2016

Population Dynamics of Gelatinous Zooplankton in the Chesapeake Bay and Sargasso Sea, and Effects on Carbon Export

Joshua Paul Stone
College of William and Mary - Virginia Institute of Marine Science, joshuapstone@gmail.com

Population Dynamics of Gelatinous Zooplankton in the Chesapeake Bay and Sargasso Sea, and Effects on Carbon Export

---

A Dissertation

Presented to

The Faculty of the School of Marine Science

The College of William and Mary in Virginia

In Partial Fulfillment

of the Requirements for the Degree of

Doctor of Philosophy

---

by

Joshua Paul Stone

August 2016

APPROVAL SHEET

This dissertation is submitted in partial fulfillment of

the requirements for the degree of

Doctor of Philosophy

Joshua P. Stone

Approved by the Committee July 19, 2016

Deborah K. Steinberg, Ph.D.
Committee Chair/Advisor

Mark J. Brush, Ph.D.

Robert H. Condon, Ph.D.
University of North Carolina Wilmington
Wilmington, NC, USA

J. Emmett Duffy, Ph.D.

Courtney K. Harris, Ph.D.

DEDICATION

This dissertation is dedicated to my father, Roger Stone,
for passing his love of biology on to me.

TABLE OF CONTENTS

ACKNOWLEDGMENTS

I owe a huge debt of gratitude to the many people who have been a part of my life during graduate school. First, Debbie Steinberg has been an amazing advisor throughout the past six years, and not only has she taught and guided me through my dissertation work with patience and infectious excitement, but has also been a wonderful friend and mentor. I am also grateful to my committee – Rob Condon, Emmett Duffy, Courtney Harris, and Mark Brush – for their advice and guidance in my research.

I am proud to be a member of the Steinbergler family, and all of the past, present, and future members of the Zooplankton Ecology Lab have my thanks. My lab family, Brandon Conroy, Kim Bernard, Joe Cope, Kate Ruck, Lori Garzio, Miram Gleiber, Jeanna Hudson, Jami Ivory, Tricia Thibodeau, and Jack Conroy, have all been amazing friends and helpful in so many ways. The highlight of my time at VIMS has undoubtedly been becoming friends with this group of people, stumbling through the graduate school experience with them, and sharing in our love of discovery.

The wider VIMS community has also been the best fraternity I could have hoped for. There are too many people to name here, but my many fantastic friends have made the years here way too much fun for my own good. Not only am I thankful for the games, parties, and comraderie, but also for the constant shared interest in science, and I learned so much from each interaction with every friend. I know that I will remain friends with all of them, and make new ones from VIMS, for many years to come.

My family has been incredibly supportive and encouraging of me every day of my life. I owe everything to my parents, Roger and Kathy, for teaching and guiding me through every aspect of my education and growing up. I can't say enough how much they've helped me, and I want to make them proud. Thank you to my first friends, Skyla and Clara, for all of your support and love.

Most importantly, I want to thank my best friend and wife, Nicole Trimmer, who has been far beyond anything I could have asked for. Not only is she the smartest, funniest, and most beautiful person I have ever met, but her constant encouragement and support have helped more than anything in completing this dissertation.

Finally, I would like to acknowledge my funding sources. The BATS program has been funded by the National Science Foundation (NSF) Chemical and Biological Oceanography programs for over two decades, with the most recent grant OCE-1258622 to D. Steinberg and colleagues funding this current effort. Data collected onboard the 'Trophic BATS' cruise was supported by OCE-1090149 to R. Condon. Research in the Chesapeake Bay was funded by Virginia Sea Grant (V718500) to D. Steinberg and myself, and by grants from the Virginia Resources Commission, Virginia Recreational Fishing Advisory Board, and NOAA-Chesapeake Bay Office to Mary Fabrizio.

LIST OF TABLES

LIST OF FIGURES

Chapter 3 Page

Chapter 4 Page

ABSTRACT

Gelatinous zooplankton (GZ; cnidarians, ctenophores, and pelagic tunicates) periodically are the dominant members of the zooplankton throughout the majority of the world's oceans. Their unique body plans and life cycles allow them to rapidly take advantage of favorable environmental conditions, which has far-ranging consequences for food web dynamics and biogeochemical cycles. GZ populations have been speculated to respond to anthropogenic changes, but few long-term studies exist to test this hypothesis and even fewer have examined the consequent effects on carbon export. I analyzed two long-term time series in the Chesapeake Bay and one in the Sargasso Sea for annual and interannual changes in GZ populations and the environmental drivers of these changes. I also conducted mesocosm experiments in the Chesapeake Bay and developed a carbon flux model for the Sargasso Sea to evaluate the role that GZ play in vertical carbon flux in these two regions. In the Chesapeake Bay, summer populations of the dominant scyphozoan medusae, *Chrysaora quinquecirrha*, are positively correlated with spring salinity and negatively with dissolved oxygen concentrations. *C. quinquecirrha* biovolume has been decreasing from 1985-2011, reducing predation pressure on the ctenophore *Mnemiopsis leidyi*, with cascading effects on copepod abundances. This top-down control of the food web extends to changes in vertical carbon flux, with the presence of *M. leidyi* reducing copepod fecal pellet flux by 50%. In the Sargasso Sea, large salp blooms can completely dominate the zooplankton community, and both cyclonic mesoscale eddies and seasonal changes in primary production can regulate annual salp population dynamics. Long-term salp population trends are correlated with changes in decadal climate oscillations, and a long-term increase in the most abundant salp species, *Thalia democratica,* was observed from 1994-2011. During blooms, salps can graze more than 100% of the primary production, and rapidly export carbon to depth through sinking fecal pellets and carcasses, and through active transport via respiration at depth. This carbon export to 200 m (average of 2.3 mg C m^{-2} d^{-1}) is equivalent to 11% of the measured sediment trap flux at the same depth, but salp fecal pellets and carcasses attenuate slowly and can be equivalent to > 100% of measured sediment trap carbon at 3200 m, representing a large export of carbon to the bathypelagic zone during salp blooms. GZ populations in both the Chesapeake Bay and Sargasso Sea are sensitive to seasonal changes in the environment on annual and interannual time scales. Long-term changes in GZ abundances could continue into the future, causing corresponding changes in carbon export.

Joshua Paul Stone

SCHOOL OF MARINE SCIENCE
THE COLLEGE OF WILLIAM AND MARY

Population Dynamics of Gelatinous Zooplankton in the Chesapeake Bay and Sargasso Sea, and Effects on Carbon Export

CHAPTER 1

Introduction to the dissertation

Importance of gelatinous zooplankton

The term ‘gelatinous zooplankton’ (GZ) refers to a taxonomically diverse group of marine organisms that share a similar gelatinous body with a high water (>95%) and low carbon content (Lucas et al., 2011). This term traditionally includes medusae and siphonophores (Phylum: Cnidaria, Class: Scyphozoa, Hydrozoa, and Cubozoa), comb jellies (Phylum: Ctenophora), and pelagic tunicates (Phylum: Chordata, Subphylum: Urochordata or Tunicata, Class: Thaliacea–salps, doliolids, pyrosomes, and Appendicularia–larvaceans). This low carbon to wet-weight ratio, along with their unique body plans, allows GZ to grow quickly and maintain much higher clearance rates than non-gelatinous animals with similar carbon content (Acuña et al., 2011; Pitt et al., 2013). Additionally, GZ have unique life histories and extremely fast reproduction rates when environmental conditions are optimal (reviewed in Purcell, 2005), allowing them to have episodic or seasonal large population increases, or ‘blooms’ (where populations are several orders of magnitude higher than base levels). Both medusae and comb jellies are important and voracious predators of zooplankton and ichthyoplankton (reviewed in Purcell & Arai, 2001), and during blooms they can have extensive top-down effects on the food web (Purcell & Decker, 2005; Daskalov et al., 2007; Condon & Steinberg, 2008; West et al., 2009). Blooms of pelagic tunicates can similarly exert top-down control on their food source, phytoplankton (Zeldis et al., 1995; Hereu et al., 2006; Madin et al., 2006; Hereu et al., 2010). The extremely high abundances that GZ are able to attain during blooms not only affect food web dynamics, but also make them important in biogeochemical cycling of carbon and nutrients.

GZ can affect biogeochemical cycling, including vertical export, through a variety of mechanisms. During the life of the animal, GZ not only excrete highly labile dissolved organic matter (DOM) (Condon et al., 2011), but also produce sinking material in the form of fecal pellets (Bruland & Silver, 1981; Madin, 1982) or mucous masses (Kremer, 1979; Reeve et al., 1989). Some GZ undergo diel vertical migration, with their respiration, excretion, and egestion of fecal pellets at depth contributing to carbon export (Steinberg et al., 2000). The sinking of dead GZ carcasses is also a significant, episodic pulse of carbon to the benthos in a variety of environments (reviewed in Lebrato et al., 2012). In addition to these direct influences, GZ may also regulate carbon and nutrient flux through their top-down control of food webs. Because phytoplankton and other zooplankton have diverse contributions to export, GZ-induced changes in the abundance and community composition of these other groups may have numerous secondary effects on the amount and content of the vertical flux. Accordingly, future changes in GZ populations would have wide-ranging effects on carbon flux through numerous mechanisms.

Globally, GZ populations oscillate through decadal periods of increase and decrease (Condon et al., 2013), although there are long-term directional increases, and decreases, documented in some regions (reviewed in Brotz et al., 2012; Condon et al., 2013). There is a perception and concern that globally GZ populations are largely increasing (Daskalov et al., 2007; Richardson et al., 2009), likely in response to various anthropogenic effects (reviewed in Purcell et al., 2007). However, this notion appears to be overstated and studies used to support this claim are often miscited (Condon et al., 2012; Sanz-Martín et al., 2016). Much of the ambiguity around this issue is a result of

the paucity of long-term GZ time series in most systems, thus estimates of trends are often based on only several years of data. The question of whether GZ populations are changing is an important one, as GZ have wide-ranging effects on many human activities, including interference with commercial fishing, stinging of recreational swimmers, clogging intakes of power and desalination plants, and harming aquaculture operations (reviewed in Purcell et al., 2007; Richardson et al., 2009; Graham et al., 2014). In addition to these direct effects, long-term changes in GZ populations would cause concurrent long-term changes in trophic interactions and carbon cycling in the ecosystems they inhabit. Two examples of ecosystems where GZ can seasonally account for the majority of biomass in the zooplankton are the Chesapeake Bay and the Sargasso Sea, and the goal of this dissertation is to: 1) quantify long-term changes in GZ populations in these contrasting ecosystems and 2) calculate the effect of those changes on vertical flux.

Chesapeake Bay

The Chesapeake Bay is a large, highly productive estuary on the eastern coast of the United States and is an important nursery ground for a wide variety of commercially and ecologically important species. The dominant and seasonally abundant GZ in the Chesapeake Bay are the lobate ctenophore *Mnemiopsis leidyi* and the scyphozoan medusa *Chrysaora quinquecirrha*. Adult *M. leidyi* feed primarily on crustacean zooplankton, and during *M. leidyi* peak abundance, can effectively control copepod populations (Purcell et al., 2001; Purcell & Decker, 2005; Condon & Steinberg, 2008). *M. leidyi* also has a significant negative effect on survival of other small zooplankton and on fish eggs (Cowan et al., 1992; Houde et al., 1994; Purcell & Arai, 2001), and larval *M. leidyi* feed

almost exclusively on microzooplankton and even consume phytoplankton (Sullivan & Gifford, 2004). Each year, *M. leidyi* are highest in abundance during April and May following increases in water temperature and copepod concentrations (Kremer, 1994; Costello et al., 2006), and they continue to be abundant through August (Condon & Steinberg, 2008). This is then followed by a bloom of *C. quinquecirrha*, starting in late May, which feeds voraciously on *M. leidyi* (Cargo & King, 1990). *C. quinquecirrha* can exert strong top-down control on ctenophore populations during summers with high medusa abundance, causing a trophic cascade (Purcell & Cowan, 1995; Purcell & Decker, 2005; Condon & Steinberg, 2008). However, the factors controlling the relative abundances of *M. leidyi* and *C. quinquecirrha* differ and are linked to their contrasting reproductive strategies.

M. leidyi reproduces as a simultaneous hermaphrodite and releases sperm and eggs into the water column, often self-fertilizing, while *C. quinquecirrha* alternates between a sexual, pelagic medusa stage, and an asexual, benthic polyp stage (Steinberg & Condon, 2009). The strength of the *C. quinquecirrha* bloom is stronger in years with warmer temperatures, reduced freshwater flow, and higher solar irradiance (Gatz et al., 1973; Cargo & King, 1990; Purcell et al., 1999). Because *C. quinquecirrha* feeds heavily on *M. leidyi*, years that are environmentally favorable for *C. quinquecirrha* exhibit low *M. leidyi* abundance (Purcell & Cowan, 1995). A smaller *M. leidyi* population reduces overall predation on copepod populations, and copepod populations are much higher during years with few ctenophores (Burrell & van Engel, 1976; Purcell & Decker, 2005). Purcell and Decker (2005) showed that years with a negative North Atlantic Oscillation (NAO) Index, which leads to higher water temperatures and salinities, had higher *C.*

quinquecirrha abundances, lower *M. leidyi* abundances, and higher copepod abundances. During the spring and summer, *C. quinquecirrha* can control the plankton community and affect all levels of the food web. However, prior studies of long-term changes in Chesapeake Bay GZ populations are limited in scope either spatially (Cargo and King, 1990) or temporally (Purcell and Decker, 2005).

Because GZ in the Chesapeake Bay can form large blooms and become the keystone species in the zooplankton community, they have the potential to greatly affect nutrient cycling in the Bay, both directly through their own feeding and metabolism, and indirectly through trophic cascades (Pitt et al., 2009). In addition to affecting copepod abundance, *C. quinquecirrha* and *M. leidyi* shunt carbon (C) away from the main food web and toward the microbial loop by releasing colloidal and dissolved organic matter that is enriched in C over N and is readily respired by bacteria (Condon et al., 2011). In several studies, GZ have been shown to increase primary productivity through release of nutrients, as well as initiating top-down trophic cascades in the zooplankton (West et al., 2009; McNamara et al., 2014; Hosia et al., 2015). What has not been previously studied is how trophic interactions and the relative abundances of these two gelatinous species influence particulate organic matter flux to the benthos.

Sargasso Sea

The Sargasso Sea is an oligotrophic region in the North Atlantic subtropical gyre, and salps can periodically become the dominant GZ in this area (Madin et al. 1996, Madin et al. 2001, Roman et al. 2002). Salps (Class: Thaliacea, Order: Salpa) are tubular GZ that filter-feed on phytoplankton and microzooplankton which during blooms

increase in biomass to levels much higher than other zooplankton. Large salp blooms occur in other environments (Everett et al., 2011; Loeb & Santora, 2012), and salp blooms can consume over 100% of the daily primary production until standing stocks of phytoplankton are depleted (Hereu et al., 2006), outcompete crustacean zooplankton for food (Dubischar & Bathmann, 1997), and have significant effects on particle export (Madin, 1982; Caron et al., 1989; Phillips et al. 2009) as detailed further below. Thus, we predict salps in the Sargasso Sea will also be important grazers and contributors to export. The life history of salps includes alternation between a sexual stage (the blastozooid) and an asexual stage (the oozoid) which enables them to rapidly replicate and form high density blooms when conditions are favorable (Godeaux et al. 1998; Henschke et al., 2015). A number of salp species can form these blooms, but for the majority of species, almost nothing is known of the causes or fates of the blooms. In other systems, salp populations have exhibited sensitivity to interannual or long-term changes in the environment (Ménard et al., 1994; Atkinson et al., 2004; Licandro et al., 2006), but studies on long-term population changes in the western Atlantic Ocean, or any oligotrophic region, are sorely lacking.

Mesozooplankton biomass has been increasing in the Sargasso Sea at the Bermuda Atlantic Time-series Study (BATS) site over the past 17 years (Steinberg et al., 2012), and the role that salps play in this increase is unknown. Ménard et al. (1994) found that salp populations increased along with increases in upwelling due to lower temperatures and higher winds, and Li et al. (2011) found that salp and doliolid abundance in the South China Sea was affected by an increase in chlorophyll *a* concentration caused by coastal upwelling and injection of nutrients into surface waters

by cold core eddies in summer. Henschke et al. (2015) modeled salp populations in the Tasman Sea, and found that both temperature and phytoplankton concentrations were the dominant drivers of salp population changes. In the Sargasso Sea, long-term changes in net primary productivity (Saba et al., 2010) have been documented, with unknown effects on salp populations. Additionally, cold core mesoscale eddies are an important periodic source of nutrient upwelling in the Sargasso Sea (McGillicuddy et al., 2007; Mouriño-Carballido, 2009), that can increase zooplankton abundance and fecal pellet production (Goldthwait & Steinberg, 2008; Eden et al., 2009). The links between these large-scale processes, decadal climate oscillations, and salp population changes in the Sargasso Sea remain to be explored.

Salps feed efficiently on small phytoplankton and bacteria and produce large, fast-sinking fecal pellets (Caron et al., 1989; Sutherland et al., 2010), making them important in biogeochemical cycling. Salps have some of the highest clearance rates of any zooplankton– several liters hr^{-1} $salp^{-1}$ (Harbison & McAlister, 1979; Madin & Purcell, 1992; Madin & Kremer, 1995). Salps feed by filtering water though a mucous mesh that they then consume along with any particles caught on the mesh (Bone et al., 2003). Because of this, they ingest a large amount of material that passes through their guts undigested and becomes packaged into fecal pellets that are much larger and faster-sinking than those of other zooplankton (Andersen, 1998). For example, copepod fecal pellet sinking rates can range from 5-220 m day^{-1} (Turner, 2002; Patonai et al., 2011) while salp fecal pellet sinking rates range from 42-2700 m day^{-1} (Andersen et al., 1998; Yoon et al., 2001; Phillips et al., 2009). Salp fecal pellet production potentially represents a fast, efficient pathway for organic matter in the surface waters to move to

depth, and during a salp bloom, salps can be major contributors to the total carbon flux from the surface to the deep sea, as demonstrated in the Mediterranean Sea (Yoon et al., 1996; Fernex et al., 1996), North Pacific (Iseki, 1981), Sargasso Sea (Conte et al., 2001), and Southern Ocean (Phillips et al., 2009).

While contribution to vertical carbon flux through salp fecal pellets has been widely studied, salp contributions to flux through vertical migration and sinking carcasses have been considered less frequently. GZ are low in per individual carbon content (carbon content is typically ~10 % of dry weight and dry weight is ~4-5% of wet weight; Madin et al., 1981; Clarke et al., 1992; Bailey et al., 1995; Madin & Deibel, 1998) compared to values for total zooplankton where carbon content is 36% of dry weight and dry weight is 19% of wet weight at BATS (Madin et al. 2001). Even huge falls of GZ could be an important source of carbon to the benthos, and a more important contributor to global carbon flux than previously thought. Appropriately, the contribution of GZ carcasses to vertical export has recently been receiving more attention (Lebrato et al., 2013), and salp carcasses have been shown to be a major source of benthic organic carbon in at least one region (Henschke et al., 2013). In addition to sinking carcasses, vertically migrating zooplankton consume particulate organic carbon in the surface waters and respire or excrete it at depth (Steinberg et al., 2000), further contributing to vertical flux. Calculating the contributions of these other mechanisms of vertical carbon export by salps is crucial to understanding the role they play in biogeochemical cycling in the Sargasso Sea.

Structure of dissertation

This dissertation examines the population dynamics of GZ in the Chesapeake Bay and Sargasso Sea as well as GZ effects on vertical carbon export. It is separated into four main chapters, examining GZ in the Chesapeake Bay in chapters 1 and 2, and in the Sargasso Sea in chapters 3 and 4. This is one of the few studies worldwide to examine GZ population dynamics using long-term time series, and the only one in the Sargasso Sea. Additionally, the work includes novel calculations of lifetime salp contributions to vertical carbon flux and experimental measurements of top-down control of vertical carbon flux.

Chapter 1 – Introduction to dissertation

Chapter 2 – utilizes two long-term time series to analyze the population dynamics of GZ in the Chesapeake Bay. These time series include the Virginia Institute of Marine Science Juvenile Fish and Blue Crab Survey from 1999-2012 and the Chesapeake Bay Program Mesozooplankton Survey from 1984-2002. Both annual and interannual variation in GZ abundances are discussed, along with environmental drivers, and potential responses to climate change.

Chapter 3 – experimentally measures the effects of top-down control by GZ in the Chesapeake Bay on vertical carbon flux. Mesocosm experiments were conducted using different combinations of GZ, allowing us to examine how both the quantity and quality of carbon and nitrogen flux changes as a result.

Chapter 4 – utilizes the Bermuda Atlantic Time-series Study (BATS) zooplankton time series from 1994-2011 to analyze changes in salp population dynamics in the Sargasso Sea. The annual and interannual variation of multiple species were analyzed to

explore the influence of environmental drivers, climate change, and mesoscale eddies. Published in Marine Ecology Progress Series as Stone & Steinberg (2014).

Chapter 5 – quantifies the contributions of salps in the Sargasso Sea to vertical carbon flux. Salp carcass sinking and decomposition rate experiments were conducted, and these results are combined with published rates of other processes to develop a model of salp contributions to carbon export. Annual and interannual variation in carbon export and attenuation with depth is discussed. Published in Deep-Sea Research I as Stone & Steinberg (2016).

Chapter 6 – Summary and conclusions of dissertation

REFERENCES

Acuña JL, López-Urrutia Á, Colin S (2011) Faking giants: The evolution of high prey clearance rates in jellyfishes. Science 333: 1627-1629

Andersen V (1998) Salp and pyrosomid blooms and their importance in biogeochemical cycles, p. 125-137. In Q. Bone [ed.], The biology of pelagic tunicates. Oxford University Press

Atkinson A, Siegel V, Pakhomov E, Rothery P (2004) Long-term decline in krill stock and increase in salps within the Southern Ocean. Nature 432, 100–103

Bailey TG, Youngbluth MJ, Owen GP (1995) Chemical composition and metabolic rates of gelatinous zooplankton from midwater and benthic boundary layer environments off Cape Hatteras, North Carolina, USA. Mar Ecol Prog Ser 122: 121-134

Bone Q, Carre C, Chang P (2003) Tunicate feeding filters. J Mar Biol Assoc UK 83: 907–919

Brotz L, Cheung WWL, Kleisner K, Pakhomov E, Pauly D (2012) Increasing jellyfish populations: trends in Large Marine Ecosystems. Hydrobiologia 690: 3-20

Bruland KW, Silver MW (1981) Sinking rates of fecal pellets from gelatinous zooplankton (Salps, Pteropods, Doliolids). Mar Biol 63: 295-300

Burrell VG, van Engel WA (1976) Predation by and distribution of a ctenophore, *Mnemiopsis leidyi* A. Agassiz, in the York River estuary. Est Coast Shelf Sci 4:235–242

Cargo DG, King DR (1990) Forecasting the abundance of the sea nettle, *Chrysaora quinquecirrha*, in the Chesapeake Bay. Estuaries 13(4): 486-491

Caron DA, Madin LP, Cole JJ (1989) Composition and degradation of salp fecal pellets: implications for vertical flux in oceanic environments. J Mar Res 47: 829-850

Clarke A, Holmes LJ, Gore DJ (1992) Proximate and elemental composition of gelatinous zooplankton from the Southern Ocean. J Exp Mar Biol Ecol 155: 55-68

Condon RH, Duarte CM, Pitt KA, Robinson KL, Lucas CH, Sutherland KR, Mianzan HW, Bogeberg M, Purcell JE, Decker MB, Uye S, Madin L, Brodeur RD, Haddock SHD, Malej A, Parry GD, Eriksen E, Quiñones J, Acha M, Harvey M, Arthur JM, Graham WM (2013) Recurrent jellyfish blooms are a consequence of global oscillations. PNAS 110(3): 1000-1005

Condon RH, Graham WM, Duarte CM, Pitt KA, Lucas CH, Haddock SHD, Sutherland KR, Robinson KL, Dawson MN, Decker MB, Mills CE, Purcell JE, Malej A, Mianzan H, Uye S, Gelcich S, Madin LP (2012) Questioning the rise of gelatinous zooplankton in the world's oceans. BioScience 62(2): 160-169

Condon RH, Steinberg DK (2008) Development, biological regulation, and fate of ctenophore blooms in the York River estuary, Chesapeake Bay. Mar Ecol Prog Ser 369: 153-168

Condon RH, Steinberg DK, del Giorgio PA, Bouvier TC, Bronk DA, Graham WM, Ducklow HW (2011) Jellyfish blooms result in a major microbial respiratory sink of carbon in marine systems. PNAS 108(25): 10225-10230

Conte MH, Ralph N, Ross EH (2001) Seasonal and interannual variability in deep ocean

particle fluxes at the Oceanic Flux Program (OFP)/Bermuda Atlantic Time Series (BATS) site in the western Sargasso Sea near Bermuda. Deep-Sea Res II 48: 1471-1505

Costello JH, Sullivan BK, Gifford DJ, Van Keuren D, Sullivan LJ (2006) Seasonal refugia, shoreward thermal amplification, and metapopulation dynamics of the ctenophore *Mnemiopsis leidyi* in Narragansett Bay, Rhode Island. Limnol Oceanogr 51(4): 1819-1831

Cowan Jr. JH, Birdsong RS, Houde ED, Priest JS, Sharp WC, Mateja GB (1992) Enclosure experiments on survival and growth of black drum eggs and larvae in lower Chesapeake Bay. Coast Estuar Res Fed 15(3): 392-402

Daskalov GM, Grishin AN, Rodionov S, Mihneva V (2007) Trophic cascades triggered by overfishing reveal possible mechanisms of ecosystem regime shifts. PNAS 104(25): 10518-10523

Dubischar CD, Bathmann UV (1997) Grazing impact of copepods and salps on phytoplankton in the Atlantic sector of the Southern Ocean. Deep-Sea Res II 44: 415–433

Eden BR, Steinberg DK, Goldthwait SA, McGillicuddy DJ (2009) Zooplankton community structure in a cyclonic and mode-water eddy in the Sargasso Sea. Deep-Sea Research I 56: 1757-1776

Everett JD, Baird ME, Suthers IM (2011) Three-dimensional structure of a swarm of the salp *Thalia democratica* within a cold-core eddy off southeast Australia. J Geophysical Res 116: C12046

Fernex FE, Braconnot JC, Dallot S, Boisson M (1996) Is ammonification rate in marine

sediment related to plankton composition and abundance? A time-series study in Villefranche Bay (NW Mediterranean). Estua Coast Shelf Sci 43: 359-371

Gatz Jr. AJ, Kennedy VS, Mihursky JA (1973) Effects of temperature on activity and mortality of the scyphozoan medusa, *Chrysaora quinquecirrha*. Chesapeake Sci 14(3): 171-180

Godeaux J, Bone Q, Braconnot JC (1998) Anatomy of Thaliacea, p. 1-24. In Q. Bone [ed.], The biology of pelagic tunicates. Oxford University Press

Goldthwait SA, Steinberg DK (2008) Elevated biomass of mesozooplankton and enhanced fecal pellet flux in cyclonic and mode-water eddies in the Sargasso Sea. Deep-Sea Res II 55: 1360-1377

Graham WM, Gelcich S, Robinson KL, Duarte CM, Brotz L, Purcell JE, Madin LP, Mianzan H, Sutherland KR, Uye S, Pitt KA, Lucas CH, Bøgeberg, Brodeur RD, Condon RH (2014) Linking human well-being and jellyfish: ecosystem services, impacts, and societal responses. Front Ecol Environ 12(9): 515-523

Harbison GR, McAlister VL (1979) The filter-feeding rates and particle retention efficiencies of three species of *Cyclosalpa* (Tunicata, Thaliacea). Limnol Oceanogr 24: 875−892

Henschke N, Bowden DA, Everett JD, Holmes SP, Kloser RJ, Lee RW, Suthers IM (2013) Salp-falls in the Tasman Sea: a major food input to deep-sea benthos. Mar Ecol Prog Ser 491: 165-175

Henschke N, Smith JA, Everett JD, Suthers IM (2015) Population drivers of a *Thalia democratica* swarm: insights from population modelling. J Plankton Res 37: 1042-1055

Hereu CM, Lavaniegos BE, Gaxiola-Castro G, Ohman MD (2006) Composition and potential grazing impact of salp assemblages off Baja California during the 1997−1999 El Niño and La Niña. Mar Ecol Prog Ser 318: 123−140

Hereu CM, Lavaniegos BE, Goericke R (2010) Grazing impact of salp (Tunicata, Thaliacea) assemblages in the eastern tropical North Pacific. J Plankton Res 32(6): 785-804

Hosia A, Augustin CB, Dinasquet J, Granhag L, Paulsen ML, Riemann L, Rintala J-M, Setälä O, Talvitie J, Titelman J (2015) Autumnal bottom-up and top-down impacts of *Cyanea capillata*: a mesocosm study. J Plankton Res 37(5) 1042-1055

Houde ED, Gamble JC, Dorsey SE, Cowan Jr. JH (1994) Drifting mesocosms: the influence of gelatinous zooplankton on mortality of bay anchovy, *Anchoa mitchilli*, eggs and yolk-sac larvae. ICES J Mar Sci 51: 383-394

Iseki (1981) Particulate organic matter transport to the deep sea by salp fecal pellets. Mar Ecol Prog Ser 5: 55-60

Kremer P (1979) Predation by the Ctenophore *Mnemiopsis leidyi* in Narragansett Bay, Rhode Island. Estuaries 2(2): 97-105

Kremer P (1994) Patterns of abundance for *Mnemiopsis* in US coastal waters: a comparative overview. ICES J Mar Sci 51: 347-354

Lebrato M, Molinero J-C, Cartes JE, Lloris D, Mélin F, Beni-Casadella L (2013) Sinking jelly-carbon unveils potential environmental variability along a continental margin. PLoS ONE 8(12): e82070

Lebrato M, Pitt KA, Sweetman AK, Jones DOB, Cartes JE, Oschlies A, Condon RH,

Molinero JC, Adler L, Gaillard C, Lloris D, Billet DSM (2012) Jelly-falls historic and recent observations: a review to drive future research directions. Hydrobiologica 690: 227-245

Li K, Yin J, Huang L, Shang J, Lian S, Liu C (2011) Distribution and abundance of thaliaceans in the northwest continental shelf of South China Sea, with response to environmental factors driven by monsoon. Continental Shelf Res 31: 979-989

Licandro P, Ibañez F, Etienne M (2006) Long-Term Fluctuations (1974-1999) of the salps *Thalia democratica* and *Salpa fusiformis* in the Northwestern Mediterranean Sea: Relationships with hydroclimatic variability. Limnol Oceanogr 51:4 1832-1848

Loeb VJ, Santora JA (2012) Population dynamics of *Salpa thompsoni* near the Antarctic Peninsula: Growth rates and interannual variations in reproductive activity (1993–2009). Prog Oceanogr 96: 93-107

Madin LP (1982) Production, composition and sedimentation of salp pellets in oceanic waters. Mar Biol 67: 39−45

Madin LP, Cetta CM, McAlister VL (1981) Elemental and biochemical composition of salps (Tunicata: Thaliacea). Mar Biol 63: 217-226

Madin LP, Deibel D (1998) Feeding and energetics of Thaliacea. In: Bone Q (ed) The biology of pelagic tunicates. Oxford University Press, Oxford, UK:81-103

Madin LP, Horgan EF, Steinberg DK (2001) Zooplankton at the Bermuda Atlantic Time-series Study (BATS) station: Diel, seasonal and interannual variation in biomass, 1994–1998. Deep Sea Res II 48(8–9): 2063–2082

Madin LP, Kremer P (1995) Determination of the filter feeding rates of salps (Tunicata,

Thaliacea). ICES J Mar Sci 52: 583-595

Madin LP, Kremer P, Hacker S (1996) Distribution and vertical migration of salps (Tunicata, Thaliacea) near Bermuda. J Plankton Res 18:5 747-755

Madin LP, Kremer P, Wiebe PH, Purcell JE, Horgan EH, Nemazie DA (2006) Periodic swarms of the salp *Salpa aspera* in the Slope Water off the NE United States: biovolume, vertical migration, grazing and vertical flux. Deep-Sea Res I 53: 804−819

Madin LP, Purcell JE (1992) Feeding, metabolism, and growth of *Cyclosalpa bakeri* in the subarctic Pacific. Limnol Oceanogr 37: 1236-1251

McGillicuddy DJ, Anderson LA, Bates NR, Bibby T, Buesseler KO, Carlson C, Davis CS, Ewart C, Falkowski PG, Goldthwait SA, Hansell DA, Jenkins WJ, Johnson R, Kosnyrev VK, Ledwell JR, Li QP, Siegel DA, Steinberg DK (2007) Eddy/wind interactions stimulate extraordinary mid-ocean plankton blooms. Science 316: 1021−1026

McNamara ME, Lonsdale DJ, Cerrato RM (2014) Role of eutrophication in structuring planktonic communities in the presence of the ctenophore *Mnemiopsis leidyi*. Mar Ecol Prog Ser 510: 151-165

Ménard F, Dallot S, Thomas G, Braconnot JC (1994) Temporal fluctuations of two Mediterranean salp populations from 1967 to 1990. Analysis of the influence of environmental variables using a Markov chain model. Marine Ecology Progress Series 104: 139-152

Mills CE (2001) Jellyfish blooms: are populations increasing globally in response to changing ocean conditions? Hydrobiologia 451: 55-68

Mouriño-Carballido B (2009) Eddy-driven pulses of respiration in the Sargasso Sea. Deep-Sea Res I 56: 1242-1250

Patonai K, El-Shaffey H, Paffenhöffer G (2011) Sinking velocities of fecal pellets of doliolids and calanoid copepods. J Plankton Res 33: 1146-1150

Phillips B, Kremer P, Madin LP (2009) Defecation by *Salpa thompsoni* and its contribution to vertical flux in the Southern Ocean. Mar Biol 156: 455–467

Pitt KA, Duarte CM, Lucas CH, Sutherland KR, Condon RH, Mianzan H, Purcell JE, Robinson KL, Uye S (2013) Jellyfish body plans provide allometric advantages beyond low carbon content. PLoS ONE 8(8): e72683

Pitt KA, Welsh DT, Condon RH (2009) Influence of jellyfish blooms on carbon, nitrogen, and phosphorus cycling and plankton production. Hydrobiologia 616: 133-149

Purcell JE (2005) Climate effects on formation of jellyfish and ctenophore blooms: a review. J Mar Biol Assoc UK 85: 461–476

Purcell JE, Arai MN (2001) Interactions of pelagic cnidarians and ctenophores with fish: a review. Hydrobiologia 451: 27-44

Purcell JE, Cowan Jr. JH (1995) Predation by the scyphomedusan *Chrysaora quinquecirrha* on *Mnemiopsis leidyi* ctenophores. Mar Ecol Prog Ser 128: 63-70

Purcell JE, Decker MB (2005) Effects of climate on relative predation by scyphomedusae and ctenophores on copepods in Chesapeake Bay during 1987-2000. Limnol Oceanogr 50(1): 376-387

Purcell JE, Shiganova TA, Decker MB, Houde ED (2001) The ctenophore *Mnemiopsis* in native and exotic habitats: U.S. estuaries versus the Black Sea basin. Hydrobiologia 451 (Dev Hydrobiol 155): 145-176

Purcell JE, Uye S, Lo WT (2007) Anthropogenic causes of jellyfish blooms and their direct consequences for humans: a review. Mar Ecol Prog Ser 350: 153–174

Purcell JE, White JR, Nemazie DA, Wright DA (1999) Temperature, salinity and food effects on asexual reproduction and abundance of the scyphozoan *Chrysaora quinquecirrha*. Mar. Ecol. Prog. Ser. 180: 187-196

Reeve MR, Syms MA, Kremer P (1989) Growth dynamics of a ctenophore (*Mnemiopsis*) in relation to variable food supply. I. Carbon biomass, feeding, egg production, growth and assimilation efficiency. J Plankton Res 11(3): 535-552

Richardson AJ, Bakun A, Hays GC, and Gibbons MJ (2009) The jellyfish joyride: causes, consequences and management responses to a more gelatinous future. Trends Ecol Evol 24: 312–22

Roman MR, Adolf HA, Landry MR, Madin LP, Steinberg DK, Zhang X (2002) Estimates of oceanic mesozooplankton production: a comparison using the Bermuda and Hawaii time-series data. Deep-Sea Res II 49: 175–192

Saba VS, Friedrichs MAM, Carr M-E, Antoine D, Armstrong RA, Asanuma I, Aumont O, Bates NR, Behrenfeld MJ, Bennington V, Bopp L, Bruggemann J, Buitenhuis ET, Church MJ, Ciotti AM, Doney SC, Dowell M, Dunne J, Dutkiewicz S, Gregg W, Hoepffner N, Hyde KJW, Ishizaka J, Karneda T, Karl DM, Lima I, Lomas MW, Marra J, McKinley GA, Mélin F, Moore JK, Morel A, O'Reilly J, Salihoglu B, Scardi M, Smyth TJ, Tang S, Tjiputra J, Uitz J, Vichi M, Waters K, Westberry TK, Yool A (2010) Challenges of modeling depth-integrated marine primary productivity over multiple decades: A case study at BATS and HOT. Global Biogeochemical Cycles 24: GB3020

Sanz-Martín M, Pitt KA, Condon RH, Lucas CH, de Santana CN, Duarte CM (2016) Flawed citation practices facilitate the unsubstantiated perception of a global trend toward increased jellyfish blooms. Global Ecol Biogeogr DOI: 10.1111/geb.12474

Steinberg DK, Carlson CA, Bates NR, Goldthwait SA, Madin LP, Michaels AF (2000) Zooplankton vertical migration and the active transport of dissolved organic and inorganic carbon in the Sargasso Sea. Deep-Sea Res I 47: 137-158

Steinberg DK, Carlson CA, Bates NR, Johnson RJ, Michaels AF, Knap AH (2001) Overview of the US JGOFS Bermuda Atlantic Time-series Study (BATS): a decade-scale look at ocean biology and biogeochemistry. Deep-Sea Res II 48: 1405-1447

Steinberg DK, Condon RH (2009) Zooplankton of the York River. J Coastal Res 57: 66-79.

Steinberg DK, Lomas MW, Cope JS (2012) Long-term increase in mesozooplankton biomass in the Sargasso Sea: Linkage to climate and implications for food web dynamics and biogeochemical cycling. Global Biogeochemical Cycles 26: GB1004

Stone, J.P., D. K. Steinberg. 2016. Salp contributions to vertical carbon flux in the Sargasso Sea. Deep-Sea Research I 113: 90-100

Stone, J.P., D.K. Steinberg. 2014. Long-term time-series study of salp population dynamics in the Sargasso Sea. Marine Ecology Progress Series 510:111-127

Sullivan LJ, Gifford DJ (2004) Diet of the larval ctenophore *Mnemiopsis leidyi* A. Agassiz (Ctenophore, Lobata). J Plank Res 26: 417-431

Sutherland KR, Madin LP, Stocker R (2010) Filtration of submicrometer particles by pelagic tunicates. PNAS 107(34): 15129-15134

Turner JT (2002) Zooplankton fecal pellets, marine snow and sinking phytoplankton blooms. Aquatic Microbial Ecol 27:57-102

West EJ, Pitt KA, Welsh DT, Koop K, Rissik D (2009) Top-down and bottom-up influences of jellyfish on primary productivity and planktonic assemblages. Limnol Oceanogr 54(6): 2058-2071

Yoon WD, Marty JC, Sylvain D, Nival P (1996) Degradation of fecal pellets in *Pegea confoederata* (Salpidae, Thaliacea) and its implication in the vertical flux of organic matter. J Exp Mar Biol Ecol 203:147–177

Yoon WD, Kim SK, Han KN (2001) Morphology and sinking velocities of fecal pellets of copepod, molluscan, euphausiid, and salp taxa in the northeastern tropical Atlantic. Mar Biol 139: 923-928

Zeldis JR, Davis CS, James MR, Ballara SL, Booth WE, Chang FH (1995) Salp grazing: effects on phytoplankton abundance, vertical distribution and taxonomic composition in a coastal habitat. Mar Ecol Prog Ser 126: 267−283

CHAPTER 2

Long-term changes in gelatinous zooplankton in Chesapeake Bay, USA: Environmental controls and interspecific interactions

ABSTRACT

Gelatinous zooplankton populations are sensitive to environmental perturbations, and there has been concern over regional, long-term changes in their abundance due to degraded environmental conditions. We used two time series to analyze the population dynamics of gelatinous zooplankton in the Chesapeake Bay, USA: the Virginia Institute of Marine Science Juvenile Trawl Survey (1999-2012) and the Chesapeake Bay Program Mesozooplankton Survey (1984-2002). Annual and interannual variations in population size and distribution of the scyphozoan medusae *Chrysaora quinquecirrha*, *Aurelia aurita*, *Cyanea capillata*, and *Rhopilema virrilli*, as well as the lobate ctenophore *Mnemiopsis leidyi*, were compared to environmental and other biological data collected by both surveys. All species except *R. virrilli* varied seasonally, with temperature controlling seasonal distribution and salinity controlling spatial distribution within Chesapeake Bay. Scyphozoan population control by environmental factors was primarily a result of survival and asexual reproduction by the benthic scyphistomae. *C. quinquecirrha* was present year-round, but biovolume was highest July-September and in salinities between 10 and 20. *M. leidyi* populations were primarily controlled by *C. quinquecirrha* predation, and were most abundant in June, after waters warmed above 18°C but before *C. quinquecirrha* bloomed. High spring streamflow significantly reduced summer *C. quinquecirrha* biovolume, and low bottom dissolved oxygen concentrations delayed the timing of the peak bloom. Total GZ biovolume decreased over both time series (1984-2012), likely due to decreases in *C. quinquecirrha* abundance, and the peak bloom was shifted later in the summer over the VIMS time series (1999-2012). This reduction in *C. quinquecirrha* allowed for a concurrent increase

in *M. leidyi* and decrease in copepod abundance. Predicted future increases in spring streamflow and spring hypoxia due to global climate change would further decrease *C. quinquecirrha* abundance, allowing for future increase in *M. leidyi* populations.

1. INTRODUCTION

Chesapeake Bay is a large estuary on the east coast of the United States, and is a productive habitat for a variety of commercially important fish and shellfish species. Gelatinous zooplankton (GZ) play a key role in Chesapeake Bay pelagic food web dynamics, with two species in particular that are abundant predators during the spring and summer: the lobate ctenophore *Mnemiopsis leidyi* and the scyphozoan medusa *Chrysaora quinquecirrha*. *M. leidyi* feeds voraciously on a wide variety of crustacean zooplankton, and during GZ 'bloom' periods exerts significant top-down control on the zooplankton community (Purcell et al., 1994; Purcell et al., 2001; Purcell & Decker, 2005; Condon & Steinberg, 2008). Additionally, during bloom periods it competes with and consumes ichthyoplankton and bivalve larvae of commercially important species (Govoni & Olney, 1991; Purcell et al., 1991; Cowan & Houde, 1993; Houde et al., 1994; Purcell et al., 2001). Since *C. quinquecirrha* also feeds on a wide variety of crustacean zooplankton, it can have similar effects on the food web as *M. leidyi* (Purcell, 1992). However, *C. quinquecirrha* is also a voracious predator of *M. leidyi*, and can control ctenophore populations where these species co-occur (Purcell & Cowan, 1995; Purcell & Decker, 2005; Condon & Steinberg, 2008). The timing and strength of these interspecific interactions are dependent on environmental conditions and how those conditions affect the reproduction of these two species.

M. leidyi are present in Chesapeake Bay throughout the year, but reproduce during the spring when waters warm above 10°C and there is high prey availability (Kremer, 1994; Purcell et al., 2001; Costello et al., 2006). *M. leidyi* are simultaneous hermaphrodites, holoplanktonic, and develop directly. They have extremely fast growth

and high production rates, and under ideal conditions can double their biomass within a day (Reeve et al., 1989) and produce up to 14,000 eggs d^{-1} (Kremer, 1976). *C. quinquecirrha* can also reproduce rapidly under favorable conditions and alternates between sexual and asexual reproduction. The planktonic medusae – most abundant June through October – broadcast spawn eggs and sperm into the water column, where the fertilized eggs form planulae that quickly settle on hard benthic substrate. Those planulae transform into the benthic polyps (scyphistomae) which persist throughout the year, and can encyst if conditions are unfavorable (e.g., low temperatures, low food availability) (Cargo & Schultz, 1966). Once waters warm to above 17°C in the spring (Cargo & King, 1990), these benthic polyps asexually produce planktonic ephyrae (a process called strobilation) which then develop into the adult medusae. Ephyrae production is highest in salinities ranging from 9 to 25 (Purcell et al., 1999).

In Chesapeake Bay, *C. quinquecirrha* are controlled by spring environmental conditions, with warmer temperatures and higher salinities (lower river discharge) leading to higher strobilation rates earlier in the year (Cargo & King, 1990; Purcell & Decker, 2005). These favorable spring conditions lead to higher abundances of medusae during the summer, which then exert top-down control on *M. leidyi*, and release copepods from *M. leidyi* predation pressure (Purcell & Decker, 2005; Condon & Steinberg, 2008). Thus, spring temperature and rainfall can have cascading, top-down effects on the summer food web in Chesapeake Bay. These interannual variations in *C. quinquecirrha* abundance are inversely correlated with the North Atlantic Oscillation (NAO) Index, as the NAO affects temperature and rainfall regimes in the region (Purcell & Decker, 2005). Model predictions of the effect of climate change on the region include increases in

winter and spring streamflow which cause lower salinities and increases in hypoxia, along with rising water temperatures (reviewed in Najjar et al., 2010). Additionally, increases in hypoxia are expected to also be accompanied by decreases in pH, especially in coastal regions (Melzner et al., 2013). These changes in climate could have significant and immediate effects on GZ, with cascading effects down the food web.

A variety of other GZ species occur in the Chesapeake at varying times of the year. These include the scyphozoan medusa *Cyanea capillata* in the winter, the scyphozoan *Aurelia aurita* in the fall, the predatory ctenophore *Beroe ovata* in the fall, and infrequent incursions of the scyphozoans *Stomolophus meleagris* and *Rhopilema verilli* (Condon & Steinberg, 2009). Because these other species are generally less abundant than *M. leidyi* and *C. quinquecirrha*, their respective roles in the Chesapeake ecosystem have been less studied and their relative importance in food web dynamics is unknown. Accordingly, future changes in climate and the Chesapeake Bay ecosystem would have unknown effects on these species.

Globally, GZ populations are changing in a variety of ecosystems (Mills, 2001; Purcell, 2005), and it is hypothesized that GZ populations will continue to change in response to future anthropogenic effects (reviewed in Purcell et al., 2007). While long-term increases are observed in some GZ populations (Brotz et al., 2012), average global changes in GZ populations follow decadal oscillations and increase and decrease periodically (Condon et al., 2013). In Chesapeake Bay, *C. quinquecirrha* populations declined in the mid-1980s, possibly as a result of decreases in oysters, the preferred habitat of the benthic scyphistomae (Breitburg & Fulford, 2006). This decrease led to a corresponding increase in *M. leidyi* and decrease in the copepod *Acartia tonsa* (Kimmel

et al., 2012). However, the dataset used to analyze changes in *C. quinquecirrha* populations was spatially limited, and overall changes in Chesapeake Bay GZ populations, especially after the mid-1980s, remain to be determined. To better understand how GZ populations in the Chesapeake Bay change on seasonal, interannual, and decadal time scales, we analyzed two time series of GZ abundance. These time series cover a large spatial and temporal range, and include additional physical and biogeochemical data. The goals of this study were to analyze: 1) how GZ populations in Chesapeake Bay are changing in response to environmental variables, 2) how those changes affect other zooplankton through trophic interactions, and 3) long-term trends in GZ populations and predict how these trends may change in the future.

2. METHODS

2.1 VIMS Juvenile Trawl Survey

One of the time series used to assess GZ populations in Chesapeake Bay is the Virginia Institute of Marine Science Juvenile Fish and Blue Crab Trawl Survey (hereafter referred to as the VIMS survey or dataset). This survey is primarily used to develop abundance indices for juvenile finfish and blue crabs, but the survey also recorded GZ total biovolume and species presence from February, 1999 to February, 2012. Sampling was conducted using a 9.14 m semi-balloon otter trawl with 38.1 mm stretched mesh and 6.35 mm cod end liner. Each tow was conducted during daylight hours and consisted of a 5-minute bottom trawl, and also fished during the net's descent and ascent. Sampling occurred monthly, except during January and March, in each of 19 regions in the lower (Virginia) portion of Chesapeake Bay and its tributaries (Figure 1). Within each region, 2-4 trawls were conducted at random at each of four depth strata: 1.2 – 3.7 m, 3.7 – 9.1 m, 9.1 – 12.8 m, and >12.8 m. In addition to the trawl catch data, surface and bottom temperature, salinity, and dissolved oxygen (DO) were recorded, along with wind speed, wind direction, and tidal stage. A complete description of the sampling protocol and study design is in Lowery and Geer (2000).

Because the otter trawl in the VIMS survey fished for GZ on the descent and ascent of the net, each tow fished for longer at deep stations than shallow stations. In order to standardize across trawls, catch data were converted into biovolume caught per minute fished (L tow-min^{-1}). The net descended and ascended at an average rate of 0.08 m s^{-1}, and this rate was multiplied by the depth of each station and added to the bottom

trawl time of 5 minutes to calculate the total time of the tow, which ranged from 5.5 to 20.4 min. While only total biovolume of all GZ species combined was measured, the presence of each species was recorded, and summer biovolume is primarily *C. quinquecirrha* (Tuckey pers. comm.). While dead GZ may have been captured during the benthic portion of each trawl, technicians did not record any obviously morbibund or severaly damaged individuals. Because of the large mesh size (38.1 mm), hydrozoan medusae, small ctenophores, and scyphozoan ephyrae were not caught in the net.

2.2 Chesapeake Bay Program

The second time series used to analyze GZ populations is the mesozooplankton monitoring component of the Chesapeake Bay Program (hereafter referred to as the CBP survey or dataset). These data were downloaded from the Chesapeake Bay Program online Plankton Database: www.chesapeakebay.net/data/downloads/baywide_cbp_plankton_database, where a complete description of the sampling methodology can be found. Sampling was conducted monthly from August, 1984 to December, 1992, and monthly (except for January and February) from March, 1993 to September, 2002. Ten stations in the upper (Maryland) portion of Chesapeake Bay and its tributaries were sampled (Figure 2), with some stations only sampled for a portion of the study period. Sampling consisted of duplicate stepped, oblique tows through the water column using a 0.5 m mesozooplankton net with 202 μm mesh. GZ were recorded as one of three taxonomic groups: Hydrozoans, *Mnemiopsis* sp., and Scyphozoans, and count and biovolume m^{-3} were reported for each group. *Beroe* sp. was also recorded by this survey but excluded from the analysis as they were observed too infrequently to conduct statistical analyses of

their populations. Large scyphozoans are underestimated by this sampling method, due to the small net size, and absolute abundances are unreliable. However, as the sampling method was constant across the time series, relative abundances of Scyphozoans can be compared within the time series. In addition to GZ data, abundance was measured for all other mesozooplankton within each tow, with identification to species when possible. Water temperature, salinity, DO, and chlorophyll *a* were recorded at each station for several depths. We integrated or averaged these data for the water column where appropriate for comparisons with GZ abundance.

2.3 Other data collection

In addition to the VIMS and CBP surveys, two other time series of environmental data were used in the analyses. These were the monthly North Atlantic Oscillation index from the National Weather Service Climate Prediction Center (www.cpc.ncep.noaa.gov/data/teledoc/nao.shtml) and the monthly mean streamflow for the James River from the USGS National Water Information System (waterdata.usgs.gov/nwis/sw). James River streamflow was used to represent streamflow magnitude for all data in the VIMS dataset because of its proximity to the study area. James River streamflow is highly correlated with streamflow in other river systems (e.g., Potomac, Susquehanna, etc.) in the Chesapeake Bay (Spearman correlation > 0.762, $p < 0.0001$).

2.4 Statistical analyses

All statistical analyses were conducted with SigmaPlot 11.0 software. Habitat preference analyses were conducted by averaging GZ biovolume or GZ species presence

into 0.5 °C temperature or 0.5 salinity unit bins across all years and stations or sampling regions for each season. These averages were then plotted across the range of temperatures or salinities sampled. A linear, Gaussian, exponential decay, or exponential growth model was then fit to the data as appropriate.

To analyze the effect of environment and season on spatial distribution of *C. quinquecirrha* in Chesapeake Bay, we calculated the mean center of population for each month of the VIMS time series. All biovolume observations where *C. quinquecirrha* were present in the VIMS time series were plotted in ArcGIS 10.3 for each month. These observations of population biovolume were then interpolated using the inverse distance weighted method with coastline as a boundary, and each month's resulting interpolation was divided into one of four regions (James River, York River, Rappahannock River, and mainstem Chesapeake Bay). The weighted center of each region was calculated for each month, and weighting was based on the interpolated GZ biovolume. After calculating the center of population, its distance from the mouth of its respective river along the river's midline was then measured. This gave an estimate of how far upstream or downstream the population biovolume center was for that particular month. These distances were then compared to average streamflow and temperature for each month.

Seasonality of GZ biovolume and GZ presence was calculated by averaging across all regions and years for each calendar month. Changes in seasonality were calculated by plotting the average weekly GZ biovolume for each year of the VIMS dataset. A Gaussian peak regression was then fit to data for each year, and the Julian day and magnitude of each years' fitted peak was plotted across the time series. Changes in Julian day and magnitude of the biovolume peak were then analyzed using linear

regression. The VIMS survey samples each site on a monthly basis, but this occurs over the course of the month. The weekly averaging for this analysis is not expected to bias the results as the order of sites sampled changes randomly from year to year. This seasonal analysis was also attempted for the CBP dataset, but there were not sufficient samples to accurately fit curves for each individual year.

Anomalies in environmental parameters, GZ biovolume, and taxon abundance were calculated for each month using the following formula:

$$A'_m = \log_{10}\left[\frac{\bar{A}_m}{\bar{A}_i}\right]$$

Where $\bar{A}_m$ is the average of each parameter for year/month *m*, and $\bar{A}_i$ is the climatological mean for calendar month *i* of that parameter (Steinberg et al., 2012). Anomalies were calculated for each sampling region (VIMS survey) or station (CBP survey) first, and then averaged across regions or stations for each month. Annual or seasonal anomalies were calculated by averaging monthly anomalies. Multi-year trends or correlations between environmental parameter and GZ biovolume anomalies were calculated either by linear regression or Pearson's Correlation Coefficient. Lags of 1-4 months and 1-2 years were also used to examine correlations between GZ biovolume and environmental parameters.

A variety of thresholds have been suggested for hypoxia in the Chesapeake Bay including < 2.0 mg O_2 l^{-1} (Diaz & Rosenberg, 1995), < 3.5, (Condon et al., 2001), and < 50% saturation (~ < 3.5-4.0, Breitburg et al., 2003). For this study, hypoxic conditions were defined as a bottom dissolved oxygen concentration of < 3.0 mg O_2 l^{-1}, as this

threshold is an averge of other values used and has been used previously as a cut-off for examining effects on *Chrysaora*/zooplankton interactions (Grove & Breitburg, 2005).

To combine datasets and calculate trends across a broader range of years, we standardized the GZ abundance anomalies in the lower Bay VIMS dataset to the upper Bay CBP dataset by using the values from overlapping years (1999-2002). This was accomplished by adjusting the relative magnitudes and distances from zero for each anomaly in the VIMS dataset. First, the mean ratio in anomaly magnitudes (*R*) between the two datasets for all six combinations of overlapping years was calculated as follows:

$$R = [(C_{1999} - C_{2000}) / (V_{1999} - V_{2000}) + (C_{1999} - C_{2001}) / (V_{1999} - V_{2001}) + (C_{1999} - C_{2002}) / (V_{1999} - V_{2002}) + (C_{2000} - C_{2001}) / (V_{2000} - V_{2001}) + (C_{2000} - C_{2002}) / (V_{2000} - V_{2002}) + (C_{2001} - C_{2002}) / (V_{2001} - V_{2002})] / 6$$

where C_x and V_x are the CBP and VIMS dataset anomalies respectively, for year *x* from the overlapping years 1999-2002. Each year's anomaly in the VIMS dataset (V_x) was then multiplied by *R* to obtain an adjusted VIMS dataset (AV_x) that had the same relative magnitude anomalies as the CBP dataset:

$$AV_x = R * V_x$$

We then calculated the average difference (*S*) between the datasets *AV* and *C* for each of the four overlapping years as follows:

$$S = [(AV_{1999} - C_{1999}) + (AV_{2000} - C_{2000}) + (AV_{2001} - C_{2001}) + (AV_{2002} - C_{2002})] / 4$$

This average difference *S* was then subtracted from each year in the dataset *AV* to obtain the final adjusted VIMS abundance anomaly for each year *x* (FA_x):

$$FA_x = AV_x - S$$

Overlapping years (1999-2002) were then calculated as an average of the original CBP dataset (*C*) and the new standardized VIMS dataset (*FA*). We acknowledge that the low number of overlapping years (4) may contribute to error in this calculation.

3. RESULTS

3.1 Habitat preference

Both salinity and temperature affect the distributions of all GZ taxa studied in both time series, with temperature controlling temporal distribution on a seasonal basis and salinity controlling spatial distribution within a season.

3.2 Salinity

For *C. quinquecirrha*, peak biovolume occurs at a salinity of 16.4 and peak presence at 16.2 in the VIMS dataset (Fig. 3A, 4B) for the lower portion of Chesapeake Bay, while peak scyphozoan biovolume (primarily *C. quinquecirrha*) occurs at a lower salinity of 11.3 (Fig. 3C) in the CBP dataset for the upper Bay. Even though peak salinity is different between datasets, biovolume is very low for both at salinities less than 6 (Fig. 3A, 3C). This trend between biovolume and salinity is significant for February, March, and June-October, and salinity explains presence of *C. quinquecirrha* most strongly in summer (June-August; Fig. 5). The weighted center of population for *C. quinquecirrha* was significantly farther downstream in both the York and Rappahannock Rivers in summer during years with higher streamflow (Pearson's Correlation Coefficient = 0.511, $p < 0.001$) (Figure 6).

M. leidyi biovolume in the CBP dataset is highest at salinities of 6-17, but below a salinity of 5 there is a sharp decrease in biovolume (Fig. 7A). Very low salinities were not sampled in the VIMS survey, and ctenophore presence (primarily *M. leidyi*) decreases linearly with increasing salinity from 4 to 26 (Fig. 4C). Percent presence of both the medusae *A. aurita* and *C. capillata* peaked at intermediate salinity ranges, but the

relationship was stronger for *A. aurita* (peaking at 20.0, Figure 3D) than for *C. capillata* (peaking at 15.4, Figure 3E). *R. verrilli* presence increases linearly with salinity up to the highest salinities sampled (~25, Fig. 3F).

3.3 Temperature

C. quinquecirrha presence and biovolume (Fig. 3B, 8B) both increased exponentially with temperature above ~15-16 °C. Temperature has a greater effect on *C. quinquecirrha* biovolume than presence, and has no significant ($p > 0.05$) control on presence distribution within any particular month. Ctenophores are present at all temperatures, and percent presence increases linearly with increasing temperature (Fig. 8C). *M. leidyi* biovolume increases exponentially with temperature, with a sharp increase above ~18 °C (Fig. 7B). *A. aurita* presence increases exponentially with temperature and was almost excluded from temperatures below ~13 °C (Fig. 8D). Conversely, *C. capillata* is only present in temperatures < 21 °C, and percent presence is highest at temperatures lower than ~15 °C (Figure 8E). Temperature has only a very weak effect on *R. verrilli* presence, and it is absent only from the highest temperatures (>27 °C, Fig. 8F).

3.4 Seasonality

There are considerable seasonal changes in total GZ biovolume as well as presence of all GZ taxa in the lower Bay (VIMS dataset, Fig. 9). Total GZ biovolume begins to increase in April, peaks in June/July, and decreases until November, after which winter biovolume remains low through March (Fig. 9A). *C. quinquecirrha* is present in the lower Bay year-round, but is most frequently found from July-September (Figure 9B). This pattern in seasonality in presence corresponds well with the upper Bay (CBP dataset,

Figure 10A) where scyphozoan biovolume is highest in July and August, decreases September-November, and remains low December-June (Fig. 10B). Ctenophores (primarily *M. leidyi*) are also present year-round, and peak in percent presence in May and June in the lower Chesapeake Bay (Figure 9C) and June-September in the upper Chesapeake Bay (Figure 10C). *M. leidyi* biovolume increases sharply in June in the upper Chesapeake Bay, and then decreases steadily throughout the summer and fall until November (Figure 10D). *A. aurita* is present in the lower Bay from August to November (Figure 9D), *C. capillata* from December to May (Figure 9E), and *R. verrilli* from September to December (Figure 9F). Hydrozoan medusae are most often present in the upper Bay from May to November (Figure 10E), with higher biovolume in May through July (Figure 10F).

3.5 Changes in seasonality

On average, total GZ biovolume (primarily comprised of *C. quinquecirrha*) peaks on Julian day 186 ±12 (July 5) in the lower Bay (VIMS dataset, 2000-2011). The day of peak biomass shifted to later in the year over the course of the time series (Figure 11A). Additionally, the magnitude of this bloom decreased over the course of the time series (Figure 11B). However, the magnitude of the bloom is not dependent on the timing of the peak, and these two trends do not significantly co-vary ($p = 0.57$). The timing of the bloom is significantly and negatively correlated with bottom dissolved oxygen (DO) concentrations in June (Figure 11C), but DO concentrations do not affect the magnitude of the calculated peak total GZ biovolume, which is instead negatively correlated with the June temperature anomaly (Fig. 11D). No change in timing or magnitude of the peak scyphozoan medusae or *M. leidyi* bloom is present in the upper Chesapeake Bay.

3.6 Effects of hypoxia on GZ

When hypoxic conditions are present (dissolved O_2 < 3.0 mg/L), median total GZ biovolume in the lower Chesapeake Bay is significantly reduced during both June and July, but not August and September (Fig. 12). Similarly, higher DO is correlated with higher GZ biovolume, and GZ biovolume anomaly in June is positively correlated with June DO anomaly from 1999-2011 (Pearson's correlation = 0.558, p = 0.048), and the same positive relationship between DO anomaly and scyphozoan medusae anomaly is present in the upper Bay in July (CBP dataset, Pearson's correlation = 0.592, p = 0.008). However, this relationship reverses later in the summer, with total GZ biovolume anomaly for both August (Pearson's correlation = -0.574, p = 0.040) and September (Pearson's correlation = -0.650, p = 0.016) negatively correlated with July DO anomaly in the lower Bay.

3.7 Long-term changes

Annual summer to early fall (June-October) biovolume anomaly of scyphozoan medusae decreased over the long term in the upper Bay (1985-2002, CBP dataset) and was accompanied by a corresponding increase in *M. leidyi* biovolume anomaly and decrease in copepod abundance anomaly (Fig. 13). Similarly there was a long-term decrease in June-October total GZ biovolume (primarily *C. quinquecirrha*) in the lower Bay from 1999-2011, and this decrease was strongest in June. The standardized, combined upper and lower Bay datasets (see Methods) show a significant decrease over the combined time series in scyphozoan/total GZ biovolume from 1985-2011 is evident (Fig. 14).

These long-term changes in biovolume are correlated with changes in several environmental drivers. Summer to early fall total GZ biovolume in the lower Bay (1999-2011) is most highly correlated with changes in bottom salinity over the same time period (Fig. 15A). However, as the summer progresses, environmental influence on GZ biovolume changes. May total GZ biovolume anomaly was negatively correlated with streamflow (Pearson's correlation = -0.588, $p = 0.047$) and June total GZ biovolume anomaly was positively correlated with salinity (Fig. 15B), while GZ biovolume in August and September were most strongly and negatively correlated with a 2-month lag in bottom DO (Fig. 15C, Fig. 15D respectively). June total GZ biovolume was also positively correlated with June NAO (0.710, $p = 0.007$), but NAO (including lagged winter NAO, as found in Purcell & Decker, 2005) was not correlated with biovolume overall for any other month.

In the upper Bay, summer scyphozoan medusae biovolume was weakly negatively correlated with chlorophyll *a* (Pearson's correlation = -0.217, $p = 0.025$), and positively with bottom DO in July only (Pearson's correlation = 0.737, $p < 0.001$). Summer *M. leidyi* biovolume anomaly was more closely, and negatively, correlated with scyphozoan anomaly (Pearson's correlation = -0.240, $p = 0.013$) than any physical environmental driver. Hydrozoan medusae summer anomaly was positively correlated with both bottom DO and salinity (Pearson's correlation = 0.243, $p = 0.019$; Pearson's correlation = 0.222, $p = 0.032$, respectively).

4. DISCUSSION

4.1 Effects of salinity

The distribution of *C. quinquecirrha* medusae in Chesapeake Bay is primarily controlled by salinity during the summer months when their biovolume is highest. While *C. quinquecirrha* were present in Chesapeake Bay across a wide range of salinities (3.5 – 25), their biovolume approached zero below a salinity of 7. This lower salinity limit for *C. quinquecirrha* is likely due to their death at salinities below 5 (Wright & Purcell, 1997). *C. quinquecirrha* biovolume and presence also decreased at higher salinities, although not to the same extent as at lower salinities, as *C. quinquecirrha* was still present in 18% of the tows at the highest salinity sampled (25). The range in salinity in which peak biovolume occurred differed between upper and lower regions of the Bay (9 – 15 in the upper Bay and 12.5 – 19.5 in the lower Bay). This range in peak biovolume for the upper Bay is consistent with results from a prior study in the mainstem of both the upper and lower Bay that found the highest concentrations of *C. quinquecirrha* at salinities of 10 – 16, and peak presence at 13.5 (Decker et al., 2007). However, we found peak *C. quinquecirrha* biovolume in the lower Chesapeake Bay occupied higher salinities than previously reported.

Salinity further limits *C. quinquecirrha* distribution by affecting the benthic scyphistomae. While Decker et al. (2007) suggested that *C. quinquecirrha* medusae vertically migrate in tidal streams to remain in preferred salinities, a recent study of fine-scale distribution of *C. quinquecirrha* (Breitburg & Burrell, 2014) found no evidence for selective tidal stream transport. Thus, we posit that medusae distribution is a secondary

result of benthic scyphistomae habitat selection and estuarine water circulation patterns. Scyphistomae are limited to salinities of 7 – 25 (Cargo & Schultz, 1966 and 1967), and strobilation is highest at salinities of 11 – 25 (Purcell et al., 1999). It is likely that after ephyrae are produced at optimum salinities of ~10 – 20, they grow and disperse randomly through physical forcing throughout the Bay. We posit that while ephyrae die if they reach salinities below 5, they survive but are widely dispersed at higher salinities in the lower mainstem of Chesapeake Bay. This is supported by the seasonal effect of salinity on *C. quinquecirrha* presence. Salinity exerts the strongest influence on *C. quinquecirrha* medusae presence in early summer (June and July) immediately after strobilation, but this effect weakens with each passing month (August through October) and disappears in the overwintering population of medusae. In addition to reducing salinity, higher river flow may also cause a faster and greater physical transport of medusae downriver in surface waters.

Salinity also significantly affects interannual variation in summer GZ (primarily *C. quinquecirrha*) biovolume. Both Cargo & King (1990) and Purcell & Decker (2005) found long-term changes in *C. quinquecirrha* abundance to be primarily influenced by differences in spring salinity. While we did find a significant positive effect of salinity on GZ biovolume in the lower Chesapeake Bay, especially in May and June, no effect of salinity on long-term trends in the biovolume of scyphozoan medusae was evident in the upper Bay.

Ctenophore presence was also significantly correlated with salinity. Ctenophores (primarily *M. leidy*) were nearly absent at the lowest salinities (0 – 4), but were most abundant at salinities immediately above that limit (~6 – 12). At salinities above the peak

abundance and presence of *M. leidyi*, both measures of abundance decreased linearly. Although *M. leidyi* egg production increases with salinity (Jaspers et al., 2011), successful reproduction and population increase of ctenophores at higher salinities in Chesapeake Bay are likely limited by the presence of *C. quinquecirrha* during the summer. Not only does *C. quinquecirrha* prey heavily on *M. leidyi*, but non-lethal interactions such as escape from predation also reduce *M. leidyi* fecundity (Purcell & Cowan, 1995). *M. leidyi* are able to tolerate lower salinities (0.1 – 25.6) than *C. quinquecirrha* (Purcell & Decker, 2005; this study), and low salinity zones may act as refugia from predation. If *M. leidyi* population sources are primarily in these low salinity zones, an individual's chance of encountering a *C. quinquecirrha* medusa increases cumulatively as it moves downstream, explaining the salinity distribution of *M. leidyi* we found. As Breitburg & Burrell (2014) also found no evidence for behavioral regulation of spatial distribution in *M. leidy*i, the effect of salinity on *M. leidyi* abundance and presence is likely a secondary effect of the probability of *M. leidyi* encounters with *C. quinquecirrha* medusae.

Aurelia aurita presence was restricted by salinity in a similar pattern to *C. quinquecirrha*, but in a higher range of salinities (~10 – 25). Distribution of *A. aurita* has been little studied in Chesapeake Bay, but *A. aurita* is reported to be well distributed throughout the water column in a variety of other regions (reviewed in Albert, 2011). Both *A. aurita* and *A. labiata* did not use tidally synchronized vertical migration to regulate their distribution within the Wadden Sea (van der Veer & Oorthuysen, 1985) or Roscoe Bay (Albert, 2010). If *A. aurita* in Chesapeake Bay are not using tidal circulation to control their location, then we suggest *A. aurita* distribution, like that of *C.*

quinquecirrha, is a secondary effect of scyphistomae reproduction. We posit that scyphistomae are present in a narrow salinity range (~18 – 23), and distribution outside of this range is governed randomly by estuarine circulation. Salinity had a weaker influence on *C. capillata* presence, and while medusae were present at all salinities sampled (3.5 – 25), there was a peak in percent presence at salinities of 11 – 19. This is consistent with observations that *C. capillata* reproduces at estuarine salinities down to 12 (Holst & Jarms, 2010). Unlike the other scyphomedusae, *R. verrilli* had the highest percent presence at the highest sampled salinities; their presence decreased linearly with decreasing salinity and this species was virtually absent below salinities of 12. This pattern strongly suggests that *R. verrilli* reproduce outside of Chesapeake Bay and are advected into the Bay from the Atlantic Ocean, most likely from the south (Harper & Runnels, 1990).

4.2 Effects of temperature

While salinity controls *C. quinquecirrha*, *A. aurita*, and *C. capillata* spatial distributions, temperature controls their biovolume and frequency of presence seasonally. *C. quinquecirrha* biovolume increased exponentially above 15 °C in both the upper and lower regions of the Bay, as scyphistomae began spring strobilation at approximately that temperature (Cargo & Schultz, 1966; Purcell et al., 1999). This control of temperature on *C. quinquecirrha* biovolume is strictly a seasonal phenomenon, as temperature had no effect on the distribution of biovolume after removing the seasonal trend. While percent presence of *C. quinquecirrha* also increased above 15 °C, medusae were commonly present throughout the year and at temperatures as low as 1.5 °C**.** This result contrasts with previous reports that medusae die off at the end of the summer (Cargo & King,

1990; Decker et al., 2007) or at temperatures below 10 °C (Gatz et al., 1973). *C. quinquecirrha* medusae pulsation rate is linearly related to temperature, and is too slow to counteract their negative buoyancy below 15 °C (Gatz et al., 1973; Sexton et al., 2010). While this temperature-induced drop in pulsation rate causes *C. quinquecirrha* to disappear from surface waters during the winter, our data suggest they are present near the bottom during these months. Because the VIMS survey samples using a benthic trawl, it collects these 'hibernating' medusae at temperatures below 15 °C. These medusae are caught in good condition (Lowery, pers. comm.), and do occasionally pulse, albeit infrequently. While the majority of medusae likely die in the winter due to dropping temperatures or starvation, as evidenced by the significant drop in biovolume below 15 °C, some individuals do survive and are present throughout the winter months.

Ctenophore percent presence (primarily *M. leidyi*) increased linearly with temperature, and *M. leidyi* biovolume was significantly higher at temperatures above 18 °C. This was expected as *M. leidyi* reproduction is controlled by a combination of temperature and food availability (reviewed in Kremer, 1994). The rapid increase in *M. leidyi* percent presence and biovolume in June is followed by a steady decrease in biovolume, but not percent presence, throughout the summer and fall. This decrease in biovolume is most likely due to predation by *C. quinquecirrha*, which typically blooms one month later in July, and can effectively control *M. leidyi* populations (Purcell & Decker, 2005; Condon & Steinberg, 2008; Breitburg & Burrell, 2014).

Temperature has opposing effects on *A. aurita* and *C. capillata* presence; percent presence of *A. aurita* increases while *C. capillata* decreases exponentially with temperature. *A. aurita* is only present in Chesapeake waters July – November, and *C.*

capillata is present December – May. As with *C. quinquecirrha*, temperature controls their populations by influencing the timing and intensity of strobilation by the scyphistomae. The timing of *A. aurita* blooms is affected by both light and temperature (Liu et al., 2009), but temperature can be negatively or positively correlated with strobilation depending on the region, suggesting that *A. aurita* populations are locally adapted to time their production of medusae with peak zooplankton biomass (Han & Uye, 2010; Purcell et al., 2012; Wang et al., 2015; Sokolowski et al., 2016). However, peak *A. aurita* presence in Chesapeake Bay appears after the peak zooplankton bloom. This may be an adaptation to avoid competition with *C. quinquecirrha* by blooming two months later. In contrast, *C. capillata* only begins strobilation at temperatures below 15 °C (Cargo & Schultz, 1967) explaining the seasonality in its presence in Chesapeake Bay. Temperature has only a weak effect on *R. verrilli* presence, although it is absent in the lower Bay in July and August during the highest water temperatures.

4.3 Effects of dissolved oxygen

Because the VIMS survey preferentially samples bottom waters, avoidance of low DO waters by *C. quinquecirrha* may contribute to reduced catches of scyphozoan medusae in hypoxic conditions. However, this is not likely the case as lower biovolumes in hypoxic conditions were only observed in June and July but not in August and September (Fig. 12), supporting our interpretation that low DO conditions do not cause a sampling bias and do have an effect on population growth. While both *C. quinquecirrha* medusae and *M. leidyi* can survive DO concentrations as low as 0.5 mg L^{-1} (Breitburg et al., 2003), polyp survival and asexual reproduction of *C. quinquecirrha* are reduced at concentrations of 3.5 mg L^{-1} and below (Condon et al., 2001), and *M. leidyi* growth and

reproduction are also decreased by reduced DO concentration (Grove & Breitburg, 2005). However, while *C. quinquecirrha* medusae and *M. leidyi* ctenophores are able to regulate their depth in the water column to avoid low DO levels (Breitburg et al., 2003), benthic polyps are unable to escape low oxygen conditions. In our analysis, bottom DO concentrations had a significant effect on the timing of the summer GZ bloom (primarily *C. quinquecirrha*), with lower DO concentrations during the strobilation period delaying the onset of the bloom (Fig. 11B). Spring and summer DO concentrations did not have an effect on the overall GZ biovolume, but low DO concentrations in May and June were negatively correlated with August and September GZ biovolume. This suggests that while hypoxic conditions can suppress strobilation, it still occurs, albeit at a lower rate, and overall biovolume of *C. quinquecirrha* is not affected by the later strobilation.

4.4 Long-term trends

We observed declines in summer total GZ biovolume from 1984 – 2012, in scyphozoan medusae biovolume in the upper Chesapeake Bay from 1984 – 2002 and in total GZ biovolume in the lower Bay from 1999 – 2012. These declines are largely due to a decrease in *C. quinquecirrha* medusae, as this species accounts for the majority of summer biovolume in both time series. A previous study which utilized three GZ datasets, one of visual counts in surface waters from a pier at a single location, and two using a 1 m^{-2} Tucker trawl at various sites in the Patuxent River and mainstem Chesapeake Bay, also found a decline in *C. quinquecirrha* medusae in the upper Chesapeake from 1960 – 2005 (Breitburg & Fulford, 2006). This decline began in the mid-1980s, which was attributed to the concurrent rapid decline in oyster (*Crassostrea virginica*) populations. Oyster shells are the primary substrate for the *C. quinquecirrha*

scyphistomae, and polyps have a higher abundance on oyster shells than other natural and artificial substrates (Cones & Haven, 1969). It was suggested that the greatly reduced population of Chesapeake oysters after the mid-1980s greatly reduced the habitat availability for scyphistomae (Breitburg & Fulford, 2006). Our time series began in 1984, after the observed population reduction in oysters and *C. quinquecirrha*. While we observe a decrease in *C. quinquecirrha* populations since 1984, oyster populations have remained stable or increased in Chesapeake Bay over the same time period (Tarnowski, 2015; Southworth & Mann, 2016). Thus, the continued decline in *C. quinquecirrha* after the 1980s is likely not due to changes in oyster populations.

What then is causing the long-term decrease in *C. quinquecirrha*? The overall decrease in medusae can be attributed to factors affecting the scyphistomae and strobilation, but the environmental factors that affect these processes each have different thresholds of influence, and what may affect *C. quinquecirrha* populations one year may not the following year. Long-term changes in *C. quinquecirrha* biovolume are clearly correlated with changes in environmental conditions. Both Cargo & King (1990) and Purcell & Decker (2005) found inter-annual variability in *C. quinquecirrha* populations linked with changes in salinity and temperature, and negatively correlated with changes in NAO. We found a similar positive correlation between summer total GZ biovolume and salinity, but temperature was only weakly positively correlated with June peak biovolume (Fig. 11D). NAO was only correlated with GZ biovolume for one month – June – and it was a positive correlation, opposite to what Purcell & Decker (2005) reported. We found the interplay between environmental drivers and *C. quinquecirrha* populations is complex, with salinity driving overall abundance, low DO delaying onset

of the summer GZ bloom, and temperature windows restricting the period of bloom initiation. Additionally, temperature has an interactive effect with DO, with higher temperatures lowering DO solubility and causing higher metabolic demand. These numerous drivers of *C. quinquecirrha* abundance, coupled with previously observed effects of oyster abundance (Breitburg & Fulford, 2006), and NAO (Purcell & Decker, 2005), make it difficult to attribute the overall decrease in *C. quinquecirrha* populations to one environmental factor.

Global climate change is predicted to have a variety of wide-ranging effects on the Chesapeake Bay region (reviewed in Najjar et al., 2010; Rice & Jastram, 2015), and a number of these changes could lead to a continued decline in *C. quinquecirrha*. Increases in June water temperature could further decrease the magnitude of the peak biovolume. January-May streamflow is predicted to increase, causing decreases in spring salinity (Najjar et al., 2010) and increases in hypoxia (Hagy et al., 2004). While the volume of hypoxic waters in early summer has been increasing over the last 60 years, late summer hypoxia has been slightly decreasing, effectively shifting the hypoxic period earlier in the year (Murphy et al., 2011). Although we did not observe any effect of hypoxia on overall GZ biovolume, early summer hypoxia did delay bloom formation. It may be that future increases in early summer hypoxia, and further shifting of hypoxic events earlier into the year, will delay *C. quinquecirrha* blooms past a point when they can achieve their current population levels, causing further reductions in *C. quinquecirrha*.

Regardless of the causes of decreasing *C. quinquecirrha* abundance, the effects of this decrease on the rest of the Chesapeake Bay food web are clear. *C. quinquecirrha* are the primary controller of *M. leidyi* populations (Purcell & Cowan, 1995; Condon &

Steinberg, 2008; Crum et al., 2014; this study), while increases in *M. leidyi* reduce copepod abundances throughout the Chesapeake Bay (Kimmel & Roman, 2004; Purcell & Decker, 2005; this study). Additionally, decreases in *C. quinquecirrha* populations, starting in the late 1980s, led to increases in *M. leidyi* and decreases in copepod abundances in the central portion of the Chesapeake Bay (Kimmel et al., 2012). Further decreases in *C. quinquecirrha* populations may release *M. leidyi* from predation pressure throughout the summer, depleting copepod populations. Copepods are particularly important for commercial finfish, representing the major pathway for transfer of carbon from phytoplankton to finfish, especially through the bay anchovy (*Anchoa mitchilli*), an abundant, zooplanktivorous fish that is a major prey item for higher trophic level species (Kimmel et al., 2012). Thus, cascading effects down the food web caused by changes in GZ abundance are potentially as disastrous as those seen in the Caspian and Black Seas (reviewed in Costello et al., 2012), where the introduction of *M. leidyi* caused commercial fisheries collapses through increased competition with finfish for crustacean zooplankton prey and direct predation on ichthyoplankton (Oguz et al., 2008; Roohi et al., 2010). However, in Chesapeake Bay, decreases in bottom DO may partition *M. leidyi* from their prey and ameliorate the predation impact (Kolesar et al., 2010).

5. SUMMARY AND CONCLUSION

Analysis of multi-decadal datasets indicates that GZ populations in the Chesapeake Bay vary on a seasonal and interannual timescale largely as a result of patterns in salinity and temperature. The most abundant summer species, *C. quinquecirrha*, is present year-round, but is most abundant in the summer when temperatures exceed 20 °C and salinities range from 10 – 20. Other species also vary seasonally, with *A. aurita* present July – November, *C. capillata* December – May, and *M. leidyi* with highest biovolumes June – August. The presence and distribution of the three scyphozoan medusa species is regulated by the temperature and salinity tolerances of their benthic scyphistomae, with distribution of the medusae radiating from the asexual reproduction hotspots. Overall *C. quinquecirrha* biovolumes are positively correlated with spring salinities, and low DO concentrations during the spring reduce early summer biovolume and delay the onset of the summer bloom. *M. leidyi* biovolume and distribution is primarily controlled by predation by *C. quinquecirrha*, and increases in *M. leidyi* decrease the abundances of their primary prey, copepods. Total *C. quinquecirrha* biovolume has been decreasing from 1984 – 2012, and these decreases have led to a long-term increase in *M. leidyi* and decrease in copepods. Further decreases in *C. quinquecirrha* populations, due to future increases in spring streamflow and increases in early summer hypoxia, could continue to release top-down control of *M. leidyi*, reducing copepod abundances and increasing competition with commercially important finfish for copepod prey in the Chesapeake Bay.

Acknowledgments

We are grateful to the numerous technicians and crew of the Virginia Institute of Marine Science Juvenile Trawl Survey and Chesapeake Bay Program Mesozooplankton Survey for the many years of tireless sampling. Special thanks to Mary Fabrizio, Troy Tuckey, and Wendy Lowery for assistance with analysis of the VIMS Trawl Survey data. This research was funded by Virginia Sea Grant (V718500) to D.K.S. and J.P.S., and grants from the Virginia Resources Commission, Virginia Recreational Fishing Advisory Board, and NOAA-Chesapeake Bay Office to Mary C. Fabrizio

References

Albert DJ (2010) Vertical distribution of *Aurelia labiata* (Scyphozoa) jellyfish in Roscoe Bay is similar during flood and ebb tides. J Sea Res 64: 422-425

Albert DJ (2011) What's on the mind of a jellyfish? A review of behavioural observations on *Aurelia* sp. jellyfish. Neuroscience Biobehavioral Rev 35: 474-482

Breitburg DL, Adamack A, Rose KA, Kolesar SE, Decker MB, Purcell JE, Keister JE, Cowan Jr. JH (2003) The pattern and influence of low dissolved oxygen in the River, a seasonally hypoxic estuary. Estuaries 26(2A): 280-297

Breitburg D, Burrell R (2014) Predator-mediated landscape structure: seasonal patterns of spatial expansion and prey control by *Chrysaora quinquecirrha* and *Mnemiopsis leidyi*. Mar Ecol Prog Ser 510: 183-200

Breitburg DL, Fulford RS (2006) Oyster-sea nettle interdependence and altered control within the Chesapeake Bay ecosystem. Estuaries Coasts 29(5): 776-784

Brotz L, Cheung WWL, Kleisner K, Pakhomov E, Pauly D (2012) Increasing jellyfish populations: trends in Large Marine Ecosystems. Hydrobiologia 690: 3-20

Cargo DG, King DR (1990) Forecasting the abundance of the sea nettle, *Chrysaora quinquecirrha*, in the Chesapeake Bay. Estuaries 13(4): 486-491

Cargo DG, Schultz LP (1966) Notes on the biology of the sea nettle, *Chrysaora quinquecirrha*, in Chesapeake Bay. Chesapeake Sci 7: 95–100

Cargo DG, Schultz LP (1967) Further observations on the biology of the sea nettle and jellyfishes in Chesapeake Bay. Ches Science 8(4): 209-220

Condon RH, Decker MB, Purcell JE (2001) Effects of low dissolved oxygen on survival

and asexual reproduction of scyphozoan polyps (*Chrysaora quinquecirrha*). Hydrobiologia 451: 89-95

Condon RH, Duarte CM, Pitt KA, Robinson KL, Lucas CH, Sutherland KR, Mianzan HW, Bogeberg M, Purcell JE, Decker MB, Uye S, Madin L, Brodeur RD, Haddock SHD, Malej A, Parry GD, Eriksen E, Quiñones J, Acha M, Harvey M, Arthur JM, Graham WM (2013) Recurrent jellyfish blooms are a consequence of global oscillations. PNAS 110(3): 1000-1005

Condon RH, Steinberg DK (2008) Development, biological regulation, and fate of ctenophore blooms in the York River estuary, Chesapeake Bay. Mar Ecol Prog Ser 369: 153-168

Condon RH, Steinberg DK (2009) Zooplankton of the York River. J Coastal Res 57: 66-79

Cones HN, Haven DS (1969) Distribution of *Chrysaora quinquecirrha* in the York river. Chesapeake Sci 10: 75-84

Costello JH, Bayha KM, Mianzan HW, Shiganova TA, Purcell JE (2012) Transitions of *Mnemiopsis leidyi* (Ctenophora: Lobata) from a native to an exotic species: a review. Hydrobiologia 690(1): 21-46

Costello JH, Sullivan BK, Gifford DJ, Van Keuren D, Sullivan LJ (2006) Seasonal refugia, shoreward thermal amplification, and metapopulation dynamics of the ctenophore *Mnemiopsis leidyi* in Narragansett Bay, Rhode Island. Limnol Oceanogr 51(4): 1819-1831

Cowan Jr. JH, Houde ED (1993) Relative predation potentials of scyphomedusae,

ctenophores and planktivorous fish on ichthyoplankton in Chesapeake Bay. Mar Ecol Prog Ser 95: 55-65

Crum KP, Fuchs HL, Bologna PAX, Gaynor JJ (2014) Model-to-data comparisons reveal influence of jellyfish interactions on plankton community dynamics. Mar Ecol Prog Ser 517: 105-119

Decker MB, Brown CW, Hood RR, Purcell JE, Gross TF, Matanoski, Bannon RO, Setzler-Hamilton EM (2007) Predicting the distribution of the scyphomedusa *Chrysaora quinquecirrha* in Chesapeake Bay. Mar Ecol Prog Ser 329: 99-113

Diaz RJ, Rosenberg R (1995) Marine benthic hypoxia: a review of its ecological effects and the behavioral responses of benthic macrofauna. Oceanogr Mar Biol, An Annual Review 33: 245-303

Gatz Jr. AJ, Kennedy VS, Mihursky JA (1973) Effects of temperature on activity and mortality of the scyphozoan medusa, *Chrysaora quinquecirrha*. Chesapeake Sci 14(3): 171-180

Govoni JJ, Olney JE (1991) Potential predation on fish eggs by the lobate ctenophore *Mnemiopsis leidyi* within and outside the Chesapeake Bay plume. Fishery Bull 89: 181-186

Grove M, Breitburg DL (2005) Growth and reproduction of gelatinous zooplankton exposed to low dissolved oxygen. Mar Ecol Prog Ser 301: 185-198

Hagy JD, Boynton WR, Keefe CW, Wood KV (2004) Hypoxia in Chesapeake Bay, 1950–2001: Long-term change in relation to nutrient loading and river flow. Estuaries 27: 634–658

Han C, Uye S (2010) Combined effects of food supply and temperature on asexual

reproduction and somatic growth of polyps of the common jellyfish *Aurelia aurita* s.l. Plankton Benthos Res 5(3): 98-105

Harper DE, Runnels RJ (1990) The occurrence of *Rhopilema verrilli* (Cnidaria: Scyphozoa: Rhizostomeae) on Galveston Island, Texas and a discussion on its distribution in U.S. waters. Northeast Gulf Sci 11(1): 19-27

Holst S, Jarms G (2010) Effects of low salinity on settlement and strobilation of Scyphozoa (Cnidaria): Is the lion's mane *Cyanea capillata* (L.) able to reproduce in the brackish Baltic Sea? Hydrobiologia 645: 53-68

Houde ED, Gamble JC, Dorsey SE, Cowan Jr. JH (1994) Drifting mesocosms: the influence of gelatinous zooplankton on mortality of bay anchovy, *Anchoa mitchilli*, eggs and yolk-sac larvae. ICES J Mar Sci 51: 383-394

Jaspers C, Møller LF, Kiørboe T (2011) Salinity gradient of the Baltic Sea limits the reproduction and population expansion of the newly invaded comb jelly *Mnemiopsis leidyi*. PLoS ONE 6(8): e24065

Kimmel DG, Boynton WR, Roman MR (2012) Long-term decline in the calanoid copepod *Acartia tonsa* in central Chesapeake Bay, USA: An indirect effect of eutrophication?. Estuarine Coastal Shelf Sci 101: 76-85

Kimmel DG, Roman MR (2004) Long-term trends in mesozooplankton abundance in Chesapeake Bay, USA: influence of freshwater input. Mar Ecol Prog Ser 267: 71-83

Kolesar SE, Breitburg DL, Purcell JE, Decker MB (2010) Effects of hypoxia on *Mnemiopsis leidyi*, ichthyoplankton and copepods: clearance rates and vertical habitat overlap. Mar Ecol Prog Ser 411: 173-788

Kremer P (1976) Population dynamics and ecological energetics of a pulsed zooplankton predator, the ctenophore *Mnemiopsis leidyi*. In Wiley, M. L. (ed.), Estuarine Processes. Academic Press, New York 1: 197–215

Kremer P (1994) Patterns of abundance for *Mnemiopsis* in US coastal waters: a comparative overview. ICES J Mar Sci 51: 347-354

Liu W-C, Lo W-T, Purcell J, Chang H-H (2009) Effects of temperature and light intensity on asexual reproduction of the scyphozoan, *Aurelia aurita* (L.) in Taiwan. Hydrobiologia 616: 247-258

Lowery WA, Geer PJ (2000) Juvenile finfish and blue crab stock assessment program bottom trawl survey annual data summary report series. Volume 1999. Virginia Institute of Marine Science Special Scientific Report No. 124. Virginia Institute of Marine Science, Gloucester Point, VA

Melzner F, Thomsen J, Koeve W, Oschlies A, Gutowska MA, Bange HW, Hansen HP, Körtzinger A (2013) Future ocean acidification will be amplified by hypoxia in coastal habitats. Mar Biol 160: 1875-1888

Mills CE (2001) Jellyfish blooms: are populations increasing globally in response to changing ocean conditions? Hydrobiologia 451: 55-68

Murphy RR, Kemp WM, Ball WP (2011) Long-term trends in Chesapeake Bay seasonal hypoxia, stratification, and nutrient loading. Estuaries Coasts 34: 1293-1309

Najjar RG, Pyke CR, Adams MB, Breitburg D, Hershner C, Kemp M, Howarth R, Mulholland MR, Paolisso M, Secor D, Sellner K, Wardrop D, Wood R (2010) Potential climate-change impacts on the Chesapeake Bay. Estuarine Coast Shelf Sci 86: 1-20

Oguz T, Fach B, Salihoglu B (2008) Invasion dynamics of the alien ctenophore *Mnemiopsis leidyi* and its impact on anchovy collapse in the Black Sea. J Plankton Res 30: 1385–1397

Purcell JE (1992) Effects of predation by the scyphomedusan *Chrysaora quinquecirrha* on zooplankton populations in Chesapeake Bay. Mar Ecol Prog Ser 87: 65-76

Purcell JE (2005) Climate effects on formation of jellyfish and ctenophore blooms. J Mar Biol Assoc U.K. 85: 461-476

Purcell JE, Atienza D, Fuentes V, Olariaga A, Tilves U, Colahan C, Gili J-M (2012) Temperature effects on asexual reproduction rates of scyphozoan species from the northwest Mediterranean Sea. Hydrobiologia 690: 169-180

Purcell JE, Cowan Jr. JH (1995) Predation by the scyphomedusan *Chrysaora quinquecirrha* on *Mnemiopsis leidyi* ctenophores. Mar Ecol Prog Ser 128: 63-70

Purcell JE, Cresswell FP, Cargo DG, Kennedy VS (1991) Differential ingestion and digestion of bivalve larvae by the scyphozoan *Chrysaora quinquecirrha* and the ctenophore *Mnemiopsis leidyi*. Biol Bull 180: 103-111

Purcell JE, Decker MB (2005) Effects of climate on relative predation by scyphomedusae and ctenophores on copepods in Chesapeake Bay during 1987-2000. Limnol Oceanogr 50: 376-387

Purcell JE, Shiganova TA, Decker MB, Houde ED (2001) The ctenophore *Mnemiopsis* in native and exotic habitats: U.S. estuaries versus the Black Sea basin. Hydrobiologia 451 (Dev Hydrobiol 155): 145-176

Purcell JE, Uye S, Lo WT (2007) Anthropogenic causes of jellyfish blooms and their direct consequences for humans: a review. Mar Ecol Prog Ser 350: 153–174

Purcell JE, White JR, Nemazie DA, Wright DA (1999) Temperature, salinity and food effects on asexual reproduction and abundance of the scyphozoan *Chrysaora quinquecirrha*. Mar. Ecol. Prog. Ser. 180: 187-196

Purcell JE, White JR, Roman MR (1994). Predation by gelatinous zooplankton and resource limitation as potential controls of *Acartia tonsa* copepod populations in Chesapeake Bay. Limnol Oceanogr 39: 263-278

Reeve MR, Syms MA, Kremer P (1989) Growth dynamics of a ctenophore (*Mnemiopsis*) in relation to variable food supply. I. Carbon biomass, feeding, egg production, growth and assimilation efficiency. J Plankton Res 11: 535–552

Rice KC, Jastram JD (2015) Rising air and stream-water temperatures in Chesapeake Bay region, USA. Climatic Change 128: 127-138

Roohi A, Kideys AE, Sajjadi A, Hashemian A, Pourgholam R, Fazli H, Khanari AG, Eker-Develi E (2010) Changes in biodiversity of phytoplankton, zooplankton, fishes and macrobenthos in the Southern Caspian Sea after the invasion of the ctenophore *Mnemiopsis leidyi*. Biol Invasions 12: 2343-2361

Sexton MA, Hood RR, Sarkodee-adoo J, Liss AM (2010) Response of *Chrysaora quinquecirrha* medusae to low temperature. Hydrobiologia 645: 125-133

Sokolowski A, Brulinska D, Olenycz M, Wolowicz M (2016) Does temperature and salinity limit asexual reproduction of *Aurelia aurita* polyps (Cnidaria: Scyphozoa) in the Gulf of Gdansk (southern Baltic Sea)? An experimental study. Hydrobiologia 773(1): 49-62

Southworth M, Mann R (2016) The status of Virginia's public oyster resource, 2015.

Molluscan Ecology Program, Virginia Institute of Marine Science, Gloucester Point, Virginia. 50 pp

Steinberg DK, Lomas MW, Cope JS (2012) Long-term increase in mesozooplankton biomass in the Sargasso Sea: linkage to climate and implications for food web dynamics and biogeochemical cycling. Global Biogeochem Cycles 26: GB1004

Tarnowski M (2015) Maryland oyster population status report: 2014 fall survey. Maryland Department of Natural Resources Publ. No. 17-782015-769, Annapolis, MD. 68 pp

van der Veer HW, Oorthuysen W (1985) Abundance, growth and food demand of the scyphomedusa *Aurelia aurita* in the western Wadden Sea. Neth J Sea Res 19: 28–44

Wang N, Li C, Liang Y, Shi Y, Lu J (2015) Prey concentration and temperature effect on budding and strobilation of *Aurelia sp.* 1 polyps. Hydrobiologia 754(1): 125-134

Wright DA, Purcell JE (1997) Effect of salinity on ionic shifts in mesohaline scyphomedusae, *Chrysaora quinquecirrha*. Biol Bull 192: 332-339

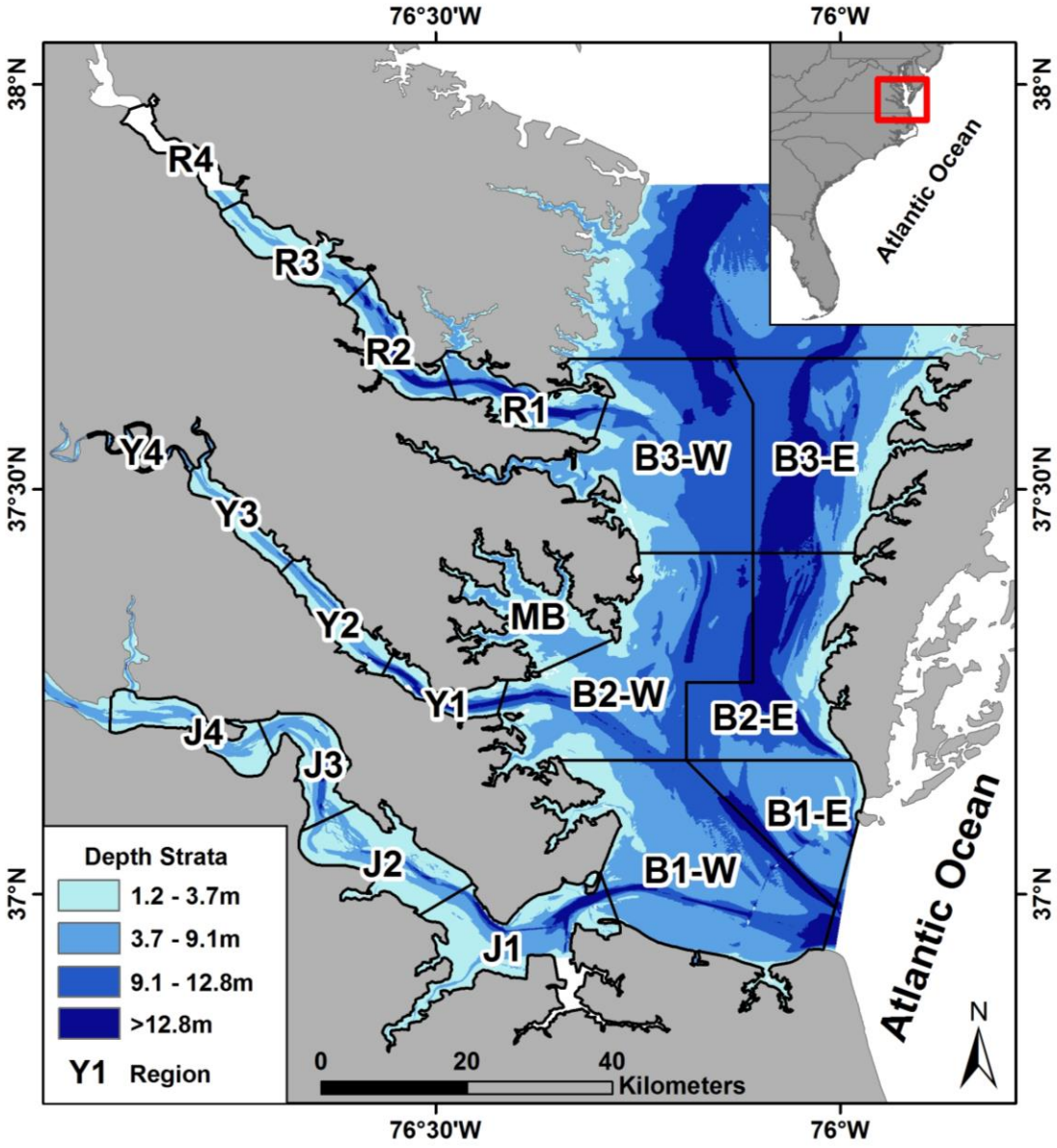

Figure 1: Map of the sampling regions and depth strata for the Virginia Institute of Marine Science Juvenile Fish and Blue Crab Trawl Survey (VIMS survey) in lower Chesapeake Bay. Sampling occurred 2-4 times within each region and strata monthly from 1999-2012, except during January and March.

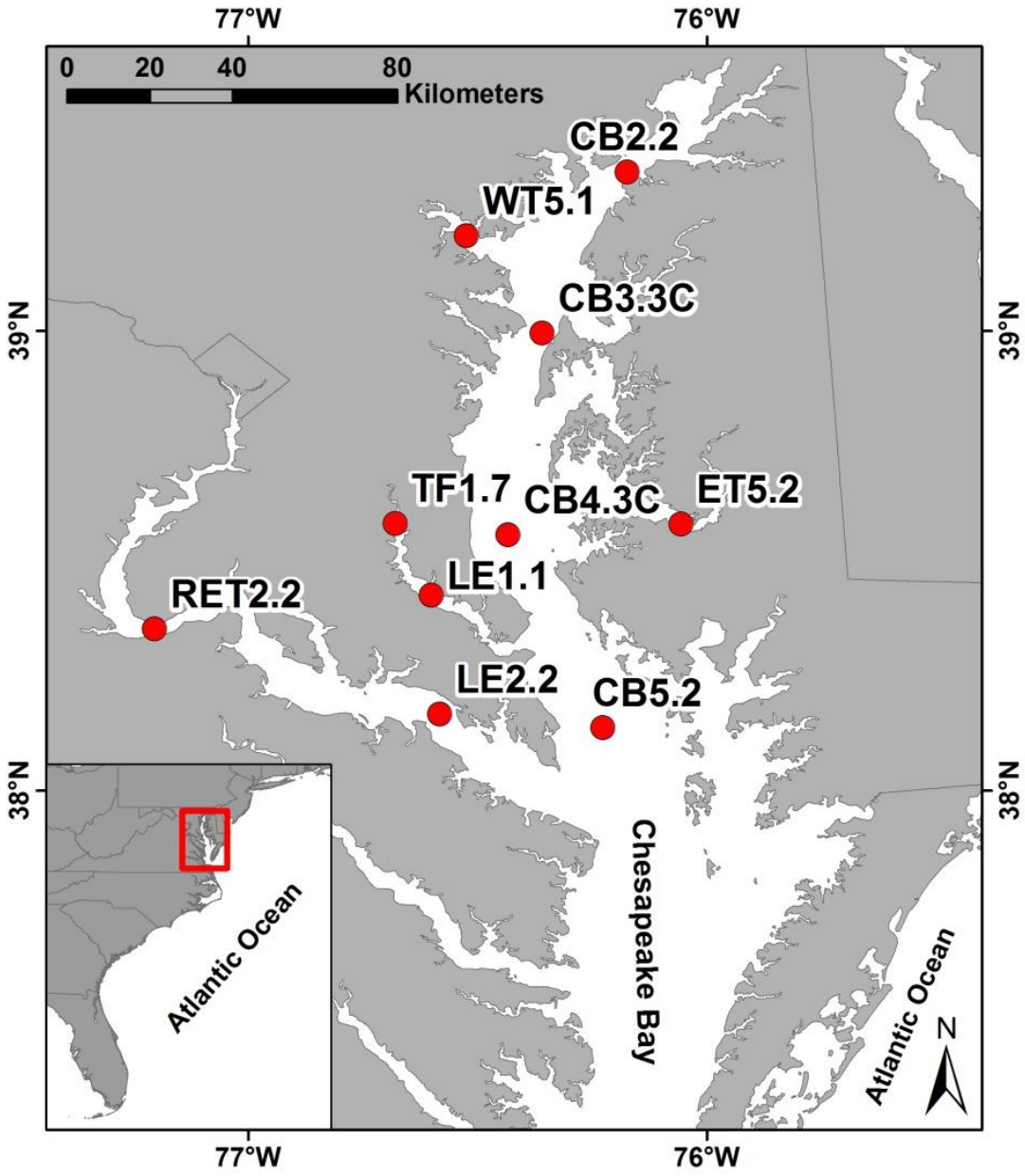

Figure 2: Map of the Chesapeake Bay Program's mesozooplankton monitoring program (CBP survey) stations used in this study to analyze changes in GZ populations in upper Chesapeake Bay. Sampling occurred monthly at each of the ten stations from 1984-1992, and monthly except during January and February from 1993-2002.

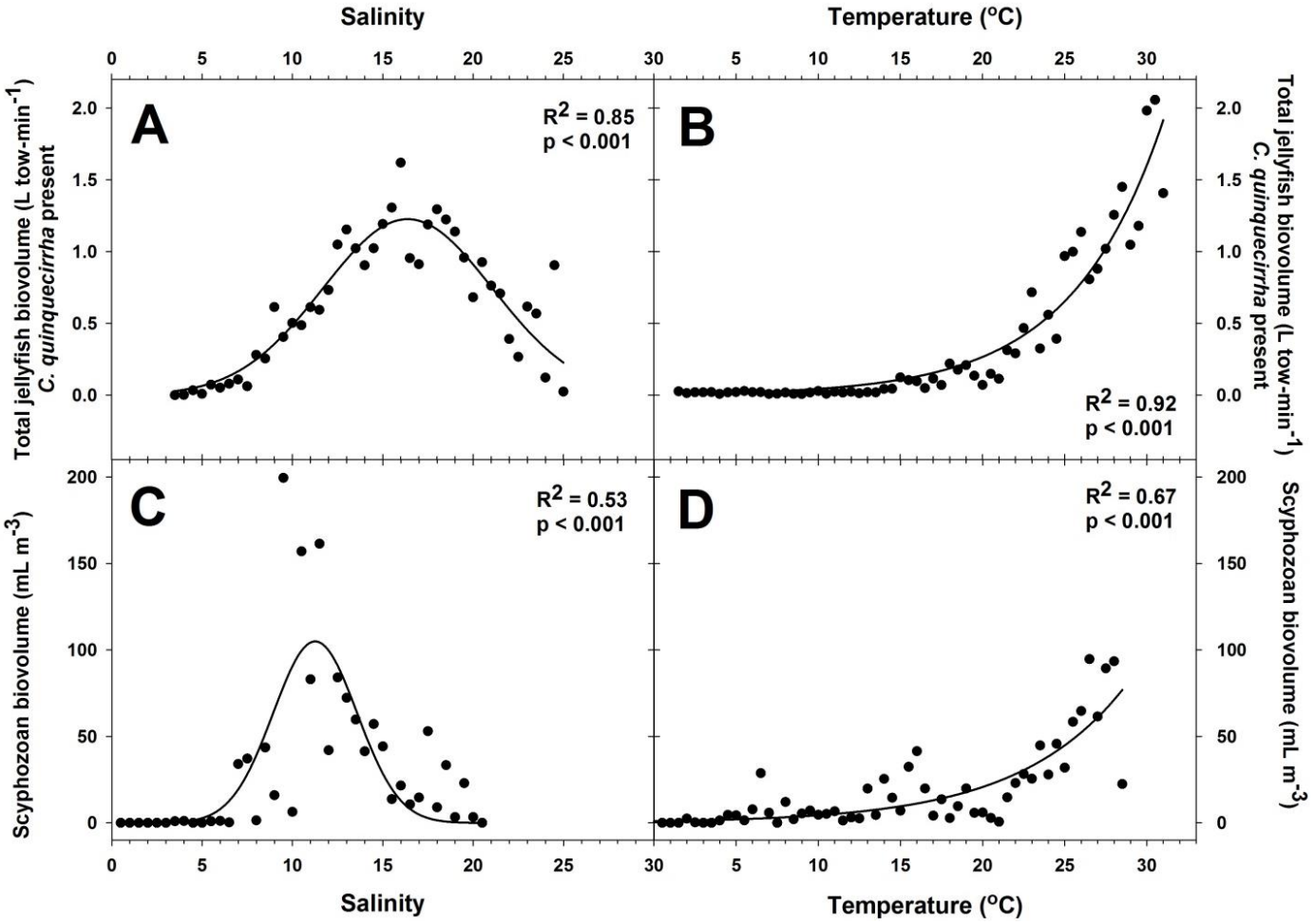

Figure 3: Response of GZ biovolume to salinity and temperature changes averaged in bins of 0.5 units from June-October (A and C) and the entire year (B and D). Panels A) and B) are total GZ biovolume averaged across the VIMS dataset only for samples in which *Chrysaora quinquecirrha* are present (2000-2012, in lower Chesapeake Bay). Panels C) and D) are total scyphozoan medusae biovolume averaged across the entire CBP dataset (1984-2002, in upper Chesapeake Bay).

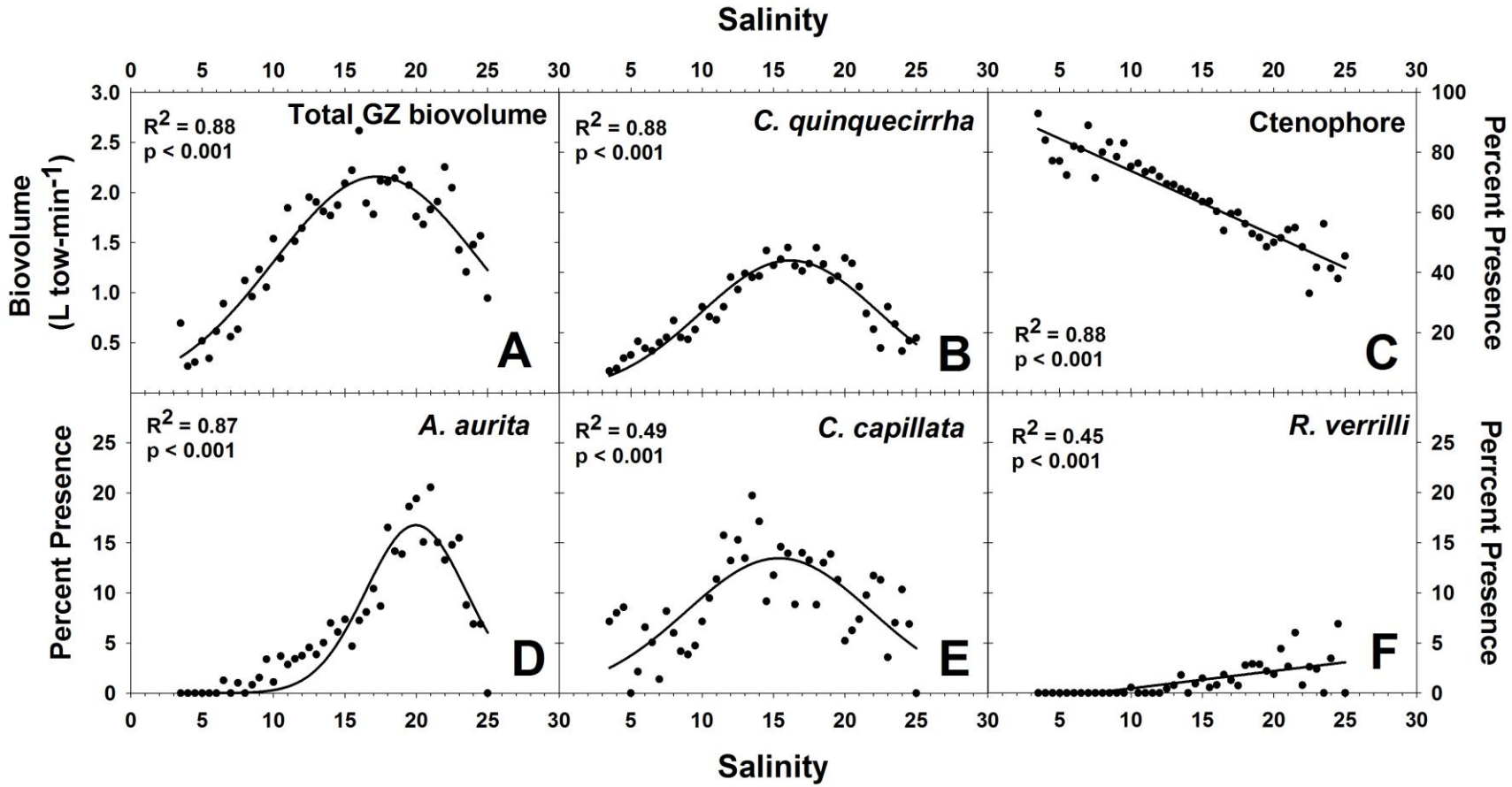

Figure 4: Effect of salinity on total GZ biovolume (A) and percent presence of individual GZ taxa (B-F) averaged across June-October for the VIMS dataset (1999-2012) in lower Chesapeake Bay. 'Percent presence' is the percentage of all tows for each salinity bin that had a particular taxon present. Scyphozoan medusae species are (B*) Chrysaora quinquecirrha*, (D*) Aurelia aurita*, (E*) Cyanea capillata,* and (F*) Rhopilema verilli.*

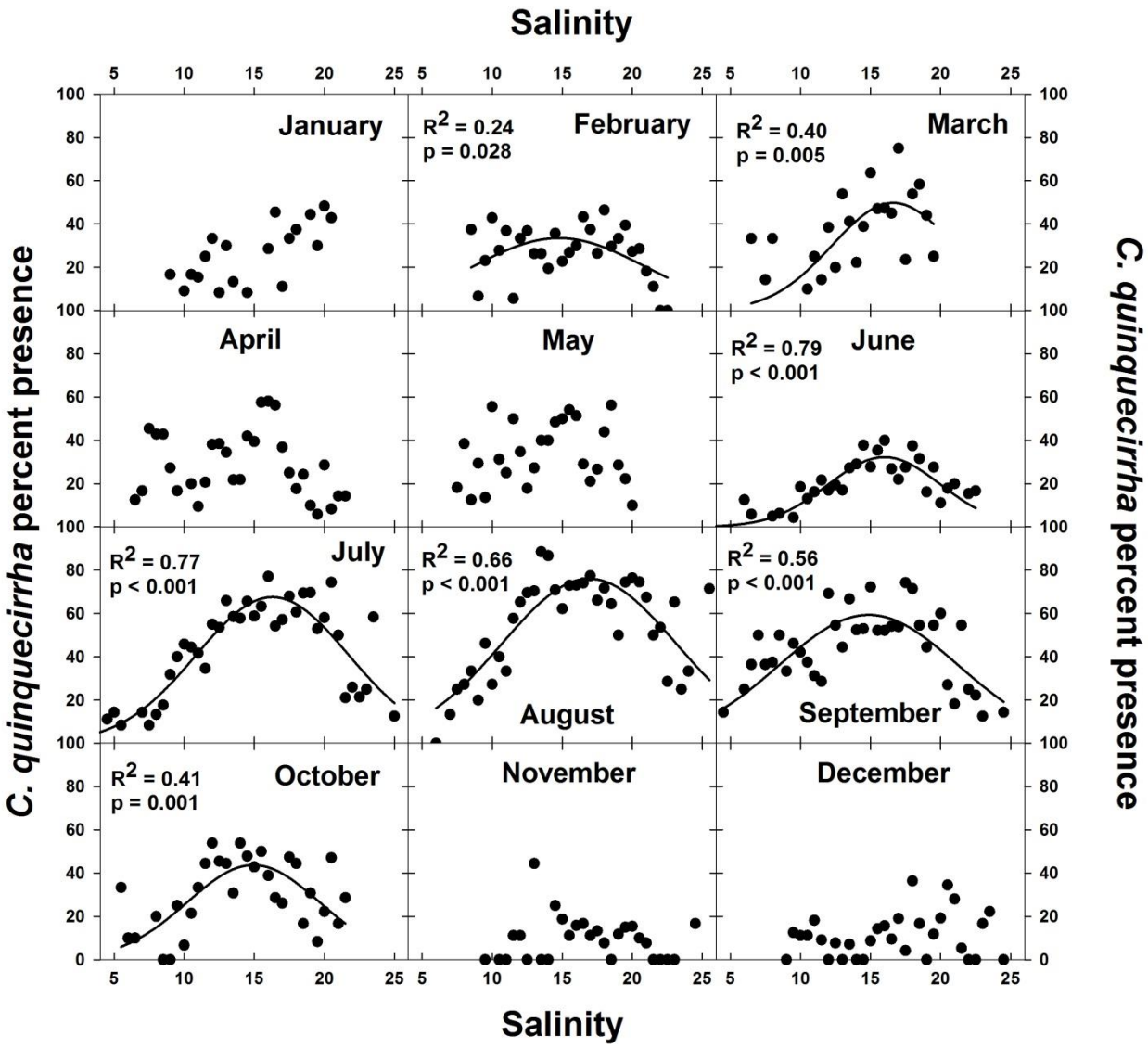

Figure 5: Monthly effect of salinity on *Chrysaora quinquecirrha* presence in lower Chesapeake Bay. Data were averaged for the VIMS dataset (1999-2012) within bins of 0.5 salinity units for each month.

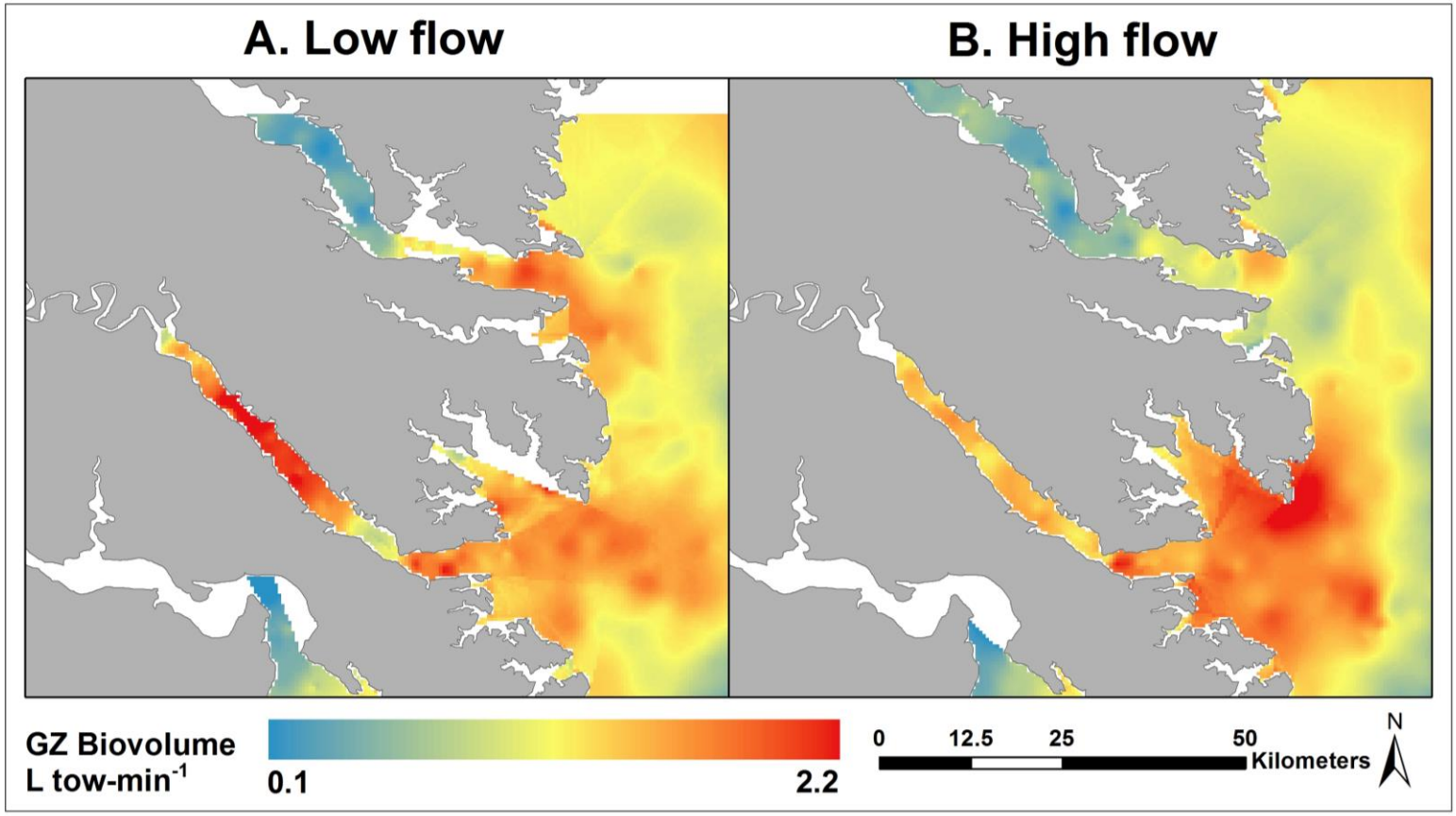

Figure 6: Map of total-GZ biovolume for summers (average of June-August) with A) low James River streamflow (2000-2002, 2005, 2007, and 2010; average 127 m^3 s^{-1}) and B) high James River streamflow (2003, 2004, 2006, 2008, 2009, 2011; average 274 m^3 s^{-1}) . Data are interpolated monthly from the VIMS dataset (2000-2011).

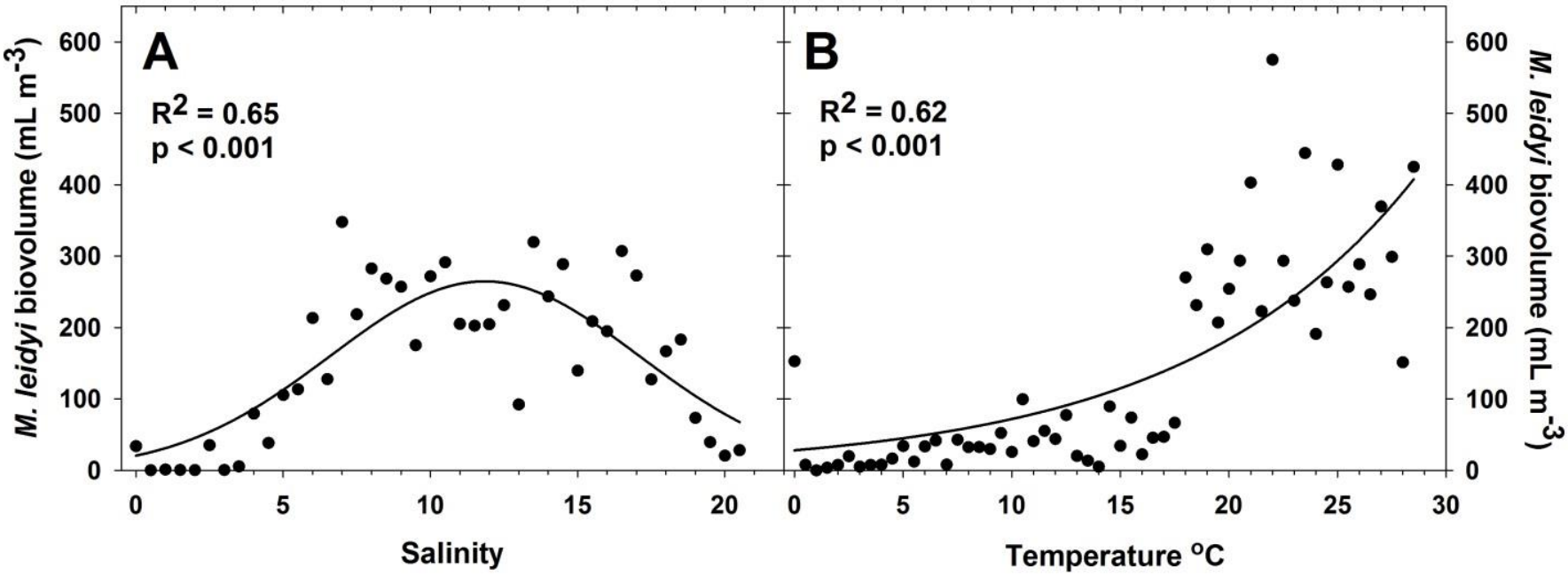

Figure 7: Effect of salinity (A) and temperature (B) on ctenophore *Mnemiopsis leidyi* biovolume averaged across all stations for the entire CBP dataset (1984-2002) in upper Chesapeake Bay.

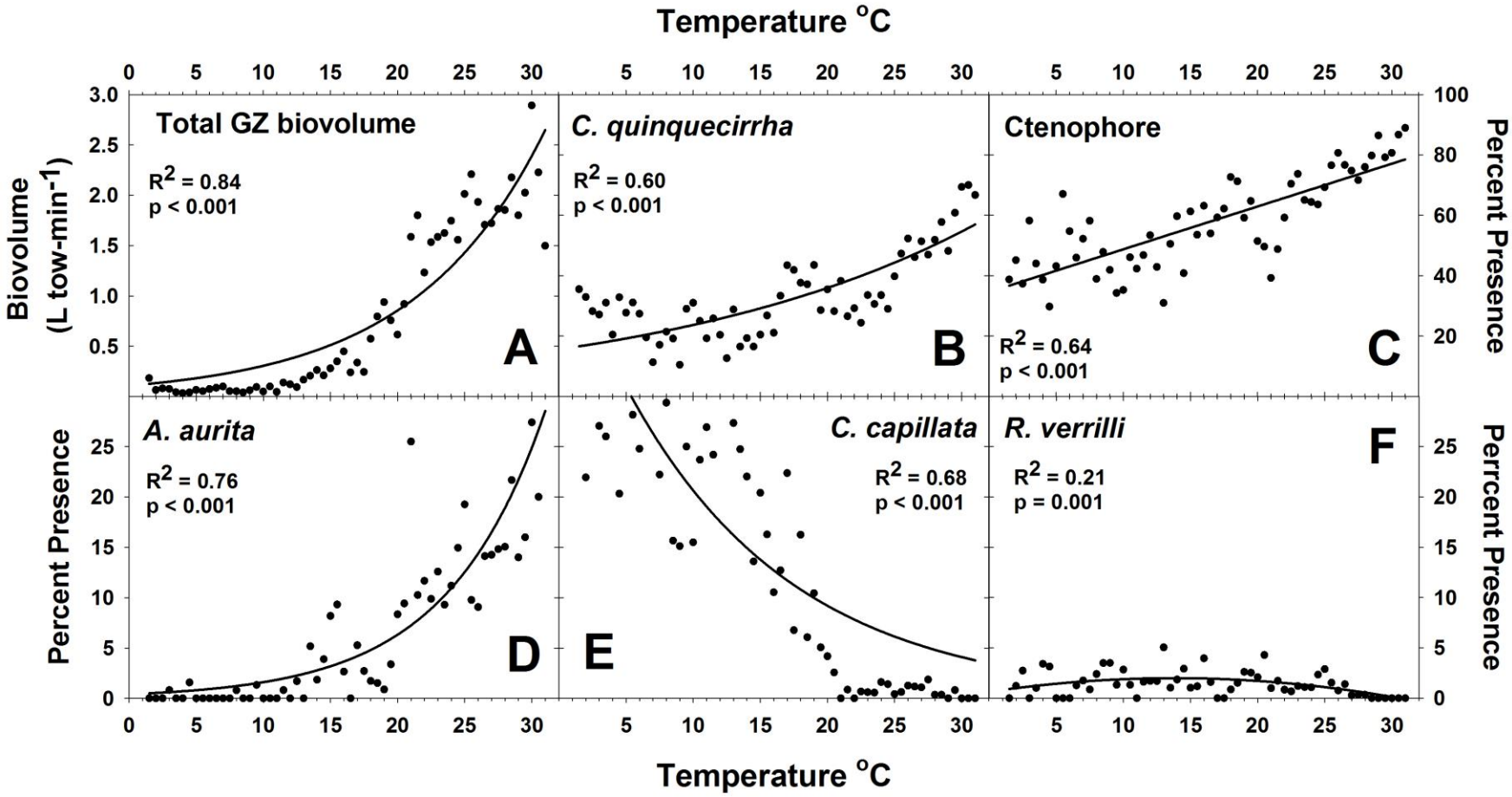

Figure 8: Effect of temperature on total GZ biovolume (A) and percent presence (B-F) of individual GZ taxa averaged across all stations for the entire VIMS dataset (1999-2012) in lower Chesapeake Bay. 'Percent presence' is the percentage of all tows for each temperature bin that had a particular taxon present. Scyphozoan medusae species are (B*) Chrysaora quinquecirrha,* (D*) Aurelia aurita*, (E*) Cyanea capillata,* and (F*) Rhopilema verilli.*

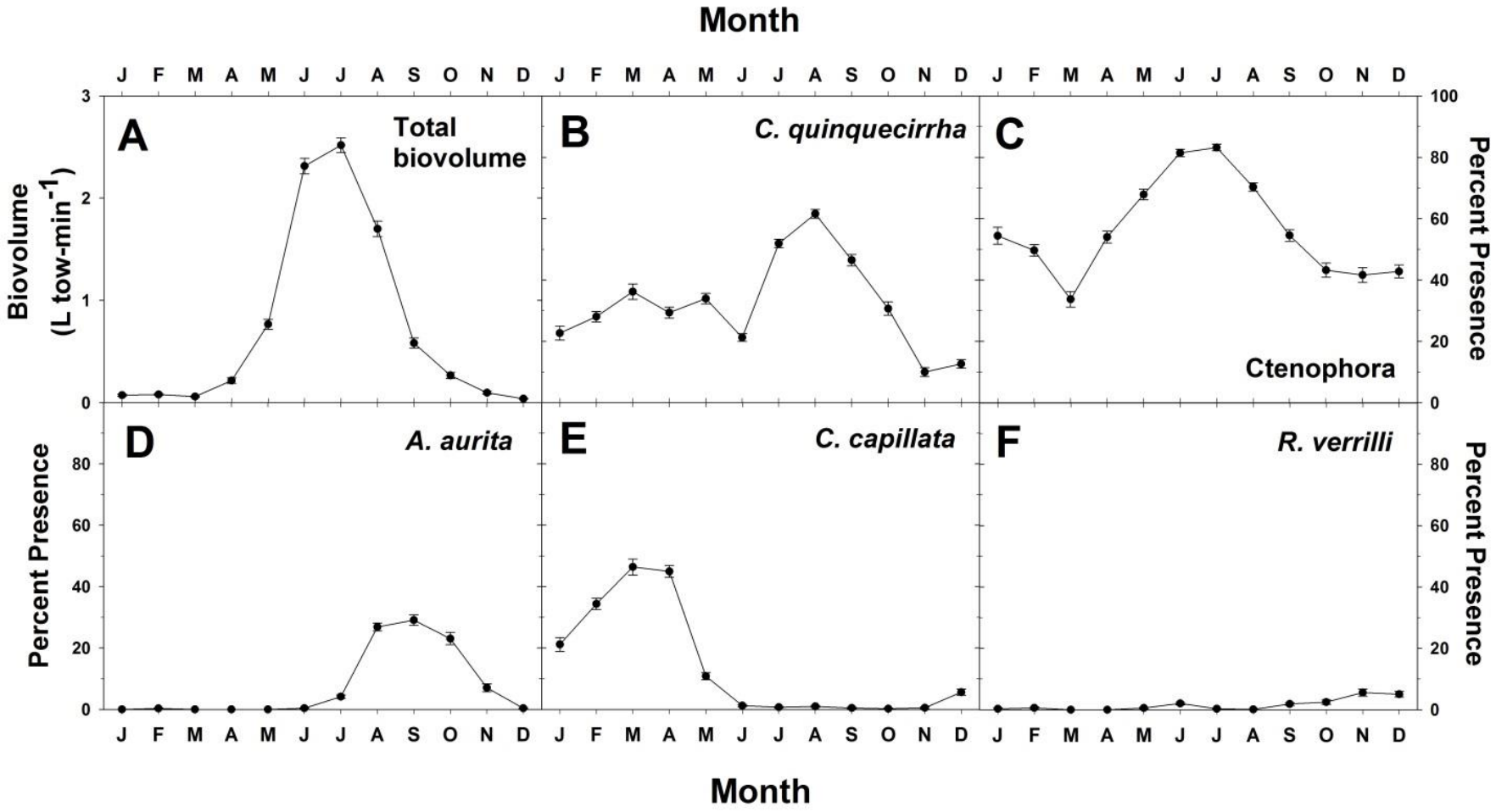

Figure 9: Seasonality of total GZ average biovolume (A) and average percent presence (B-F) of individual GZ taxa. Data are monthly averages (±SE) for the entire VIMS dataset (1999-2012) in lower Chesapeake Bay. Scyphozoan medusae species are (B*) Chrysaora quinquecirrha*, (D*) Aurelia aurita*, (E*) Cyanea capillata*, and (F*) Rhopilema verilli.*

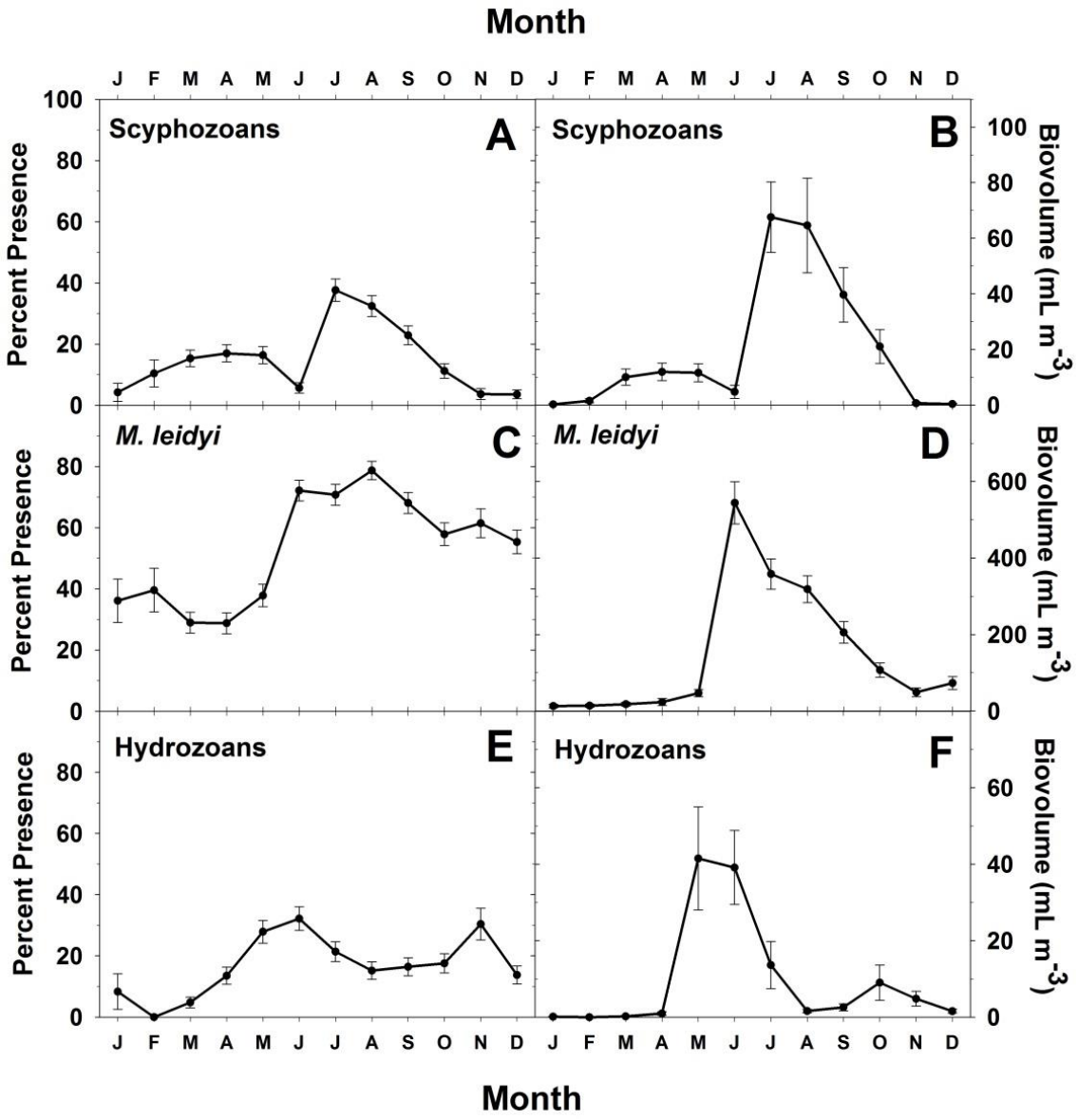

Figure 10: Seasonality of total GZ average percent presence (A, C, and E) and average biovolume (B, D, and F) of individual GZ taxa. Data are monthly averages (±SE) for the entire CBP dataset (1984-2002) in upper Chesapeake Bay. Taxa shown are scyphozoan and hydrozoan medusae, and the ctenophore *Mnemiopsis leidyi*.

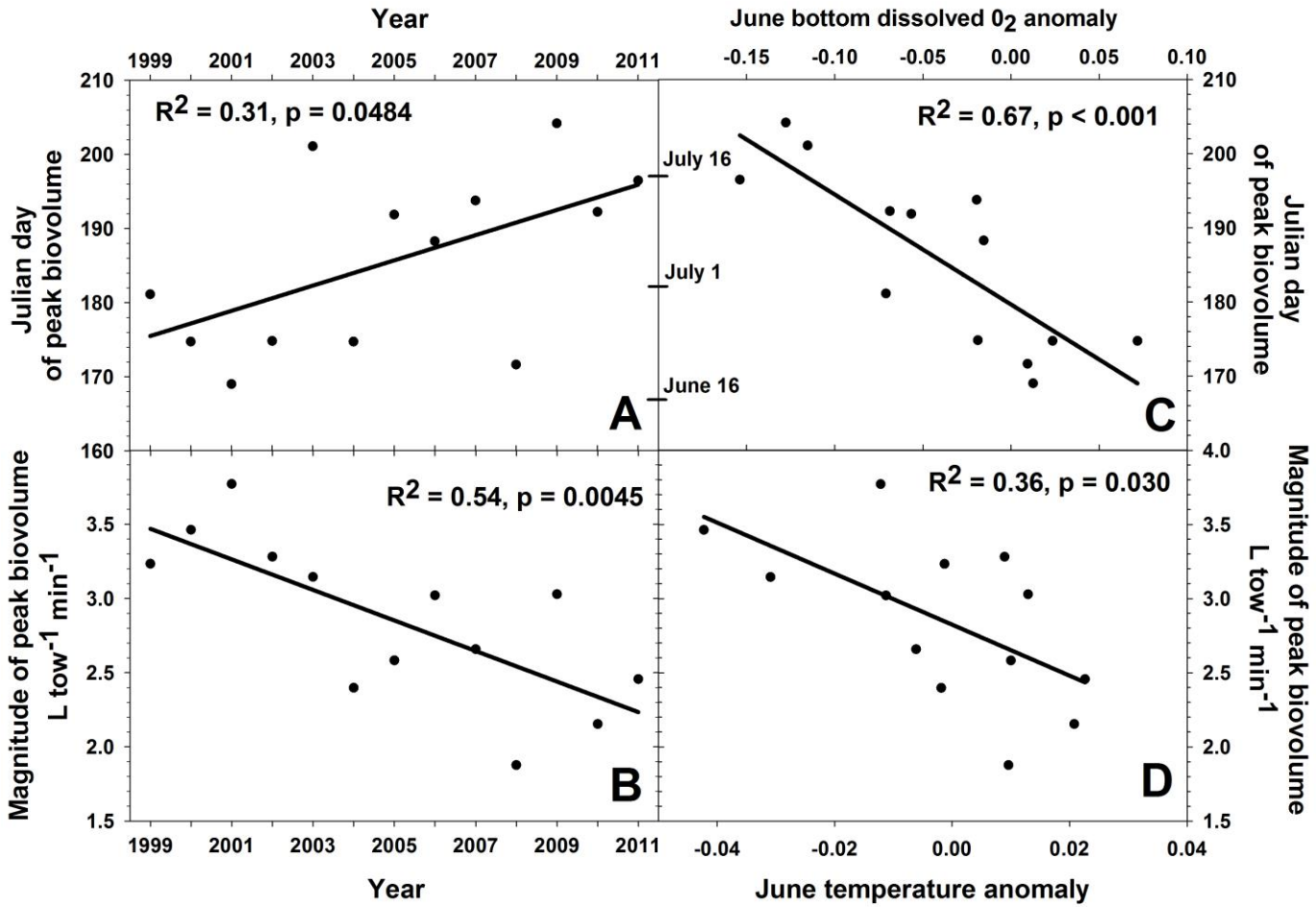

Figure 11: Changes in the timing and magnitude of the peak GZ bloom in lower Chesapeake Bay (VIMS dataset, 2000-2011). A) Changes in the Julian day of the peak total GZ biovolume over the time series, B) changes in the magnitude of peak total GZ biovolume over the time series, C) June bottom dissolved oxygen anomaly vs. timing of the peak total GZ biovolume, and D) June temperature anomaly vs. magnitude of the peak total GZ biovolume.

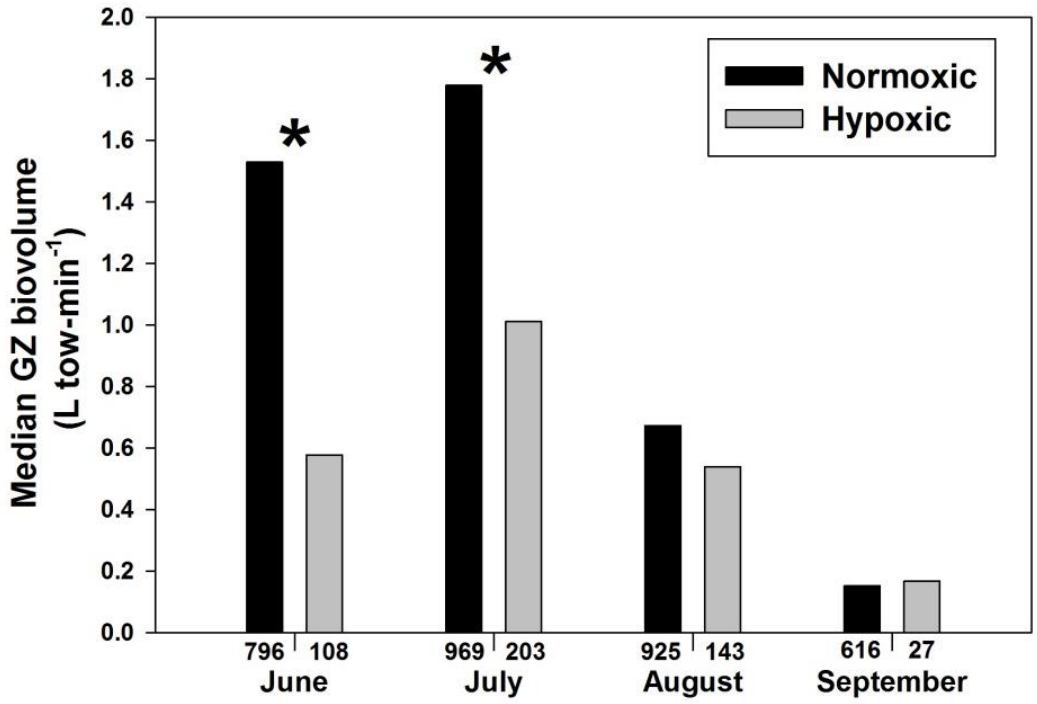

Figure 12: Effects of hypoxia (dissolved O_2 < 3.0 mg/L) on total GZ biovolume by month in lower Chesapeake Bay (VIMS dataset, 1999-2011). Asterisks mark significant differences (t-test, $p < 0.05$) between normoxic and hypoxic conditions. Sample sizes are indicated below bars.

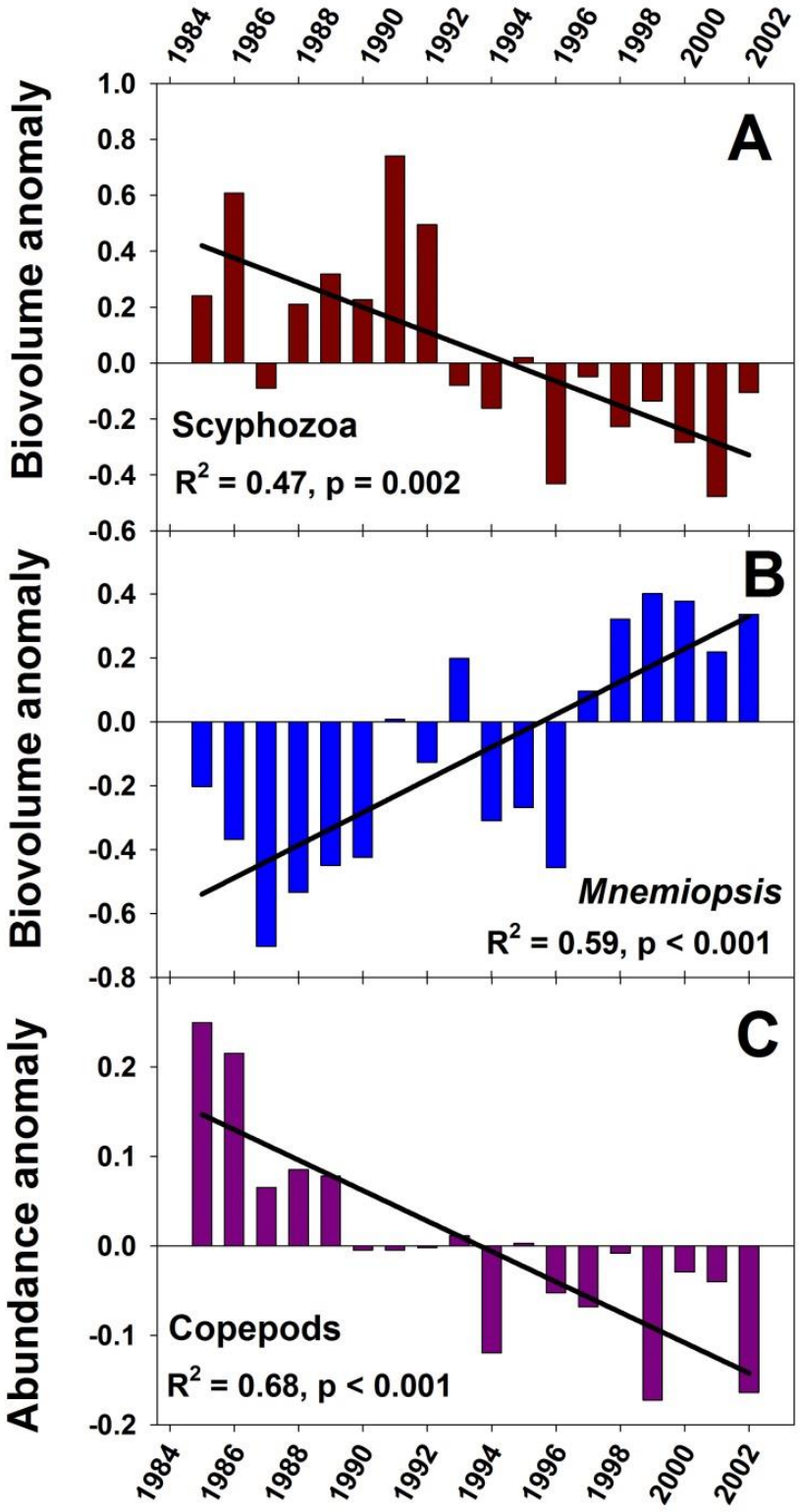

Figure 13: Long-term changes in GZ anomalies from 1985-2002 in upper Chesapeake Bay. A) scyphozoan medusae biovolume, B) ctenophore *Mnemiopsis leidyi* biovolume, and C) total copepod abundance. Data are from the CBP dataset.

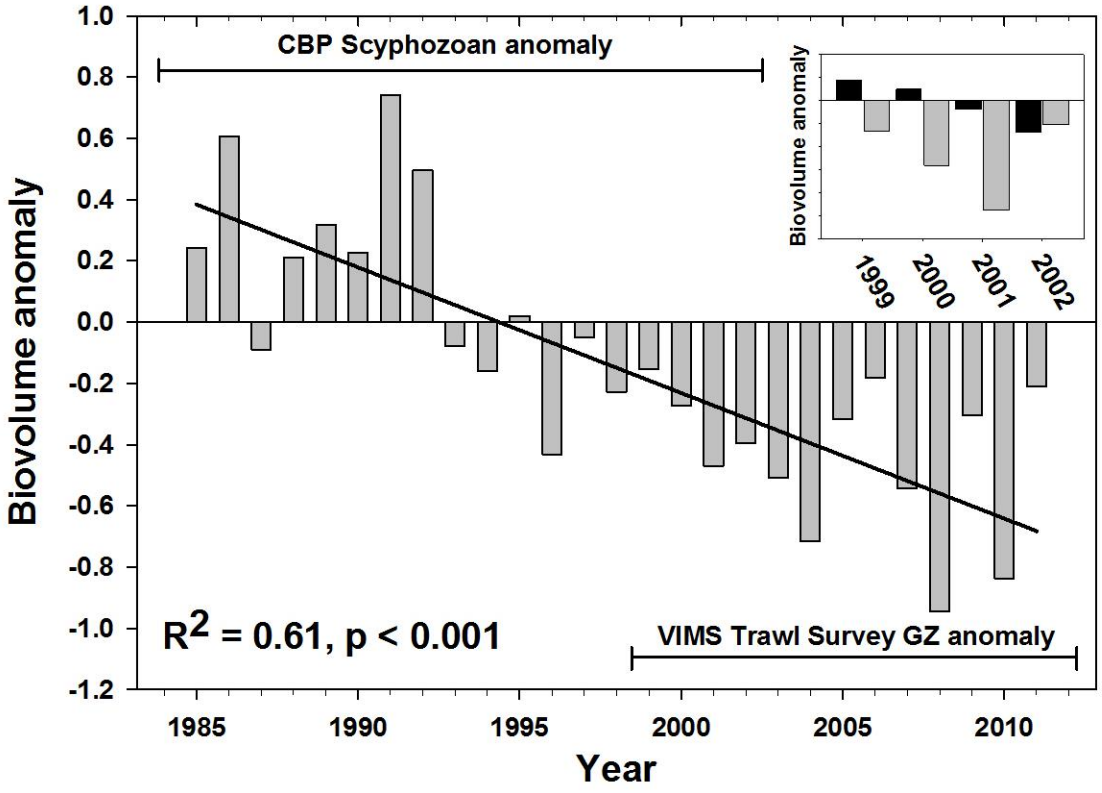

Figure 14: Summer to early fall (June-October) biovolume anomaly for scyphozoan medusae in upper Chesapeake Bay from 1984-2002 (CBP dataset) and total GZ in lower Chesapeake Bay from 1999-2011 (VIMS dataset). VIMS dataset anomaly was standardized relative to the CBP dataset, and overlapping years (1999-2002) are averages of the two datasets. Inset shows original data for overlapping years of the CBP dataset (black bars) and the VIMS dataset (gray bars).

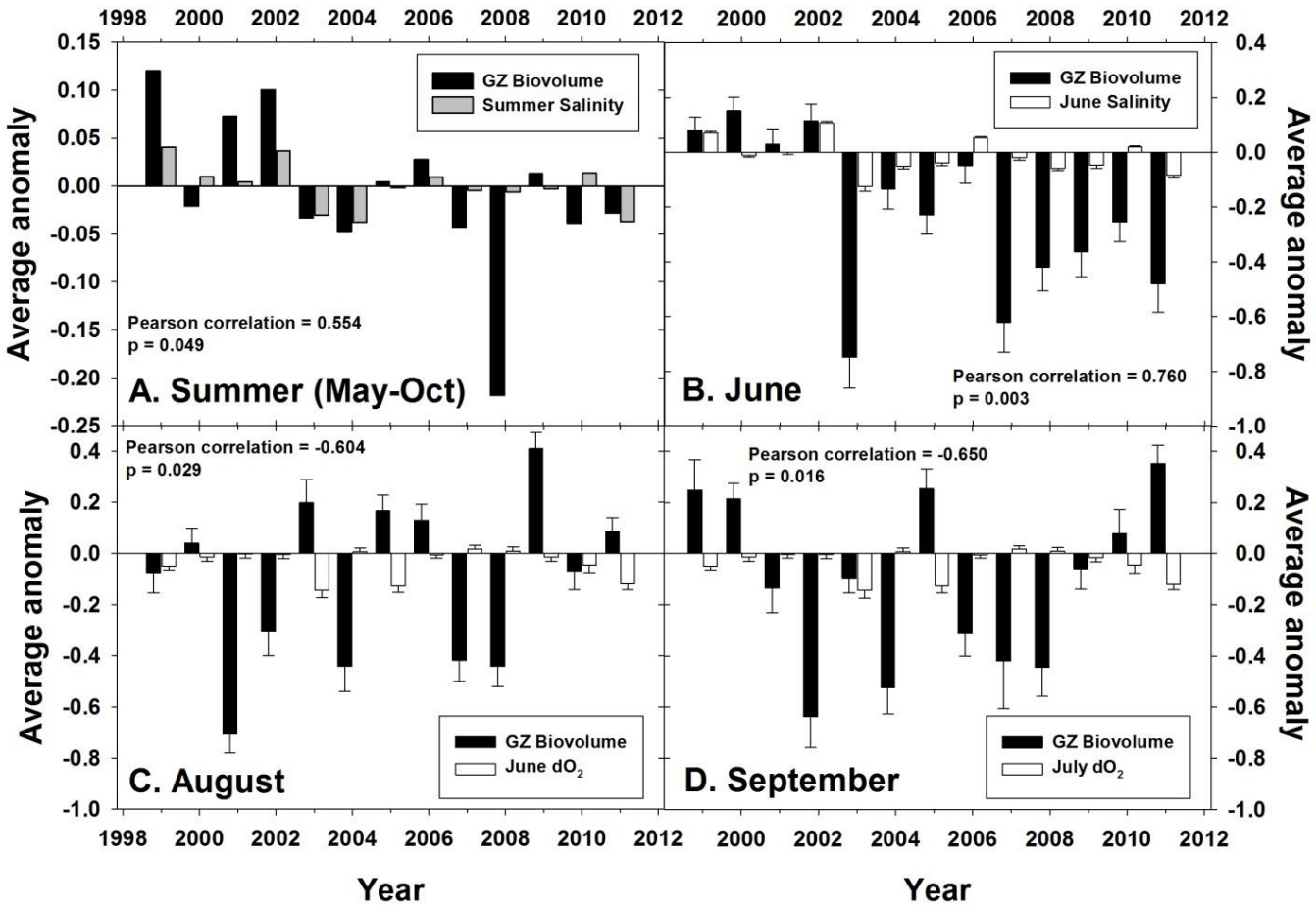

Figure 15: Correlations between total GZ biovolume and environmental anomalies in lower Chesapeake Bay (1999-2011, VIMS dataset). A) Summer to early fall total GZ biovolume anomaly and salinity anomaly, B) June total GZ biovolume anomaly and salinity anomaly, C) August total GZ biovolume anomaly and June bottom dissolved oxygen anomaly, and D) September total GZ biovolume anomaly and July bottom dissolved oxygen anomaly. Error bars are standard error.

CHAPTER 3

Influence of top-down control in the plankton food web on vertical carbon flux: a mesocosm study in the Chesapeake Bay

ABSTRACT

The effect of predation on carbon export in planktonic food webs is poorly known, but could play an important role in modulating the strength of the biological pump. Carnivorous gelatinous zooplankton (GZ) dominate the zooplankton community in Chesapeake Bay during summer months, exerting considerable top-down control on the planktonic food web. To examine the cascading effects of GZ blooms on the plankton food web and particulate organic carbon (POC) flux, we conducted multiple 2-day mesocosm experiments in the York River tributary of Chesapeake Bay in July-August, 2015. Mesocosms contained a natural assemblage of phytoplankton, microzooplankton, and copepods, and each treatment received additions of the ctenophore (*Mnemiopsis leidyi*), the scyphozoan medusae (*Chrysaora quinquecirrha*), or both *M. leidyi* and *C. quinquecirrha*. Mean clearance rate of *C. quinquecirrha* on *M. leidyi* was 32.1 L ind.$^{-1}$ h^{-1}, and *M. leidyi* on copepods was 1.9 L ind.$^{-1}$ h^{-1}. There was no significant difference between treatments in total POC or PON flux, and average POC flux was 0.62 mg C d^{-1} m^{-3} across all treatments and experiments. However, presence of *M. leidyi* reduced the abundance of copepods, in turn significantly decreasing copepod fecal pellet (FP) carbon flux compared to treatments without *M. leidyi* by 50% (from 36 to 18 μg C d^{-1} m^{-3}, or 6% to 3% of total POC flux). Total POC export fluxes were small (<1%) compared to previously measured sedimentation rates in the Chesapeake Bay. But, these top-down changes in copepod FP carbon flux are equivalent to a modest portion (~10%) of previously calculated *C. quinquecirrha* carcass flux. Future experiments and models of zooplankton contributions to vertical carbon flux should include top-down processes.

1. INTRODUCTION

The relative importance of bottom-up vs. top-down control in food webs has been examined extensively in a wide variety of ecosystems, and trophic cascades initiated by top-down control have been demonstrated repeatedly throughout terrestrial, aquatic, and marine environments (Micheli, 1999; Borer et al., 2005; Borer et al., 2006; Duffy et al., 2007). The effects of top-down control and community composition on cycling of organic matter and nutrients have been examined in terrestrial and freshwater ecosystems (reviewed in Brett & Goldman, 1996; Vanni, 2002; Schmitz et al., 2010). For example, presence of zooplanktivorous fish in freshwater systems reduce herbivorous crustacean zooplankton, increasing phytoplankton biomass and changing composition of sediment organic matter (SOM) (Attayde & Hansson, 2001; Allard et al., 2011). However, the top-down effects on SOM deposition have only recently been examined in marine ecosystems. In a benthic marine system, the presence of the predator blue crab (*Callinectes sapidus*) reduced epiphyte grazers in seagrass beds, leading to increases in epiphytes, decreases in seagrass, and complex changes in sediment organic matter amount and composition (Canuel et al., 2007; Spivak et al., 2007; Spivak et al., 2009). However, there is a paucity of data on how top-down control affects cycling and export of carbon and nutrients in marine planktonic ecosystems.

Carnivorous gelatinous zooplankton (GZ) (e.g., cnidarians, ctenophores) are conspicuous and effective marine planktonic predators that are known to initiate trophic cascades (reviewed in Verity & Smetacek, 1996; West et al., 2009; Dinasquet et al., 2012; McNamara et al., 2014). GZ are taxonomically diverse, but share two key characteristics: alternation of generations between sexual and asexual reproduction and

large, fast-growing, gelatinous bodies. These traits allow them to reproduce extremely rapidly under good environmental conditions (Purcell et al., 2005) and to be extremely efficient predators (Acuña et al., 2011; Pitt et al., 2013). These advantages allow GZ to exert top-down control during blooms that can extend several trophic levels down (Purcell & Decker, 2005; Compte et al., 2010).

In the Chesapeake Bay, phytoplankton biomass is highest during the spring, and primary production increases to a peak during the summer months. This mismatch between the peaks of phytoplankton biomass and production is caused by the high grazing of crustacean zooplankton, primarily calanoid copepods which are more abundant in the late spring and summer than early spring (White & Roman, 1992; Steinberg & Condon, 2009). This spring progression of blooms – phytoplankton followed by copepods – is followed by two species of carnivorous GZ that exert wide-ranging top-down control throughout the zooplankton food web in summer in Chesapeake Bay: the lobate ctenophore *Mnemiopsis leidyi* and the scyphozoan medusa *Chrysaora quinquecirrha* (Cargo & King, 1990). *M. leidyi* is present year-round throughout the mesohaline and polyhaline regions of Chesapeake Bay and its tributaries, but is most abundant from June through October (Purcell et al., 2001; Purcell & Decker, 2005; Steinberg & Condon, 2009). *M. leidyi* is a voracious predator of crustacean mesozooplankton and can exert high predation pressure on copepods, as well as icthyoplankton during *M. leidyi* blooms (Purcell et al., 1994; Purcell & Roman, 1994; Purcell et al, 2001; Condon & Steinberg, 2008).

In contrast to *M. leidyi*, C. *quinquecirrha* medusae populations are greatly reduced in the winter as they often do not survive temperatures below 10^{o}C (Gatz et al.

1973). C. *quinquecirrha* overwinter as benthic polyps and begin to produce planktonic medusae when water temperatures rise above 17^{o} C in the late spring (Purcell & Decker, 2005). These medusae are present from May to October, but the highest abundances are from July to September (Purcell 1992). *C. quinquecirrha* feed on a wide variety of meso- and macrozooplankton, and are the primary predator of *M. leidyi* (Purcell & Cowan, 1995; Suchman et al., 1998). When present, *C. quinquecirrha* can exert strong top-down control of *M. leidyi* and significantly reduce their populations (Purcell & Cowan, 1995). This reduction of *M. leidyi* in turn releases their prey (primarily copepods) from predation pressure, allowing the copepods to continue to have high summer abundances (Purcell & Decker, 2005). This sets up a trophic cascade where years with higher abundance of *C. quinquecirrha* have lower abundance of *M. leidyi* and therefore higher abundance of copepods, increasing grazing on phytoplankton by copepods. The populations of the top predator, *C. quinquecirrha*, are regulated by the timing of spring warming and rainfall, with earlier warming and low rainfall (higher salinities) leading to years with higher medusae abundances (Cargo & King 1990). Thus, changes in weather patterns (Purcell & Decker, 2005) from year to year may have significant top-down effects on the Chesapeake Bay food web, and consequently–as we hypothesize–on vertical carbon and nitrogen flux to the benthos.

GZ can affect vertical flux through a variety of mechanisms (Pitt et al., 2008). At the end of a bloom, sinking GZ carcasses provide a large, episodic pulse of carbon to the benthos (Lebrato et al., 2013), but throughout the life of a bloom, GZ produce mucus which may entrain phytoplankton and other particles, causing it to sink out of the water column as a loose, sticky aggregate (Deason & Smayda, 1982). Additionally, both *C.*

quinquecirrha and *M. leidyi* egest waste material as loose, poorly defined 'fecal fluff' which sinks more slowly and disintegrates more quickly than the compact fecal pellets (FP) produced by copepods (Kremer, 1979; Alldredge & Gotschalk, 1988). Because of the sinking speed and disintegration differences between the GZ-produced fecal material and the copepod-produced FP, the quality and overall mass flux to the benthos may change depending on which species is dominant in the plankton. It is these interactions between top-down effects and vertical flux that we explore in this study.

We hypothesized that increases in *C. quinquecirrha* medusae during the summer months will lead to top-down control and a resulting trophic cascade in which *M. leidyi* abundance decreases, releasing copepods from predation pressure and leading to an increase in POC and PON export in the form of copepod fecal pellets. Conversely, absence of *C. quinquecirrha* will allow *M. leidyi* to decrease the abundance of copepods, decreasing predation pressure on phytoplankton and increasing the export of particulate organic carbon and nitrogen (POC, PON) in the form of phytoplankton aggregates. To test this hypothesis, we conducted mesocosm experiments in the Chesapeake Bay with four treatments of zooplankton communities: 1) natural copepod assemblage with no GZ, 2) natural assemblage plus *M. leidyi*, 3) natural assemblage plus *C. quinquecirrha*, and 4) natural assemblage plus both *M. leidyi* and *C. quinquecirrha*. By analyzing the changes in zooplankton abundance, total PON and POC flux, and flux from fecal pellets for each treatment, we were able to examine top-down controls on vertical particle flux.

2. METHODS

2.1 Mesocosm design

Mesocosm experiments were conducted in July and August, 2015 in a large, cylindrical fiberglass tank (3.5 m tall, 3.66 m diameter) with a continuous supply of water pumped from the York River–a tidal, brackish estuary of the Chesapeake Bay. Water flow was approximately 110 L min^{-1}, thus the tank water was completely flushed every ~4.5 h, and temperature, salinity, and dissolved oxygen were equal to ambient conditions in York River surface waters. Water conditions for each experiment are listed in Table 1. Within the tank, we placed four 1.83 m^3 mesocosms, each 1 m in diameter and 3 m long with a 2 L, PVC cod end. The mesocosms were the same as those used in Cowan and Houde (1990), with the top 2 m being cylindrical and consisting of 2.2 oz Dacron sail cloth with an average mesh aperture of ~25 μm, and the bottom conical portion constructed of 53 μm Nitex mesh. Two 6 mm stainless steel hoops were attached outside of the central portion to keep it from collapsing, and bricks were attached to the cod end to keep it positioned upright and at the bottom of the mesocosm. The top of the mesocosm was placed above the surface of the water and open to allow sunlight to enter. These mesocosms allowed free exchange of water, almost immediate response to changes in the surrounding temperature, salinity, and dissolved oxygen, and retention of zooplankton (de Lafontaine and Leggett, 1987).

2.2 Experimental procedure

Mesocosms were filled by diffusion of water through the mesh, with a small amount (~100 L) of water entering through the top to allow large phytoplankton to

colonize the mesocosm. Each experiment was conducted over ~2 days using 4 mesocosms per experiment. Animals were collected from the York River the same day as the start of each experiment, with *M. leidyi* and *C. quinquecirrha* collected by gently dip netting from the surface, and copepods collected using a 1-m diameter zooplankton net with 200 μm mesh and a non-filtering cod end. All mesocosms first received a natural copepod assemblage (primarily *Acartia tonsa* copepods), containing copepod numbers comparable to those naturally found in the York River during peak abundances (6.5 – 11 L^{-1}) (Condon and Steinberg, 2008). Copepods were added first and allowed to disperse through the mesocosm before any GZ were added. One mesocosm also received 10 *Mnemiopsis leidyi*, one received 1 *Chrysaora quinquecirrha*, and the last mesocosm received both 10 *M. leidyi* and 1 *C. quinquecirrha*. These abundances of *M. leidyi* and *C. quinquecirrha* are also similar to their natural abundances in the York River during the summer. For some experiments *C. quinquecirrha* were unavailable; in these experiments, two mesocosms were used as the copepod-only controls and two as replicate *M. leidyi* treatments. One additional pilot experiment was conducted on July 22-25, and while the GZ used were healthy, the copepods used in the experiments did not survive for unknown reasons and only the results of *C. quinquecirrha* grazing on *M. leidyi* are included from that study.

At the start and end of each experiment, salinity, temperature, and dissolved oxygen were measured in the center of the tank using a YSI EXO Sonde. Chlorophyll *a* concentrations were collected from the NOAA data buoy YRK005.40 (37.24728 °N, 76.49937 °W, www.ndbc.noaa.gov). Over the course of the experiment, sinking material in the mesocosm was funneled into the cod end. At the end of each experiment, the mesh

immediately above the cod end was cinched off to prevent exchange of material back into the mesocosm. The cod end was then brought to the surface, removed, capped, and an empty cod end was put in its place. After the new cod end was in place, the entire mesocosm was lifted from the water, allowing copepods and other mesozooplankton, GZ, and other contents that were suspended in the water column to drain into the cod end. GZ were first quickly removed to prevent continued feeding on copepods, and the remainder of the cod end contents saved for subsequent analysis. Remaining GZ and copepods were also checked for swimming activity to ensure they were still alive and active. Clearance rate (C) of GZ predators on their prey was calculated from the formula:

Equation 1: $C = (V / (n \times t)) * \ln(P_0 / P_t)$

Where V = volume of experimental container (1832 L), n = number of predators (*C. quinquecirrha* or *M. leidyi*), t = time of the experiment in hours, P_0 = number of prey (copepods or *M. leidyi*) at start of the experiment, and P_t = number of prey at the end of the experiment.

2.3 Analyses of sinking particles and mesocosm contents

Cod ends containing either sedimented particles (hereafter particulate organic matter; POM) or live zooplankton plus other suspended mesocosm material were returned to the laboratory, and stored at 4 °C until analysis, within 24 h. Oral-aboral length (*M. leidyi*), diameter (*C. quinquecirrha*), and biovolume (both) were measured for each surviving GZ (i.e., uneaten *M. leidyi*; there was no natural death of either GZ species in our 2 day experiments, with GZ actively swimming at the end of experiments). Copepods and other mesozooplankton were preserved in 4% formalin and counted under

a dissecting microscope. Sedimented POM was split into two fractions, one for elemental analysis and the other for visual analysis of particle type.

The fraction of POM used for elemental analysis was filtered through a 150 μm sieve to remove copepods and other mesozooplankton, and then filtered through a pre-combusted, pre-weighed, 0.7 μm pore, glass microfiber (GF/F) filter. Some of the copepods that were removed from this fraction may have included copepod carcasses that sank out of the water column, and would thus be included as particle export. However, whether these copepods died as a result of interactions with GZ or other causes could not be determined, and thus they were not included as POM export. Filters were then placed in a 60 °C drying oven for at least 7 d. After drying, filters were re-weighed to obtain bulk dry weight of POM, and then analyzed for particulate organic carbon and nitrogen (POC and PON) using an Exeter Elemental Analyzer CE440.

The fraction of sedimented POM used for analysis of particle type was preserved in 4% formalin, with fecal pellets (FP) quantified using a dissecting microscope at 16-32 magnification. At least 50 copepod FP were measured for each mesocosm using CellSens 1.13 software to determine an average volume per FP, and total volume of pellets per mesocosm calculated. To calculate total FP carbon, we used two methods and averaged the results of each approach for each mesocosm: we applied a volume to carbon conversion factor for *Acartia tonsa* FP of 0.34 pg C μm^{-3} using our calculated mean FP volume (Hansen et al., 1999), and we also multiplied the total number of FP by 17.7 ng C $pellet^{-1}$ (Saba et al., 2011).

2.4 Statistical analysis

Both t-tests and one-way ANOVAs were used to test differences in mass flux and FP POC and PON flux between treatments. When appropriate, results from each treatment were averaged between experiments and compared using t-tests and ANOVAs. Statistical analyses were done using Sigma Plot 11 software.

3. RESULTS

3.1 Experimental conditions

While average temperature (27.4 – 28.6 °C) and salinity (20.0 – 20.7) were similar between experiments conducted on different days, both dissolved oxygen (2.5 – 6.29 mg/L) and chlorophyll *a* (6.7 – 20.3 μg/L) varied considerably between experiments (Table 1).

3.2 Clearance rates

The clearance rate of *M. leidyi* on copepods was calculated from all experiments, and averaged 1.9 L ind.$^{-1}$ h^{-1} (± 0.7 SE) including experiment 2 where no predation on copepods was observed (Figure 1A). The clearance rate of *C. quinquecirrha* on copepods was negligible, with no feeding occurring in the *C. quinquecirrha*-only treatments in experiments 1 and 2. The clearance rate of *C. quinquecirrha* consuming *M. leidyi* was also calculated from experiments 1, 2, and the pilot study and averaged 32.1 L ind.$^{-1}$ h^{-1} (± 13.9) (Figure 1B).

3.3 Particulate organic carbon and nitrogen flux

Overall, there was no significant difference in total POC (ANOVA, $p = 0.87$) or PON (ANOVA, $p = 0.77$) flux between treatments, and no treatments were significantly different from each other for POC or PON as a percentage of the control (ANOVA, $p = 0.70$ and 0.66, respectively) when flux was calculated as a percentage of the flux in controls (Figure 2). Flux of POC and PON ranged from 0.39–1.02 mg C day^{-1} m^{-3} and 0.04–0.17 mg N day^{-1} m^{-3}, respectively (Table 2). The C:N ratios of sinking POM were

more similar between treatments within an experiment than between experiments (ranging from an average of 5.5 in experiment 1 to 9.7 in experiment 2).

3.4 Fecal pellet flux

Flux of *Acartia tonsa* fecal pellets (Fig. 3) ranged from 0.55–41.1 mg C day^{-1} m^{-3} (Table 2), and was lower in the *M. leidyi* treatments than controls in both experiments 3 and 4, but there was no significant difference (ANOVA, $p > 0.05$) in FP POC flux between treatments for experiments 1 and 2 (Table 2; see also Fig. 4). Small copepod FP (from *A. tonsa*) were present in all mesocosms, and large crustacean FP (Fig. 3) were present in about half of the mesocosms. POC from large fecal pellets, when present, varied from 1.7-173 μg C day^{-1} m^{-3} (equivalent to 8–1300% of *A. tonsa* fecal pellet C), but the absence of large fecal pellets from 6 mesocosms through all experiments and high variability prevented comparisons between treatments or experiments to be conducted. In all treatments and controls *Acartia tonsa* fecal pellets made up a small proportion (<1 to 8.6%) of the exported material (Table 2), with other larger fecal pellets (0 to 39%) and phyto-detritus (Fig. 3) or unidentified aggregates constituting the rest. After combining the results of experiments 3 and 4, FP carbon was significantly lower (t-test, $p = 0.003$) in *M. leidyi* treatments (18.0 μg C day^{-1} m^{-3}) than in the controls (36.1 μg C day^{-1} m^{-3}), and was equivalent to a 50% decrease in FP POC flux over the 2-day experiments. Small FP carbon was about 20 times higher in all of the treatments and controls for experiments 3 and 4 than for experiments 1 and 2 (Table 2).

4. DISCUSSION

4.1 Clearance rates

Clearance rates in our study were similar to those previously reported. Average clearance rate of *C. quinquecirrha* feeding on *M. leidyi* (32.1 L ind.$^{-1}$ h^{-1}) was similar to that reported by Purcell and Cowan (1995) for experiments conducted in a 1 m^3 mesocosm (29.2 L ind.$^{-1}$ h^{-1}) but less than reported for a 3.2 m^3 mesocosm (69.1 L ind.$^{-1}$ h^{-1}). Average clearance rate of *M. leidyi* feeding on copepods (1.9 L ind.$^{-1}$ h^{-1}) was similar to experiments using large container sizes reviewed in Purcell et al. (2001) (1.9 and 2.2 L ind.$^{-1}$ h^{-1}) as well as in Purcell and Decker (2005) (1.3-2.0 L ind.$^{-1}$ h^{-1} for ctenophores 35-53 mm). *M. leidyi* clearance rate of copepods was higher than those reported in Madsen and Riisgård (2010) (0.1-1.2 L ind.$^{-1}$ h^{-1}) and Mazlum and Syhan (2007) (0.18-1.25 L ind.$^{-1}$ h^{-1}), although those studies used smaller ctenophores and smaller containers, respectively. Low DO concentrations do not affect *C. quinquecirrha* or *M. leidyi* clearance rate of copepods (Breitburg et al., 1997; Kolesar et al., 2010), therefore low DO in experiment 2 likely did not alter feeding rates. While copepod clearance rates were not measured in these experiments, grazing on phytoplankton may be reduced in treatments with *M. leidyi* present, as the presence of *M. leidyi* significantly reduces the number of grazing copepods. Thus, the trophic cascade caused by *C. quinquecirrha* could extend down to the level of primary producers, reducing phytoplankton concentrations when *C. quinquecirrha* are present.

4.2 Effect of trophic cascades on export

A trophic cascade initiated by *C. quinquecirrha* was observed in copepod abundances, and this top-down control led to changes in POC flux. A decrease in *A. tonsa* copepod fecal pellet POC flux occurred in treatments containing *M. leidyi* ctenophores, which we interpret as consumption of copepods leading to their reduced abundance and subsequent reduced overall copepod grazing and fecal pellet production (Fig. 5). This suggests a reduction in *A. tonsa* FP flux could occur *in situ* during the summer months when *M. leidyi* is present. Using the rates determined in our study and known abundances of copepods and GZ, we can estimate the effects GZ presence would have on *A. tonsa* FP flux in the Chesapeake Bay. Typically, *C. quinquecirrha* are abundant in the Chesapeake Bay from early July to late September, and exert high predation on *M. leidyi* during those three months (Condon and Steinberg, 2008; Stone et al., in prep.). Copepod densities can reach up to 20,000 m^{-3} in Chesapeake Bay, and are significantly reduced by the presence of *M. leidyi* (Purcell and Decker, 2005; Condon and Steinberg, 2008). To estimate the change in FP POC flux caused by *C. quinquecirrha* over the summer months, we can multiply *A. tonsa* FP production (C m^{-3} day^{-1}) measured by this experiment in both the average control and average *M. leidyi*-only treatments by the average depth of the Chesapeake Bay (6.4 m) and 90 days. In this scenario, *A. tonsa* FP production would increase from 10.4 to 20.8 mg C m^{-2}. This estimate is conservative, as the short duration (2 d) of the experiments means *M. leidyi* predation on copepods is likely an underestimate. This 10.4 mg C m^{-2} increase over three months represents a modest portion (3%) of the 357 mg C m^{-2} total POC flux measured by this study over the same depth and time period. However, these fluxes are over two orders of magnitude lower than those reported from other studies that measured total POC flux to the benthos

in the Chesapeake Bay using sediment traps (126 g C m^{-2}, Boynton et al., 1993; 76.8 g C m^{-2}, Roden et al., 1995) and a deposition model (45.9 g C m^{-2}, Hagy et al., 2005) for the same 3 months (July, August, and September). While the presence of *M. leidyi* has an appreciable effect on *A. tonsa* abundances and FP flux, this represents only a small portion of overall summer carbon flux in the Chesapeake Bay. However, the final fate of copepod FP may differ greatly from that of phytodetritus, and future research should examine how decomposition, burial, and consumption of these flux components differs.

In addition to top-down effects, GZ may also influence phytoplankton through bottom-up processes. There were no significant differences in total POC and PON flux between treatments containing GZ and those that did not, and this is most likely due to the high abundance of aggregates of phytodetritus which made up the majority of the flux in all treatments. In our experiments, while *M. leidyi*-only treatments had lower FP flux, this reduction in FP POC flux may be offset by higher GZ mucus production or higher phytoplankton aggregate flux (due to decreased copepod grazing), although we were unable to quantify this. In other systems, GZ have been shown to alter phytoplankton composition and abundance both through top-down control of phytoplankton grazers (Compte et al., 2010; Dinasquet et al., 2012) and stimulating growth through the release of nutrients (Pitt et al., 2009; West et al., 2009; Hosia et al., 2014; McNamara et al., 2014) although this bottom-up effect is dependent on the extent of nutrient limitation in the system. While this experiment was not designed to measure GZ effects on phytoplankton growth, it is possible that the presence of either *M. leidyi* or *C. quinquecirrha* would increase phytoplankton production through the release of dissolved nutrients via excretion, although these nutrients may be shunted into the microbial loop

for use in bacterioplankton metabolism (Condon et al., 2011). During blooms of *M. leidyi*, this bottom-up process would be additive with the top-down control of mesozooplankton grazers such as copepods, further increasing phytoplankton production. However, during blooms of *C. quinquecirrha* the bottom-up and top-down effects on phytoplankton production would counteract each other. These bottom-up effects would explain the lack of differences seen between treatments in the overall flux, although excretion of DON and DOP by GZ was estimated to support < 4% of primary production in the Chesapeake Bay (Condon et al., 2010). Even large blooms of GZ would only excrete enough dissolved inorganic N to support a small portion (3%) of microplankton production in the Chesapeake Bay (Nemazie et al., 1993).

While changes in carbon flux due to top-down control were relatively small, one of the primary pathways GZ can contribute to flux is through the sinking of dead GZ as carcasses, which has been shown to represent a substantial, seasonal carbon pulse in the deep sea (Lebrato et al. 2013). Sexton et al. (2010) found that as temperatures cool in October and November in the Chesapeake Bay, *C. quinquecirrha* medusae pulse more slowly, and sink to the bottom before waters are too cold to survive. This, combined with their lack of significant predators, means that the majority of *C. quinquecirrha* biomass produced during the summer returns to the benthos at a rate over 100 mg C m^{-2} yr^{-1} (Sexton et al. 2010). However, because *M. leidyi* ctenophores can better survive winter water temperatures in the Chesapeake Bay and quickly disintegrate upon death, it is unlikely that their carcasses reach the benthos. Thus, the presence of *C. quinquecirrha* not only increases copepod FP, but also shifts carbon away from the non-sinking *M. leidyi* carcasses. This carcass carbon flux of *C. quinquecirrha* at the end of the year is 10

times higher than our estimated increase in flux due to top-down effects of *C. quinquecirrha* presence over the summer, although the fates of these two carbon sources (GZ carcass vs. copepod FP) may be very different once they reach the benthos or reach the benthos at different rates.

5. SUMMARY AND CONCLUSION

We observed the hypothesized trophic cascade of *C. quinquecirrha* preying on *M. leidyi* and *M. leidyi* preying on copepods, with clearance rates similar to previously published values. While there was no significant change in total POC or PON flux between treatments, the composition of the flux did change, with higher flux of *A. tonsa* FP in the controls versus treatments with added *M. leidyi* in half of the experiments. The presence of *M. leidyi* reduced this FP flux by 50% over the course of the experiments, and we estimate that this decrease in flux would lower FP deposition in the Chesapeake Bay by ~10 mg C m^{-2} over the course of the summer. While summer FP flux is extremely small compared to published values for total summer POC flux in the Chesapeake Bay, there may be differences in the fate of FP versus phytodetritus and their effect on benthic processes. Additionally, the top-down changes in carbon flux controlled by *C. quinquecirrha* is an appreciable portion of estimates of *C. quinquecirrha* carcass carbon flux for the entire year.

Top-down control in vertical carbon flux should be considered in experimental or modeling studies examining the role of plankton food webs in the biological pump. As similarly shown in freshwater pelagic (Brett & Goldman, 1996; Vanni et al., 2002; Allard et al., 2011) and marine systems (Micheli, 1999; Spivak et al., 2009), top-down control can significantly affect the composition of vertical POC flux in marine pelagic systems. This study only examined one coastal estuary, and carnivorous GZ may exert top-down control in a wide variety of ecosystems where they bloom including the Black and Caspian Seas (Daskalov et al., 2007; reviewed in Costello et al., 2012), coastal Australia (West et al., 2009), Mediterranean marshes (Compte et al., 2010), Baltic Sea (Dinasquet

et al., 2012), the Benguela Current (Roux et al., 2013), Bering Sea (Brodeur et al., 2008), Northern California Current (Suchman et al., 2008), and numerous others (reviewed in Purcell & Arai, 2001; Purcell, 2005). Furthermore, carnivorous GZ can be highly abundant in the mesopelagic zone (Robison et al., 1998; Silguero & Robison, 2000), where their top-down control may ultimately affect sinking particle attenuation and thus efficiency of POC export to depth. In each of these ecosystems, GZ have the potential to regulate multiple aspects of vertical carbon flux and could have a relatively stronger effect in regions more nutrient-limited than the Chesapeake Bay.

Acknowledgments

We are grateful to James Cowan Jr. of Louisiana State University for his advice on experimental design and for lending us the mesocosms. Thanks to Paul Panetta of Applied Research Associates, Inc. for use of his equipment, Emmett Duffy for advice on experimental design, and the VIMS field operations personnel for assistance with setting up the experiments. This research was funded by Virginia Sea Grant (V718500) to D.K.S. and J.P.S.

REFERENCES

Acuña JL, López-Urrutia Á, Colin S (2011) Faking giants: The evolution of high prey clearance rates in jellyfishes. Science 333: 1627-1629

Allard B, Danger M, Ten-Hage L, Lacroix G (2011) Influence of food web structure on the biochemical composition of seston, zooplankton and recently deposited sediment in experimental freshwater mesocosms. Aquat Sci 73: 113-126

Alldredge AL, Gotschalk C (1988) In situ settling behavior of marine snow. Limnol Oceanogr 33(3): 339-351

Attayde JL, Hansson L-A (2001) Fish mediated nutrient recycling and the trophic cascade in lakes. Can J Fish Aquat Sci 58: 1924-1931

Baird D, Ulanowicz RE (1989) The seasonal dynamics of the Chesapeake Bay ecosystem. Ecological Monographs 59: 329-364

Borer ET, Halpern BS, Seabloom EW (2006) Asymmetry in community regulation: Effects of predators and productivity. Ecology 87(11): 2813-2820

Borer ET, Seabloom EW, Shurin JB, Anderson KE, Blanchette CA, Broitman B, Cooper SD, Halpern BS (2005) What determines the strength of a trophic cascade?. Ecology 86(2): 528-537

Boynton WR, Kemp WM, Barnes JM, Matteson LL, Rohland FM, Jasinski DA, Kimble HL (1993) Ecosystem Processes Component Level 1 Interpretive Report No. 10. Chesapeake Biological Laboratory, University of Maryland System, Solomons, MD 20688-0038. Ref. No. [UMCEES]CBL 93-030a

Breitburg DL, Loher T, Pacey CA, Gerstein A (1997) Varying effects of low dissolved oxygen on trophic interactions in an estuarine food web. Ecological Monographs 67(4): 489-507

Brett MT, Goldman CR (1996) A meta-analysis of the freshwater trophic cascade. Proc Natl Acad Sci 93: 7723-7726

Brodeur RD, Decker MB, Ciannelli L, Purcell JE, Bond NA, Stabeno PH, Acuna E, Hunt Jr. GL (2008) Rise and fall of jellyfish in the eastern Bering Sea in relation to climate regime shifts. Prog Oceanogr 77: 103-111

Canuel EA, Spivak AC, Waterson EJ, Duffy JE (2007) Biodiversity and food web structure influence short-term accumulation of sediment organic matter in an experimental seagrass system. Limnol Oceanogr 52(2): 590-602

Cargo DG, King DR (1990) Forecasting the abundance of the sea nettle, *Chrysaora quinquecirrha*, in the Chesapeake Bay. Estuaries 13(4): 486-491

Compte J, Gascón S, Quintana XD, Boix D (2010) Top-predator effects of jellyfish *Odessia maeotica* in Mediterranean salt marshes. Mar Ecol Prog Ser 402: 147-159

Condon RH, Steinberg DK, Bronk DA (2010) Production of dissolved organic matter and inorganic nutrients by gelatinous zooplankton in the York River estuary, Chesapeake Bay. J Plankton Res 32(2): 153-170

Condon RH, Steinberg DK, del Giorgio PA, Bouvier TC, Bronk DA, Graham WM, Ducklow HW (2011) Jellyfish blooms result in a major microbial respiratory sink of carbon in marine systems. PNAS 108(25): 10225-10230

Costello JH, Bayha KM, Mianzan HW, Shiganova TA, Purcell JE (2012) Transitions of *Mnemiopsis leidyi* (Ctenophora: Lobata) from a native to an exotic species: a review. Hydrobiologia 690(1): 21-46

Cowan JH, Houde ED (1990) Growth and survival of bay anchovy *Anchoa mitchilli* larvae in mesocosm enclosures. Mar Ecol Prog Ser 68: 47-57

Daskalov GM, Grishin AN, Rodionov S, Mihneva V (2007) Trophic cascades triggered by overfishing reveal possible mechanisms of ecosystem regime shifts. PNAS 104(25): 10518-10523

de Lafontaine Y, Leggett WC (1987) Evaluation of in situ enclosures for larval fish studies. Can J Fish Aquat Sci 44: 54-65

Deason EE, Smayda TJ (1982) Ctenophore-zooplankton-phytoplankton interactions in Narragansett Bay, Rhode Island, USA, during 1972-1977. Journal of Plankton Research. 4(2):203-217

Dinasquet J, Titelman J, Møller LF, Setälä O, Granhag L, Andersen T, Båmstedt U, Maraldsson M, Hosia A, Katajisto T, Kragh T, Kuparinen J, Schrøter M-L, Søndergaard M, Tiselius P, Riemann L (2012) Cascading effects of the ctenophore *Mnemiopsis leidyi* on the planktonic food web in a nutrient-limited estuarine system. Mar Ecol Prog Ser 460: 49-61

Duffy JE, Cardinale BJ, France KE, McIntyre PB, Thébault E, Loreau M (2007) The functional role of biodiversity in ecosystems: incorporating trophic complexity. Ecol Letters 10: 522-538

Gatz AJ, Kennedy VS, Mihurski JA (1973) Effects of temperature on activity and mortality of the medusa, *Chrysaora quinquecirrha*. Chesapeake Science 14: 171–180

Hagy III JD, Boynton WR, Jasinski DA (2005) Modelling phytoplankton deposition to Chesapeake Bay sediments during winter-spring: interannual variability in relation to river flow. Est Coast Shelf Sci 62: 25-40

Hansen B, Fotel FL, Jensen NJ, Madsen SD (1996) Bacteria associated with a marine planktonic copepod in culture. II. Degradation of fecal pellets produced on a diatom, a nanoflagellate or a dinoflagellate diet. J Plankton Res 18(2): 275-288

Hosia A, Augustin CB, Dinasquet J, Granhag L, Paulsen ML, Riemann L, Rintala J-M, Setälä O, Talvitie J, Titelman J (2015) Autumnal bottom-up and top-down impacts of *Cyanea capillata*: a mesocosm study. J Plankton Res 37(5) 1042-1055

Kemp WM, Faganeli J, Puskaric S, Smith EM, Boynton WR. (1999) Pelagic-Benthic coupling and nutrient cycling. In: Coastal and Estuarine Studies- Ecosystems at the land-sea margin- Drainage Basin to coastal sea. T.C. Malone, A. Malej, L.W. Harding, N. Smodlaka, and R.E. Turner (eds.). American Geophysical Union, Washington D.C. pp. 295-339.

Kolesar SE, Breitburg DL, Purcell JE, Decker MB (2010) Effects of hypoxia on *Mnemiopsis leidyi*, ichthyoplankton and copepods: clearance rates and vertical habitat overlap. Mar Ecol Prog Ser 411: 173-188

Kremer P (1979) Predation by the Ctenophore *Mnemiopsis leidyi* in Narragansett Bay, Rhode Island. Estuaries. 2(2): 97-105

Lebrato M, Molinero J-C, Cartes JE, Lloris D, Mélin F, Beni-Casadella L (2013) Sinking jelly-carbon unveils potential environmental variability along a continental margin. PLoS ONE 8(12): e82070

Madsen CV, Riisgård HU (2010) Ingestion-rate method for measurement of clearance rates of the ctenophore *Mnemiopsis leidyi*. Aquatic Invasions 5(4): 357-361

Mazlum RE, Seyhan K (2007) Gastric emptying, clearance rate, feeding periodicity and food consumption of the Black Sea jelly fish, *Mnemiopsis leidyi* (Agassiz). Indian J of Mar Sci 36(1): 59-64

McNamara ME, Lonsdale DJ, Cerrato RM (2014) Role of eutrophication in structuring planktonic communities in the presence of the ctenophore *Mnemiopsis leidyi*. Mar Ecol Prog Ser 510: 151-165

Micheli F (1999) Eutrophication, fisheries, and consumer– resource dynamics in marine pelagic ecosystems. Science 285: 1396–1398

Nemazie DA, Purcell JE, Glibert PM (1993) Ammonium excretion by gelatinous zooplankton and their contribution to the ammonium requirements of microplankton in Chesapeake Bay. Mar Biol 116: 451–458

Pitt KA, Duarte CM, Lucas CH, Sutherland KR, Condon RH, Mianzan H, Purcell JE, Robinson KL, Uye S (2013) Jellyfish body plans provide allometric advantages beyond low carbon content. PLoS ONE 8(8): e72683

Pitt KA, Welsh DT, Condon RH (2009) Influence of jellyfish blooms on carbon, nitrogen and phosphorus cycling and plankton production. Hydrobiologia 616: 133-149

Purcell JE (1992) Effects of predation by the scyphomedusan *Chrysaora quinquecirrha* on zooplankton populations in Chesapeake Bay. Mar Ecol Prog Ser 87: 65-76

Purcell JE (2005) Climate effects on formation of jellyfish and ctenophore blooms: a review. J Mar Biol Assoc UK 85: 461–476

Purcell JE, Arai MN (2001) Interactions of pelagic cnidarians and ctenophores with fish: a review. Hydrobiologia 451: 27-44

Purcell JE, Cowan Jr. JH (1995) Predation by the scyphomedusan *Chrysaora quinquecirrha* on *Mnemiopsis leidyi* ctenophores. Mar Ecol Prog Ser 128: 63-70

Purcell JE, Cresswell FP, Cargo DG, Kennedy VS (1991) Differential ingestion and digestion of bivalve larvae by the scyphozoan *Chrysaora quinquecirrha* and by the ctenophore *Mnemiopsis leidyi*. Biol Bull 180: 103-111

Purcell JE, Decker MB (2005) Effects of climate on relative predation by scyphomedusae and ctenophores on copepods in Chesapeake Bay during 1987-2000. Limnol Oceanogr 50(1): 376-387.

Purcell JE, Nemazie DA, Dorsey SE, Houde ED, Gamble JC (1994) Predation mortality of bay anchove (*Anchoa mitchilli*) eggs and larvae due to scyphomedusae and ctenophores in Chesapeake Bay. Mar Ecol Prog Ser 114: 47-58

Purcell JE, Shiganova TA, Decker MB, Houde ED (2001) The ctenophore *Mnemiopsis* in native and exotic habitats: U.S. estuaries versus the Black Sea basin. Hydrobiologia 451: 145-176

Purcell JE, Roman MR (1994) Predation by gelatinous zooplankton and resource limitation as potential controls of *Acartia tonsa* copepod populations in Chesapeake Bay. Limnol Oceanogr 39: 263-278

Robison BH, Reisenbichler KR, Sherlock RE, Silguero JMB, Chavez FP (1998) Seasonal abundance of the siphonophore Nanomia bijuga, in Monterey Bay. Deep-Sea Res II 45: 1741–1752

Roden EE, Tuttle JH, Boynton WR, Kemp WM (1995) Carbon cycling in mesohaline Chesapeake Bay sediments 1: POC deposition rates and mineralization pathways. J Mar Res 53: 799-819

Roux J-P, van der Lingen CD, Gibbons MJ, Moroff NE, Shannon LJ, Smith ADM, Cury PM (2013) Jellyfication of marine ecosystems as a likely consequence of overfishing small pelagic fishes: Lessons from the Benguela. Bull Mar Sci 89(1): 249-284

Saba GK, Steinberg DK, Bronk DA (2011) The relative importance of sloppy feeding, excretion, and fecal pellet leaching in the release of dissolved carbon and nitrogen by *Acartia tonsa* copepods. J Exp Mar Biol Ecol 404: 47-56

Schmitz OJ, Hawlena D, Trussell GC (2010) Predator control of ecosystem nutrient dynamics. Ecol Letters 13: 1199-1209

Sexton MA, Hood RR, Sarkodee-adoo J, Liss AM (2010) Response of *Chrysaora quinquecirrha* medusae to low temperature. Hydrobiologia 645: 125-133

Silguero JMB, Robison BH (2000) Seasonal abundance and vertical distribution of mesopelagic calycophoran siphonophores in Monterey Bay, CA. J Plankton Res 22: 1139–1153

Spivak AC, Canuel EA, Duffy JE, Douglass JG, Richardson JP (2009) Epifaunal community composition and nutrient addition alter sediment organic matter

composition in a natural eelgrass *Zostera marina* bed: a field experiment. Mar Ecol Prog Ser 376: 55-67

Spivak AC, Canuel EA, Duffy JE, Richardson JP (2007) Top-down and bottom-up controls on sediment organic matter composition in an experimental seagrass ecosystem. Limnol Oceanogr 52(6): 2595-2607

Steinberg DK, Condon RH (2008) Development, biological regulation, and fate of ctenophore blooms in the York River estuary, Chesapeake Bay. Marine Ecology Progress Series 369: 153-168

Steinberg DK, Condon RH (2009) Zooplankton of the York River. Journal of Coastal Research 57: 66-79

Suchman CL, Daly EA, Keister JE, Peterson WT, Brodeur RD (2008) Feeding patterns and predation potential of scyphomedusae in a highly productive upwelling region. Mar Ecol Prog Ser 358: 161–172

Suchman CL, Sullivan BK (1998) Vulnerability of the copepod, *Acartia tonsa* to predation by the scyphomedusa *Chrysaora quinquecirrha*: effect of prey size and behavior. Mar Biol 132: 237-245

Vanni MJ (2002) Nutrient cycling by animals in freshwater ecosystems. Annu Rev Ecol Syst 33: 341-370

Verity PG, Smetacek V (1996) Organism life cycles, predation, and the structure of marine pelagic ecosystems. Mar Ecol Prog Ser 130: 277-293

West EJ, Pitt KA, Welsh DT, Koop K, Rissik D (2009) Top-down and bottom-up influences of jellyfish on primary productivity and planktonic assemblages. Limnol Oceanogr 54(6): 2058-2071

White JR, Roman MR (1992) seasonal study of grazing by metazoan zooplankton in the mesohaline Chesapeake Bay. Marine Ecology Progress Series 86: 251-261

Table 1: Mesocosm experimental set up and conditions. Dates, average environmental data, and treatments with replicates (n) listed for each experiment. Temperature, salinity, dissolved oxygen, and pH were all measured within the tank using an EXO Sonde. Chlorophyll *a* data were collected from the NOAA data buoy YRK005.40. 'Copes' = copepods and other mesozooplankton; 'Mnem' = ctenophore *Mnemiopsis leidyi*; 'Chrys' = medusa *Chrysaora quinquecirrha.* *Note, only data for treatment + Mnem, + Chrys are included in our analyses for Pilot study (see text).

Experiment	Pilot*	1	2	3	4
Dates (2015)	22-25 Jul.	3-5 Aug.	6-8 Aug.	18-20 Aug.	1-3 Sept.
Duration (h)	71	40	48	45	43
Treatments: copes only (control) + Mnem + Chrys + Mnem, + Chrys	 n=1 n=1 n=1 n=1	 n=1 n=1 n=1 n=1	 n=1 n=1 n=1 n=1	 n=2 n=2	 n=2 n=2
Temperature (°C)	29.1	28.6	28.5	27.7	27.4
Salinity	19.9	20.0	20.2	20.7	20.6
Dissolved Oxygen (mg/L)	6.8	4.4	2.5	6.3	4.4
pH	7.60	7.51	7.37	7.98	7.49
Chl *a* (µg/L)	11.2	20.3	8.9	12.5	6.7
Mean *M. leidyi* length (oral-aboral, mm)	26.9	49.0	53.1	34.7	35.9

Table 2: Comparison of exported particulate organic matter in mesocosms. Particulate organic carbon (POC) flux, particulate organic nitrogen (PON) flux, carbon to nitrogen ratio (C:N), and *A. tonsa* fecal pellet (FP) carbon for each experiment and treatment. 'Copes' = copepods and other mesozooplankton; 'Mnem' = ctenophore *Mnemiopsis leidyi*; 'Chrys' = medusa *Chrysaora quinquecirrha.*

Experiment	Treatment	POC flux (mg C day^{-1} m^{-3})	PON Flux (mg N day^{-1} m^{-3})	C:N	*A. tonsa* FP (μg C day^{-1} m^{-3})	Percent *A. tonsa* FP of total POC flux
1	Copes only (control)	0.55	0.09	5.9	2.76	0.50
1	+ Mnem	0.46	0.08	5.5	0.55	0.12
1	+ Chrys	0.39	0.08	4.9	0.79	0.20
1	+ Mnem, + Chrys	0.62	0.11	5.7	0.70	0.11
2	Copes only (control)	0.49	0.05	9.2	0.90	0.18
2	+ Mnem	0.61	0.07	8.9	1.09	0.18
2	+ Chrys	0.98	0.09	10	0.93	0.09
2	+ Mnem, + Chrys	0.47	0.04	11	0.87	0.19
3	Copes only (control) 1	0.68	0.11	6.1	40.1	5.90
3	Copes only (control) 2	0.48	0.08	6.1	41.1	8.56
3	+ Mnem 1	1.02	0.17	6.0	17.0	1.67

Table 2: Continued

Experiment	Treatment	POC flux (mg C day^{-1} m^{-3})	PON Flux (mg N day^{-1} m^{-3})	C:N	*A. tonsa* FP (μg C day^{-1} m^{-3})	Percent *A. tonsa* FP of total POC flux
3	+ Mnem 2	0.40	0.07	6.3	21.4	5.35
4	Copes only (control) 1	0.74	0.11	6.5	30.1	4.07
4	Copes only (control) 2	0.64	0.10	6.3	33.0	5.16
4	+ Mnem 1	0.55	0.09	6.3	10.7	1.95
4	+ Mnem 2	0.90	0.15	6.1	23.1	2.57
Average	All controls and treatments	0.62	0.09	6.9	14.1	2.30

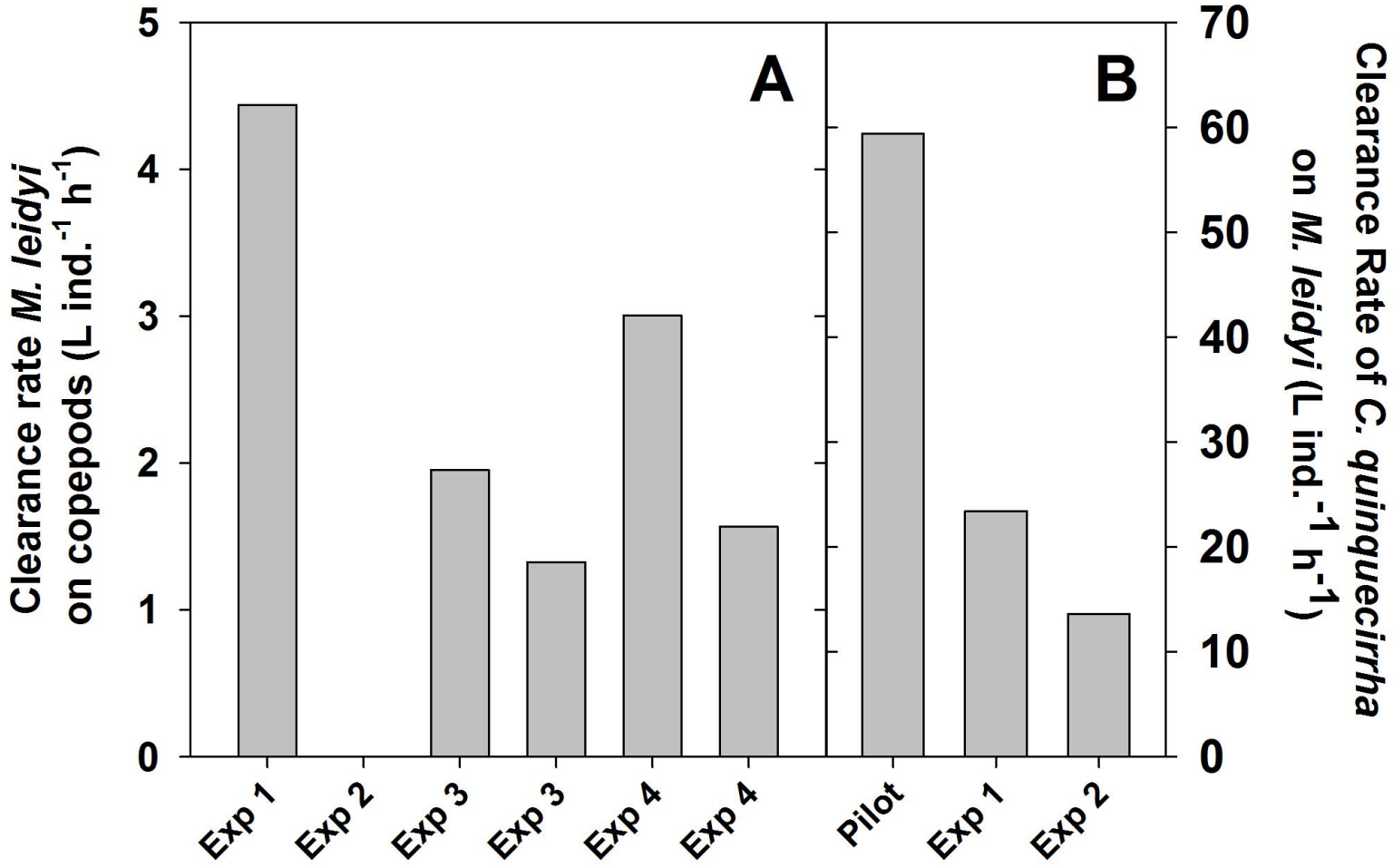

Figure 1: Clearance rates (L ind.$^{-1}$ h^{-1}) of A) copepods by *M. leidyi* and B) *M. leidyi* by *C. quinquecirrha* in each of four mesocosm experiments and one pilot experiment. Replicates from experiments 3 and 4 (see Table 1) are shown separately.

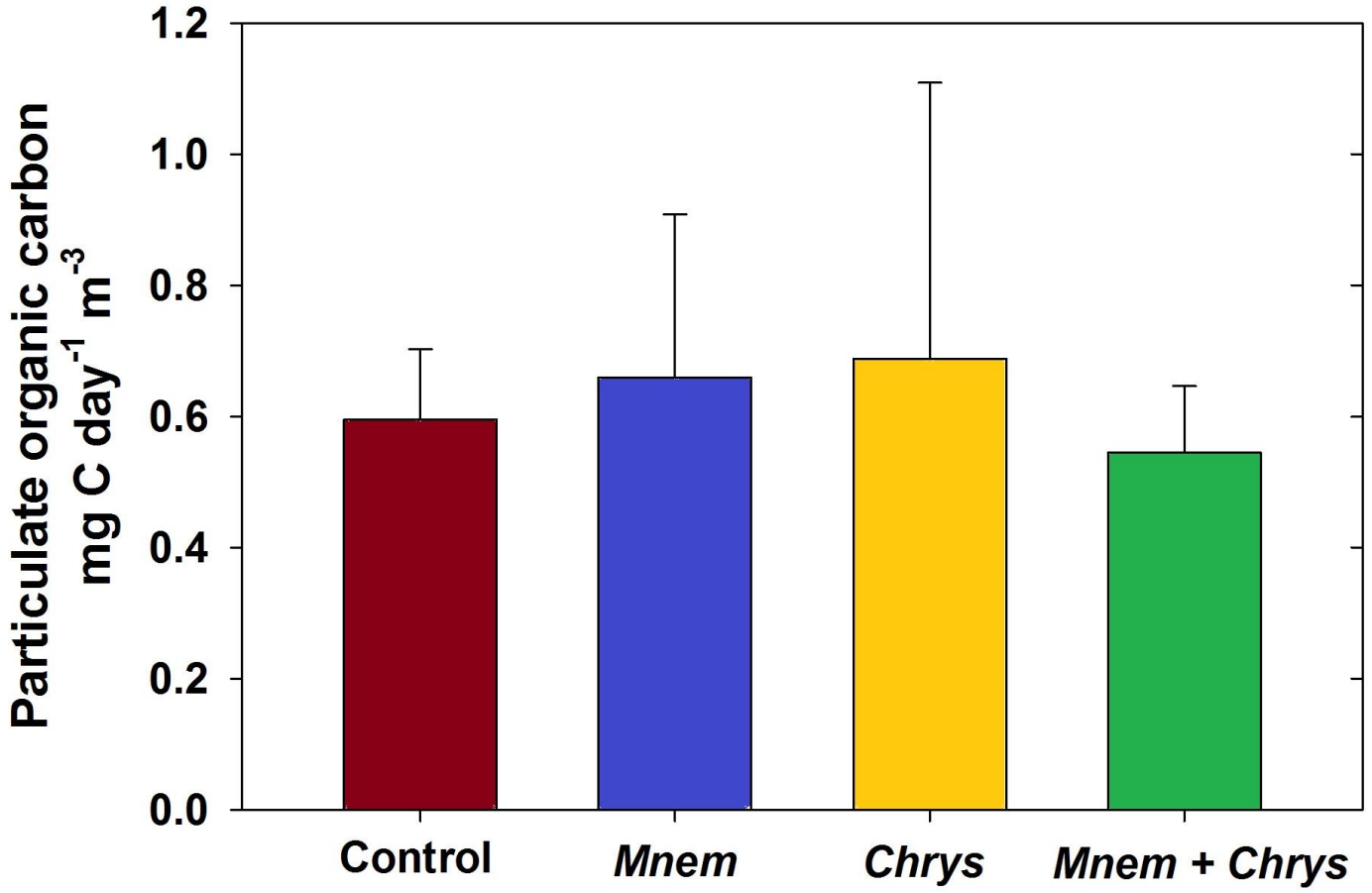

Figure 2: Total particulate organic carbon flux per day averaged for each treatment. Control (n=6) and Mnem treatments (n=6) are averaged from experiments 1, 2, 3, and 4; Chrys (n=2) and Mnem + Chrys (n=2) treatments are averaged from experiments 3 and 4. Error bars are 1 standard deviation. Control is natural assemblage of phytoplankton, microzooplankton, and copepods. 'Mnem' = *Mnemiopsis leidyi*-only, 'Chrys' = *Chrysaora quinquecirrha*-only, and 'Mnem + Chrys' = both *M. leidyi* and *C. quinquecirrha*.

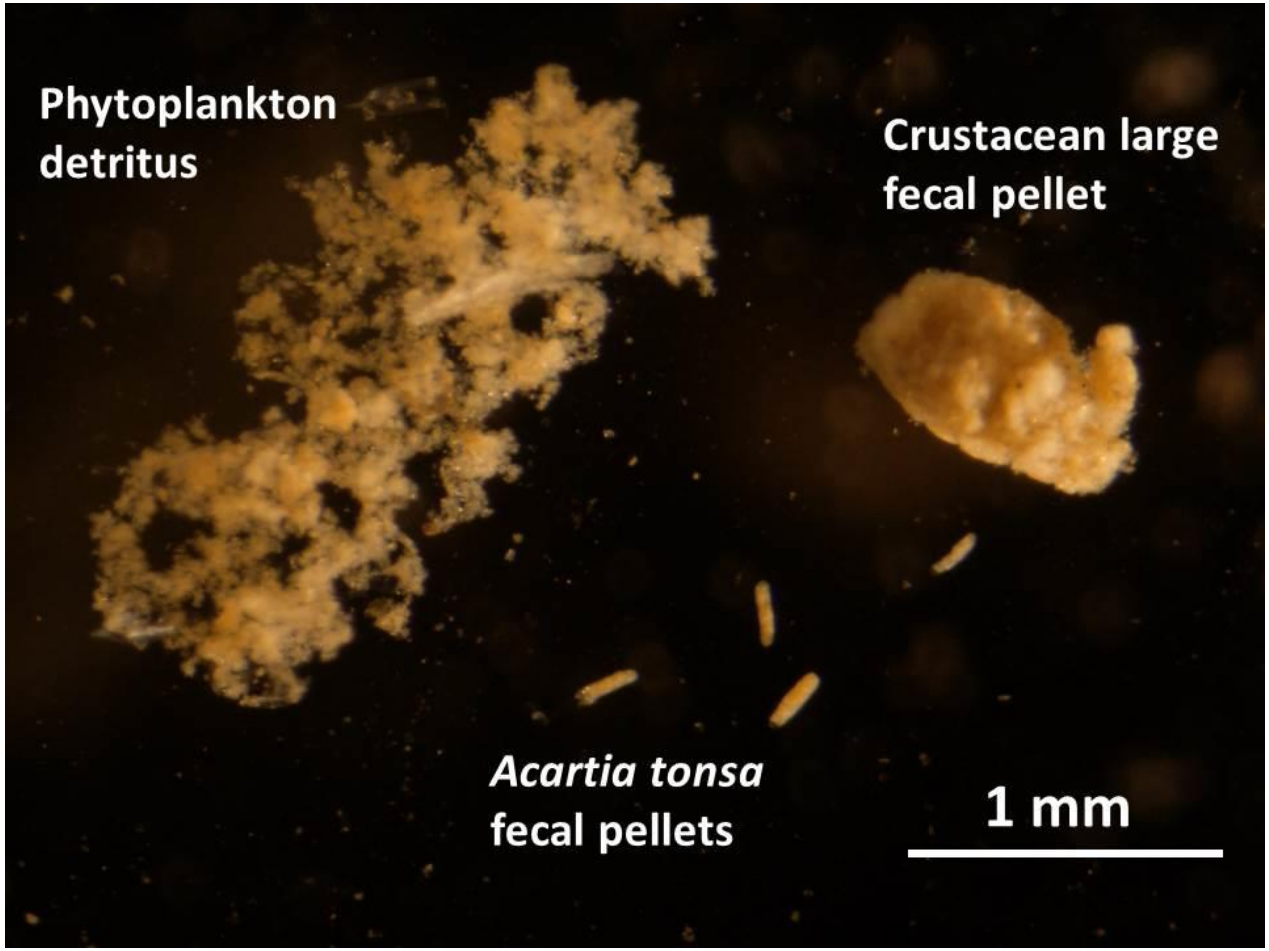

Figure 3: Examples of mesocosm sinking material, including small fecal pellets from *Acartia tonsa* copepods, a larger fecal pellet from a crustacean (likely larger copepod or decapod), and phytoplankton detritus.

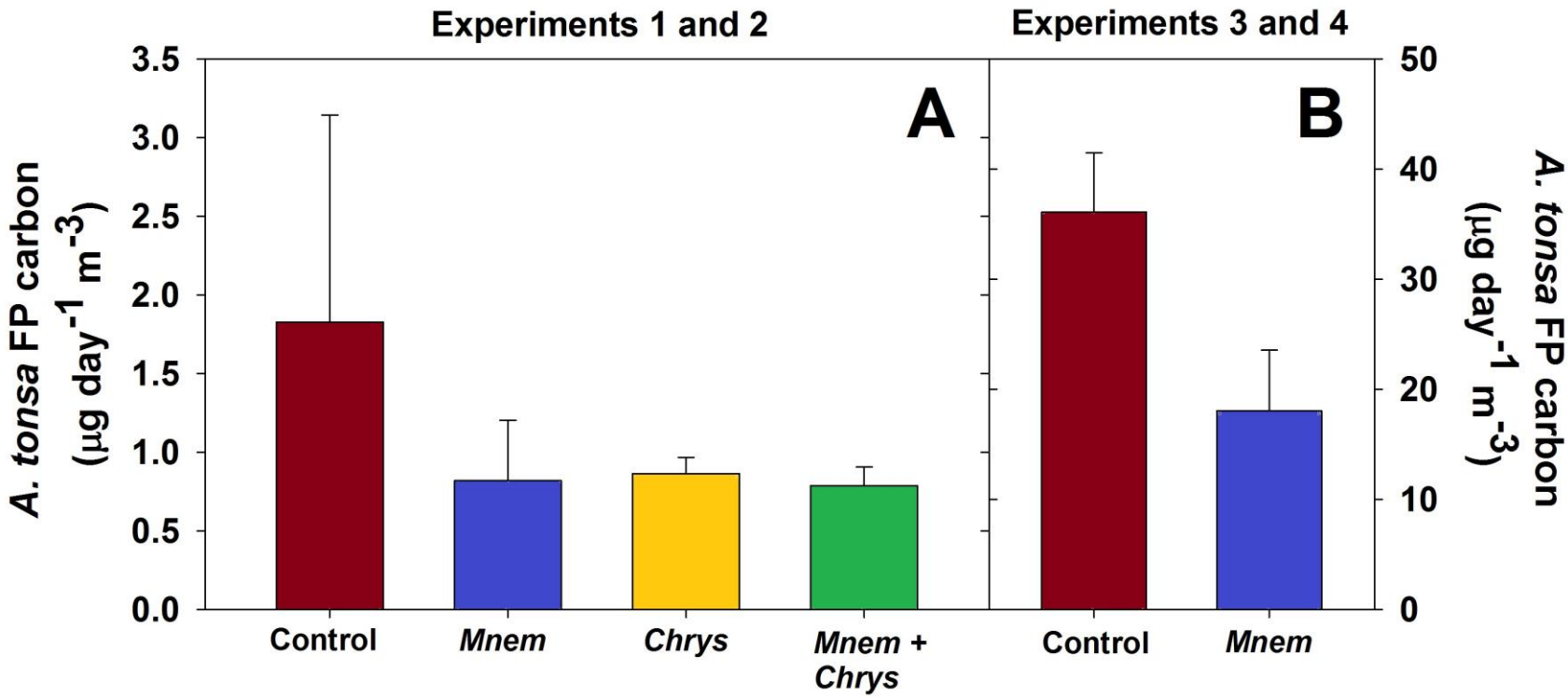

Figure 4: Comparison amongst treatments of *Acartia tonsa* fecal pellet POC production for A) average of experiments 1 and 2 (each treatment n=2), B) Average of experiments 3 and 4 (each treatment n=4). Error bars are standard deviation. Control = natural assemblage of phytoplankton, microzooplankton, and copepods, 'Mnem' = *Mnemiopsis leidyi*-only, 'Chrys' = *Chrysaora quinquecirrha*-only, and 'Mnem + Chrys' = both *M. leidyi* and *C. quinquecirrha*.

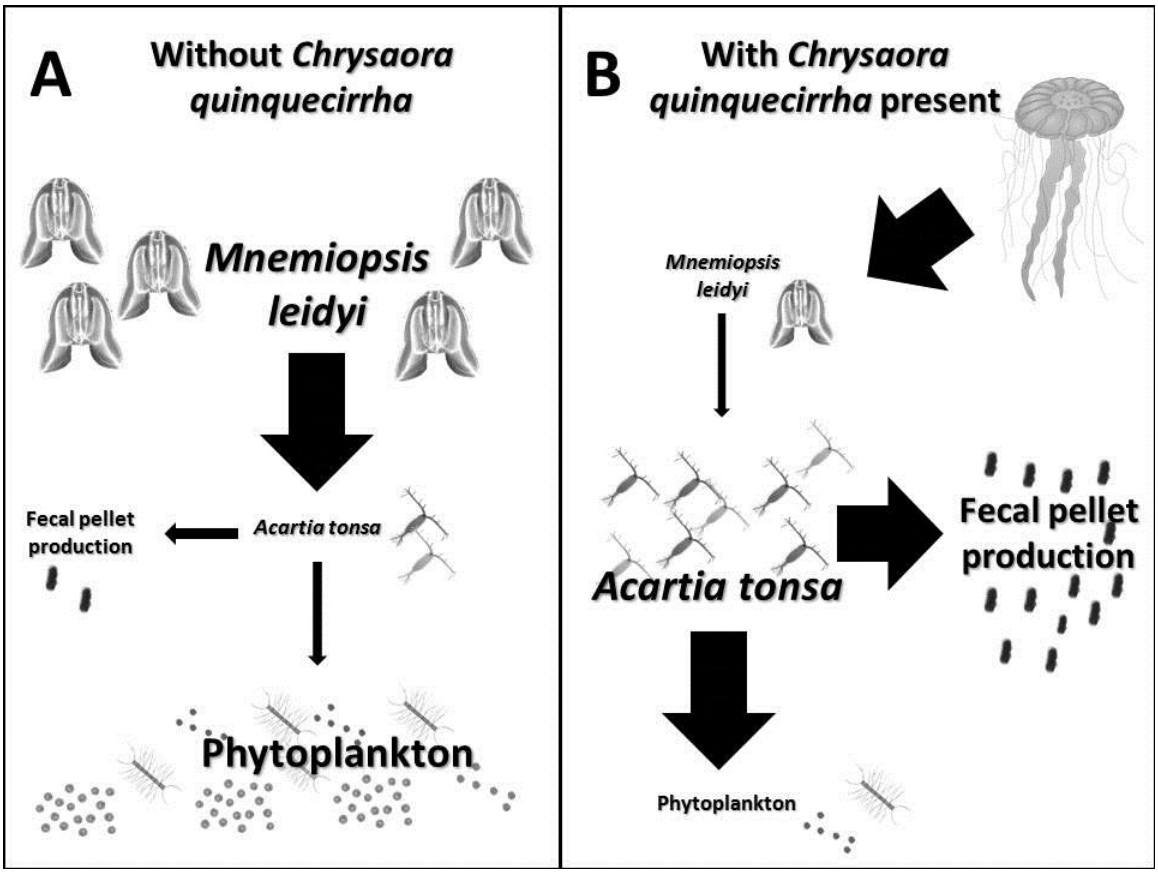

Figure 5: Conceptual diagram of the top-down effects of *Chrysaora quinquecirrha* on the relative abundances of taxa and strength of carbon transfer for the summer Chesapeake Bay ecosystem when A) *C. quinquecirrha* medusae are absent and B) *C. quinquecirrha* are present. Relative size of text and number of images represents the relative abundance of each category, and relative size of arrows represents strength of carbon transfer between categories.

CHAPTER 4

Long-term time-series study of salp population dynamics in the Sargasso Sea

This chapter published in the journal *Marine Ecology Progress Series* as:

Stone JP, Steinberg DK (2014) Long-term time-series study of salp population dynamics in the Sargasso Sea. Mar Ecol Prog Ser 510: 111-127. doi: 10.3354/meps10985

ABSTRACT

Salps are bloom-forming, pelagic tunicates with high grazing rates on phytoplankton, with the potential to greatly increase vertical particle flux through rapidly sinking fecal pellets. However, the frequency and causes of salp blooms are not well known. We quantified salps from day and night zooplankton net tows in the epipelagic zone of the North Atlantic subtropical gyre as part of the Bermuda Atlantic Time-series Study (BATS). Salp species and size were quantified in biweekly to monthly tows from April 1994 to November 2011. Twenty-one species of salps occurred at the BATS site over this time period, and the most common bloom-forming salps were *Thalia democratica*, *Salpa fusiforimis*, *Weelia* (*Salpa*) *cylindrica*, *Cyclosalpa polae*, and *Iasis zonaria*. Five species of salps exhibited diel vertical migration, and salp abundances varied seasonally, with *T. democratica*, *S. fusiformis*, and *C. polae* blooms coincident with the spring phytoplankton bloom, and *W. cylindrica* blooms occurring more often in late summer. For *T. democratica*, mean annual biomass increased slightly over the time series and was elevated every 3 yr, and biomass increased in the presence of cyclonic mesoscale eddies. Decadal climate oscillations and biogeochemical conditions influenced multi-year trends in salp abundance and biomass. Both total salp and *T. democratica* abundance were positively correlated with primary production, total salp biomass was positively correlated with the North Pacific Gyre Oscillation, and *T. democratica* biomass was negatively correlated with the Pacific Decadal Oscillation. These salp bloom dynamics have important implications for planktonic food web interactions and biogeochemical cycling.

1. INTRODUCTION

Salps are gelatinous, planktonic tunicates with a life history alternating between sexual and asexual stages, which enables them to rapidly replicate, forming high density blooms when conditions are favorable (Godeaux et al., 1998). Salps are known to form large blooms in many regions of the world's oceans, including the Sargasso Sea (Madin et al., 1996; Madin et al., 2001; Roman et al., 2002), Mediterranean Sea (Ménard et al., 1994), Southern Ocean (Atkinson et al., 2004; Loeb & Santora, 2012), western Tasman Sea (Everett et al., 2011), southwestern Atlantic (Daponte et al., 2011), and Hauraki Gulf (Zeldis et al., 1995). Salps can feed efficiently on small phytoplankton and bacteria (Bone et al., 2003), have some of the highest clearance rates of any zooplankton– up to several liters h^{-1} $salp^{-1}$ (Harbison & McAlister, 1979; Madin & Purcell, 1992; Madin & Kremer, 1995), and can consume over 100% of the daily primary production (PP) (Hereu et al., 2006). These high clearance rates contribute to salps producing large, fast-sinking fecal pellets (Caron et al., 1989; Sutherland et al., 2010b), with sinking rates ranging from 42 to 2700 m d^{-1} (Andersen, 1998; Yoon et al., 2001; Phillips et al., 2009). Because of their high fecal pellet production rates, salp blooms have a significant effect on particle export (Madin, 1982; Caron et al., 1989). This, coupled with sinking of dead carcasses (Lebrato & Jones, 2009; Henschke et al., 2013; Lebrato et al., 2013), represents an efficient and fast pathway for organic matter in the surface waters to move to depth. During a salp bloom, salps can thus be major contributors to the total carbon flux from the surface to the deep sea, as demonstrated in the Mediterranean Sea (Yoon et al., 1996; Fernex et al., 1996), Sargasso Sea (Conte et al., 2001), Southern Ocean (Phillips et al., 2009), and Tasman Sea (Henschke et al., 2013).

Salp populations are sensitive to interannual or longer-term changes in the environment (Ménard et al., 1994; Licandro et al., 2006). A long-term decrease in pelagic tunicates, particularly salps, in the California Current is attributed to a long-term increase in water column density stratification, which has weakened the eddy kinetics of the region as well as the southward flow of water and the seeding populations of salps within it (Lavaniegos & Ohman, 2007). Salp populations in some regions of the Southern Ocean have been increasing in abundance and expanding their range (Atkinson et al., 2004) as a result of long-term warming and decreases in sea ice (Vaughan et al., 2003; Stammerjohn et al., 2012). Variability in the Southern Ocean Antarctic Circumpolar Current Front causes fluctuations in salp abundance off the western Antarctic Peninsula (Loeb et al., 2010). Ménard et al. (1994) and Sutherland et al. (2010a) found salp abundance in the Mediterranean Sea declined in response to increases in temperature and stratification of the water column, which decreased mixing of nutrients to the surface and PP. Likewise, salp, doliolid, and pyrosome abundance in the South China Sea increased with an increase in chlorophyll *a* (chl *a*) concentration caused by coastal upwelling and injection of nutrients into surface waters by cold-core eddies in the summer (Li et al., 2011). While previous studies help us to understand salp population dynamics in coastal upwelling and continental shelf regions, very little is known about how salps respond to environmental changes in the open ocean.

The Sargasso Sea is an oligotrophic, open-ocean region of the western North Atlantic subtropical gyre, with patterns in the biogeochemistry of the region influenced by physical forcing with ties to decadal-scale climate oscillations (Saba et al., 2010; Álvarez-García et al., 2011; Wu et al., 2011). Long-term changes in regional

biogeochemistry of the Sargasso Sea have been documented, including: an increase in net primary productivity correlated with the North Atlantic Oscillation (NAO) (Saba et al., 2010), increases in both shallow-water particulate organic carbon export and mesopelagic zone particle attenuation in the winter-spring period (Lomas et al., 2010), and an increase in epipelagic mesozooplankton biomass (Steinberg et al., 2012). Mesoscale eddies are an important physical feature in the Sargasso Sea also affecting ecosystem structure and biogeochemical cycling. Cyclonic (cold-core) eddies are an important periodic source of nutrient injection into the euphotic zone stimulating new PP (McGillicuddy et al., 1998, 2007), leading to changes in zooplankton community structure (Eden et al., 2009) as well as an increase in mesozooplankton biomass, enhanced fecal pellet flux, and increased carbon export by diel vertical migration (DVM) (Goldthwait & Steinberg, 2008). The goals of this study are to examine seasonal, interannual, and decadal patterns in the abundance of salp species in the Sargasso Sea and to determine what physical or biogeochemical conditions lead to these patterns.

2. METHODS

2.1 Salp collection

Meszooplankton were collected as part of the Bermuda Atlantic Time-series Study (BATS) in the oligotrophic North Atlantic subtropical gyre (31°40'N, 64°10'W) (Madin et al., 2001; Steinberg et al., 2012). We identified and enumerated salps from 17 yr of the time series. Overall, 776 tows were analyzed from 238 cruises starting on April 6, 1994 and ending November 11, 2011. Mesozooplankton tows were conducted using a net with a 0.8 x 1.2 m rectangular mouth and 202 μm mesh, with replicate, double-oblique tows made during day (09:00-15:00 h) and night (20:00-02:00 h) each month (May-January) or biweekly (February-April) (Madin et al., 2001; Steinberg et al., 2012). Targeted net depth was between 150 and 200 m, and actual depth was recorded using a Vemco Minilog recorder with the exception of the first year, when depth was estimated by wire out and wire angle. Volume filtered was measured using a General Oceanics flowmeter. Tow contents were immediately split on board with one half-split size-fractionated for total mesozooplankton biomass measurements, and the other half-split preserved in 4% buffered formaldehyde for taxonomic analysis (Madin et al., 2001; Steinberg et al., 2012).

2.2 Salp enumeration and biomass determination

Salps were analyzed from archived, preserved samples using an Olympus SZX-10 dissecting microscope at 6-10x magnification under dark and bright field illumination. Salps from the entire half-split or quarter-split were identified to species and enumerated, and the oral-atrial length of each salp was measured. Samples in which small salps (e.g. *Thalia democratica*) were very abundant (>2000 salps per tow) were subsampled using a

10 ml Stempel pipette (2.5 cm in diameter) after removal of any large salps, and at least 40 individuals were measured to determine average length. This subsample was analyzed for small salps, and large salps were counted separately. Individual salp length was measured as the oral-atrial distance using an ocular micrometer, and these lengths were used in published salp live length to carbon weight regression equations for each species to calculate salp carbon biomass (see Table 5.3 in Madin & Deibel, 1998, and references therein). Total length of salps preserved in formaldehyde has been shown to decrease over time (Heron et al., 1988; Nishikawa & Terazaki, 1996). However, because this animal shrinkage is minimal and our preservation times varied, we did not correct salp length: thus our carbon biomass estimates may be conservative. Salp data are presented as total salp, *T. democratica*, *Salpa fusiformis*, *Weelia* (*Salpa*) *cylindrica*, or *Cyclosalpa polae* abundance (ind. m^{-3}) or carbon biomass (mg C m^{-3}).

2.3 Comparison to environmental parameters and data analysis

We examined potential environmental and climatological parameters influencing salp species abundance and biomass. For these analyses, salp biomass data for total salps and the 4 most abundant species on each sampling date were averaged between replicate tows and then between night and day. Average biomass for each sampling date was then compared to environmental data extracted from the BATS website (http://bats.bios.edu/) including sea-surface temperature (SST), water potential density, chl *a* integrated to 140 m, and PP integrated to 140 m (Knap et al., 1997; Steinberg et al., 2001). The water-column stratification index (WCSI) was calculated as the difference in potential density between the surface and 200 m (Steinberg et al., 2012). Salp abundance was compared to the 12-mo, centered moving average of the NAO

(www.cpc.noaa.gov/products/precip/CWlink/pna/nao/shtml), Multivariate El Niño Southern Oscillation (MEI) (www. esrl.noaa.gov/psd/people/klaus.wolter/MEI/), North Pacific Gyre Oscillation (NPGO) (http://eros/eas/gatech/edu/npgo/), and Pacific Decadal Oscillation (PDO) (http://jisao.washington/edu/pdo/) indices as described in Steinberg et al. (2012). Salp biomass anomaly was calculated for each month using the following formula:

$$A'_m = log_{10}[\frac{\bar{A}_m}{\bar{A}_i}]$$

where $\overline{A}_m$ is the average biomass for year/month *m*, and $\overline{A}_i$is the climatological median for calendar month *i*. Annual biomass anomalies were then calculated as the average of A'_m for each year (Steinberg et al., 2012), and included total salps, *T. democratica*, *S. fusiformis*, and total salps minus *T. democratica* and *S. fusiformis*.

The Spearman rank correlation coefficient was used to compare salp abundance and biomass with environmental parameters, climate indices, and date to analyze seasonal and long-term changes. Monthly time series from April 1994 to November 2011 were constructed, with one observation per month, by averaging within months that contained more than one observation. Months with missing data (n = 13 out of 212) were assigned the median measured value of that calendar month, and the smallest non-zero observation for each species was added to all observations to eliminate zeroes. The time-series data were then natural-log transformed. After constructing the time series, each species and environmental dataset was decomposed into its long-term trend (12 mo moving average), seasonal component (average of each calendar month after removing the long-term trend), and noise component (the remainder after removing both the long-term trend and seasonal component) using the *time-series* (ts) and *decompose* functions in

R 2.13.0. The Spearman rank correlation coefficients were then calculated by comparing the extracted long-term trends of each variable, and the effective degrees of freedom used in calculating significance were adjusted for autocorrelation using Eq. (1) in Pyper & Peterman (1998). In order to better examine the synergistic effects of different environmental variables on salp populations, correlations of seasonal and long-term trends were also compared using principal component analysis (PCA) in JMP 11.0.0. Bloom seasonality was analyzed by comparing the median bloom frequency between 2 seasonal periods within the year (e.g. February and March vs. the other 10 months of the year), and DVM was analyzed by comparing day and night salp abundance, both using the Mann-Whitney Rank Sum Test.

2.4 Mesoscale eddies

To examine the role that mesoscale eddies play in salp population dynamics, mesoscale eddy data in raw form were downloaded from the Cooperative Institute for Oceanographic Satellite Studies website (http://cioss.coas.oregonstate.edu/eddies/) (Chelton et al., 2011). This information included weekly eddy locations, rotation direction, amplitude, radius, and rotation speed. Using ESRI ArcGIS (version 10.0), we then determined which eddies were present at the BATS sampling location during tow sampling events. Only eddies with a total lifespan of 8 wk or more were used. As eddy location was only given weekly, any eddy that overlapped the BATS sampling site within 110% of its circumference (our own estimate to include any eddy edge effect) within 6 days of the sampling date was considered present at the time of BATS sampling. The effect of eddy type and presence on salp biomass was evaluated using an ANOVA on ranks, the Bonferroni-Dunn test was used for pairwise comparisons, and correlation

between salp biomass and eddy speed, amplitude, and radius were calculated using the Spearman rank correlation coefficient.

Additionally, eddy presence data was obtained from Mouriño-Carballido (2009), who determined eddy presence and type from 1993 to 2002 using both satellite altimetry and BATS hydrographic profiles. Mouriño-Carballido (2009) categorized eddy influence on the BATS site as cyclonic, anticyclonic, mode-water, none, or the frontal region between cyclonic and anticylconic eddies. For the purposes of our study, mode-water and anticyclonic eddies were combined into one 'anticyclonic' category, and frontal regions were delineated as no eddy present. A separate analysis was completed with these categorizations over the shorter time period, using an ANOVA on ranks to determine eddy influence on salp biomass.

3. RESULTS

3.1 Species composition and seasonality

In total, 21 species of salps were identified in the time series, with *Thalia democratica*, *Salpa fusiformis*, *Weelia* (*Salpa*) *cylindrica*, and *Cyclosalpa polae* being the most common species (present in tows from 77, 61, 21, and 16% of the 238 monthly cruises, respectively) (Fig. 1, Table 1). *Thalia democratica* was the most abundant salp species and had the highest biomass, with average abundance across all samples of the time series in day and night tows of 3.31 and 1.90 ind. m^{-3}, respectively, and biomass of 40.8 and 30.2 μg C m^{-3}, respectively. This was considerably higher than the second-most abundant and highest biomass species, *S. fusiformis*, with an average abundance in day and night tows of 1.86 x 10^{-3} and 2.56 x 10^{-2} ind. m^{-3}, respectively, and a biomass of 0.21 (day) and 3.39 (night) μg C m^{-3} (Table 1). Total salp abundance and biomass was influenced mainly by *T. democratica*, although the other 20 species contributed relatively more to total biomass than abundance (Table 1), as *T. democratica* is one of the smallest salps in the region. Qualitatively, salps were highest in biomass during the spring (February-April) throughout the entire time series, with both early and late summer peaks (July-August) as well, particularly from 1999 to 2003 (Fig. 2).

Salp 'blooms' were defined as the top 10% of biomass observations within all non-zero observations for each species. The species analyzed for blooms were *T. democratica*, *S. fusiformis*, *W. cylindrica*, and *C. polae*. All of the bloom events were more than one order of magnitude greater than the median (*T. democratica* and *S. fusiformis*) or mean (*W. cylindrica* and *C. polae*; median was zero) biomass.

Salp blooms occurred regularly, with blooms of *T. democratica*, *S. fusiformis*, and *C. polae* occurring more often in February and March, with a median total of 5.5, 4, and 1 blooms, respectively, in each of those months over the time series (Fig. 3A). The occurrence of blooms in those 2 months was significantly higher than the median occurrence in the other 10 months of the year ($p < 0.05$; Mann-Whitney Rank Sum Test). *W. cylindrica* blooms occurred more commonly in late summer (median total of 1 bloom in each of July, August, and September) compared with the rest of the year ($p = 0.002$). Blooms in all other species combined were evenly distributed throughout the year. Monthly averages of salp biomass with the long-term trend removed showed similar seasonal patterns with *T. democratica*, *S. fusiformis*, and *C. polae* peaking in the spring, *W. cylindrica* peaking in late summer, and all others remaining relatively constant throughout the year (Fig. 3B).

3.2 Diel vertical migration

Of the 21 salp species present, 5 exhibited a detectable pattern of DVM with significantly higher median biomass during the night than during the day (Fig. 4). These diel vertical migrators included 2 species of *Salpa* (*S. fusiformis*, $n = 136$, $p < 0.001$; *S. aspera*, $n = 30$, $p < 0.001$), *W. cylindrica* ($n = 48$, $p = 0.030$), *Iasis zonaria* ($n = 31$, $p < 0.001$), and *Ritteriella retracta* ($n = 11$, $p = 0.002$). Overall *T. democratica* did not demonstrate DVM (Fig. 4), with day median biomass (0.342 μg C m^{-3}) not significantly different from night median biomass (0.362 μgC m^{-3}) ($n = 165$, $p = 0.899$). When at bloom concentrations, we did detect day-night differences in *T. democratica*, with 6 blooms (out of 33) having at least 2-fold higher biomass at night compared to during the day, but also 12 blooms with at least 2-fold higher biomass in the surface waters during

the day than at night. For most other species, presence in tows was too infrequent or biomass likely too low for a significant difference between day and night to be detected.

3.3 Mesoscale eddies

A total of 56 mesoscale eddies were detected intersecting the BATS site within 6 d of a zooplankton sampling event from April 1994 to November 2011, using the Chelton and Schlax eddy data set. Of these 56 eddies, 38 were cyclonic and 18 were anticyclonic: there was no significant difference between the median amplitude, speed, and radius of the 2 eddy types (Table 2). When comparing median abundance of *T. democratica* between cyclonic, anticyclonic, and no eddies, there was a significant difference between treatments ($P = 0.017$), but there were no significant differences in pairwise comparisons. However, the median biomass of *T. democratica* was significantly higher within cyclonic eddies (0.609 μg C m^{-3}) than within anticyclonic eddies (0.129 μg C m^{-3}) (Fig. 5). Within the 38 cyclonic eddies, *T. democratica* biomass was not significantly correlated with eddy rotational speed or amplitude. No significant relationships between other salp species and eddy presence, type, or attributes were found.

Using the Mouriño-Carballido (2009) eddy determinations, a total of 48 sampling events between April 1994 and December 2001 were eddy influenced, with 31 cyclonic eddies and 17 anticyclonic eddies. The median biomass of *T. democratica* was significantly higher within cyclonic eddies (0.638 μg C m^{-3}) than within anticyclonic eddies (0.165 μg C m^{-3}) or in the absence of eddies (0.202 μg C m^{-3}, Fig. 5). No significant relationships between other salp species and eddy presence or type were found.

3.4 Long-term trends

There was no significant long-term positive or negative trend in total salp biomass over the 17 yr time series; however, over the time series there were weak, but significant, increases in both *T. democratica* and *C. polae* biomass, and in water column stratification index (WCSI) (Fig. 6A, B, and C, respectively). The linear increase in WCSI is due to both a significant increase in SST and a coinciding decrease in temperature from 300 to 600 m depth ($R^2 = 0.25$, $p < 0.0001$, for both) over the time series. The increases in salp biomass were log-linear and represented an increase of 0.01 μg C m^{-3} yr^{-1} for *T. democratica* and 0.003 μg C m^{-3} yr^{-1} for *C. polae*. Mean annual biomass anomalies for *T. democratica* (Fig. 7B) were consistently positive over the last 6 yr of the time series, and for *S. fusiformis* were strongly negative over the last 4 yr (Fig. 7C). Additionally, there was a distinct shift after 2000 ($t = -3.413$, $P = 0.004$) from consistently negative to positive anomalies in total salps other than *T. democratica* and *S. fusiformis* (Fig 7D).

Additionally, a cyclical pattern in *T. democratica* biomass was evident, with average annual biomass increasing by 3-7 orders of magnitude every 3 yr (Fig. 8). This cycle is supported by the spectral density of the *T. democratica* biomass long-term trend, which was highest in value at a period of 33.3 mo (Fig. 8, inset). This pattern is mostly driven by larger spring blooms of *T. democratica* during these peak years, but also by elevated biomass throughout the year, and occasional non-spring blooms.

3.5 Environmental and climate influences

Total salp seasonality was most closely grouped with integrated PP in the PCA of seasonality in salps and environmental parameters (Fig. 9A). Additionally, *T. democratica* and *S. fusiformis* were closely grouped with PP and chl *a* concentrations. These 2 species were also seasonally negatively correlated with SST and the WCSI. *C.*

polae was weakly negatively correlated with SST and the WCSI. *W. cylindrica* and all salps other than the 'top' (highest biomass) 4 species grouped together, and were most strongly, and negatively, correlated with 300-600 m water temperature, although this only explained a small portion of their variability.

Long-term trends in salp biomass were significantly correlated with several environmental parameters (Table 3, Fig. 9B). However, the variance explained by components 1 and 2 of the PCA (Fig. 9B) is low, suggesting a complex system poorly represented by the first two components alone. Both SST the WCSI were positively correlated with *T. democratica* and *C. polae* biomass (Table 3). Additionally, *T. democratica* and *C. polae* were positively correlated with SST in the PCA (Fig. 9B). PP was negatively correlated with biomass of *S. fusiformis*, *C. polae*, and *W. cylindrica* (Table 3), but strongly positively correlated with total salp and *T. democratica* abundance (Table 3, Fig. 9B). Integrated chl *a* was negatively correlated with *W. cylindrica* and weakly so with biomass of less abundant salp species (Table 3). Chl *a* was positively correlated with *C. polae* biomass and abundance and *S. fusiformis* abundance (Table 3). Lower mesopelagic temperatures corresponded with higher biomass of total salps, *T. democratica*, *S. fusiformis*, *C. polae*, and other less abundant species (Table 3).

We compared the long-term trend of biomass of total salps, *T. democratica*, *S. fusiformis*, *W. cylindrica*, *C. polae*, and all other salp species combined with the 12-month moving average of 4 decadal climate indices (Table 4, Fig. 10). Total salp biomass was most strongly, and positively, correlated with the NPGO (Fig. 10A). *T. democratica* was most strongly, and negatively, correlated with the PDO (Fig. 10B). *S. fusiformis* was significantly positively correlated with the PDO (Fig. 10C), while all other

salps combined was most strongly positively correlated with the NPGO (Fig. 10D). Significant correlations between other salp species and climate indices can be found in Table 4.

4. DISCUSSION

4.1 Salp species composition and seasonality

We found a total of 21 species of salps present in the entire time series, compared to 16 species over 2 cruises in late summer and spring of 1989-1990 (Madin et al., 1996) and 20 species throughout the year in 1967-1972 (van Soest, 1975) in the BATS region. Of the 25 salp species van Soest (1998) reports to occur throughout the northwestern Atlantic Ocean, only 4 species were not present at the BATS site: *Salpa younti*, *Brooksia bermeri*, *Cyclosalpa bakeri*, and *Cyclosalpa foxtoni*. The most common species at the BATS site were *Thalia democratica* and *S. fusiformis,* with other species such as *Weelia* (*Salpa*) *cylindrica, C. polae, Iasis zonaria,* and *S. aspera* seasonally abundant. While van Soest (1975) and Madin et al. (1996) did not measure absolute abundance of salps, the relative abundances of species that they observed were similar to those we found. In the BATS time series, total salp abundance reached as high as 371 ind. m^{-3} (during a *T. democratica* bloom), which is comparable to documented maxima of 150 ind. m^{-3} for the Bay of Bengal (Madhupratap et al., 1980), 300 ind. m^{-3} for the Agulhas Bank (Gibbons, 1997), and 100 ind. m^{-3} in the South Atlantic Bight of the USA (Paffenhöfer & Lee, 1987). However, this is lower than off of southeast Australia where abundance exceeded 2444 ind. m^{-3} for *T. democratica* in a bloom event within an eddy (Henschke et al., 2011). The second most common species, *S. fusiformis*, reached 0.96 ind. m^{-3}, which is comparable to a *S. fusiformis* maximum of 1.6 ind. m^{-3} in coastal Taiwan (Tew & Lo, 2005) and 2 ind. m^{-3} in the Humboldt Current (González et al., 2000). But this is much lower than ~700 *S. fusiformis* ind. m^{-3} found in the North Atlantic west of Ireland (Bathmann, 1988) and 225 ind. m^{-3} off northwest Spain (Huskin et al., 2003).

There was a distinct seasonality in salp blooms, with 3 of the 4 most abundant species (*T. democratica*, *S. fusiformis*, and *C. polae*) blooming more commonly in February and March (spring), coinciding with the seasonal increase in primary production and chlorophyll biomass (Steinberg et al., 2001; Lomas et al., 2013). In contrast, *W. cylindrica* bloomed more frequently in late summer, suggesting that other processes are responsible for their rapid population increase. Similarly, Madin et al. (1996) found *W. cylindrica* present in August but absent in March and April, although van Soest (1975) found *W. cylindrica* present in low abundances year-round. Other salp species were more variable in their bloom seasonality and showed no overall trend.

4.2 Environmental influences

Environmental parameters such as SST and water column stratification (which in turn influence mixing and PP) are important seasonal regulators of salp abundance at BATS. The BATS region is characterized by a spring phytoplankton bloom in January-March that follows a period of winter mixing (Steinberg et al., 2001). Abundance and biomass of 3 of the 4 most common species of salps at BATS (*T. democratica*, *S. fusiformis*, and *C. polae*) respond to this seasonal bottom-up forcing, as shown by the increase in their abundance with increasing chl *a* and PP, and the more frequent occurrence of blooms in early spring than at other times of the year. Correspondingly, seasonally lower SST and reduced stratification, typical of conditions at the onset of the spring bloom, result in higher abundance of these 3 salp species. This response of salps to the spring phytoplankton bloom is similar to that in other systems, including *T. democratica* off the southern Atlantic coast of the USA (Deibel & Paffenhöfer, 2009) and in the Tasman Sea (Heron, 1972), *S. fusiformis* off northwestern Spain (Huskin et al.,

2003), and both *T. democratica* and *S. fusiformis* in the western Mediterranean Sea (Ménard et al., 1994). In some coastal systems, the correlation between chl *a* and salp abundance becomes negative at very high chl *a* concentrations (Zeldis et al., 1995; Liu et al., 2012) presumably due to the clogging of the salp's mucous feeding net (i.e., at chl *a* concentrations > 1 μg l^{-1}, Harbison et al.,1986). However, phytoplankton biomass in the oligotrophic BATS region, typically ranging from 0 to 0.8 μg l^{-1} (Steinberg et al., 2001; Lomas et al., 2013), rarely would approach the level required to negatively impact salp feeding.

In contrast to other salps species, *W. cylindrica* abundance was positively correlated with both SST and water column stratification, while it was not significantly correlated with chl *a*, and was most abundant during the late summer (July, August, and September). This difference in seasonal abundance may be due to *W. cylindrica's* apparent preference for warm tropical waters. *W. cylindrica* is not reported in waters colder than 17 °C (van Soest, 1975), and Harbison & Campenot (1979) experimentally determined that *W. cylindrica* stopped swimming at temperatures colder than ~5 °C. However, Harbison & Campenot (1979) also reported that *C. polae* demonstrated a response to cold temperatures similar to that of *W. cylindrica*. This is in contrast to our results, which indicate higher *C. polae* abundance in cool, high-phytoplankton biomass conditions, suggesting that food availability has more influence than temperature on *C. polae* abundance.

4.3 Diel vertical migration (DVM)

Five species (*S. fusiformis*, *I. zonaria*, *S. aspera*, *Riitteriela retracta*, and *W. cylindrica*) exhibited clear DVM, with significantly higher night vs. day biomass in the

top 150 m. Madin et al. (1996) also found DVM off Bermuda in *S. fusiformis*, *I. zonaria*, *S. aspera*, and *R. retracta*, but additionally in *Ihlea punctata*. In the slope waters of the NE USA, *S. aspera* also exhibited DVM (Madin et al., 2006). The most abundant vertically migrating species, *S. fusiformis*, was also negatively correlated with mesopelagic zone temperature (300-600 m), suggesting that warming of waters at typical daytime residence depths for vertical migrators in the region (e.g. Steinberg et al., 2000, 2012; Bianchi et al., 2013) could have a negative impact on *S. fusiformis* populations, such as increasing their metabolism at depth. While the most abundant species, *T. democratica* did not exhibit DVM during times of average or low abundance, there was an indication of DVM (both 'normal' and reverse) during different large *T. democratica* blooms. However, this is likely an artifact of horizontal movement of the salps and not vertical, as extremely high abundances could amplify the patchiness of the bloom. This is supported by both 'normal' and reverse *T. democratica* DVM on different sampling days during individual blooms in both 1996 and 2011. Other studies in the Agulhas Bank (Gibbons, 1997), off SW Taiwan (Tew & Lo, 2005), and in the Kuroshio current (Tsuda & Nemoto, 1992) found that *T. democratica* did not exhibit DVM and generally stayed within the upper 200m. Thus, we conclude that the diel differences we detected in *T. democratica* were likely due to bloom patchiness and that *T. democratica* likely does not undergo significant DVM.

4.4 Mesoscale Eddies

Mesoscale eddies can enhance nutrient upwelling and PP in the BATS region (McGillicuddy et al., 2007; Mouriño-Carballido, 2009) as well as the oligotrophic North Pacific gyre (Landry et al., 2008). Eddy presence can also lead to increases in biomass

and changes in the community composition of mesozooplankton (Goldthwait & Steinberg, 2008; Eden et al., 2009). The only salp species that significantly changed in biomass in response to mesoscale eddies was *T. democratica*, which had elevated biomass in cyclonic eddies compared to the absence of eddies or anticyclonic eddies (Fig. 5). The first eddy data set we used (Chelton et al., 2011) does not distinguish between the 2 anticyclonic eddy types: anticyclonic eddies that are downwelling, and anticyclonic mode-water eddies with isopycnal displacement and upwelling. However, when using the Mouriño-Carballido (2009) data which do distinguish these eddy types, we found no significant difference between *T. democratica* median biomass between anticylonic mode-water and anticyclonic eddies, although the low number of anticyclonic eddies (4) may be an insufficient sample size with which to detect a significant difference.

Increases in *T. democratica* biomass in response to cyclonic mesoscale eddies may be the result of several processes. Everett et al. (2011) reported *T. democratica* blooming within a 30 km cold-core, cyclonic eddy off southeast Australia, with an estimated abundance of over 5000 ind. m^{-3}. This high abundance of salps in the cyclonic eddy was linked to an uplift of the nutricline and elevated fluorescence (Everett et al., 2011). While an increase in salps and other zooplankton in cyclonic eddies compared with the absence of eddy perturbation might be predicted, it is less clear why *T. democratica* was the only salp species to significantly increase in biomass in eddies. It is possible that only this most abundant species occurs in numbers large enough to detect differences between eddy types and that other salps may be responding to eddy perturbation as well. Alternatively, differences in phytoplankton community structure between eddy types may play a role. Previous studies showed that in anticyclonic mode-

water eddies in the BATS region there was an increase in the percentage of larger phytoplankton such as diatoms and dinoflagellates (2-200 μm), while in cyclonic eddies there was an increased percentage of cyanobacteria such as *Synechococcus* and *Prochlorococcus* (0.5-1.5 μm) (Sweeney et al., 2003; Mouriño-Carballido, 2009). If *T. democratica* can outcompete other salp species in cyanobacteria-dominated phytoplankton assemblages, this shift in phytoplankton may explain why only *T. democratica* increased in the presence of cyclonic eddies. Although early studies showed that smaller salps could feed more efficiently on smaller particles (Harbison & McAlister, 1979; Kremer & Madin, 1992) and that *T. democratica* can feed on bacteria (Mullin, 1983), a recent study shows that at least one large salp (*Pegea confoederata*) can also feed on sub-micrometer particles (Sutherland et al., 2010b).

4.5 Long-term trends

The only significant long-term trends in salp abundance or biomass at BATS were slight increases in *T. democratica* and *C. polae* biomass. While the trend in *T. democratica* was consistent over the time series, the trend in *C. polae* is mostly driven by the extremely low concentrations during the first 2 yr of the study. For *T. democratica*, the increase was equivalent to an integrated (0-150 m) biomass increase of 1.43 μg C m^{-2} yr^{-1} or ~10.0 μg dry weight m^{-2} yr^{-1} (assuming C = 12.8% dry weight; Madin et al., 1981), and represents an increase of ~0.17 mg dry weight m^{-2} (85%) over the 17 yr time series. While this increase is small compared to an increase of 10.7 mg dry weight m^{-2} in total mesozooplankton biomass at BATS over the same time period (Steinberg et al., 2012), any shift in the baseline of salp biomass will have larger impacts seasonally at bloom concentrations. Significant long-term changes in salp abundance have been documented

in other regions, including a long-term decrease in the California Current (Lavaniegos & Ohman, 2007) and a range expansion in the Southern Ocean (Atkinson et al., 2004). In other regions, salp abundance was positively associated with changes in primary production (Baird et al., 2011; Li et al., 2011).

There has been a 2% increase per year in net PP from 1989 to 2007 at BATS (Saba et al., 2010). This may be driving the long-term increase in *T. democratica*, as suggested by the significant positive correlation with long-term trends in primary production and their close grouping in the PCA of long-term trends. Chl *a* was not as good a predictor of salp biomass; while PP and chl *a* are significantly positively correlated at BATS over the long term ($p < 0.001$), salps at bloom abundances may quickly deplete chl *a* concentrations. Interestingly, long-term trends in both *T. democratica* and *C. polae* are positively correlated with the WCSI which has also been increasing over the time series. While an increase in the WCSI would reduce the amount of mixing and nutrient influx into surface waters, this overall increase may not be affecting winter-time advective mixing, which is most important for driving the BATS spring phytoplankton bloom (Lomas et al., 2010; Lomas et al., 2013).

In addition to a long-term increase, there were unusually large spring blooms of *T. democratica* every third year starting in 1996, as well as elevated biomass of this species throughout the rest of that year. No other salp species showed a similar cycle of blooms or abundance. Globally, salps have been shown to follow approximately a 4 yr cycle of high and low relative abundance (Condon et al., 2013, their supplementary Fig. S2C). Condon et al. (2013) posit that this may be related to the 4.4 yr quasi-cycle of high tidal levels based on the lunar perigee (the closest distance the moon is to Earth; Haigh et

al., 2011), during which an increase in internal tidal wave energy causes an increase in turbulence and mixing over the deep ocean (Garrett, 2003). However, we have no mechanistic evidence of a link between this 4.4 yr cycle of increased mixing and the slightly offset 3 yr cycle of *T. democratica* we detected, and no other explanation for the pattern.

4.6 Climate oscillations

Decadal climate oscillations play an important role in regulating long-term trends in physical forcing and biological response in the North Atlantic (Greene et al., 2003) and specifically in the BATS region (Krause et al., 2009; Lomas et al., 2010; Saba et al., 2010; Steinberg et al., 2012). The phase of the NAO influences the ecology of the North Atlantic through changes in temperature, circulation patterns, and wind intensity (Ottersen et al., 2001). In the BATS region, a negative phase in the NAO results in increased storm activity (Dickson et al., 1996), which causes an increase in the frequency of mixing in the region (Lomas et al., 2010). This increased mixing leads to an increase in primary production (Saba et al., 2010), higher chl *a* (Lomas et al., 2010), and increased mesozooplankton biomass (Steinberg et al., 2012). In our analysis a negative NAO correlated with an increase in chl *a* and biomass and abundance of *C. polae*, but not with an increase in biomass of the 3 most abundant species of salps.

Due to climate teleconnections between the North Atlantic and other ocean basins (Kucharski et al., 2006; Müller et al., 2008), PP and mesozooplankton biomass are also positively correlated with the NPGO (Saba et al., 2010; Steinberg et al., 2012). The NPGO was positively correlated with long-term trends in total salp biomass and

abundance. The other Pacific climate indices, MEI and PDO, both decreased while total salp biomass, abundance, and the NPGO increased. This suggests that salp biomass is influenced through a similar mechanism by the 3 Pacific indices while the NAO has little or no effect on long-term trends in salp biomass. *Thalia democratica* was also significantly correlated with the Pacific oscillation indices but not with the NAO, again suggesting that variability in these climate indices affects physical forcing ultimately leading to salp blooms in the BATS region in different ways. The PDO was negligibly correlated with long-term trends in *S. fusiformis* and no climate index was correlated with *W. cylindrica* biomass. It is likely that the processes affecting their long-term trends are unrelated to the mechanism linking the Pacific indices and *T. democratica*. El Niño Southern Oscillation (ENSO) forcing affects Southern Ocean salp populations (*S. thompsoni*), but the nature of the environmental conditions driven by this forcing leading to years with large summer blooms of *S. thompsoni* is still unknown (Loeb & Santora, 2012). Similarly, the mechanism by which forcing associated with these Pacific climate oscillations affect changes in BATS region ecology remains to be determined.

5. SUMMARY AND CONCLUSION

The high diversity and seasonal increase in abundance of salps in the BATS region has important implications for trophic interactions in the planktonic food web, as during blooms, salps periodically make up more than 90% of the mesozooplankton biomass. Grazing by salp blooms and competition with other mesozooplankton could alter the phytoplankton and zooplankton community structure in ways that persist after the salp blooms have died off by changing the relative ratios of different phytoplankton groups. These high abundances, coupled with the high filtration rates of salps, could also efficiently transfer carbon to the deep pelagic ocean and benthos, through rapid sinking of their large fecal pellets, sinking of salp carcasses, and active transport by DVM. In conjunction with a long-term increase in PP at BATS, there has been a corresponding long-term increase in *T. democratica* and *C. polae* biomass, and long-term trends in other species may emerge as the data set continues. Salp populations are clearly sensitive to both seasonal and multi-year changes in environmental conditions, and each species responds uniquely to environmental changes. While the links between climate oscillations and changes in salp populations need to be further explored, increased warming of the oceans and resultant changes in decadal climate oscillations could lead to future changes in salp abundance.

Acknowledgments

We are grateful to the many Bermuda Atlantic Time-series Study (BATS) technicians and personnel involved in the sampling and maintenance of the zooplankton time series over the last two decades. We appreciate the support of the officers and crew of the R/V *'Weatherbird II*' and the R/V *'Atlantic Explorer*' for help with sample collection. Special

thanks goes to Joseph Cope for assistance with data management and analysis and to Rob Condon for helpful discussions about our results. The BATS zooplankton time series was initially funded by National Science Foundation (NSF) grant OCE-9202336 to L.P. Madin, and continued by the BATS program through the NSF Chemical and Biological Oceanography programs (OCE-9301950, OCE-9617795, and OCE-0326885), and through OCE-0752366 and OCE-1258622 to D.K.S., which funded this current effort. This is Contribution No. 3396 of the Virginia Institute of Marine Science, The College of William and Mary.

REFERENCES

Álvarez-García FJ, Ortiz-Bevia MJ, Cabos-Narvaez WD (2011) On the structure and teleconnections of North Atlantic decadal variability. J Climate 24: 2209-2223

Andersen V (1998) Salp and pyrosomid blooms and their importance in biogeochemical cycles. In Bone Q [ed.], The biology of pelagic tunicates. Oxford University Press. p 125-137

Atkinson A, Siegel V, Pakhomov E, Rothery P (2004) Long-term decline in krill stock and increase in salps within the Southern Ocean. Nature 432: 100–103

Baird ME, Everett JD, Suthers IM (2011) Analysis of southeast Australian zooplankton observations of 1938-42 using synoptic oceanographic conditions. Deep-Sea Res Pt II 58: 699-711

Bathmann UV (1988) Mass occurrence of *Salpa fusiformis*, in the spring of 1984 off Ireland: implications of sedimentation processes. Mar Biol 97: 127–135

Bianchi D, Galbraith ED, Carozza DA, Mislan KAS, Stock CA (2013) Intensification of open-ocean oxygen depletion by vertically migrating animals. Nat Geosci 6: 545-548

Bone Q, Carre C, Chang P (2003) Tunicate feeding filters. J Mar Biol Assoc UK 83: 907–919Caron DA, Madin LP, Cole JJ (1989). Composition and degradation of salp fecal pellets:

implications for vertical flux in oceanic environments. J Mar Res 47: 829-850

Chelton DB, Schlax MG, Samelson RM (2011) Global observations of nonlinear mesoscale eddies. Prog Oceanogr 91: 167-216

Condon RH, Duarte CM, Pitt KA, Robinson KL, Lucas CH, Sutherland KR, Mianzan

HW, Bogeberg M, Purcell JE, Decker MB, Uye S, Madin LP, Brodeur RD, Haddock SHD, Malej A, Parry GD, Eriksen E, Quiñones J, Acha M, Harvey M, Arthur JM, Graham WM (2013) Recurrent jellyfish blooms are a consequence of global oscillations. P Natl Acad Sci USA 110(3): 1000-1005

Conte MH, Ralph N, Ross EH (2001) Seasonal and interannual variability in deep ocean particle fluxes at the Oceanic Flux Program (OFP)/Bermuda Atlantic Time Series (BATS) site in the western Sargasso Sea near Bermuda. Deep-Sea Res Pt II 48: 1471-1505

Daponte MC, Calcagno JA, Acevedo-Luque MJJ, Martos P, Machinandiarena L, Esnal GB (2011) Composition, density, and biomass of Salpidae and Chaetognatha in the southwestern Atlantic Ocean (34.5^{o}S-39^{o}S). B Mar Sci 87(3): 437-461

Deibel D, Paffenhöfer G-A (2009) Predictability of patches of neritic salps and doliolids (Tunicata, Thaliacea). J Plankton Res 31(12): 1571-1579

Dickson R, Lazier J, Meincke J, Rhines P, Swift J (1996) Long-term coordinated changes in the convective activity of the North Atlantic. Prog Oceanogr 38: 241-295

Eden BR, Steinberg DK, Goldthwait SA, McGillicuddy DJ (2009) Zooplankton community structure in a cyclonic and mode-water eddy in the Sargasso Sea. Deep-Sea Res Pt I 56: 1757-1776

Everett JD, Baird ME, Suthers IM (2011) Three-dimensional structure of a swarm of the salp *Thalia democratica* within a cold-core eddy off southeast Australia. J Geophys Res 116: C12046

Fernex FE, Braconnot JC, Dallot S, Boisson M (1996) Is ammonification rate in marine

sediment related to plankton composition and abundance? A time-series study in Villefranche Bay (NW Mediterranean). Estuar Coast Shelf S 43: 359-371

Garrett C (2003) Internal tides and ocean mixing. Science 301: 1858-1859

Gibbons M J (1997) Vertical distribution and feeding of *Thalia democratica*, on the Agulhas Bank during March 1994. J Mar Biol Assoc UK 77: 493–505

Godeaux J, Bone Q, Braconnot JC (1998) Anatomy of Thaliacea. In Bone Q [ed.], The biology of pelagic tunicates. Oxford University Press, p 1-24

Goldthwait SA, Steinberg DK (2008) Elevated biomass of mesozooplankton and enhanced fecal pellet flux in cyclonic and mode-water eddies in the Sargasso Sea. Deep-Sea Res Pt II 55: 1360-1377

González HE, Sobarzo M, Figueroa D, Nöthig E-M (2000) Composition, biomass and potential grazing impact of the crustacean and pelagic tunicates in the northern Humboldt Current area off Chile: differences between El Niño and non-El Niño years. Mar Ecol-Prog Ser 195: 201–220

Greene CH, Pershing AJ, Conversi A, Planque B, Hannah C, Sameoto D, Head E, Smith PC, Reid PC, Jossi J, Mountain D, Benfield MC, Wiebe PH, Durbin E (2003) Trans-Atlantic responses of *Calanus finmarchicus* populations to basin-scale forcing associated with the North Atlantic Oscillation. Prog Oceanogr 58: 301-312

Haigh ID, Eliot M, Pattiaratchi C (2011) Global influences of the 18.61 year nodal cycle and 8.85 year cycle of lunar perigee on high tidal levels. J Geophys Res 1 16: C06025

Harbison GR, Campenot RB (1979) Effects of temperature on the swimming of salps

(Tunicata, Thaliacea): Implications for vertical migration. Limnol Oceanogr 24(6): 1081-1091

Harbison GR, McAlister VL (1979) The filter-feeding rates and particle retention efficiencies of three species of *Cyclosalpa* (Tunicata, Thaliacea). Limnol Oceanogr 24: 875-892

Harbison GR, McAlister VL, Gilmer RW (1986) The response of the salp, *Pegea confoederata*, to high levels of particulate material: Starvation in the midst of plenty. Limnol Oceanogr 31(2): 371-382

Henschke N, Bowden DA, Everett JD, Holmes SP, Kloser RJ, Lee RW, Suthers IM (2013) Salp-falls in the Tasman Sea: a major food input to deep-sea benthos. Mar Ecol-Prog Ser 491: 165-175

Henschke N, Everett JD, Baird ME, Taylor MD, Suthers IM (2011) Distribution of life-history stages of the salp *Thalia democratica* in shelf waters during a spring bloom. Mar Ecol-Prog Ser 430: 49-62

Hereu CM, Lavaniegos BE, Gaxiola-Castro G, Ohman MD (2006) Composition and potential grazing impact of salp assemblages off Baja California during the 1997–1999 El Niño and La Niña. Mar Ecol-Prog Ser 318: 123-140

Heron AC (1972) Population ecology of a colonizing species: The pelagic tunicate *Thalia democratica*. I. Individual growth rate and generation time. Oecologia 10(4): 269-293

Heron AC, McWilliam PS, Dal Pont G (1988) Length-weight relation in the salp *Thalia democratica* and potential of salps as a source of food. Mar Ecol-Prog Ser 42: 125-132

Huskin I, Elices MA, Anadón R (2003) Salp distribution and grazing in a saline intrusion off NW Spain. J Mar Syst 42: 1–11

Knap AH, Michaels AF, Steinberg DK, Bahr F, Bates N, Bell S, Countway P, Close A, Doyle A, Howse F, Gundersen K, Johnson R, Little R, Orcutt K, Parsons R, Rathbun C, Sanderson M, Stone S (1997) BATS Methods Manual. U.S. JGOFS Planning Office, Woods Hole

Krause JW, Nelson DM, Lomas MW (2009) Biogeochemical responses to late-winter storms in the Sargasson Sea, II: Increased rates of biogenic silica production and export. Deep-Sea Res Pt I 56: 861-874

Kremer P, Madin LP (1992) Particle retention efficiency of salps. J Plankton Res 14(7): 1009-1015

Kucharski F, Molteni F, Bracco A (2006) Decadal interactions between the western tropical Pacific and the North Atlantic Oscillation. Clim Dynam 26: 79-91

Landry MR, Brown SL, Rii YM, Selph KE< Bidigare RR, Yang EJ, Simmons MP (2008) Depth-stratified phytoplankton dynamics in Cyclone *Opal*, a subtropical mesoscale eddy. Deep-Sea Res Pt II 55: 1348-1359

Lavaniegos BE, Ohman MD (2007) Coherence of long-term variations of zooplankton in two sectors of the California Current System. Prog Oceanogr 75: 42-69

Lebrato M, Jones DOB (2009) Mass deposition event of *Pyrosoma atlanticum* carcasses off Ivory Coast (West Africa). Limnol Oceanogr 54(4): 1197-1209

Lebrato M, Mendes PJ, Steinberg DK, Cartes JE, Jones BM, Birsa LM, Benavides R, Oschlies A (2013) Jelly biomass sinking speed reveals a fast carbon export mechanism. Limnol Oceanogr 58(3): 1113-1122

Li K, Yin J, Huang L, Shang J, Lian S, Liu C (2011) Distribution and abundance of thaliaceans in the northwest continental shelf of South China Sea, with response to environmental factors driven by monsoon. Cont Shelf Res 31: 979-989

Licandro P, Ibañez F, Etienne M (2006) Long-Term Fluctuations (1974-1999) of the Salps *Thalia democratica* and *Salpa fusiformis* in the Northwestern Mediterranean Sea: Relationships with Hydroclimatic Variability. Limnol Oceanogr 51(4): 1832-1848

Liu Y, Sun S, Zhang G (2012) Seasonal variation in abundance, diel vertical migration and body size of pelagic tunicate *Salpa fusiformis* in the Southern Yellow Sea. Chin J Oceanol Limn 30(1): 92-104

Loeb VJ, Hofmann EE, Klinck JM, Osmund H-H (2010) Hydrographic control of the marine ecosystem in the South Shetland-Elephant Island and Bransfield Strait region. Deep-Sea Res Pt II 57: 519-542

Loeb VJ, Santora JA (2012) Population dynamics of Salpa thompsoni near the Antarctic Peninsula: Growth rates and interannual variations in reproductive activity (1993–2009). Prog Oceanogr 96: 93-107

Lomas MW, Steinberg DK, Dickey T, Carlson CA, Nelson NB, Condon RH, Bates NR (2010) Increased ocean carbon export in the Sargasso Sea linked to climate variability is countered by its enhanced mesopelagic attenuation. Biogeosciences 7: 57-70

Lomas MW, Bates NR, Johnson RJ, Knap AH, Steinberg DK, Carlson CA (2013) Two decades and counting: 24-years of sustained open ocean biogeochemical measurements in the Sargasso Sea. Deep-Sea Res Pt II 93: 16-32

Madhupratap M, Devassy VP, Sreekumaran-Nair SR, Rao TSS (1980) Swarming of pelagic tunicates associated with phytoplankton bloom in the Bay of Bengal. Ind J Mar Sci 9(1): 69–71

Madin LP, Cetta CM, McAlister VL (1981) Elemental and biochemical composition of salps (Tunicata: Thaliacea). Mar Biol 63: 217-226

Madin LP (1982) Production, composition and sedimentation of salp pellets in oceanic waters. Mar Biol 67: 39–45

Madin LP, Purcell JE (1992) Feeding, metabolism, and growth of *Cyclosalpa bakeri* in the subarctic Pacific. Limnol Oceanogr 37: 1236-1251

Madin LP, Kremer P (1995) Determination of the filter feeding rates of salps (Tunicata, Thaliacea). ICES J Mar Sci 52: 583-595

Madin LP, Kremer P, Hacker S (1996) Distribution and vertical migration of salps (Tunicata, Thaliacea) near Bermuda. J Plankton Res 18(5): 747-755

Madin LP, Deibel D (1998) Feeding and energetics of Thaliacea. In: Bone Q (ed) The biology of pelagic tunicates. Oxford University Press, Oxford, UK, p 81-103

Madin LP, Horgan EF, Steinberg DK (2001), Zooplankton at the Bermuda Atlantic Time-series Study (BATS) station: Diel, seasonal and interannual variation in biomass, 1994–1998. Deep Sea Res Pt II 48(8–9): 2063–2082

Madin LP, Kremer P, Wiebe PH, Purcell JE, Horgan EH, Nemazie DA (2006) Periodic swarms of the salp *Salpa aspera* in the Slope Water off the NE United States: biovolume, vertical migration, grazing and vertical flux. Deep-Sea Res Pt I 53: 804–819

McGillicuddy DJ, Robinson AR, Siegel DA, Jannasch HW, Johnson R, Dickey TD,

McNeil J, Michaels AF, Knap AH (1998) Influence of mesoscale eddies on new production in the Sargasso Sea. Nature 394: 263-266

McGillicuddy DJ, Anderson LA, Bates NR, Bibby T, Buesseler KO, Carlson CA, Davis CS, Ewart C, Falkowski PG, Goldthwait SA, Hansell DA, Jenkins WJ, Johnson R, Kosnyrev VK, Ledwell JR, Li QP, Siegel DA, Steinberg DK (2007) Eddy/wind interactions stimulate extraordinary mid-ocean plankton blooms. Science 316: 1021-1026

Ménard F, Dallot S, Thomas G, Braconnot JC (1994) Temporal fluctuations of two Mediterranean salp populations from 1967 to 1990. Analysis of the influence of environmental variables using a Markov chain model. Mar Ecol-Prog Ser 104: 139-152

Mouriño-Carballido B (2009) Eddy-driven pulses of respiration in the Sargasso Sea. Deep-Sea Res Pt I 56: 1242-1250

Müller WA, Frankignoul C, Chouaib N (2008) Observed decadal tropical Pacific-North Atlantic teleconnections. Geophys Res Lett 35: L24810

Mullin MM (1983) *In situ* measurement of filtering rates of the salp, *Thalia democratica*, on phytoplankton and bacteria. J Plankton Res 5(2): 279-288

Nishikawa J, Terazaki M (1996) Tissue shrinkage of two gelatinous zooplankton, *Thalia democratica* and *Dolioletta gegenbauri* (Tunicata: Thaliacea) in preservative. Bull Plankton Soc Jap 43(1): 1-7

Ottersen G, Planque B, Belgrano A, Post E, Reid PC, Stenseth NC (2001) Ecological effects of the North Atlantic Oscillation. Oecologia 128(1): 1-14

Paffenhöfer G-A, Lee TN (1987) Development and persistence of patches of Thaliacea. S

Afr J Mar Sci 5: 305–318

Phillips B, Kremer P, Madin LP (2009) Defecation by *Salpa thompsoni* and its contribution to vertical flux in the Southern Ocean. Mar Biol 156: 455–467

Pyper BJ, Peterman RM (1998) Comparison of methods to account for autocorrelation in correlation analyses of fish data. Can J Fish Aquat Sci 55: 2127-2140.

Roman MR, Adolf HA, Landry MR, Madin LP, Steinberg DK, Zhang X (2002) Estimates of oceanic mesozooplankton production: a comparison using the Bermuda and Hawaii time-series data. Deep-Sea Res Pt II 49: 175–192

Saba VS, Friedrichs MAM, Carr M-E, Antoine D, Armstrong RA, Asanuma I, Aumont O, Bates NR, Behrenfeld MG, Bennington V, Bopp L, Bruggeman J, Buitenhuis ET, Church MJ, Ciotti AM, Doney SC, Dowell M, Dunne J, Dutkiewicz S, Gregg W, Hoepffner N, Hyde KJW, Ishizaka, J, Kameda T, Karl DM, Lima I, Lomas MW, Marra J, McKinley GA, Mélin F, Moore JK, Morel A, O'Reilly J, Salihoglu B, Scardi M, Smyth TJ, Tank S, Tjiputra J, Uitz J, Vichi M, Waters K, Westberry TK, Yool A (2010) Challenges of modeling depth-integrated marine primary productivity over multiple decades: A case study at BATS and HOT. Global Biogeochem Cy 24: GB3020

Sutherland KR, Beet AR, Solow AR (2010a) Re-analysis of a salp population time-series. Mar Ecol-Prog Ser 418: 147-150

Sutherland KR, Madin LP, Stocker R (2010b) Filtration of submicrometer particles by pelagic tunicates. P Natl Acad Sci USA 107(34): 15129-15134

Stammerjohn S, Massom R, Rind D, Martinson D (2012) Regions of rapid sea ice change: An inter-hemispheric seasonal comparison. Geophys Res Lett 39: L06501

Steinberg DK, Carlson CA, Bates NR, Goldthwait SA, Madin LP, Michaels AF (2000) Zooplankton vertical migration and the active transport of dissolved organic and inorganic carbon in the Sargasso Sea. Deep-Sea Res I 47: 137-158

Steinberg DK, Carlson CA, Bates NR, Johnson RJ, Michaels AF, Knap AH (2001) Overview of the US JGOFS Bermuda Atlantic Time-series Study (BATS): a decade-scale look at ocean biology and biogeochemistry. Deep-Sea Res II 48:1 405-1447

Steinberg DK, Lomas MW, Cope JS (2012) Long-term increase in mesozooplankton biomass in the Sargasso Sea: Linkage to climate and implications for food web dynamics and biogeochemical cycling. Global Biogeochem Cy 26: GB1004

Sweeney EN, McGillicuddy DJ, Buesseler KO (2003) Biogeochemical impacts due to mesoscale eddy activity in the Sargasso Sea as measured at the Bermuda Atlantic Time-series Study (BATS). Deep-Sea Res Pt II 50: 3017-3039

Tew KS, Lo T (2005) Distribution of Thaliacea in SW Taiwan coastal water in 1997, with special reference to *Doliolum denticulatum*, *Thalia democratica*, and *T. orientalis*. Mar Ecol-Prog Ser 292: 181–193

Tsuda A, Nemoto T (1992) Distribution and growth of salps in a Kuroshio warm-core ring during summer 1987. Deep-Sea Res 39(S1): S219-S229

van Soest RWM (1975) Thaliacea of the Bermuda area. Bull Zool Mus Univ Amsterdam 5(2): 7-12

van Soest RWM (1998) The cladistics biogeography of salps and pyrosomas. In Bone Q [ed.], The biology of pelagic tunicates. Oxford University Press. p 231-249

Vaughan DG, Marshall GJ, Connolley WM, Parkinson C, Mulvaney R, Hodgson DA,

King JC, Pudsey CJ, Turner J (2003) Recent raid regional climate warming on the Antarctic Peninsula. Climate Change 60: 243-274

Wu S, Liu Z, Zhang R, Delworth TL (2011) On the observed relationship between the Pacific Decadal Oscillation and the Atlantic Multi-decadal Oscillation. J Oceanogr 67: 27-35

Yoon WD, Marty JC, Sylvain D, Nival P (1996) Degradation of fecal pellets in *Pegea confoederata* (Salpidae, Thaliacea) and its implication in the vertical flux of organic matter. Journal of Experimental Mar Biol Ecol 203: 147–177

Yoon WD, Kim SK, Han KN (2001) Morphology and sinking velocities of fecal pellets of copepod, molluscan, euphausiid, and salp taxa in the northeastern tropical Atlantic. Mar Biol 139: 923-928

Zeldis JR, Davis CS, James MR, Ballara SL, Booth WE, Chang FH (1995) Salp grazing: effects on phytoplankton abundance, vertical distribution and taxonomic composition in a coastal habitat. Mar Ecol-Prog Ser 126: 267-283

Table 1: Day (n = 227) and night (n = 222) biomass and abundance (mean ± SD) for each salp species in the epipelagic zone at the Bermuda Atlantic Time-series Study (BATS) site. Mean and maximum day and night biomass and abundance are given for each species for the entire 17 yr time series. Species are listed in decreasing order of frequency of presence (see Fig. 1). See 'Methods' for biomass calculations.

	Abundance (ind. m^{-3})				Biomass (μg C m^{-3})			
Species	**Day mean**	**Night mean**	**Day max**	**Night max**	**Day mean**	**Night mean**	**Day max**	**Night max**
Total salps	3.32 ±25.5	1.95 ±17.5	281	221	43.1 ±361	41.5 ±245	4470	2630
Thalia democratica	3.31 ±25.5	1.90 ±17.5	281	221	40.8 ±361	30.2 ±245	4470	2630
Salpa fusiformis	1.86E-3 ±7.35E-3	2.56E-2 ±7.11E-2	0.073	0.962	0.211 ±1.24	3.39 ±13.6	14.1	178
Weelia* (*Salpa*) *cylindrica	3.44E-3 ±14.4E-3	6.32E-3 ±30.9E-3	0.133	0.293	0.245 ±1.10	0.587 ±4.40	8.45	62.6
Cyclosalpa polae	7.52E-4 ±34.3E-4	2.98E-3 ±17.6E-3	0.033	0.186	0.150 ±0.810	0.240 ±1.11	6.72	11.6
Iasis zonaria	1.37E-4 ±10.9E-4	2.01E-3 ±7.09E-3	0.012	0.061	0.070 ±0.934	1.22 ±5.23	14.0	60.6
Salpa aspera	4.24E-4 ±40.1E-4	1.41E-2 ±10.3E-2	0.054	1.44	0.034 ±0.347	3.77 ±15.4	4.07	136
Ritteriella retracta	6.09E-5 ±64.9E-5	1.03E-3 ±7.67E-3	0.007	0.098	0.057 ±0.836	0.202 ±1.29	12.6	12.6
Pegea confoederata	1.23E-3 ±11.7E-3	1.69E-3 ±17.5E-3	0.143	0.239	0.298 ±3.11	0.242 ±2.53	44.4	35.8
Ihlea punctata	4.04E-4 ±41.2E-4	8.05E-4 ±62.3E-4	0.053	0.071	0.035 ±0.396	0.134 ±1.02	5.69	12.6
Pegea socia	8.34E-4 ±83.3E-4	2.57E-4 ±20.7E-4	0.114	0.023	1.10 ±14.1	0.148 ±1.64	210	23.7
Traustedtia multitentaculata	1.84E-4 ±13.6E-4	2.53E-4 ±27.8E-4	0.015	0.040	0.019 ±0.232	0.017 ±0.200	3.45	2.90
Cyclosalpa floridana	8.50E-5 ±98.4E-5	2.22E-4 ±16.9E-4	0.014	0.016	0.002 ±0.017	0.003 ±0.027	0.22	0.34
Salpa maxima	6.42E-5 ±70.3E-5	4.72E-3 ±69.2E-3	0.009	1.03	0.005 ±0.055	1.20 ±16.7	0.78	249
Thalia orientalis	6.02E-4 ±61.3E-4	3.22E-4 ±34.6E-4	0.083	0.047	0.013 ±0.124	0.008 ±0.092	1.45	1.35
Cyclosalpa pinnata	8.32E-5 ±73.7E-5	2.63E-5 ±39.2E-5	0.008	0.006	0.017 ±0.199	0.008 ±0.120	2.93	1.79
Thalia cicar	2.29E-5 ±34.5E-5	7.04E-5 ±75.2E-5	0.005	0.009	0.001 ±0.018	0.001 ±0.020	0.27	0.30
Brooksia rostrata	3.16E-5 ±47.6E-5	6.32E-5 ±94.1E-5	0.007	0.014	0.000	0.014 ±0.215	0.07	3.20
Cyclosalpa affinis	1.96E-4 ±29.6E-4	2.86E-5 ±42.6E-5	0.045	0.006	0.001 ±0.009	0.003 ±0.050	0.14	0.75
Pegea bicaudata	2.48E-5 ±37.4E-5	5.33E-4 ±79.4E-4	0.006	0.118	0.002 ±0.028	0.061 ±0.907	0.42	13.5
Helicosalpa virgula	0.00	1.64E-5 ±24.4E-5	0.000	0.004	0.000	0.001 ±0.016	0.00	0.24
Thetys vagina	0.00	1.83E-5 ±27.3E-5	0.000	0.004	0.000	0.015 ±0.222	0.00	3.31

Table 2: Mean (± SD) and range for the amplitude, rotation speed, and radius of the 56 mesoscale eddies that passed through the Bermuda Atlantic Time-series Study (BATS) site within 6 d of a zooplankton sampling event. Eddies were considered to have passed through the BATS site if 110% of their circumference encompassed the BATS site. Eddy data were collected from the online database http://cioss.coas.oregonstate.edu/eddies/ (Chelton et al., 2011).

	Cyclonic	**Anticyclonic**
Number	**38**	**18**
Mean amplitude (cm)	**8.0 ±4.4**	**8.1 ±2.8**
Amplitude range (cm)	**1.2 – 16.5**	**4.2 – 14.2**
Mean rotational speed (cm/s)	**17.0 ±6.4**	**17.5 ±3.8**
Rotational speed range (cm/s)	**7.1 – 33.9**	**13.1 – 26.6**
Mean radius (km)	**96 ±22.2**	**104 ±29.5**
Radius range (km)	**54 - 148**	**66 – 159**

Table 3: Spearman correlation coefficients for the 12 mo moving average of salp abundance (no m^{-3}) and biomass (mg C m^{-3}) versus environmental parameters. Not significant (NS): $p \geq 0.05$, * $0.05 > p \geq 0.01$, ** $0.01 > p \geq 0.001$, *** $p < 0.001$.

Species	Sea surface temperature	Water column stratification index	Temperature 300 to 600 m	Primary production integrated to 140 m	Chlorophyll *a* integrated to 140 m
Total salp abundance	**NS**	**NS**	**NS**	**0.42*** **	**NS**
Total salp biomass	**NS**	**NS**	**-0.23****	**0.18***	**NS**
***Thalia democratica* abundance**	**NS**	**0.20***	**-0.24****	**0.32*** **	**NS**
***Thalia democratica* biomass**	**0.23****	**0.48*** **	**-0.43*** **	**0.22****	**NS**
***Salpa fusiformis* abundance**	**NS**	**NS**	**-0.29*** **	**NS**	**0.20***
***Salpa fusiformis* biomass**	**NS**	**NS**	**-0.36*** **	**-0.19****	**NS**
***Weelia* (*Salpa*) *cylindrica* abundance**	**NS**	**NS**	**NS**	**-0.30*** **	**-0.32*** **
***Weelia* (*Salpa*) *cylindrica* biomass**	**NS**	**NS**	**NS**	**-0.38****	**-0.23*** **
***Cyclosalpa polae* abundance**	**0.34*** **	**0.29*** **	**NS**	**NS**	**0.20****
***Cyclosalpa polae* biomass**	**0.31*** **	**0.30*** **	**-0.16***	**-0.16***	**0.24*** **
Others combined abundance	**NS**	**NS**	**NS**	**NS**	**NS**
Others combined biomass	**NS**	**NS**	**-0.19***	**NS**	**-0.20***

Table 4: Spearman correlation coefficients for the 12 mo moving average of climate index anomalies versus the 12 mo moving average of salp biomass and abundance. MEI: Multivariate El Niño Southern Oscillation; NAO: North Atlantic Oscillation; NPCO: North Pacific Gyre Oscillation; PDO: Pacific Decadal Osciallation. Not significant (NS): * $0.05 > p \geq 0.01$, ** $0.01 > p \geq 0.001$, *** $p < 0.001$.

Species	MEI	NAO	NPGO	PDO
Total salp abundance	**-0.40*** **	**NS**	**0.55*** **	**-0.37*** **
Total salp biomass	**-0.22****	**0.20****	**0.57*** **	**-0.45*** **
***Thalia democratica* abundance**	**-0.44*** **	**NS**	**0.28*** **	**-0.35*** **
***Thalia democratica* biomass**	**-0.44*** **	**NS**	**0.40*** **	**-0.54*** **
***Salpa fusiformis* abundance**	**NS**	**NS**	**NS**	**0.25****
***Salpa fusiformis* biomass**	**NS**	**NS**	**NS**	**0.27*** **
***Weelia* (*Salpa*) *cylindrica* abundance**	**NS**	**NS**	**NS**	**NS**
***Weelia* (*Salpa*) *cylindrica* biomass**	**NS**	**NS**	**NS**	**NS**
***Cyclosalpa polae* abundance**	**NS**	**-0.33*** **	**0.26*** **	**NS**
***Cyclosalpa polae* biomass**	**NS**	**-0.32*** **	**0.22****	**NS**
Others combined abundance	**NS**	**0.25*** **	**0.47*** **	**-0.25****
Others combined biomass	**NS**	**0.38*** **	**0.46*** **	**-0.27****

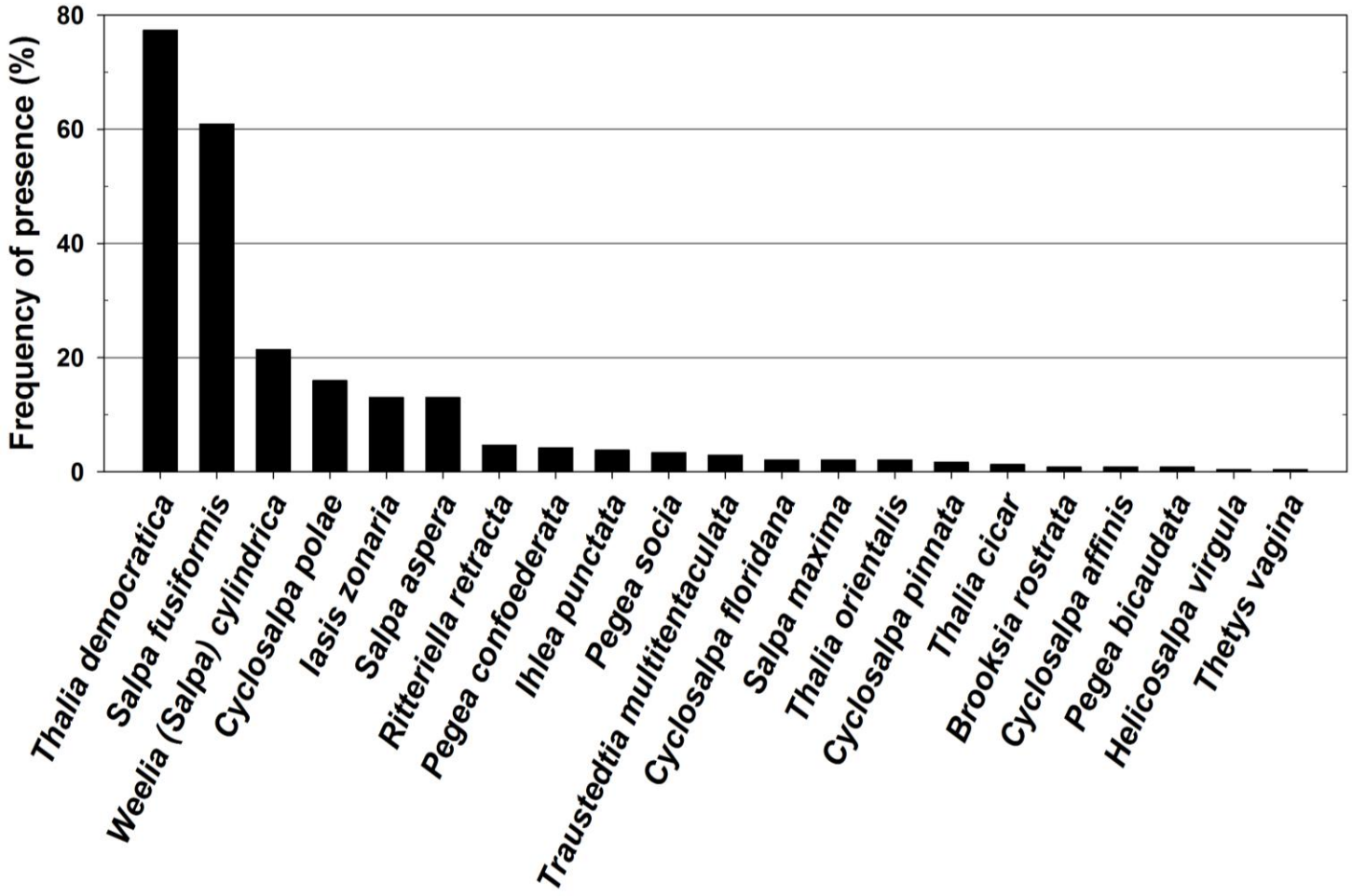

Figure 1: Frequency of presence (as %) of each salp species in monthly cruises (n=238). A total of 776 tows were analyzed from all cruises between April, 1994 and November, 2011.

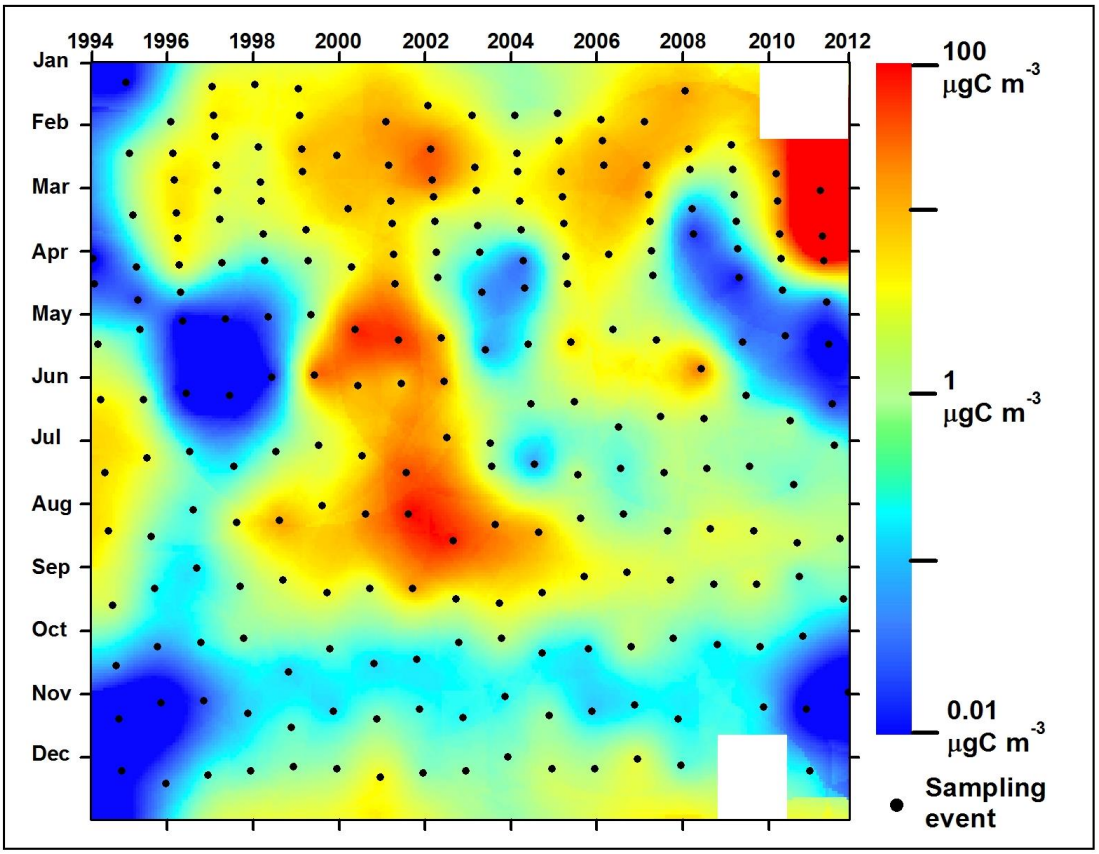

Figure 2: Seasonal and interannual total salp biomass at the Bermuda Atlantic Time-series Study (BATS) site. Total combined (all species) salp biomass across the time series (April 1994-November 2011). Note that biomass is depicted on a natural log scale.

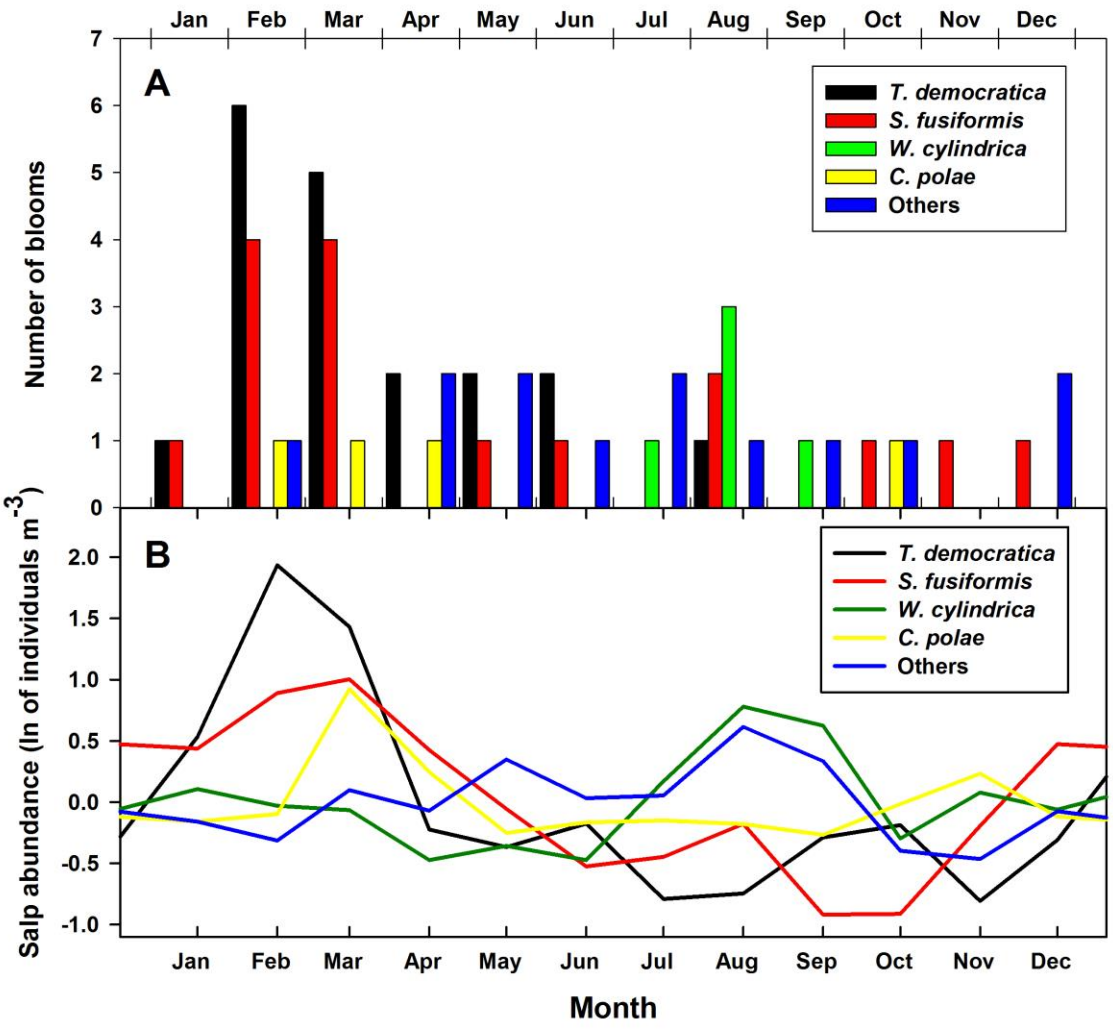

Figure 3: Monthly distribution of (A) salp blooms and (B) average monthly biomass after removal of the long-term trend. Blooms are defined as salp biomass in the top 10% of the entire time series for that species. Shown are the sums of all blooms in each month for the 4 most abundant species: *Thalia democratica*, *Salpa fusiformis*, *Weelia* (*Salpa*) *cylindrica*, and *Cyclosalpa polae*, and all other salps combined over the entire time series (April 1994-November 2011).

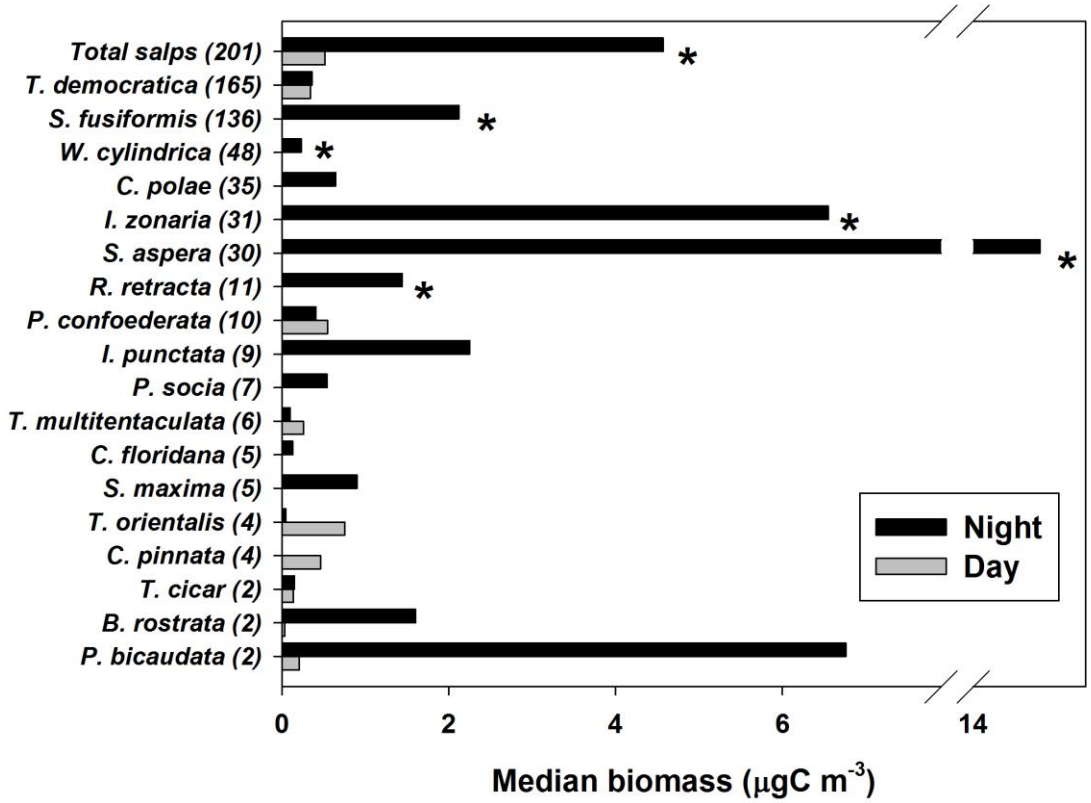

Figure 4: Salp diel vertical migration. Day and night median biomass of total salps and 18 species of salps at the Bermuda Atlantic Time-series Study (BATS) site across the time series (April 1994 - November 2011). Day and night biomasses that are significantly different (i.e. the species demonstrates diel vertical migration) are marked with an asterisk, and the number of day-night observation pairs for each species is in parentheses. Full species names given in Fig. 1.

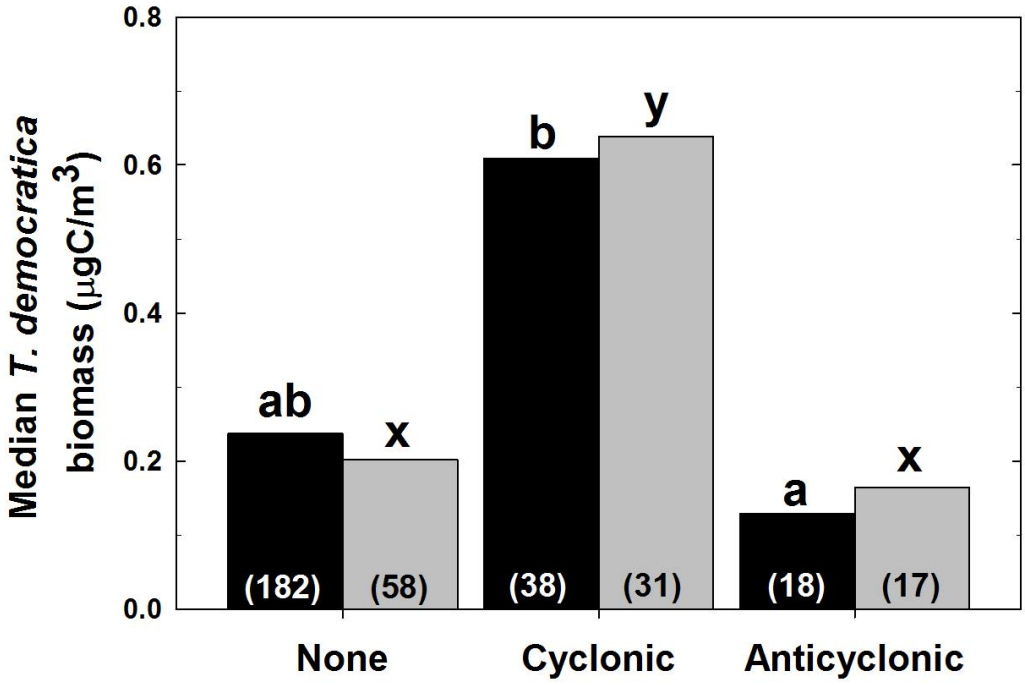

Figure 5: Median biomass of *Thalia democratica* within cyclonic and anticyclonic eddies, and when no eddies are present, at the Bermuda Atlantic Time-series Study (BATS) site. Black bars represent salp median biomass for eddies from the Chelton and Schlax database (http://cioss.coas.oregonstate.edu/eddies/) that encompassed the BATS site within 110% of their circumference within 6 d of a zooplankton sampling event, and represents our entire salp time series (April 1994 - November 2011). Gray bars represent salp median biomass for eddies listed in Mouriño-Carballido (2009) that influenced BATS from April 1994 to December 2001. Numbers in parentheses indicate the number of eddy-influenced samples within each category. Bars with different letters are significantly different (Bonferroni-Dunn test, $p < 0.05$) from other bars within that database ('a' and 'b' for Chelton and Schlax, and 'x' and 'y' for Mouriño-Carballido), and bars with the same letters are not significantly different ($p < 0.05$).

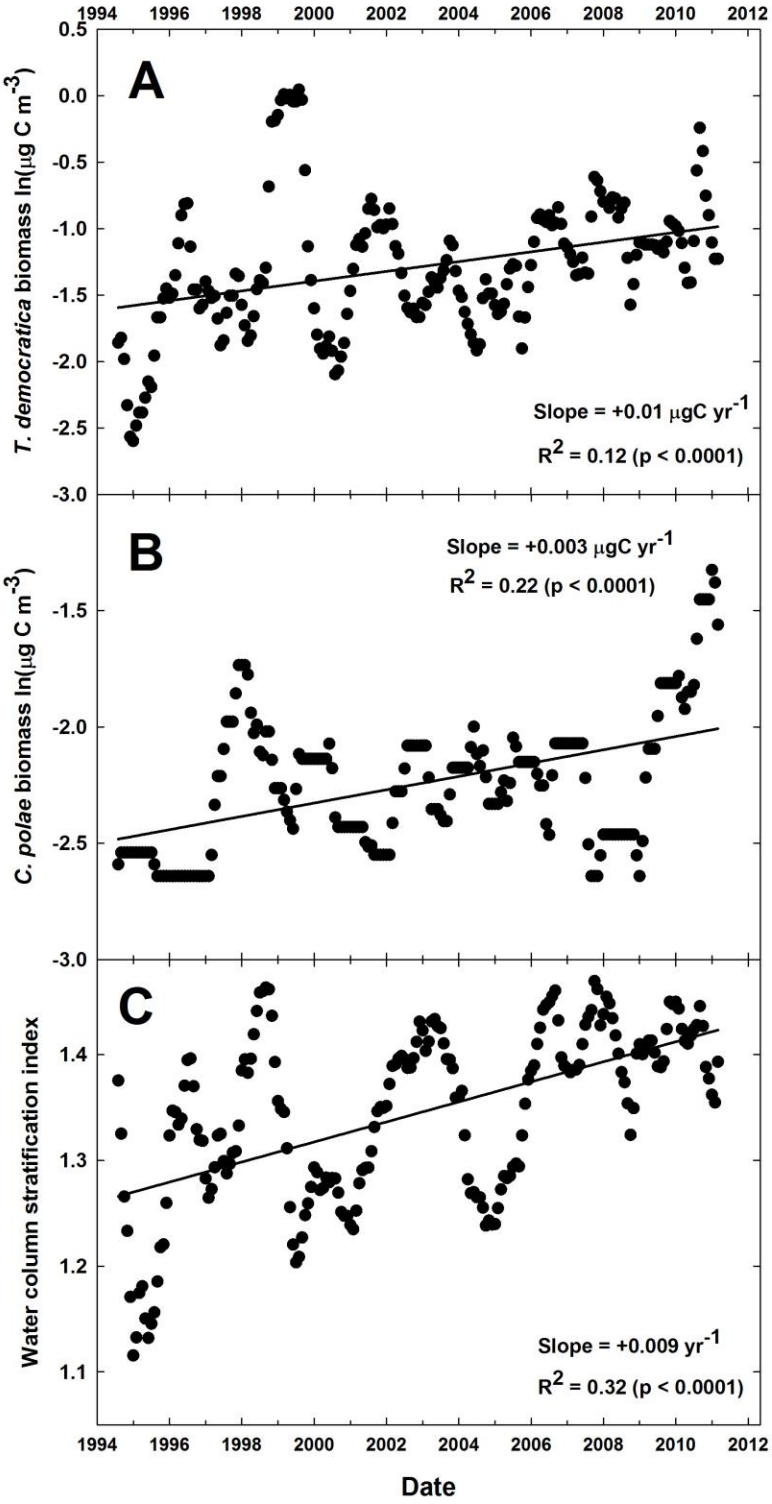

Figure 6: Twelve month moving average of (A) *Thalia democratica* biomass (B) *Cyclosalpa polae* biomass, and (C) the water column stratification index (WCSI) across the time series (October 1994 - May 2011). Note the natural log scale for the salp biomass plots. All regressions are log-linear.

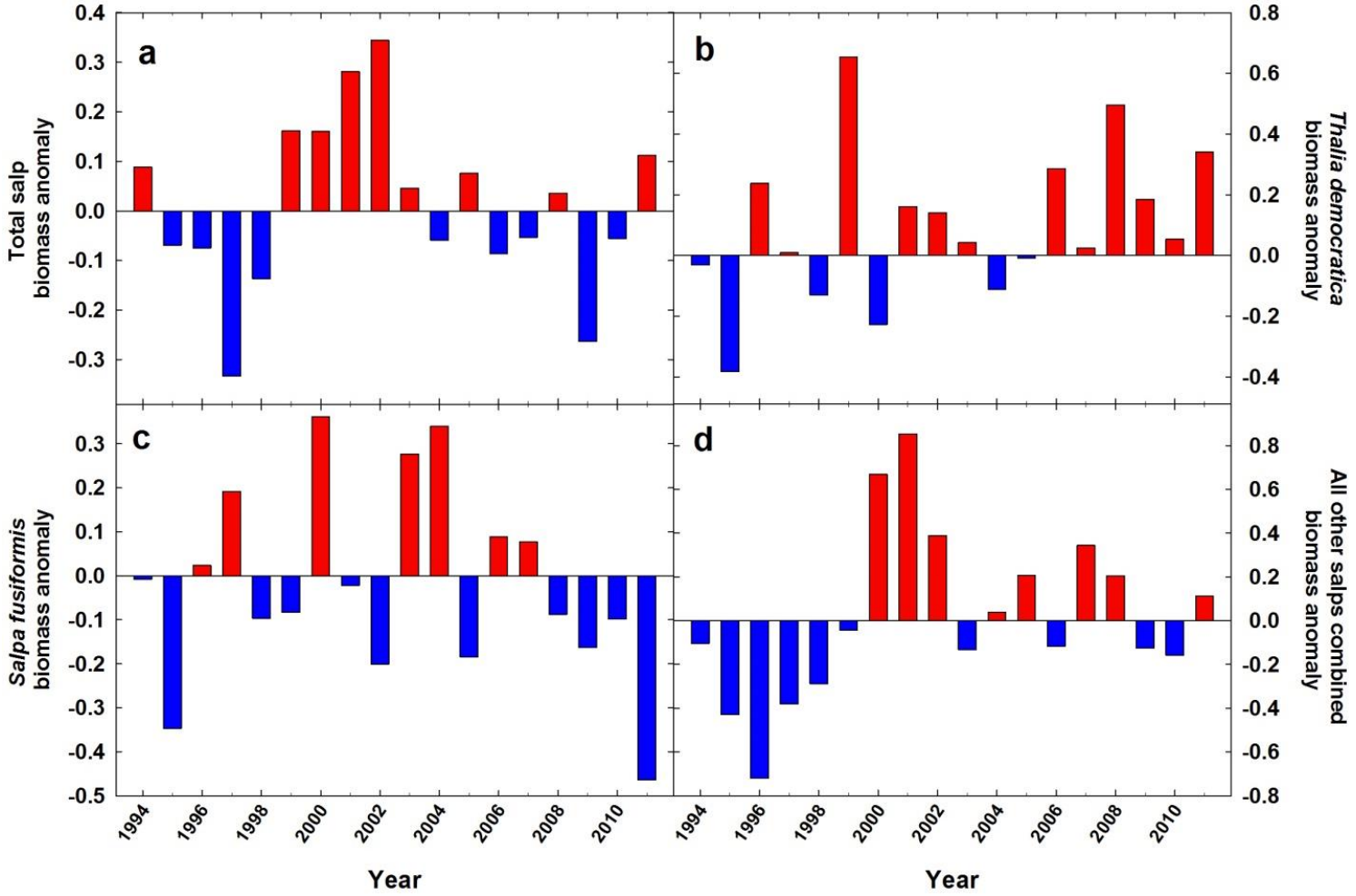

Figure 7: Yearly average biomass anomaly for (A) total salps, (B) *Thalia democratica*, (C) *Salpa fusiformis*, and (D) total salps minus *T. democratica* and *S. fusiformis.* Red and blue bars indicate higher and lower biomass, respectively, for that year compared to the annual median of the whole time series.

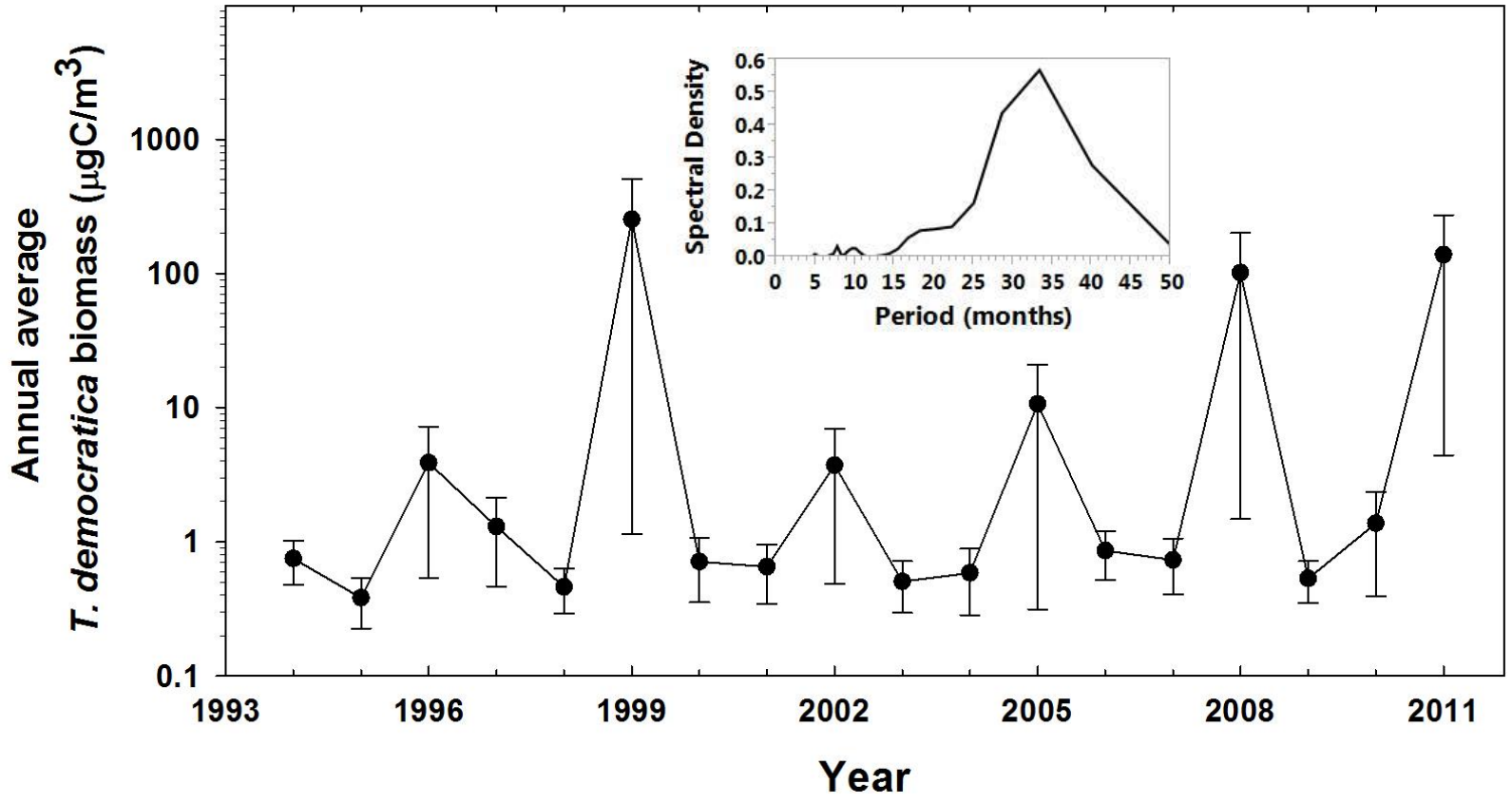

Figure 8: Annual average biomass of *Thalia democratica*. Monthly averages were calculated first to avoid bias towards the more frequently sampled spring period, and the median monthly value of each month was used for missing data points. Error bars represent standard error. Note natural log scale and the cycle of higher average biomass every 3 yr. Inset is the calculated spectral density of the monthly time series 12 mo moving average showing the most significant periodicity.

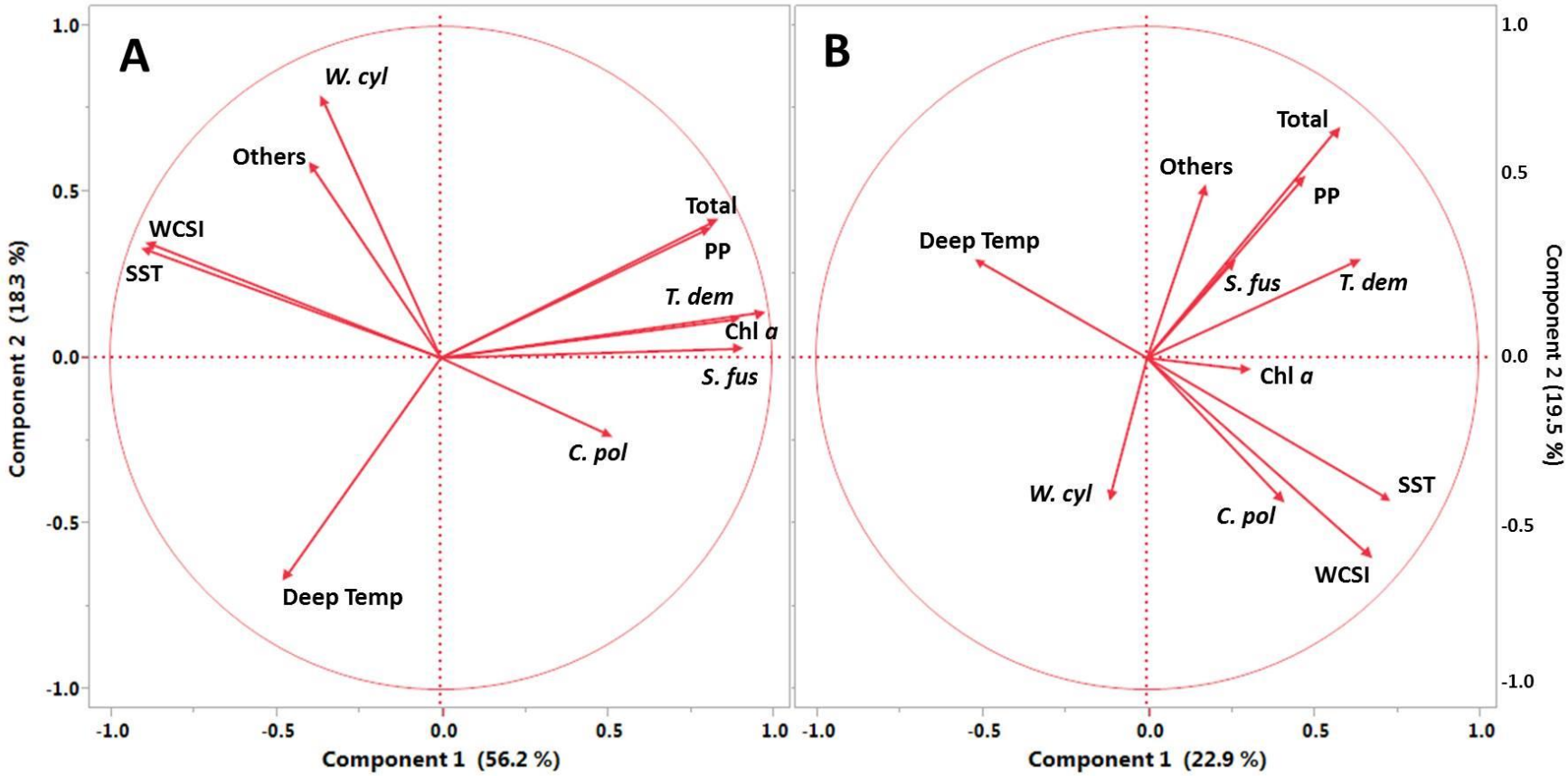

Figure 9: Principal component analysis of salp biomass and environmental parameters for (A) seasonal averages after removing the long-term trend and (B) the long-term trend. Total: total salps; *T. dem*: *Thalia democratica*; *S. fus*: *Salpa fusiformis*; *C. pol*: *Cyclosalpa polae*; *W. cyl*: *Weelia* (*Salpa*) *cylindrica*; Others: all other salp biomass combined; PP: primary production integrated to 140 m; Chl *a*: chlorophyll *a* integrated to 140 m; WCSI: water column stratification index; SST: sea surface temperature; Deep Temp: mean temperature in mesopelagic zone from 300 to 600 m.

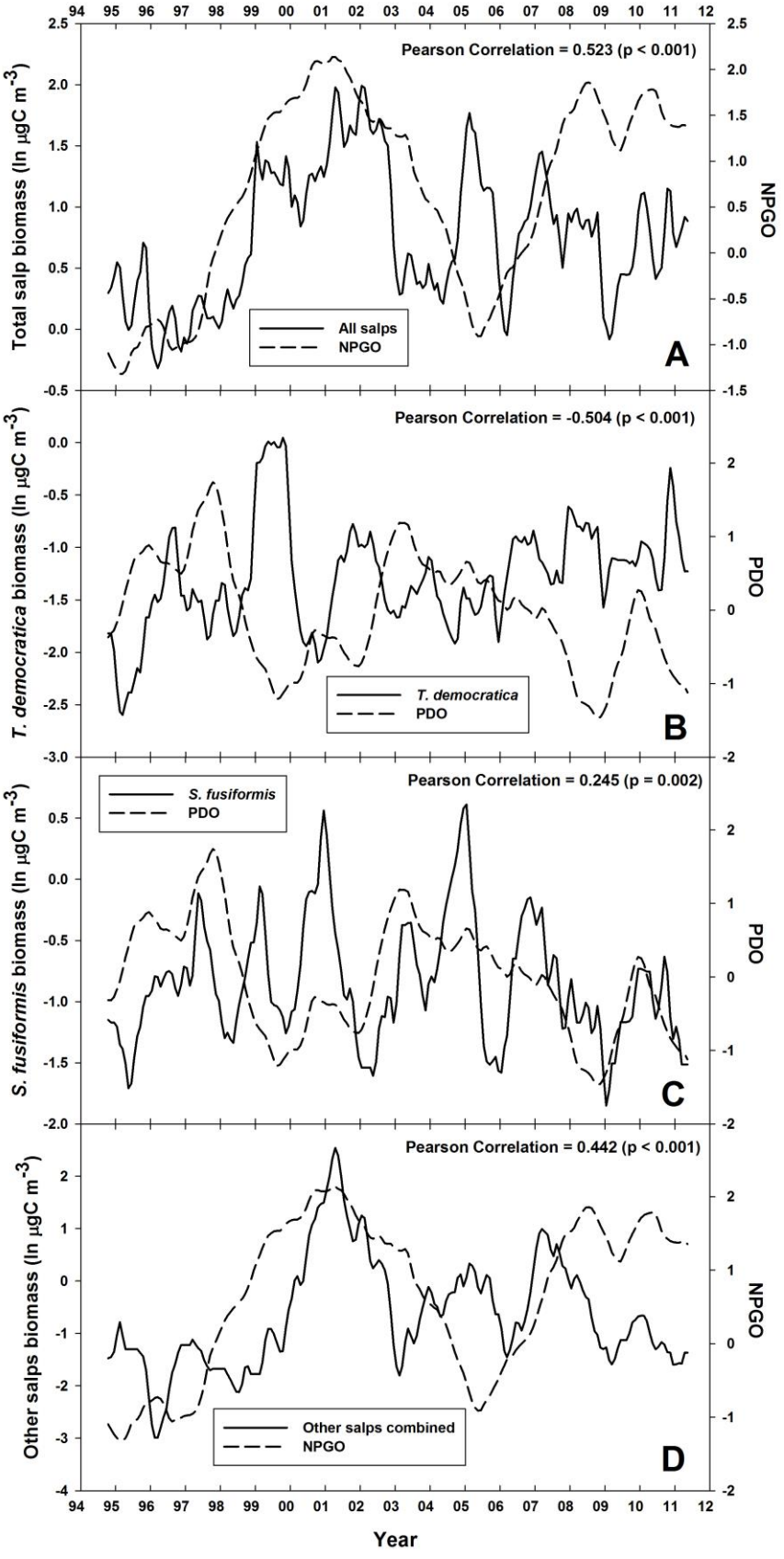
Pearson Correlation = 0.523 (p < 0.001)
Total salp biomass (ln µgC m-3)
NPGO
All salps
NPGO
A
Pearson Correlation = -0.504 (p < 0.001)
T. democratica biomass (ln µgC m-3)
PDO
T. democratica
PDO
B
Pearson Correlation = 0.245 (p = 0.002)
S. fusiformis biomass (ln µgC m-3)
PDO
S. fusiformis
PDO
C
Pearson Correlation = 0.442 (p < 0.001)
Other salps biomass (ln µgC m-3)
NPGO
Other salps combined
NPGO
D
94 95 96 97 98 99 00 01 02 03 04 05 06 07 08 09 10 11 12
Year

Figure 10: Salp biomass and climate index 12 mo moving average. Monthly salp biomass trend (solid line) is shown with the most strongly correlated monthly climate index trend (dashed line). (A) total salps with North Pacific Gyre Oscillation (NPGO), (B) *Thalia democratica* and (C) *Salpa fusiformis* with Pacific Decadal Oscillation (PDO), and (D) total salps minus *T. democratica*, *S. fusiformis*, *Weelia* (*Salpa*) *cylindrica*, and *Cyclosalpa polae* with the NPGO. Correlations between salp trends and climate indices were tested using the Pearson correlation (see Table 3 for full results of analysis) for the period of the salp time series (October 1994-May 2011).

CHAPTER 5

Salp contributions to vertical carbon flux in the Sargasso Sea

This chapter published in the journal *Deep-Sea Research I* as:

Stone JP, Steinberg DK (2016) Salp contributions to vertical carbon flux in the Sargasso Sea. Deep-Sea Res I 113: 90-100. doi: 10.1016/j.dsr.2016.04.007

ABSTRACT

We developed a one-dimensional model to estimate salp contributions to vertical carbon flux at the Bermuda Atlantic Time-series Study (BATS) site in the North Atlantic subtropical gyre for a 17-yr period (April 1994 to December 2011). We based the model parameters on published rates of salp physiology and experimentally determined sinking and decomposition rates of salp carcasses. Salp grazing was low during non-bloom conditions, but routinely exceeded 100% of chlorophyll standing stock and primary production during blooms. Fecal pellet production was the largest source of salp carbon flux (78% of total), followed by respiration below 200 m (19%), sinking of carcasses (3%), and DOC excretion below 200m (<0.1%). *Thalia democratica*, *Salpa fusiformis*, *Salpa aspera*, *Wheelia cylindrica*, and *Iasis zonaria* were the five highest contributors, accounting for 95% of total salp-mediated carbon flux. Seasonally, salp flux was higher during spring-summer than fall-winter, due to seasonal changes in species composition and abundance. Salp carbon export to 200m was on average 2.3 mg C m^{-2} d^{-1} across the entire time series. This is equivalent to 11% of the mean 200 m POC flux measured by sediment traps in the region. During years with significant salp blooms, however, annually-averaged salp carbon export was the equivalent of up to 60% of trap POC flux at 200 m. Salp carbon flux attenuated slowly, and at 3200 m the average modeled carbon from salps was 109% of the POC flux measured in sediment traps at that depth. Migratory and carcass carbon export pathways should also be considered (alongside fecal pellet flux) as facilitating carbon export to sequestration depths in future studies.

1. INTRODUCTION

The Sargasso Sea is an oligotrophic region in the North Atlantic subtropical gyre, with patterns in biogeochemistry influenced by physical forcing, moderated by strength of winter mixing, and tied to decadal-scale climate oscillations (Saba et al. 2010, Álvarez-García et al. 2011, Wu et al. 2011). In years with increased frequency of winter mixing, increased surface nutrients fuel new production, ultimately leading to higher particulate organic carbon (POC) fluxes to 150 m (Lomas et al. 2010). This POC flux is significantly attenuated in the meso- and bathypelagic zones of the Sargasso Sea (Conte et al., 2001), where flux to these depths consists of phytodetritus, amorphous aggregates, zooplankton fecal pellets, and foraminifera shells (Shatova et al., 2012; Conte and Weber, 2014), with variation in mass flux closely coupled to seasonal changes in epipelagic particle flux (Conte et al., 2001; Lomas et al., 2010). Flux is also influenced by climate oscillations, with higher nitrogen flux to 3200 m in years with a negative North Atlantic Oscillation (NAO) anomaly (Conte & Weber 2014). Interannual variations in mesozooplankton biomass in this region also affect vertical export (Steinberg et al., 2012); we examine here how fluctuations in salp populations (Stone and Steinberg, 2014) contribute to vertical carbon flux through a variety of mechanisms.

Salps are gelatinous, tubular zooplankton which alternate life stages between solitary, sexually-produced individuals and aggregated, asexually-produced colonies– ranging in size from a few mm's to tens of m's in length (Godeaux et al., 1998). Salps are highly efficient filter feeders, with clearance rates up to several liters $salp^{-1}$ $hour^{-1}$ (Madin & Cetta, 1984; Andersen, 1985; Vargas & Madin, 2004), and they can consume a broad size range of phytoplankton and bacteria (Bone et al., 2003; Sutherland et al.,

2010). Salps feed incessantly as they propel themselves through the water, and when numerous, can consume more than 100% of the primary production (Hereu et al., 2006). Their continuous ingestion of a wide range of particle sizes promotes rapid rates of growth, reproduction, and defecation. Salp fecal pellets are relatively large (Caron et al., 1989; Sutherland et al., 2010), and sink at rates up to 1600 m day^{-1} (Bruland & Silver, 1981; Phillips et al., 2009). Due to fast sinking velocities, salp pellets can reach bathypelagic depths relatively intact, and are found in high numbers in sediment traps (Iseki, 1981; Matsueda et al., 1986; Caron et al., 1989; Conte et al., 2001). This observation suggests remineralization or scavenging of these particles by microbes or other metazoans may be limited.

Dead carcasses of salps also contribute to vertical export of organic matter (Lebrato et al., 2013a). While the fate of many salp blooms is unknown, seasonal blooms of salps often quickly collapse (Purcell et al., 2001), and this sudden production of carcasses can represent an important source of food for deep-sea animals and bacteria (Cacchione et al., 1978; Wiebe et al., 1979; Lebrato et al., 2012). Flux from salp fecal pellets and carcasses are estimated to contribute up to 72% of the measured flux in the coastal Mediterranean (Andersen & Nival, 1988), and a *Salpa* sp. bloom in the northeastern Pacific resulted in a major deposition of fecal pellets and carcasses to the seafloor (Smith et al., 2014). In addition to producing fecal pellets and carcasses, several abundant species of salps in the Sargasso Sea and elsewhere undergo diel vertical migration, spending time well below the pycnocline during the day and migrating to surface waters at night (Wiebe et al., 1979; Madin et al., 1996; Stone & Steinberg, 2014). While at depth, vertical migrators metabolize particulate organic carbon (POC) consumed

in surface waters, respiring it as CO_2 and excreting dissolved organic carbon (DOC), contributing to vertical transport of carbon to depth (Steinberg et al., 2000).

While salps are important contributors to vertical carbon flux while they are present, their populations are quite variable. Salps periodically bloom throughout the world's oceans, including in the Sargasso Sea (Madin et al., 1996, 2001; Roman et al., 2002, Stone & Steinberg, 2014), where they are occasionally the dominant epipelagic zooplankton (Stone & Steinberg, 2014). Salps are sensitive to interannual and longer-term changes in the environment, mostly related to variations in temperature and stratification. Shifts in prevailing wind led to temperature and primary production changes that caused salp species composition in the Mediterranean to alternate between *Thalia democratica* and *Salpa fusiformis* (Ménard et al., 1994; Licandro et al., 2006). Increases in temperature, as measured by the Northern Hemisphere Temperature anomaly, caused observed increases in the pelagic tunicate *Pyrosoma atlanticum* due to more stable water masses and decreases in phytoplankoton community size (Lebrato et al., 2013b). Long-term regional changes in salp populations have been reported in the California Current (Lavaniegos & Ohman, 2007) where shifts in temperature regimes caused changes to both their species composition and biomass. In the Southern Ocean, changes in El Niño–Southern Oscillation (ENSO) and regional warming are correlated with increases in salps (Atkinson et al., 2004; Loeb et al., 2010), and worldwide, gelatinous zooplankton fluctuations are linked to oscillations in climate indices (Condon et al., 2013). In the Sargasso Sea, biomass of the salps *Thalia democratica* and *Cyclosalpa polae* increased over the last 20 years, and was positively correlated with water column stratification (Stone & Steinberg, 2014). *T. democratica* abundance was

also higher within cyclonic eddies in the Sargasso Sea, possibly through increased eddy-induced production or through eddy-wind aggregation (Stone & Steinberg, 2014). These long-term changes in salps in the Sargasso Sea could increase carbon export to the deep sea.

In this study, we hypothesize that all three mechanisms of salp-mediated carbon export –1) sinking of fecal pellets, 2) sinking of carcasses, and 3) respiration and excretion at depth– represent significant pathways of export. To test this hypothesis, we used salp abundance and species composition data from the Bermuda Atlantic Time-series Study (BATS) to individually model each species' contributions to vertical carbon flux. This one-dimensional model includes previously-published rates of salp fecal pellet production and sinking, newly measured rates of salp carcass decomposition and sinking, and previously published rates of salp metabolism. By modeling each species and export mechanism separately, we can estimate total salp contributions to vertical flux in an oligotrophic, open-ocean environment and how those fluxes change through the water column as salp abundance and species composition change.

2. METHODS

2.1 Sinking and decomposition rate experiments

Salps used in sinking and decomposition rate experiments were collected in the western North Atlantic subtropical gyre at stations within ~100 km of the Bermuda Atlantic Time-series Study (BATS) sampling site ($31^{o}40$'N, $64^{o}10$'W). Cruises were aboard the R/V *Atlantic Explorer* during the 'Trophic BATS' project from July 19-31, 2012 and on regular monthly BATS cruises from March 4–7, April 28–May 3, and August 19–23, 2014. Salps were collected using a net with a 0.8 x 1.2 m rectangular mouth, 202 μm mesh, and a non-filtering cod end to minimize damage to the salps. Tows were conducted during both day and night to depths of 50-150 m, and lasted ~50 min each. Immediately after each tow, captured salps were separated from other zooplankton and brought into the lab for experimentation. Any particles or other zooplankton stuck to the outside or inside of the salps were first removed. Salps were then identified to species and life stage, and individual salp length was measured as the oral-atrial distance using digital calipers. Salps that were not already dead post capture were killed by placing them in a shallow pan of seawater (~2 mm deep) to collapse and suffocate them while allowing them to remain moist.

To determine sinking rates, dead salps were placed individually into a sinking chamber comprised of a clear acrylic tube 60 cm long and 15 cm in diameter filled with surface seawater. This experimental set up and sinking chamber is similar to those used in Lebrato et al., (2013a), which were 12.5 cm and 19 cm in diameter. The chamber diameter in relation to the size of some of the salps may allow flow interactions between

the salp and the wall, slowing the salp sinking rate. To correct for this, we used equation 12 from Ristow (1997) to apply a sidewall correction factor to each individual salp's sinking rate based on the size of the salp. Water temperature was measured using a Cole-Parmer Traceable® 90205-22 temperature probe, and salinity was determined from the ship's flow-through salinometer. Water temperature in the sinking chamber changed less than 1 °C throughout each experimental run, and salps were stored in water with the same temperature and salinity as the sinking chamber. After placement in the sinking chamber using forceps, salps were gently shaken to remove any bubbles on or inside the salps. If any bubbles remained, the salp was discarded. Each salp was then gently released and allowed to sink. Depth of each salp in the sinking chamber was determined by comparison to measurement markings on the outside of the chamber. Once each salp appeared to reach terminal velocity (after ~20 cm), a timer was started, and the time to sink a distance between 5 and 30 cm was recorded. Different sinking distances were used when an individual salp sank particularly quickly or slowly, as we attempted to time each sinking salp for 30-60 s. Each salp was sunk once to avoid retrieving the salp from the bottom of the chamber and introducing turbulence.

Decomposition rate experiments were conducted with *Cyclosalpa polae*, *Iasis zonaria, Salpa fusiformis, S. maxima, Thalia democratica, Wheelia cylindrica,* and *Ritteriella retracta* in March, May, and August of 2014. Dead salps were placed in small (~5x5 cm) 200 μm mesh bags submerged in a large beaker in the dark with a continuous flow-through of surface seawater (19-23 °C) for the duration of the experiment, simulating the decomposition process in warm epipelagic waters with the resident microbial assemblage. Several salps were removed at each time point from their mesh

bags and "sacrificed" from the experiment to be frozen for analysis onshore. This removal occurred at regular intervals (~8-12 h) until all salps were either removed or completely decomposed. Once onshore, salp remains were placed in a drying oven at 60 °C for at least one week and then weighed. Initial salp dry weight (i.e., T_0) was estimated from length measurements of freshly caught, whole salps using published salp live length to carbon weight regression equations for each species (see Table 5.3 in Madin & Deibel, 1998, and references therein). Occasionally, the measured dry weights of the initial, undecomposed salps were consistently different from the dry weights calculated by the regression equations. When this occurred, a correction factor was applied to all salps in that experiment by adding or subtracting the difference between the mean calculated and mean measured dry weights of the time zero (t_0) salps. Decay rate of salp carcasses was calculated by plotting the percent remaining of initial salp dry weight over time and fitting a first-order exponential decay curve:

$$P = a*e^{(-k*t)}$$

where 'P' is percent of starting salp dry weight remaining at time 't,' 'a' is the percent remaining at time zero t_0, 'k' is the decay constant, and 't' (hours) is time from the start of the experiment. Similar experiments were carried out at 8 °C using water collected from 1000 m, to simulate meso- and bathypelagic conditions. For these experiments, instead of water continuously flowing through the decomposition chamber, carcasses were placed in 4 L bottles in a refrigerator, and the water in each bottle was replenished every 12 h.

2.2 Model development

We developed a one-dimensional model to calculate salp contributions to total vertical carbon flux (Fig. 1). Fecal pellet production, grazing, production of carcasses, and respiration at depth was calculated daily for each species' biomass. Data forced into the model included biological, environmental, and process rate data (e.g., salp biomass, temperature, primary production) collected through the BATS program (http://bats.bios.edu/), previously published rates of salp metabolic and export processes (fecal pellet production, respiration, and DOC excretion), as well as results from the above sinking and decomposition experiments. Salp 'blooms' were defined as in Stone and Steinberg (2014), i.e., when total salp biomass is in the top 10% of all observations.

Salp biomass (mg C m^{-2}) and vertical migration was calculated from monthly and bimonthly tows at the BATS site as detailed in Stone and Steinberg (2014). Species-specific biomass was averaged from duplicate day and night tows, with only the night tow biomass used for species that exhibited diel-vertical migration. Salp blooms are generally short-lived, and typically do not remain at high abundance for several months. Because the duration of each salp bloom could not be accurately estimated from monthly sampling, the biomass data were linearly interpolated between each sampling date to give a biomass estimate for each day from April 15, 1994 to November 14, 2011. This was done for each of the 21 species and 4 higher taxa categories (*Pegea* sp., Salpidae, *Salpa* sp., and *Thalia* sp.) in the dataset; the 25 biomass time series were then used to force the flux model. Based on Stone and Steinberg (2014), all species were split into those which exhibited diel vertical migration (DVM; *Salpa fusiformis*, *Wheelia cylindrica*, *Iasis zonaria*, *S. aspera*, and *Ritteriella retracta*) and those that did not exhibit DVM (*Brooksia rostrata, Cyclosalpa affinis, C. floridana, C. pinnata, C. polae, Helicosalpa virgula, Ihlea*

punctata, Pegea bicaudata, P. confoederata, P. socia, Pegea sp., S. maxima, Salpa sp., Salpidae, *Thalia cicar, T. democratica, T. orientalis, Thetys vagina,* and *Traustedtia multitentaculata*). For each DVM species, an overall average migrating proportion of the biomass was calculated by dividing each sampling date's day biomass by night biomass and subtracting from 1 to obtain a percentage of biomass that was migrating. These percentages were then averaged for each species across the entire time series. For non-DVM species, we calculated the amount of carbon reaching 200 m from both fecal pellet production (FPP) and from sinking of carcasses (i.e., the 'passive flux'). For DVM species, we additionally calculated respiration and dissolved organic carbon (DOC) excretion while at depth (i.e., the 'active flux').

Fecal pellet production, sinking of dead carcasses, respiration and DOC excretion at depth, and grazing were all resolved daily from April 1994 to November 2011 as described in the following sections. For fecal pellet production, species-specific FPP rates were used when available from the literature; for species without a specific rate, rates from the same genus or family were averaged (Supplementary Table 1; Deibel, 1982; Madin, 1982; Mullin, 1983; Small et al., 1983; Cetta et al., 1986; Andersen, 1985; Huntley et al., 1989; Madin & Purcell, 1992; Sreekumaran Nair et al., 1995). Fecal pellet decomposition was based on rates averaged from Caron et al. (1989), who measured the loss of ash free dry weight over a 10-day experiment. Based on literature values for fecal pellet sinking rates (Bruland & Silver, 1981; Caron et al., 1989; Phillips et al., 2009), salp fecal pellets would reach the Sargasso Sea floor well within 10 days. Because the experiments in Caron et al. (1989) measured fecal pellet decomposition over a total of 10 days through a temperature gradient (1 day at 22 °C followed by 9 days at 5 °C) and did

not measure pellet decomposition at only one temperature, we were unable to separately model the decomposition taking place in the warm surface waters from that at colder depths. Thus, we applied the total 10-day decomposition measured by Caron et al. (1989), and no additional decomposition parameter was applied after the fecal pellets reached 200 m. Because fecal pellets would sink below 200 m much more quickly than 10 days, our estimates are conservative. For DVM species, we assumed the following: 1) FPP was the same in the surface waters and at depth, as salps with full guts would continue to produce fecal pellets after migrating to depth for some time and would not immediately begin producing them again after returning to the surface, 2) migrators spent 12 h per day above 200 m and 12 h per day below 200 m, and 3) while physical breakup or resuspension of fecal material may occur, we had no reliable estimates of these processes, and they were not included in the model.

We modeled carcass sinking and decomposition by incorporating the experimentally-determined rates for each species (Fig. 2 and Table 1), and averaging across genus or family when species-specific rates were not available. Daily biomass of each species and life stage was multiplied by the proportion dying each day (the mortality rate), which gave a biomass of dead salps produced each day. All salps were conservatively assumed to have died at the surface, and the amount of time required to sink 200 m was calculated by using the species-specific corrected rates in Fig. 2. The decomposition equations in Table 1 were then used with the time required to sink 200 m to determine the sinking carcass biomass. The monthly proportion of salp biomass in each life stage (blastozooid or oozoid) was calculated from BATS count data, and then linearly interpolated to obtain a daily value. Life spans were estimated as 3 days for

Thalia blastozooids, 14 days for *Thalia* oozoids, 15 days for all other salp blastozooids, and 30 days for all other salp oozoids (Henschke et al., 2011, Deibel & Lowen, 2012). Daily death rates were estimated as the proportion of the population reaching the end of its lifespan each day; for example, the 14-day lifespan of *Thalia* oozoids translates as 1/14 of *Thalia* oozoid biomass dying each day. For DVM species, we estimated that half of the population died above 200 m, and half below 200 m. Since we did not measure decomposition at colder temperatures or under increased pressure at depth, we calculated biomass of carcasses produced below 200 m (reaching depths of 300 m, 500 m, 1500 m, and 3200 m) by applying the decomposition rates of Lebrato et al. (2011) (2013a) separately to *T. democratica* (due to slower sinking speeds of this species), and then to all other species combined. We assumed a constant temperature of 18 °C from 200 to 500 m, 8 °C from 500 to 1000 m, 5 °C from 1000 to 1500 m, and 3 °C from 1500 to 3200 m (http://batsftp.bios.edu/BATS/ctd/).

Salp active transport–respiration and DOC excretion at depth– was calculated for the five DVM species while they were below 200 m. One rate for each parameter was applied to all species. An average respiration rate (2.2% body C h^{-1}) was calculated from data compiled in Madin and Purcell (1992) and Cetta et al. (1986). There is no published DOC excretion rate of salps, thus DOC excretion rate for this model was averaged from those of other gelatinous zooplankton (ctenophores and cnidarians) in Condon et al. (2011) (0.182 mg C h^{-1} g dry body $weight^{-1}$).

Daily salp grazing (mg C m^{-3} d^{-1}) was calculated by multiplying the volume of water cleared by the average carbon biomass of phytoplankton 0-140 m, as phytoplankton biomass is not significant below 140 m. Both daily chlorophyll *a* and

primary production were linearly interpolated from the monthly BATS sampling (http://batsftp.bios.edu/BATS/bottle/bats_pigments.txt and http://batsftp.bios.edu/BATS/production/bats_production.dat). Phytoplankton carbon biomass was calculated by multiplying the daily chlorophyll *a* concentration by a seasonal carbon to chlorophyll ratio (C:Chl). These C:Chl ratios (g/g) were calculated from seasonal averages of BATS chlorophyll *a* concentration and average seasonal values of phytoplankton carbon from Wallhead et al. (2014), and were as follows (months in parentheses): 52 – winter (JFM), 60 – spring (AMJ), 52 – summer (JAS), and 47 – fall (OND). Species-specific clearance rates were used when available; otherwise, average rates for genus or family were used (Supplementary Table 1; Harbison and Gilmer, 1976; Harbison & McAlister, 1979; Deibel, 1982; Mullin, 1983; Madin & Cetta, 1984; Andersen, 1985; Deibel, 1985; Reinke, 1987; Madin & Purcell, 1992; Sreekumaran Nair et al., 1995; Vargas & Madin, 2004; Hereu et al., 2010). Because salps are considered non-discriminant filter feeders (Madin, 1974) and only cease feeding when their internal filters become clogged at very high phytoplankton concentrations (i.e., above ~1 ug chl *a* L^{-1}, Andersen, 1985 and Harbison et al., 1986; concentrations rarely reached at BATS), we assumed clearance rates to be constant regardless of phytoplankton concentration. While some DVM species may migrate at different times of the day (Madin et al., 1996), further research is needed to quantify these differences, and all DVM species were assumed to graze 12 h each 24-h period in surface waters. All salp grazing rates were based on phytoplankton standing stocks, and FPP rates for this model were independent of calculated grazing (see above). If grazing rates were to be used in an energetic model or to calculate FPP, consumption of microzooplankton (such as

dinoflagellates and ciliates shown in Vargas & Madin, 2004) would also need to be taken into consideration.

2.3 Sediment trap flux

Sediment trap POC flux data (mg C m^{-2} day^{-1}) for sediment traps at 150 m, 200 m, and 300 m from April 1994 to November 2011 were downloaded from the BATS database (bats.bios.edu). Mean POC flux for traps at 500 m (1984-1986, 1989-1982, and 1997-1998), 1500 m (1984-1992, and 1997-1998), and 3200 m (1978-1998) was calculated from Table 1 in Conte et al. (2001).

3. RESULTS

3.1 Sinking and decomposition rates

Mean salp carcass sinking rate was measured for 8 species ranging in average size from 8 mm *T. democratica* to 30 mm *S. maxima*. Sinking rates ranged from 414-871 m d^{-1} and 467-1002 m d^{-1}, before and after correcting for wall-interaction effects, respectively (Fig. 2), with a mean (corrected) sinking rate across all species of 727 m d^{-1} (n=293). The corrected rates were used throughout the model calculations. There were weak linear correlations between salp length vs. sinking rate ($p<0.001$; $r^2 = 0.21$) and water density vs. sinking rate ($p>0.05$; $r^2 < 0.01$). We posit that sinking rate was not dependent on water density due to the high water content of salp carcasses, and thus there was an equally proportional change in their body density as in the surrounding seawater after adjusting to the new temperature. However, there were significant differences in sinking rate between individual species, with *Wheelia cylindrica* (1002 m d^{-1}) and *Salpa maxima* (927 m d^{-1}) sinking faster than the two slowest sinking species, *Cyclosalpa polae* (526 m d^{-1}) and *Thalia democratica* (467 m d^{-1}) (Kruskal-Wallis ANOVA on ranks; Fig. 2). Thus, the average rates of similar taxa were used in model calculations, and sinking was not based on salp size or variance in water density.

Species-specific decomposition rates were calculated for species with sufficient replication to obtain a significant exponential decay curve (*I. zonaria, S. fusiformis,* and *T. democratica*), while an average of all of the warm-water experiments was used to fit a decay curve for the rest of the species (Table 1; Fig. 3). No measurable decomposition occurred over 3 days during the cold-water experiments. As described in the methods, actual measured salp weights at t_0 were used to adjust the calculated starting weights.

This method was successful, as measured/modeled weight ratio at t_0 was distributed normally (Shapiro-Wilk p=0.132) and the mean ratio was 1.07 (± 0.27 SD). Modeled salp decomposition was rapid within the first several hours, with 50% of the starting dry weight lost after only 8 h. Decomposition of the subsequent 49% took much longer, ~44 additional hours, with some salp biomass still present 56 h into the experiment.

3.2 Grazing model

Total daily salp grazing was, on average, 0.05 mg chl *a* m^{-3} d^{-1} (± 0.003 standard error, SE), or 26% of the chlorophyll biomass over the 17+ year model run (6423 days). However, median daily salp grazing was only 0.004 mg chl *a* m^{-3} d^{-1}, or 2% of the chlorophyll biomass; this difference being driven by periodically high salp abundances. Likewise, while salp grazing impact was typically low (an average of 3.9% of the chlorophyll biomass during non-bloom salp abundances), during salp blooms, calculated grazing was an average of 220% of the phytoplankton standing stock present in epipelagic waters (Fig. 4A). Grazing was also seasonally variable, with elevated mean grazing in spring and early summer (March-June; 6.5 mg C m^{-2} d^{-1}) compared to the rest of the year (July-February; 0.7 mg C m^{-2} d^{-1}). Annual grazing across the time series was a median of 17% of the annual primary production (Fig. 4B), with annual grazing exceeding 100% of the primary production in 1999, 2002, and 2008. Additionally, the proportion of primary production exported by salps was low (<0.5%) for much (86%) of the time series, but increased to as much as 35% during large blooms (Fig. 5B). On average, 0.5% of all primary production at BATS, from April 1994 to November 2011, was exported to below 200 m by salps.

3.3 Flux model results

The daily salp-mediated carbon flux to 200 m for each of 25 salp taxa from April 15, 1994 to November 15, 2011 was computed in the model. This included fecal pellet production (FPP) and export, sinking of salp carcasses, and respiration and DOC excretion by DVM at depth. The total carbon flux was generally low, with salp-mediated carbon export less than 1.0 mg C m^{-2} day^{-1} in 76% of the time series. However, due to the population dynamics of salps, this low baseline was punctuated with large salp blooms causing spikes in the flux of several orders of magnitude (Fig. 5). These salp blooms cumulatively accounted for 79% of the total modeled salp POC flux across the time series, over half of which was produced by the blooms in 1999, 2008, and 2011. Total salp-mediated export to 200m was highly correlated with total salp grazing (Pearson's correlation coefficient = 0.93, $p < 0.001$), and averaged across the entire time series salp carbon flux was 1.6% of the total carbon grazed by salps. The average daily salp-mediated carbon export across the time series was 2.3 mg C m^{-2} day^{-1} and the median flux was 0.4 mg C m^{-2} day^{-1}. The largest proportion of salp-mediated carbon export came from fecal pellets, with an annual average of 78% (586 mg C m^{-2} $year^{-1}$) (Table 2). The second largest contribution to export was from respiration at depth (19%; 139 mg C m^{-2} $year^{-1}$), followed by sinking of carcasses (3%; 23 mg C m^{-2} $year^{-1}$), and DOC excretion at depth (< 0.1%; 0.1 mg C m^{-2} $year^{-1}$) (Table 2).

Seasonal trends in salp carbon flux varied according to the source of the flux, and trends were slightly different dependent upon whether mean or median values of export were considered (Fig. 6). As salp export is several orders of magnitude higher during periodic salp blooms, mean values were much higher than median values for much of the

model output. Mean export due to salp fecal pellets was elevated in spring and early summer (March-June), while respiration and carcass carbon flux were more elevated in late summer (July-September) (Fig. 6A). Median fecal pellet and carcass fluxes were elevated through all of the spring and summer (February-September), while median respiration peaked in late winter (February and March) and summer (July-September) (Fig. 6B). DOC excretion was negligible in all seasons. Both mean and median total salp carbon flux were higher in spring and summer than in fall and winter.

Five species accounted for 96% of the total salp-mediated carbon flux at BATS, with *Thalia democratica* contributing the most, followed by *Salpa aspera*, *S. fusiformis*, *Iasis zonaria*, and *Wheelia cylindrica* (Fig. 7A). The other 20 species and taxa combined contributed the remaining 4%. This was calculated by summing the total flux contributed by each species for the entire time series. However, when each species' annual total contribution was averaged for each year of 1995-2010, *S. fusiformis* was the largest contributor to flux, followed by *T. democratica*, *S. aspera*, *W. cylindrica*, and *I. zonaria* (Fig. 7B).

Overall, total annual salp carbon flux ranged widely, from 97 to 4580 mg C m^{-2} y^{-1} in 1997 and 1999, respectively (Fig. 8A), with a mean and standard deviation of 748 ± 1133 mg C m^{-2} y^{-1} for the time series. Annual BATS 200 m sediment trap flux ranged from 5260 to 9710 mg C m^{-2} y^{-1} in 2005 and 2002, respectively (Fig. 8B) with a mean and standard deviation of 7530 ± 1050 mg C m^{-2} y^{-1}. Annual salp-mediated export flux was equivalent to a mean of 10% ± 15 (range 1-60%) of the 200 m sediment trap POC flux over the time series (Fig. 8C).

While there was no consistent long-term change in total salp C export over the time series ($r^2 < 0.01$), there was a periodicity to export. We performed spectral analysis on monthly totals of salp C export to 200 m, and the highest spectral densities were found at 9, 12, and 36 months (approximate p-value < 0.001, Bartlett's Kolmogorov–Smirnov statistic, Fuller, 1996), indicating total salp carbon export cycles on seasonal (9 months between the late summer and spring blooms), annual, and interannual time scales, respectively.

Relatively little of the total salp-exported carbon was lost as it sank through the water column (Fig. 9), due to fast sinking and slow decomposition of fecal pellets and carcasses. Average daily salp carbon flux at 200 m across the time series was 2.3 mg C m^{-2} day^{-1} and only attenuated to 1.9 mg C m^{-2} day^{-1} at 3200 m. This was a decrease of only 19%, whereas average daily POC flux captured in sediment traps decreased by 92% between 200 m and 3200 m (from 20.6 to 1.7 mg C m^{-2} day^{-1}). At 3200 m, calculated salp carbon (mostly from fecal pellets) was equivalent to 109% of the POC collected in the sediment traps (Fig. 9).

4. DISCUSSION

4.1 Carcass sinking rates

Salp carcass sinking rates varied between 467 and 1002 m d^{-1}, similar to the few previously published measurements. Moseley (1880) recorded a sinking rate of ~860 m d^{-1} for an unknown species of salp, and Wiebe et al. (1979) reported *Salpa aspera* carcasses sank 240-480 m d^{-1}. Lebrato et al. (2013a) found *Salpa thompsoni* carcasses sink 800-1700 m d^{-1}, and other gelatinous zooplankton, including *Cyanea* sp., *Pelagia noctiluca*, *Mnemiopsis leidyi*, and *Pyrosoma atlanticum*, had average sinking rates of 400-1500 m d^{-1}. While Lebrato et al. (2013a) found a positive relationship between salp biovolume and sinking rate, we found no significant relationship overall between salp length and sinking rate but that there were some significant differences between species. In our study the smallest species of salp (*Thalia democratica*) did have the slowest sinking rate. Differences between species in sinking rate other than body size could be related to different relative sizes of the dense, phytoplankton-filled gut or sinking orientation of each individual salp.

4.2 Decomposition rates

Decomposition rates of salps were fast enough that while much of the carcass carbon would be exported out of the epipelagic, very little would reach bathypelagic depths before complete decomposition. We found the exponential decay constant 'k' of all salp species combined to be 2.2 d^{-1} at 21 °C, which is close to the calculated *k* of 2.9 d^{-1} for all gelatinous zooplankton using Equation 2 in Lebrato et al. (2011). However, the decay constant for *Thalia democratica* (k = 14.5) was much higher than that calculated for all

gelatinous zooplankton in Lebrato et al. (2011). While this may be due to a higher surface area-to-volume ratio of the small *T. democratica* compared to larger salps, decomposition of *T. democratica* was included in Equation 2 of Lebrato et al. (2011), albeit at a lower experimental temperature of 16.5 °C (Sempéré et al., 2000). Sempéré et al. (2000) observed that salp carcasses consist of a quickly decomposing, labile fraction and a more slowly decomposing fraction, which is consistent with our experimental results showing exponential decay.

While slow-sinking salp species or small individuals, which make up the majority of salp biomass at BATS, may decompose before reaching the benthos, less common blooms of larger and faster sinking species would be able to reach the deep sea. Additionally, DVM species could die at their daytime mesopelagic residence depth, and thus be more likely to reach the benthos since much of the decomposition occurs in warmer surface waters. While we used a depth horizon of salp DVM of 200 m for the purpose of our model, at least one species of salp in the North Atlantic subtropical gyre (*Salpa aspera*) migrates to depths >800 m (Wiebe et al., 1979), where temperatures are ~10 °C and decomposition much slower. Thus, our estimates of salp carcass carbon export to the deep sea are likely conservative.

4.3 Grazing

Salp grazing had relatively low impact on phytoplankton standing stock and primary production (PP) for much of the year, but periodically extremely high grazing during salp blooms resulted in demand often exceeding phytoplankton supply, with grazing over 100% phytoplankton standing stock and PP. Similarly, salp grazing in the

Humboldt Current averaged 16% but was up to 60% of PP (González et al., 2000), off NW Spain averaged 7% of chlorophyll standing stock but was as much as 77% (Huskin et al., 2003), in the California current system ranged from <1 to >100% of daily PP and phytoplankton biomass (Hereu et al., 2006), and in the Eastern Tropical North Pacific ranged from 0.01 to 3.5% of chlorophyll standing stock each day (Hereu et al., 2010). The high grazing impact seen during salp blooms would only be sustained for a short time before phytoplankton standing stocks were depleted, suggesting bottom-up control and a mechanism for the rapid demise of salp blooms (Henschke et al., 2014).

Seasonal patterns of grazing by salps were similar to other mesozooplankton at BATS, with elevated grazing in spring compared to the rest of the year. Total mesozooplankton (>64 μm) grazing in the Sargasso Sea was 88 mg C m^{-2} day^{-1} in March/April 1990 (82% of PP) and 13 mg C m^{-2} day^{-1} in August 1989 (25% of PP) (Roman et al., 1993). In both seasons, salps contributed a similar proportion to the total mesozooplankton grazing, with average salp grazing in both March/April and August 6% of the total grazing reported in Roman et al. (1993).

4.4 Salp-mediated carbon flux

On average, total salp-mediated C flux is significant compared to the POC flux measured by sediment traps at 200 m, consistent with previous studies of fecal pellet contributions to carbon flux in the Sargasso Sea (Steinberg et al., 2012) and the temperate North Pacific (Iseki, 1981). Annual average salp fecal pellet flux in our study is equivalent to 7.8% of sinking trap POC flux and active transport by DVM is 1.9% of trap POC flux. During blooms, however, salps account for a higher portion of C flux out of

the euphotic zone, and high-abundance years can produce total salp-mediated carbon fluxes up to 60% (as in 1999) of trap POC flux at 200 m. These high fluxes are mostly a result of *Thalia democratica* blooms, where daily total export fluxes reached up to 144 mg C m^{-2} d^{-1}, and these bloom fluxes are more comparable to those found in coastal regions. For example, Madin et al. (2006) found FPP by *Salpa aspera* in the summer in slope waters off New England was 5-91 mg C m^{-2} $night^{-1}$, and Phillips et al. (2009) found *S. thompsoni* produced up to 20 mg C m^{-2} day^{-1} in fecal pellets off the Antarctic Peninsula.

Dissolved organic carbon flux was low compared to other sources of salp carbon export, likely because the most abundant species, *Thalia democratica*, did not vertically migrate, and any DOC excretion by non-DVM species would remain in the surface waters. However, uncertainties in our applied weight-specific salp DOC excretion rate could lead to underestimates of DOC export. There are limited measurements of DOC excretion by zooplankton, and none for salps. We used DOC excretion rates based on those measured for gelatinous zooplankton by Condon et al. (2011). Kremer (1977) found that DOC excretion by the ctenophore *Mnemiopsis leidyi* is equal to 61% of respiration, and Steinberg et al. (2000) found that average DOC excretion was 31% of respiration for several migrating crustacean zooplankton taxa and a gelatinous polychaete. Using an intermediate DOC excretion rate of 40% of respiration, our estimates of salp DOC export at BATS would increase to 56 mg C m^{-2} y^{-1}, or 7% of the yearly total salp-mediated carbon flux. Experimental measurements of salp DOC excretion rates are needed to resolve this issue.

Seasonality in average carbon export by salps can be explained by seasonality in salp blooms, with the peaks driven by periodic large blooms. The general pattern of higher flux in late winter and spring, and lower flux in late summer and fall, is consistent with the general pattern of primary production at BATS (Steinberg et al., 2001; Lomas et al., 2013). Higher respiratory DVM flux in the early spring and late summer is due to seasonal increases in large, vertically migrating species like *S. fusiformis* in the spring and *W. cylindrica* in the late summer (Stone & Steinberg, 2014). Because biomass of salps increases by several orders of magnitude during blooms, average salp fluxes are often driven by a few large blooms over the time series. Thus when summing across an entire year, the difference between mean and median may not be great; however, when summing across smaller time periods, such as a single season, the difference may be large.

Differences between salp species' effect on carbon export are primarily dependent on the size of the salp, due to increases in FPP and respiration rates with body size, and whether they vertically migrate. Vertically migrating species (*Salpa aspera*, *S. fusiformis, Wheelia cylindrica, Iasis zonaria*, and *Ritteriella retracta*) produce fecal pellets and carcasses and respire at depths already below the pycnocline, not only decreasing the distance they have to sink, but also spending less time in warmer surface waters where bacterial decomposition is faster. Carcasses from small species, such as *Thalia* sp., not only sink more slowly, but also decompose more rapidly. Thus, a small species such as *T. democratica* would overall export less carbon than an equivalent biomass of a larger, vertically migrating species such as *S. aspera*. However, in the

Sargasso Sea this difference is often masked by the considerably higher biomass of *T. democratica* blooms compared to all other species.

There were no significant long-term trends in total annual salp C export, which is dependent on the frequency and size of blooms, and peaks in export every three years is consistent with a three-year cycle of *Thalia democratica* peak biomass (Stone & Steinberg, 2014). However, there is a recorded long-term increase in total sinking POC flux to 150 m as measured by sediment traps during the high production winter-spring transition period at BATS (Lomas et al., 2010; although there was no significant increase when averaged over the entire year). Steinberg et al. (2012) also calculated an increase in both fecal pellet POC export and active C transport by diel migrating zooplankton over time due to a long-term increase in BATS mesozooplankton biomass (including an increase in DVM zooplankton biomass). This contrast between increases in winter-spring period trap flux and no change in calculated salp flux may indicate that other, non-salp-mediated pathways of export are as efficient as salp-mediated ones during this period. Comparisons between measured trap flux and calculated flux are further complicated by sediment traps not reliably capturing exported particles from spatially and temporally variable salp blooms.

Salps contribute an increasingly higher proportion of C export with increasing depth compared to sinking POC flux measured with sediment traps. At 200 m, salp flux only accounts for 11% of the daily POC flux on average. Comparatively, average daily POC flux at 3200 m of 1.7 mg C m^{-2} day^{-1} at BATS (Conte et al., 2001) is less than our calculated salp flux of 1.9 mg C m^{-2} day^{-1} at that same depth. This high amount of salp carbon reaching the deep sea has been directly observed on one occasion in the

northeastern Pacific, where a *Salpa* sp. bloom deposited large amounts of fecal pellets and carcasses to the seafloor (~4000 m) (Smith et al., 2014). However, Shatova et al. (2012) quantified zooplankton fecal pellets in traps at 500, 1500, and 3200 m at BATS in 2007, and found that FP carbon only contributed 4.6% of the total carbon flux at 3200 m, much lower than our calculated values. Additionally, they found that fecal pellets are subject to high rates of recycling and repackaging in the deep water column. Our higher estimates of deep salp export may be explained by: including carcasses–which baffles on sediment traps are likely to exclude, including DVM–which is not measured by sediment traps, and not including scavenging and consumption of salp fecal pellets and carcasses.

5. SUMMARY AND CONCLUSION

Salp populations in the oligotrophic Sargasso Sea play an important role in transporting carbon from the epipelagic zone to the deep sea. The primary source of salp-mediated carbon flux is the sinking of fecal pellets, but contributions from respiration at depth by diel vertically migrating species and sinking of salp carcasses are also important. Salp carbon flux is relatively low for much of the year, punctuated by several orders of magnitude higher fluxes during periodic population blooms, especially in spring. Salp grazing follows a similar pattern, with relatively low levels of grazing interspersed with removal of 100% of phytoplankton standing stock and PP during blooms. *Thalia democratica* is the highest contributor to salp flux, but due to its small size and absence of vertical migration, most of this species' contribution is from sinking fecal pellets. Larger species that vertically migrate (such as *Salpa fusiformis*, *S. aspera*, *Iasis zonaria*, and *Wheelia cylindrica*) respire carbon consumed in the epipelagic in the mesopelagic zone, and produce carcasses at depth that can reach the benthos (Cacchione et al., 1978; Wiebe et al., 1979). While low and high periods of salp flux average out to be a small percentage of total flux captured annually in sediment traps at 200 m, salp flux contributes a much higher percentage of the total flux in the bathypelagic zone, mostly due to slow decomposition and fast sinking of fecal pellets and carcasses.

Future changes in the diversity and abundance of salp populations could affect the efficiency of the biological pump in the Sargasso Sea. As shown in Stone and Steinberg (2014), *Thalia democratica* and *Cyclosalpa polae* populations have increased, and *T. democratica* biomass was three-fold higher within cyclonic eddies than outside eddies. If

these population increases continue, carbon flux would significantly increase, especially to the bathypelagic and benthos–carbon sequestration depths.

Acknowledgements

We are grateful to the many Bermuda Atlantic Time-series Study (BATS) technicians involved in the sampling and maintenance of the zooplankton time series over the last 2 decades. We appreciate the support of the officers and crew of the R/V '*Weatherbird II*' and the R/V '*Atlantic Explorer*' for help with sample collection. Special thanks go to Mark Brush and Courtney Harris for assistance with model development. The BATS zooplankton time series was initially funded by National Science Foundation (NSF) grant OCE-9202336 to L.P. Madin, and continued by the BATS program through the NSF Chemical and Biological Oceanography programs (OCE-9301950, OCE- 9617795, and OCE-0326885), and through OCE-0752366 and OCE-1258622 to D.K.S., which funded this current effort. Data collected onboard the 'Trophic BATS' cruise was supported by OCE -1090149 to R. Condon. This paper is Contribution no. 3545 of the Virginia Institute of Marine Science, College of William & Mary.

REFERENCES

Álvarez-García FJ, Ortiz-Bevia MJ, Cabos-Narvaez WD (2011) On the structure and teleconnections of North Atlantic decadal variability. J Clim 24: 2209−2223

Andersen V (1985) Filtration and ingestion rates of *Salpa fusiformis* Cuvier (Tunicata: Thaliacea): Effects of size, individual weight and algal concentration. J Exp Mar Biol Ecol 87: 13-29

Andersen V, Nival P (1988) A pelagic ecosystem model simulating production and sedimentation of biogenic particles: role of salps and copepods. Mar Ecol Prog Ser 44: 37-50

Atkinson A, Siegel V, Pakhomov E, Rothery P (2004) Longterm decline in krill stock and increase in salps within the Southern Ocean. Nature 432: 100−103

Bone Q, Carre C, Chang P (2003) Tunicate feeding filters. J Mar Biol Assoc UK 83: 907−919

Bruland KW, Silver MW (1981) Sinking rates of fecal pellets from gelatinous zooplankton (Salps, Pteropods, Doliolids). Mar Biol 63: 295-300

Cacchione DA, Rowe GT, Malahoff A (1978) Submersible investigation of outer Hudson submarine canyon. In: Stanley DJ, Kelling F (eds) Sedimentation in Submarine Canyons, Fans, and Trenches. Dowden, Hutchinson & Ross, Inc. Stroudsburg, PA, p42-50

Caron DA, Madin LP, Cole JJ (1989) Composition and degradation of salp fecal pellets:

implications for vertical flux in oceanic environments. J Mar Res 47: 829−850

Cetta CM, Madin LP, Kremer P (1986) Respiration and excretion by oceanic salps. Mar Biol 91: 529-537

Condon RH, Duarte CM, Pitt KA, Robinson KL, Lucas CH, Sutherland KR, Mianzan HW, Bogeberg M, Purcell JE, Decker MB, Uye S, Madin LP, Brodeur RD, Haddock SHD, Melej A, Parry GD, Eriksen E, Quiñones J, Acha M, Harvey M, Arthur JM, Graham WM (2013) Recurrent jellyfish blooms are a consequence of global oscillations. PNAS 110(3): 1000-1005

Condon RH, Steinberg DK, del Giorgio PA, Bouvier TC, Bronk DA, Graham WM, Ducklow HW (2011) Jellyfish blooms result in a major microbial respiratory sink of carbon in marine systems. PNAS 108(25): 10225-10230

Conte MH, Ralph N, Ross EH (2001) Seasonal and interannual variability in deep ocean particle fluxes at the Oceanic Flux Program (OFP)/Bermuda Atlantic Time Series (BATS) site in the western Sargasso Sea near Bermuda. Deep-Sea Res II 48: 1471−1505

Conte MH, Weber JC (2014) Particle flux in the Deep Sargasso Sea: The 35-year Oceanic Flux Program time series. Oceanography 27(1): 142-147

Deibel D (1982) Laboratory-measured grazing and ingestion rates of the salp, *Thalia democratica* Forskal and *Dolioletta gegenbauri* Uljanin (Tunicata, Thaliacea). J Plankton Res 4: 143-153

Deibel D (1985) Clearance rates of the salp *Thalia democratica* fed naturally occurring particles. Mar Biol 86: 47-54

Deibel D, Lowen B (2012) A review of the life cycles and life-history adaptations of

pelagic tunicates to environmental conditions. ICES J of Mar Sci 69(3): 358

Fuller WA (1996) Introduction to Statistical Time Series. John Wiley & Sons, New York, NY, p. 698

Godeaux J, Bone Q, Braconnot JC (1998) Anatomy of Thaliacea. In: Bone Q (ed) The biology of pelagic tunicates. Oxford University Press, New York, NY, p 1−24

González HE, Sobarzo M, Figueroa D, Nöthig EM (2000) Composition, biomass and potential grazing impact of the crustacean and pelagic tunicates in the northern Humboldt Current area off Chile: differences between El Niño and non-El Niño years. Mar Ecol Prog Ser 195: 201-220

Harbison GR, Gilmer RW (1976) The feeding rates of the pelagic tunicate *Pegea confoederata* and two other salps. Limnol and Oceanogr 21: 517-528

Harbison GR, McAlister (1979) The filter-feeding rates and particle retention efficiencies of three species of Cyclosalpa (Tunicata: Thaliacea). Limnol and Oceanogr 24: 875-892

Harbison GR, McAlister VL, Gilmer RW (1986) The response of the salp, *Pegea confoederata*, to high levels of particulate material: starvation in the midst of plenty. Limnol Oceanogr 31: 371−382

Henschke N, Bowden DA, Everett JD, Holmes SP, Kloser RJ, Lee RW, Suthers IM (2013) Salp-falls in the Tasman Sea: a major food input to deep-sea benthos. Mar Ecol Prog Ser 491: 165−175

Henschke N, Everett JD, Baird ME, Taylor MD, Suthers IM (2011) Distribution of life-history stages of the salp *Thalia democratica* in shelf waters during a spring bloom. Mar Ecol Prog Ser 430: 49−62

Henschke N, Everett JD, Doblin MA, Pitt KA, Richardson AJ, Suthers IM (2014) Demography and interannual variability of salp swarms (*Thalia democratica*). Mar Biol 161: 149-163

Hereu CM, Lavaniegos BE, Gaxiola-Castro G, Ohman MD (2006) Composition and potential grazing impact of salp assemblages off Baja California during the 1997−1999 El Niño and La Niña. Mar Ecol Prog Ser 318: 123−140

Hereu CM, Lavaniegos BE, Goericke R (2010) Grazing impact of salp (Tunicata, Thaliacea) assemblages in the eastern tropical North Pacific. J Plankton Res 32(6): 785-804

Huntley ME, Sykes PF, Marin V (1989) Biometry and trophodynamics of *Salpa thompsoni* Foxton (Tunicata: Thaliacea) near the Antarctic peninsula in Austral summer, 1983-1984. Polar Biol 10:59-70

Huskin I, Elices Ma.J, Anadón R (2003) Salp distribution and grazing in a saline intrusion off NW Spain. J Mar Syst 42: 1-11

Iseki K (1981) Particulate organic matter transport to the deep sea by salp fecal pellets. Mar Ecol Prog Ser 5: 55-60

Kremer P (1977) Respiration and excretion by the ctenophore *Mnemiopsis leidyi*. Mar Biol 44:1 43-50

Lavaniegos BE, Ohman MD (2007) Coherence of long-term variations of zooplankton in two sectors of the California Current System. Prog Oceanogr 75: 42−69

Lebrato M, Mendes PJ, Steinberg DK, Cartes JE and others (2013a) Jelly biomass sinking speed reveals a fast carbon export mechanism. Limnol Oceanogr 58: 1113−1122

Lebrato M, Molinero J-C, Cartes J, Lloris D, Mélin F, Beni-Casadella L (2013b) Sinking jelly-carbon unveils potential environmental variability along a continental margin. PLoS ONE 8(12): e82070

Lebrato M, Pahlow M, Oschlies A, Pitt KA, Jones DOB, Molinero JC, Condon RH (2011) Depth attenuation of organic matter export associated with jelly falls. Limnol Oceanogr 56(5): 1917-1928

Lebrato M, Pitt KA, Sweetman AK, Jones DOB, Cartes JE, Oschlies A, Condon RH, Molinero JC, Adler L, Gaillard C, Lloris D, Billett DSM (2012) Jelly-falls historic and recent observations: a review to drive future research directions. Hydrobiologia 690: 227-245

Licandro P, Ibañez F, Etienne M (2006) Long-term fluctuations (1974–1999) of the salps *Thalia democratica* and *Salpa fusiformis* in the Northwestern Mediterranean Sea: relationships with hydroclimatic variability. Limnol Oceanogr 51: 1832−1848

Loeb VJ, Hofmann EE, Klinck JM, Osmund HH (2010) Hydrographic control of the marine ecosystem in the South Shetland-Elephant Island and Bransfield Strait region. Deep-Sea Res II 57: 519−542

Lomas MW, Bates NR, Johnson RJ, Knap AH, Steinberg DK, Carlson CA (2013) Two decades and counting: 24-years of sustained open ocean biogeochemical measurements in the Sargasso Sea. Deep-Sea Res II 93: 16-32

Lomas MW, Steinberg DK, Dickey T, Carlson CA, Nelson NB, Condon RH, Bates NR (2010) Increased ocean carbon export in the Sargasso Sea linked to climate variability is countered by its enhanced mesopelagic attenuation. Biogeosciences 7: 57−70

Madin LP (1974) Field observations on the feeding behavior of salps (Tunicata: Thaliacea). Mar Biol 25: 143-147

Madin LP (1982) Production, composition and sedimentation of salp pellets in oceanic waters. Mar Biol 67: 39−45

Madin LP, Cetta CM (1984) The use of gut fluorescence to estimate grazing by oceanic salps. J Plankton Res 6(3): 475-492

Madin LP, Deibel D (1998) Feeding and energetics of Thaliacea. In: Bone Q (ed) The biology of pelagic tunicates. Oxford University Press, Oxford, p 81−103

Madin LP, Kremer P, Hacker S (1996) Distribution and vertical migration of salps (Tunicata, Thaliacea) near Bermuda. J Plankton Res 18: 747−755

Madin LP, Kremer P, Wiebe PH, Purcell JE, Horgan EH, Nemazie DA (2006) Periodic swarms of the salp *Salpa aspera* in the Slope Water off the NE United States: Biovolume, vertical migration, grazing, and vertical flux. Deep-Sea Res I 53: 804-819

Madin LP, Horgan EF, Steinberg DK (2001) Zooplankton at the Bermuda Atlantic Time-series Study (BATS) station: diel, seasonal and interannual variation in biomass, 1994−1998. Deep-Sea Res II 48: 2063−2082

Madin LP, Purcell JE (1992) Feeding, metabolism, and growth of *Cyclosalpa bakeri* in the subarctic Pacific. Limnol and Oceanogr 37: 1236-1251

Matsueda H, Handa N, Inoue I, Takano H (1986) Ecological significance of salp fecal pellets collected by sediment traps in the eastern North Pacific. Mar Biol 91: 421-431

Ménard F, Dallot S, Thomas G, Braconnot JC (1994) Temporal fluctuations of two

Mediterranean salp populations from 1967 to 1990. Analysis of the influence of environmental variables using a Markov chain model. Mar Ecol Prog Ser 104: 139−152

Moseley HN (1880) Deep-sea dredging and life in the deep sea III. Nature 21: 591-593

Mullin MM (1983) In situ measurement of filtering rates of the salp, *Thalia democratica*, on phytoplankton and bacteria. J Plankton Res 5: 279-288

Phillips B, Kremer P, Madin LP (2009) Defecation by *Salpa thompsoni* and its contribution to vertical flux in the Southern Ocean. Mar Biol 156: 455−467

Purcell JE, Graham WM, Dumont H (eds) (2001) Jellyfish blooms: ecosystem and societal importance. Developments in hydrobiology 155. Kluwer Academic Publishers, Dordrecht

Reinke M (1987) On the feeding and locomotory physiology of *Salpa thompsoni* and *Salpa fusiformis*. Rep Polar Res 36: 89

Ristow GH (1997) Wall correction factor for sinking cylinders in fluids. Phys Rev E 55(3): 2808-2813

Roman MR, Adolf HA, Landry MR, Madin LP, Steinberg DK, Zhang X (2002) Estimates of oceanic mesozooplankton production: a comparison using the Bermuda and Hawaii time-series data. Deep-Sea Res II 49: 175−192

Roman MR, Dam HG, Gauzens AL, Napp JM (1993) Zooplankton biomass and grazing at the JGOFS Sargasso Sea time series station. Deep-Sea Res I 40(5): 883-901

Saba VS, Friedrichs MAM, Carr M-E, Antoine D and others (2010) Challenges of

modeling depth-integrated marine primary productivity over multiple decades: a case study at BATS and HOT. Global Biogeochem Cycles 24: GB3020, doi:10.1029/2009GB003655

Sempéré R, Yoro SC, Wambeke FV, Charrière B (2000) Microbial decomposition of large organic particles in the northwestern Mediterranean Sea: an experimental approach. Mar Ecol Prog Ser 198: 61-72

Shatova O, Koweek D, Conte MH, Weber JC (2012) Contribution of zooplankton fecal pellets to deep ocean particle flux in the Sargasso Sea assessed using quantitative image analysis. J Plankton Res 34(10): 905-921

Small LF, Fowler SW, Moore SA, La Rosa J (1983) Dissolved and fecal pellet carbon and nitrogen release by zooplankton in tropical waters. Deep-Sea Res 30: 1199-1220

Smith Jr. KL, Sherman AD, Huffard CL, McGill PR, Henthorn R, Von Thun S, Ruhl HA, Kahru M, Ohman MD (2014) Large salp bloom export from the upper ocean and benthic community response in the abyssal northeast Pacific: Day to week resolution. Limnol Oceanogr 59(3): 745-757

Sreekumaran Nair SR, Achuthankutty CT, Bhattathiri PMA, Madhupratap M (1995) Feeding behaviour of salp Thalia democratica (Thaliacea). Indian J Mar Sci 24: 102-103

Steinberg DK, Carlson CA, Bates NR, Goldthwait SA, Madin LP, Michaels AF (2000) Zooplankton vertical migration and the active transport of dissolved organic and inorganic carbon in the Sargasso Sea. Deep-Sea Res I 47: 137-158

Steinberg DK, Carlson CA, Bates NR, Johnson RJ, Michaels AF, Knap AH (2001)

Overview of the US JGOFS Bermuda Atlantic Time-series Study (BATS): a decade-scale look at ocean biology and biogeochemistry. Deep-Sea Res II 48: 1405−1447

Steinberg DK, Lomas MW, Cope JS (2012) Long-term increase in mesozooplankton biomass in the Sargasso Sea: linkage to climate and implications for food web dynamics and biogeochemical cycling. Global Biogeochem Cycles 26: GB1004, doi:10.1029/2010GB004026

Stone JP, Steinberg DK (2014) Long-term time-series study of salp population dynamics in the Sargasso Sea. Mar Ecol Prog Ser 510: 111-127

Sutherland KR, Madin LP, Stocker R (2010) Filtration of submicrometer particles by pelagic tunicates. Proc Natl Acad Sci USA 107: 15129−15134

Vargas CA, Madin LP (2004) Zooplankton feeding ecology: clearance and ingestion rates of the salps *Thalia democratica, Cyclosalpa affinis* and *Salpa cylindrica* on naturally occurring particles in the Mid-Atlantic Bight. J Plankton Res 26(7): 827-833

Wallhead PJ, Garçon, Casey JR, Lomas MW (2014) Long-term variability of phytoplankton carbon biomass in the Sargasso Sea. Global Biogeochem Cycles 28, doi:10.1002/2013GB004797

Wiebe PH, Madin LP, Haury LR, Harbison GR, Philbin LM (1979) Diel vertical migration by *Salpa aspera* and its potential for large-scale particulate organic matter transport to the deep-sea. Mar Biol 53: 249-255

Wu S, Liu Z, Zhang R, Delworth TL (2011) On the observed relationship between the

Pacific Decadal Oscillation and the Atlantic Multi-decadal Oscillation. J Oceanogr 67: 27−35

Yoon WD, Kim SK, Han KN (2001) Morphology and sinking velocities of fecal pellets of copepod, molluscan, euphausiid, and salp taxa in the northeastern tropical Atlantic. Mar Biol 139: 923−928

Table 1: Warm-water decomposition rates for three species of salps and for all measured species combined. The equation solves for the percent (P) of the starting salp dry weight remaining after t hours. Decomposition follows an exponential decay curve, with a faster decay rate followed by slower decomposition.

Species	Equation	R^2	p
Iasis zonaria	$P = 108 * e(-0.033 * t)$	0.67	< 0.001
Salpa fusiformis	$P = 101 * e(-0.164 * t)$	0.87	< 0.001
Thalia democratica	$P = 95 * e(-0.605 * t)$	0.84	< 0.001
All species combined	$P = 104 * e(-0.090 * t)$	0.64	< 0.001

Table 2: Average annual carbon flux from the 9 largest contributors to flux and all other species combined. Shown are fluxes of fecal pellets, sinking of dead carcasses, respiration at depth of diel-vertical migrators, and the total of those three categories. Values are in mg carbon m^{-2} $year^{-1}$, and ± standard deviation. DOC excretion is less than 0.1 mg C m^{-2} $year^{-1}$ for all species combined.

Species	Fecal pellets mg C m^{-2} $year^{-1}$	Carcasses mg C m^{-2} $year^{-1}$	Respiration mg C m^{-2} $year^{-1}$	Total mg C m^{-2} $year^{-1}$
Thalia democratica	417 ± 1160	0.4 ± 1.1	0	418 ± 1160
Salpa aspera	60.9 ± 117	7.6 ± 14.0	58.4 ± 112	127 ± 243
Salpa fusiformis	47.9 ± 42.9	6.5 ± 5.8	46.0 ± 41.2	100 ± 90
Iasis zonaria	18.3 ± 24.7	3.9 ± 5.5	14.5 ± 19.6	37 ± 50
Wheelia cylindrica	10.4 ± 26.7	1.3 ± 2.8	18.9 ± 48.6	31 ± 78
Salpa maxima	13.0 ± 50.1	1.1 ± 4.3	0	14 ± 54
Pegea confoederata	6.7 ± 17.6	0.4 ± 1.2	0	7.1 ± 19
Pegea socia	4.9 ± 16.1	0.9 ± 3.1	0	5.9 ± 19.2
Ritteriella retracta	1.9 ± 3.6	0.2 ± 0.6	1.3 ± 3.1	3.5 ± 8.1
Other	4.8 ± 5.1	0.6 ± 0.5	0	5.3 ± 5.5
Total	586 ± 1140	23.0 ± 19.5	139 ± 126	749 ± 1130

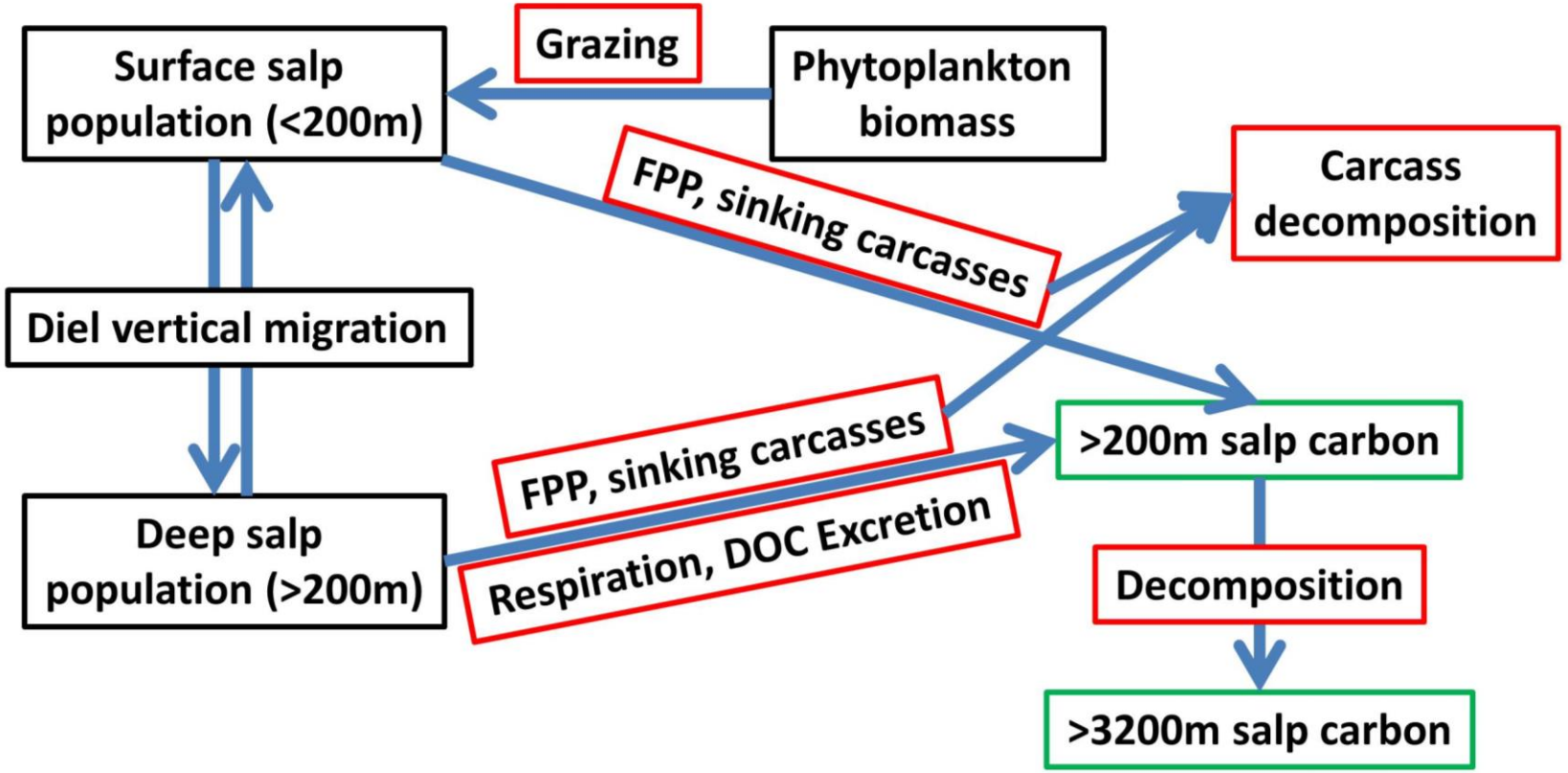

Figure 1: A summary of the model. Black boxes indicate forced values from BATS data (phytoplankton biomass, salp biomass, and salp diel vertical migration), red boxes indicate modeled rates (grazing, fecal pellet production (FPP), sinking carcasses, respiration, dissolved organic carbon (DOC) excretion, and decomposition), green boxes indicate outputs (shallow and deep salp carbon), and blue arrows indicate carbon flow.

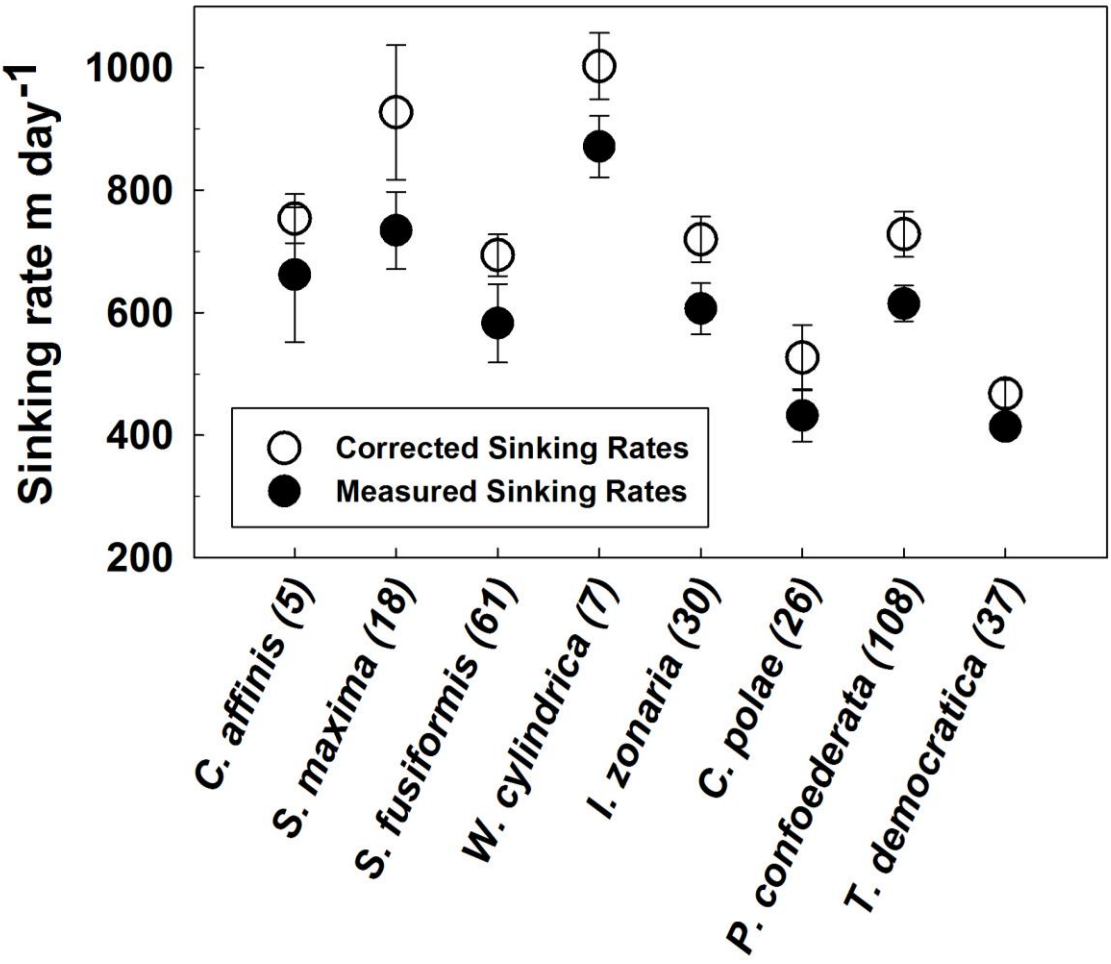

Figure 2: Mean carcass sinking rate for eight species of salps, arranged from largest salp on the left to smallest on the right. Open circles are the wall-interaction corrected values of the measured sinking rates (filled circles). Error bars are standard error, and n for each species is in parentheses after name.

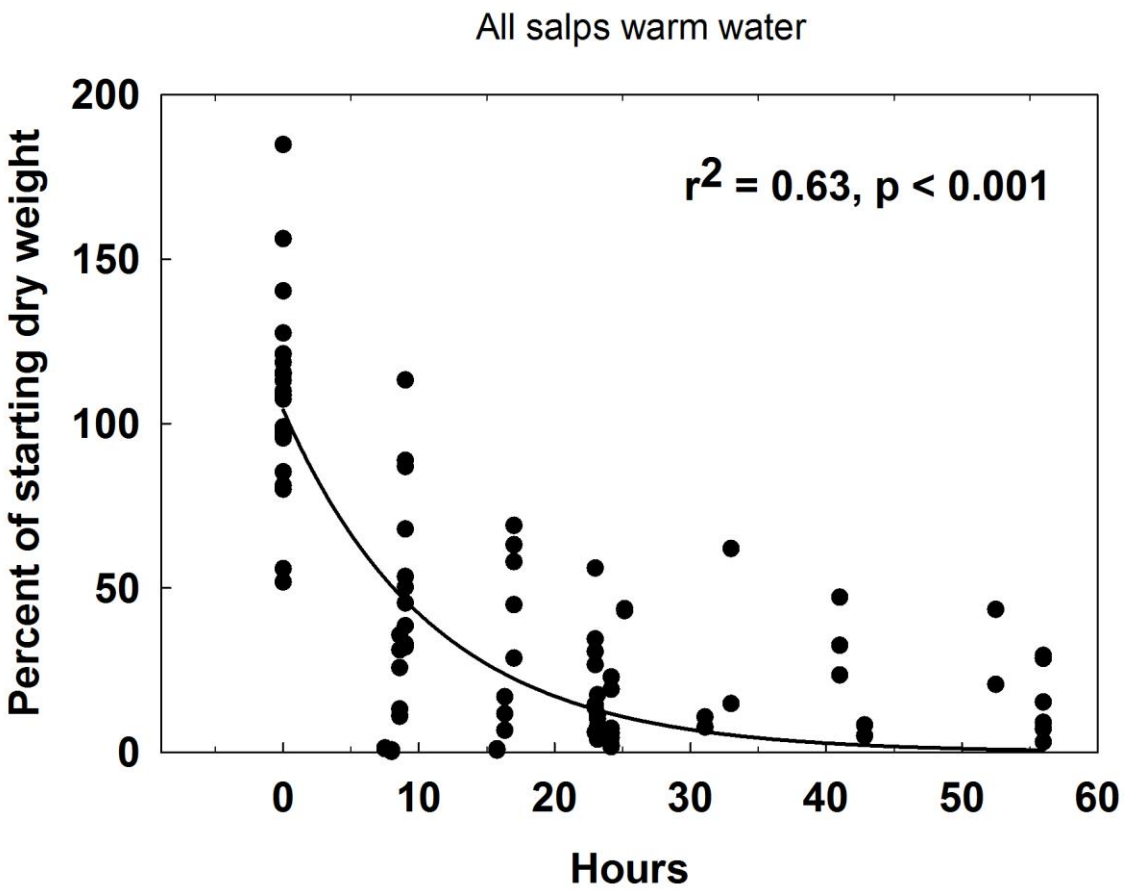

Figure 3: Percent of starting salp dry weight remaining after decomposing in surface waters. Data from 7 species and 96 individuals were used to fit the exponential decay regression. Experiments were carried out in March, May, and August of 2014 using surface water that ranged from 19-23 °C.

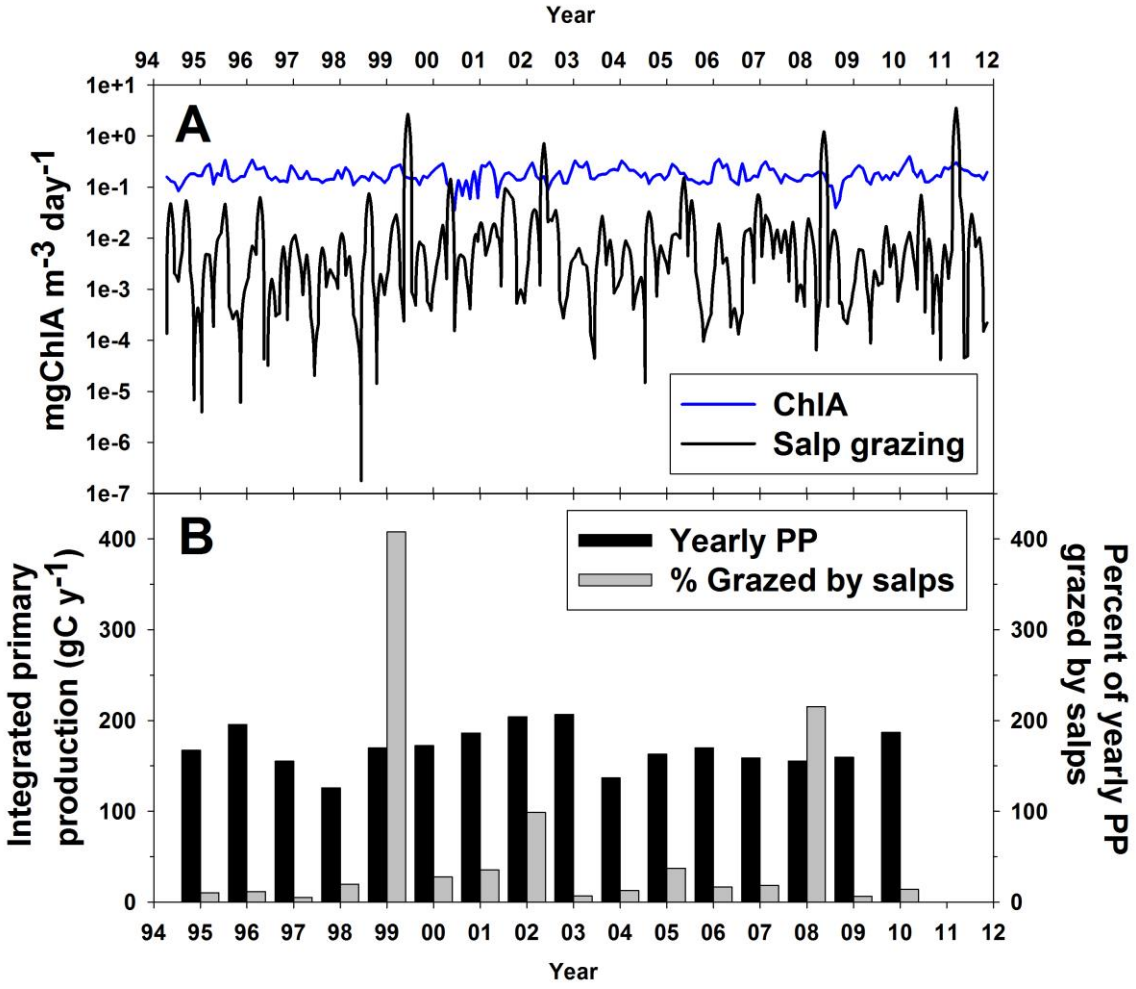

Figure 4: A) Daily chlorophyll a concentration (blue) and calculated amount of chlorophyll a grazed by total salps each day (black). B) Annual primary production (integrated to 140 m) from 1995 to 2010 (black bars) and calculated percent of that annual PP carbon grazed by total salps for each year (gray bars).

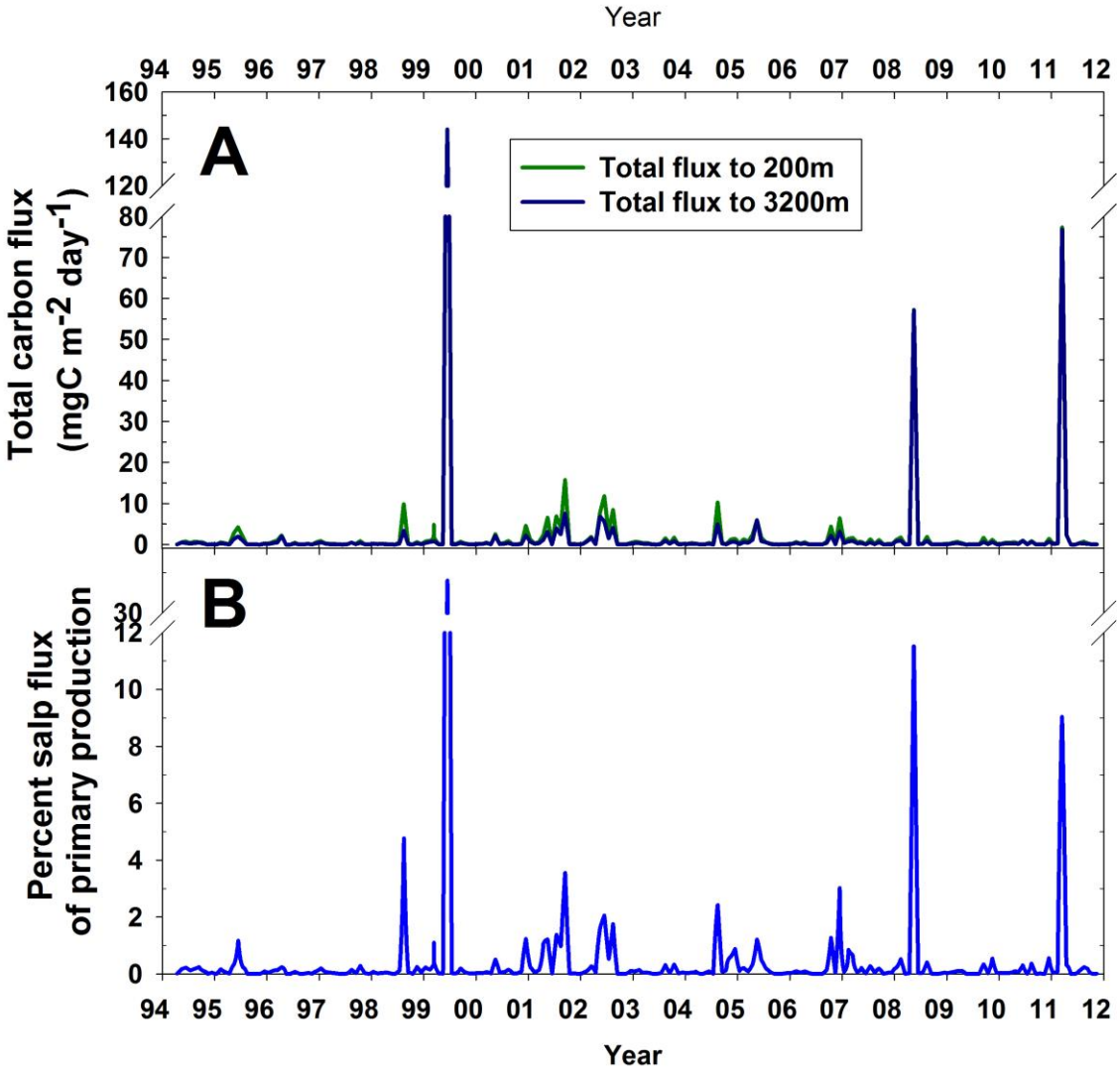

Figure 5: A) Total salp daily carbon flux to 200 m (green) and 3200 m (blue) at BATS. Total flux is from all salp species and is combined fecal pellet export, sinking of salp carcasses, and respiration and DOC excretion by DVM at depth. Blue lines without corresponding green indicate 3200 m flux that is nearly equal to the 200 m flux. B) Percent calculated total salp flux of daily primary production (integrated to 140 m).

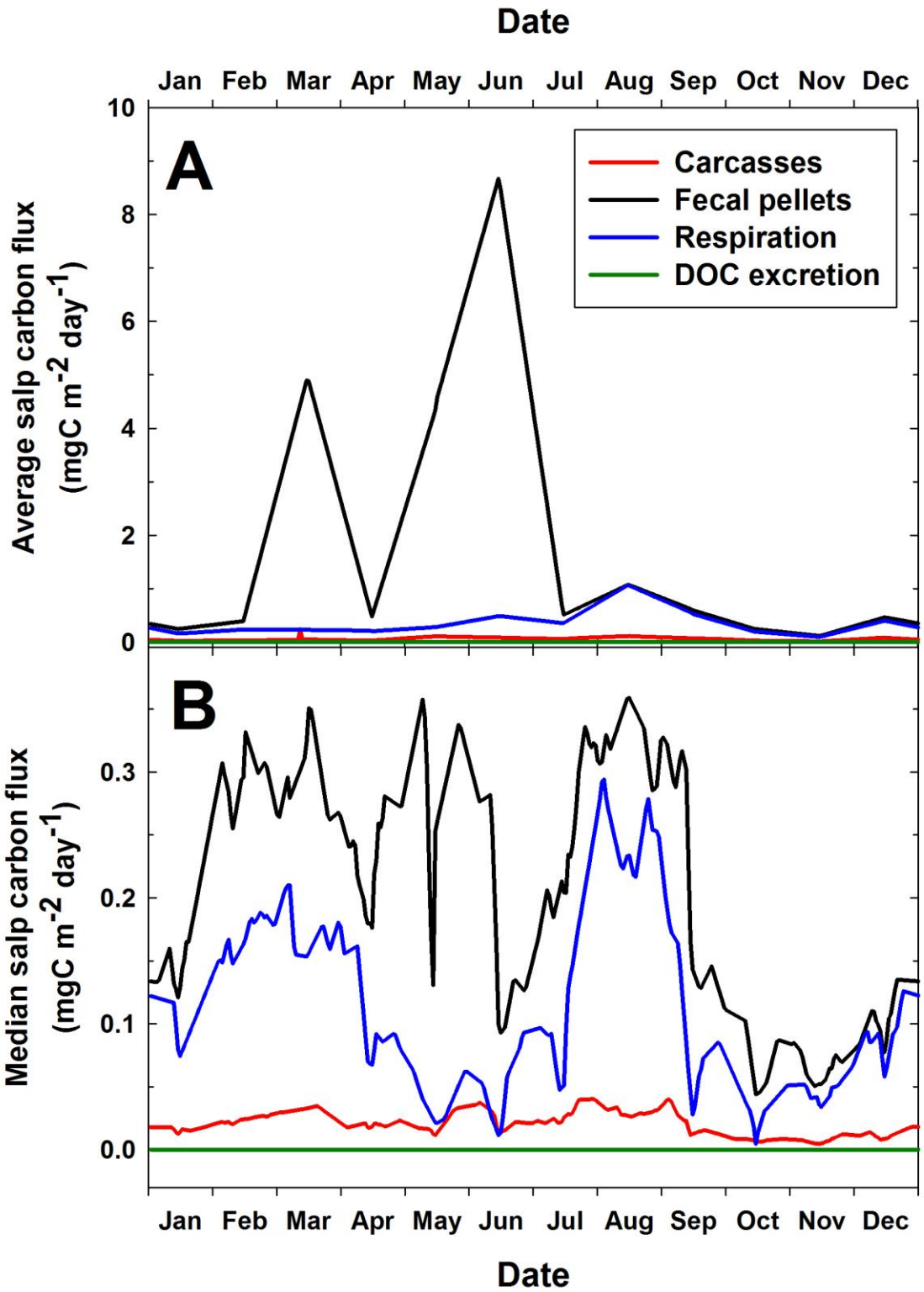

Figure 6: Seasonal variation in the salp flux to 200 m of carcasses (red), fecal pellets (black), respiration below 200 m (blue), and DOC excretion below 200 m (green). Average (A) and median (B) daily salp carbon flux for each Julian day are shown from the entire time series.

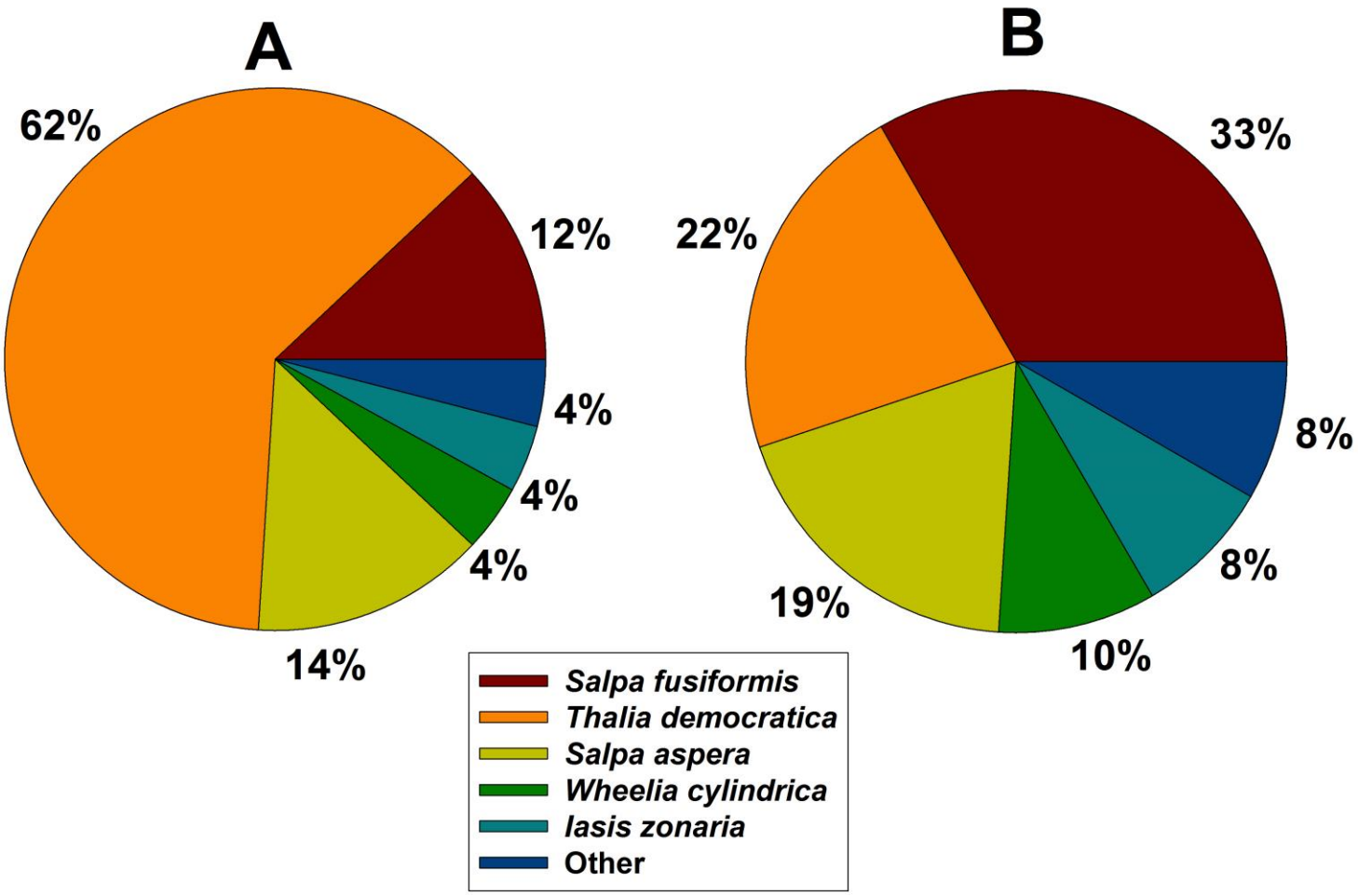

Figure 7: The percent of the total salp carbon flux at 200 m for each of the top 5 species at the BATS site for (A) the sum of each species' contribution across the entire time series and (B) the average annual percent contribution for years 1995-2010.

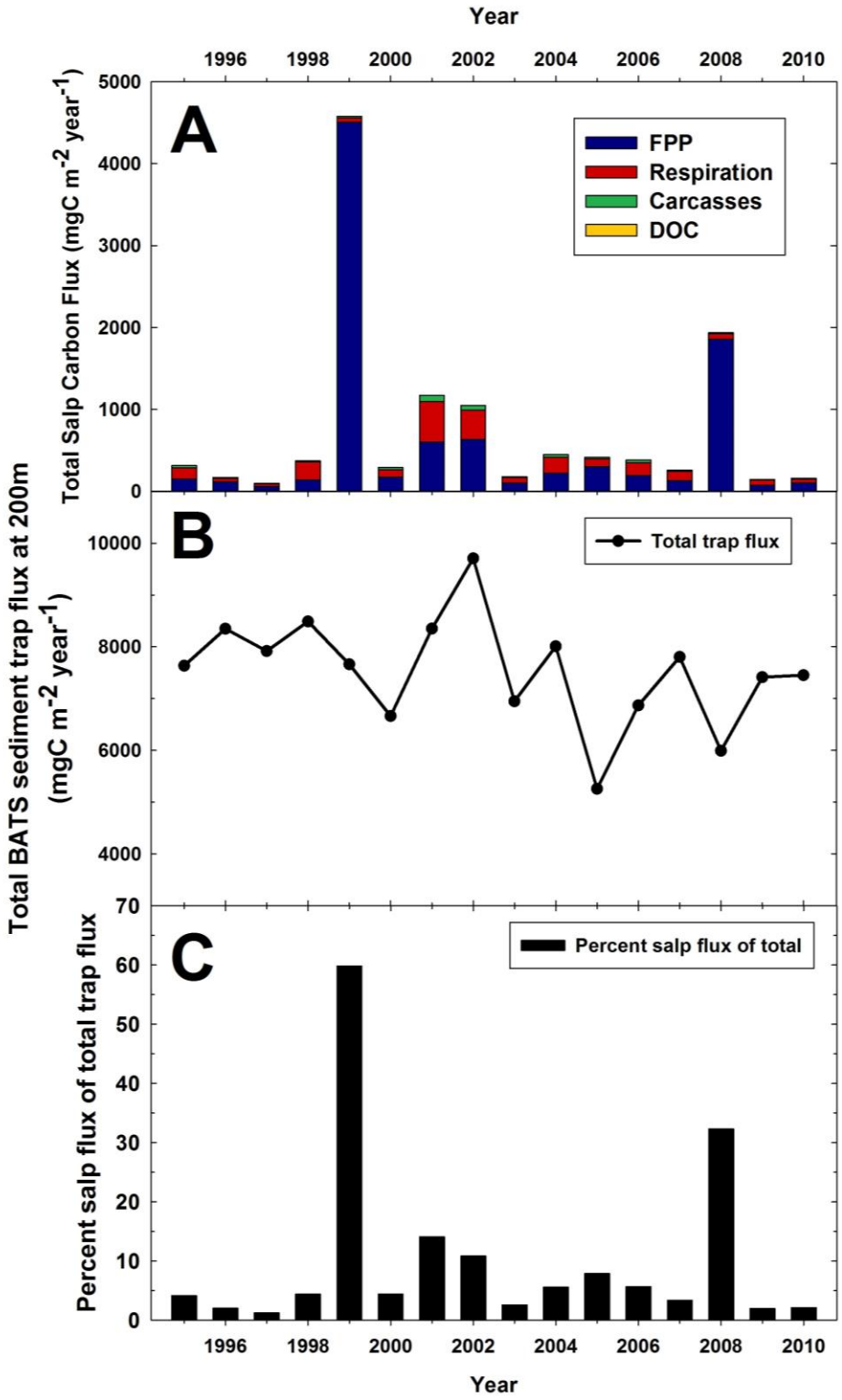

Figure 8: (A) Annual totals from 1995-2010 for combined salp carbon flux to 200 m, and the proportion different sources (fecal pellets, respiration, sinking of dead carcasses, and dissolved organic carbon excretion) contribute to those totals. These totals are compared to (B) the total annual BATS sediment trap flux at 200 m by calculating (C) the percent salp flux of the total BATS trap flux at 200 m.

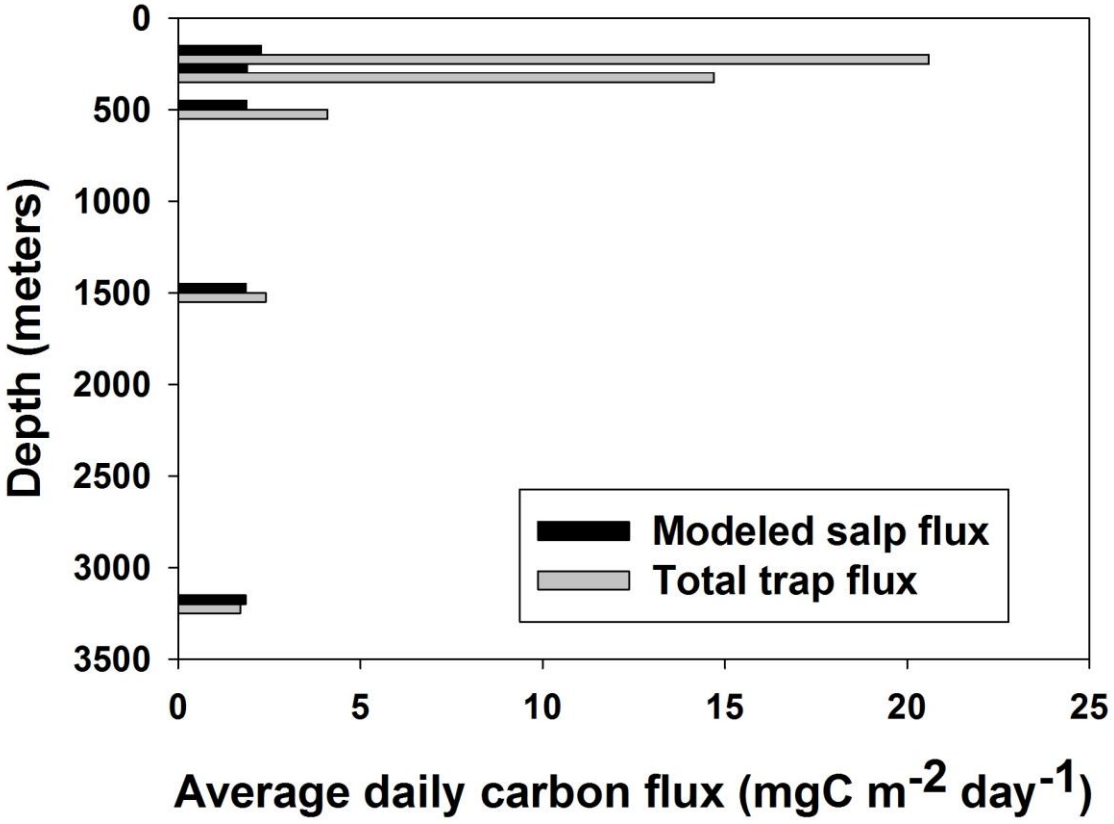

Figure 9: Depth attenuation of modeled salp carbon flux (black bars) and measured sediment trap flux (gray bars). Modeled data are averaged from January 1994 to December 2011; 200 and 300 m sediment trap fluxes are from the BATS dataset and averaged from January 1989 to December 2011; and 500, 1500, and 3200 m sediment trap fluxes are collected from Conte et al. (2001).

Supplementary Table 1: Clearance rates and fecal pellet production rates used in the salp carbon flux model. Values are averaged from multiple sources, with the individual values reported by each paper in parentheses after the citation. The standard error of each of these averages is reported below the value.

Parameter	Modeled taxa	Value	Sources
Clearance (liters cleared per mg salp C per day)	Blastozooid – *Thalia democratica, Thalia cicar, Thalia orientalis, Thalia* sp.	8.894 ± 3.8	Averaged from Deibel 1982 (19.2), Mullin 1983 (6.0, 8.4), Vargas and Madin 2004 (2.0)
	Oozoid – *T. democratica, T. cicar, T. orientalis, Thalia* sp.	5.2 ± 2.1	Averaged from Mullin 1983 (6.0, 8.4), Vargas and Madin 2004 (1.2)
	Blastozooid – *Brooksia rostrata, Helicosalpa virgula, Ihlea punctata, Iasis zonaria, Ritteriella retracta,* Salpidae, *Traustedtia multitentaculata, Thetys vagina*	14.783 ± 3.4	Averaged from Harbison and Gilmer 1976 (6.3, 15, 29.6), Harbison and McAlister 1979 (9.2, 15.9), Deibel 1982 (19.2), Mullin 1983 (6.0, 8.4), Madin and Cetta 1984 (46.8, 42.1), Andersen 1985 (4.2), Madin and Purcell 1992 (3.9, 8.5), Vargas and Madin 2004 (2.0, 17.8, 1.6)
	Oozoid – *B. rostrata, H. virgula, I. punctata, I. zonaria, R. retracta,* Salpidae, *T. multitentaculata, T. vagina*	27.265 ± 9.7	Averaged from Harbison and Gilmer 1976 (99.6 and 8.1), Harbison and McAlister 1979 (77.1 , 37.5, 8.7), Mullin 1983 (6.0, 8.4), Madin and Cetta 1984 (97.5), Andersen 1985 (5.6), Madin and Purcell 1992 (3.8, 8.5), Vargas and Madin 2004 (1.2, 17.8, 1.6)
	Blastozooid – *Cyclosalpa affinis*	5.711 ± 2.2	Averaged from Harbison and Gilmer 1976 (6.4), Harbison and McAlister 1979 (9.2), Vargas and Madin 2004 (1.6),
	Oozoid – *C. affinis*	59.455 ± 29	Averaged from Harbison and Gilmer 1976 (99.7), Harbison and McAlister 1979 (77.1), Vargas and Madin 2004 (1.6),
	Blastozooid – *Cyclosalpa floridana*	15.936	Harbison and McAlister 1979
	Oozoid – *C. floridana*	37.584	Harbison and McAlister 1979
	Blastozooid – *Cyclosalpa pinnata*	7.571 ± 2.0	Averaged from Harbison and Gilmer 1976 (6.4), Harbison and McAlister 1979 (9.2, 15.9), Madin and Purcell 1992 (3.9, 8.5), Vargas and Madin 2004 (1.6)
	Oozoid – *C. pinnata*	33.860 ± 15	Averaged from Harbison and Gilmer 1976 (99.6), Harbison and McAlister 1979 (77.1, 37.6, 8.7), Madin and Purcell 1992 (3.9, 8.5), Vargas and Madin 2004 (1.6)
	Blastozooid – *Cyclosalpa polae*	7.571 ± 2.0	Averaged from Harbison and Gilmer 1976 (6.4), Harbison and McAlister

			1979 (9.2, 15.9), Madin and Purcell 1992 (3.9, 8.5), Vargas and Madin 2004 (1.6)
	Oozoid – *C. polae*	8.712	Harbison and McAlister 1979
	Blastozooid – *Pegea bicaudata, Pegea confoederata, Pegea socia, Pegea* sp.	30.924	Averaged from Harbison and Gilmer 1976 (15.0), Madin and Cetta 1984 (46.8)
	Oozoid – *P. bicaudata, P. confoederata, P. socia, Pegea* sp.	8.112	Harbison and Gilmer 1976
	Blastozooid – *Salpa aspera, Salpa fusiformis*	4.152	Andersen 1985
	Oozoid – *S. aspera, S. fusiformis*	5.616	Andersen 1985
	Blastozooid – *Salpa maxima*	35.856	Averaged from Harbison and Gilmer 1976 (29.6), Madin and Cetta 1984 (42.1)
	Oozoid – *S. maxima*	35.856	Averaged from Harbison and Gilmer 1976 (29.6), Madin and Cetta 1984 (42.1)
	Blastozooid – *Wheelia cylindrica*	17.823	Vargas and Madin 2004
	Oozoid – *W. cylindrica*	17.823	Vargas and Madin 2004
FPP (% body C per hour)	*B. rostrata, C. floridana, H. virgula, I. punctata, I. zonaria, R. retracta,* Salpidae, *T. cicar, T. democratica, T. multitentaculata, T. orientalis, T. vagina, Thalia* sp.	1.179 ± 0.17	Averaged from Madin 1982 (0.99, 0.37, 0.65, 2.77, 0.99, 1.22, 1.30), Small et al. 1983 (1.24), Cetta et al. 1986 (0.62, 1.2, 1.3), Madin and Purcell 1992 (1.5)
	C. affinis	0.99	Madin 1982
	C. pinnata	0.37	Madin 1982
	C. polae	0.68	Averaged from Madin 1982 (0.99, 0.37)
	P. bicaudata	0.65	Madin 1982
	P. confoederata	2.77	Madin 1982
	P. socia	0.99	Madin 1982
	Pegea sp.	1.47 ± 0.65	Averaged from Madin 1982 (0.65, 2.77, 0.99)
	S. aspera, S. fusiformis	1.238 ± 0.03	Averaged from Madin 1982 (1.22, 1.3), Cetta et al. 1986 (1.2)
	S. maxima	1.3	Cetta et al. 1986
	Salpa sp.	1.26 ± 0.03	Averaged from Madin 1982 (1.22, 1.3), Cetta et al. 1986 (1.2, 1.3)
	W. cylindrica	1.22	Averaged from Madin 1982 (1.22), Cetta et al. 1986 (1.2)

CHAPTER 6

Summary and Concluding Remarks

Gelatinous zooplankton are important predators and grazers in the majority of the world's oceans and seas. Due to their unique body plans, complex life histories, and ability to bloom in extremely high abundances, their effects on food web dynamics and vertical carbon flux are strong and diverse. Additionally, GZ are sensitive to environmental changes, and future changes in global climate could greatly affect their abundance. My research is the most spatially and temporally rich long-term analysis of GZ population changes in the Chesapeake Bay (Chapter 2), and the only long-term analysis of GZ population changes in the Sargasso Sea (Chapter 4). I also present the first measurements of top-down control of vertical carbon flux (Chapter 3), and the first estimates of lifetime contributions by salps to vertical carbon flux (Chapter 5).

Previous studies of GZ population dynamics in the Chesapeake Bay have shown that abundance of the dominant species, the scyphozoan medusa *Chrysaora quinquecirrha*, is driven by changes in spring temperature and stream flow (Cargo & King, 1990), with the North Atlantic Oscillation driving interannual changes (Purcell & Decker, 2005). Relative abundances of *C. quinquecirrha* in turn control populations of the ctenophore *Mnemiopsis leidyi*, causing a trophic cascade down the food web (Purcell & Decker, 2005; Kimmel et al., 2012). My results show that spring salinity is the primary driver of overall *C. quinquecirrha* populations, with lower salinities leading to higher summer biovolume through regulation of asexual reproduction by the benthic scyphistomae. Temperature is primarily a seasonal control on the Chesapeake Bay *C. quinquecirrha* population, with warming waters regulating the timing, but not magnitude, of the bloom. Additionally, low dissolved oxygen concentrations delay the onset of the summer bloom, with hypoxic conditions negatively affecting spring *C. quinquecirrha*

biovolume. Changes in *C. quinquecirrha* abundances are the primary controller of *M. leidyi* populations, which in turn have a significant effect on the overall spring and summer copepod abundance. *C. quinquecirrha* populations in Chesapeake Bay have been decreasing from 1985-2011, with a concurrent increase in *M. leidyi* and decrease in copepod abundances, the latter similar to the decrease in *Acartia tonsa* copepods shown by Kimmel et al. (2012). Both spring streamflow and spring hypoxia are predicted to increase in Chesapeake Bay in response to global climate change (Hagy et al., 2004; Najjar et al., 2010), and both of these trends would continue to cause a decline of *C. quinquecirrha* populations in Chesapeake Bay. This reduction in *C. quinquecirrha* would further release *M. leidyi* from top-down control in the summer, reducing copepod abundances and increasing predation pressure on ichthyoplankton (Purcell et al., 1994; Purcell & Cowan, 1995) and bivalve larvae (Purcell et al., 1991; Breitburg & Fulford, 2006).

This top-down control of Chesapeake Bay food webs by *C. quinquecirrha* also has implications for vertical carbon flux. In my mesocosm experiments, I showed that the presence of *C. quinquecirrha* reduces the abundance of *M. leidyi*, releasing *Acartia tonsa* copepods from predation pressure. This in turn allows the copepods to produce more fecal pellets, and for some experiments, fecal pellet carbon flux was 2 times higher in treatments without the addition of *M. leidyi*. However, overall particulate organic carbon flux was not different between treatments, most likely due to bulk flux being dominated by phytoplankton detritus. Over the course of a summer, the presence of *C. quinquecirrha* in Chesapeake Bay increases copepod fecal pellet carbon flux by 10.4 mg C m^{-2}, equivalent to a significant portion (10%) of the calculated direct contribution to

vertical flux by *C. quinquecirrha* carcasses (~100 mg C m^{-2} yr^{-1}, Sexton et al., 2010). While this change in flux is small relative to the overall summer Chesapeake Bay carbon flux (Boynton et al., 1993; Roden et al., 1995; Hagy et al., 2005), it remains to be investigated how the fate of copepod fecal pellets may differ from phytodetritus in the benthos. Future reduction of *C. quinquecirrha* populations will reduce the overall vertical flux of copepod fecal pellets in the Chesapeake Bay.

Much work remains to be done on the role of GZ in the Chesapeake Bay. Population changes in *C. quinquecirrha* and *M. leidyi* affect the entire Chesapeake Bay ecosystem, and further investigation is needed into how hypoxia, especially in conjunction with other environmental changes, affects *C. quinquecirrha* asexual reproduction. Additionally, the fate of overwintering *C. quinquecirrha* is an intriguing issue, especially if these individuals are shown to reproduce for a second year and winter survival is increased by warmer winters. Future research should also examine the fate in the benthos of copepod fecal pellets versus GZ particulate organic matter, and the role that GZ mucous plays in aggregating phytoplankton into sinking masses. Finally, little is still known of what predators consume GZ in Chesapeake Bay.

In the Sargasso Sea, salps are the most abundant GZ and population dynamics are characterized by very low baseline abundances interspersed with short periods of extremely high abundances (up to 371 ind. m^{-3}) during blooms. Of the 21 species identified in the Bermuda Atlantic Time-series Study (BATS), *Thalia democratica* was the most common and bloomed to the highest abundances. While total salp biomass was primarily driven by *T. democratica* blooms, several other species (*Salpa fusiformis*, *Weelia cylindrica*, and *Cyclosalpa polae*) also occasionally bloomed. Blooms of *T.*

democratica, *S. fusiformis*, and *C. polae* were seasonally associated with increases in chlorophyll *a* and primary production during the onset of the spring phytoplankton bloom (Feb-Mar). A second seasonal peak in salp biomass during the late summer (Aug-Sep) was generally associated with blooms of *W. cylindrica*. Outside of this seasonal trend, *T. democratica* populations were also significantly higher in cyclonic mesoscale eddies, common oceanographic features in the Sargasso Sea. These increases may be due to physical aggregation of salps, but mesoscale eddies have also been shown to enhance primary production (McGillicuddy et al., 2007) and mesozooplankton biomass (Goldthwait & Steinberg, 2008), potentially causing bottom-up stimulation of *T. democratica* blooms. Interannual variation was tied to changes in decadal climate oscillations, including several Pacific indices. Total salp biomass remained constant throughout the time series (1994-2011), but long-term increases in *T. democratica* (+0.01 μg C m^{-3} yr^{-1}) and *C. polae* (+0.003 μg C m^{-3} yr^{-1}) biomass were observed, concurrent with an overall increase in primary production at BATS (Saba et al., 2010).

GZ can contribute to vertical carbon flux through several mechanisms, and previous studies have separately examined the contributions to flux by sinking fecal pellets (Matsueda et al., 1986; Caron et al., 1989; Shatova et al., 2012), sinking carcasses (Lebrato et al., 2013), and respiration in conjunction with diel-vertical migration (Steinberg et al., 2000). I modeled the contributions of salps to vertical carbon flux in the Sargasso Sea through all three of these mechanisms, and found that salps have the potential to transport an extremely large pulse of carbon to the deep sea during large blooms (over 100 mg C m^{-2} day^{-1}). However, because baseline salp abundance is several orders of magnitude lower than bloom abundance, average fluxes are much lower (2.3

mg C m^{-2} d^{-1}). Sinking fecal pellets were the greatest source of carbon flux to 200 m (78% of total flux), followed by respiration (19%), and sinking of carcasses (3%). Although carcasses represent a small portion of the overall calculated flux, sinking and decomposition rate experiments show that carcasses can reach the sea floor relatively intact, consistent with deep-sea observations (Lebrato et al., 2012) and be consumed by organisms that would not consume fecal pellets. While salp carbon flux was a modest portion of overall measured flux at 200 m (11%), annual salp flux to 3200 m could exceed 100% of that measured by sediment traps due to the slow attenuation of salp carcasses and fecal pellets. Future increases in salp populations, such as those observed for *T. democratica* and *C. polae*, would increase the overall carbon flux in this region.

The development and progression of individual salp blooms has not been tracked in the Sargasso Sea, and future research should focus on the short-term mechanisms that lead to the growth of blooms. Specific attention is needed to the relative importance different phytoplankton play in initiating a salp bloom, the role that mesoscale eddies play in production vs. aggregation of salps, as well as what causes salp blooms to collapse. Models of salp contributions to vertical carbon export could also be refined by determining the scavenging and consumption of salp fecal pellets and carcasses that occurs throughout the water column.

While there has been much concern over whether GZ populations are increasing globally (Daskalov et al., 2007; Richardson et al., 2009), my research shows that different taxa of GZ respond very differently to changing environmental conditions, and complex food-web interactions further complicate population dynamics. In Chesapeake Bay, *C. quinquecirrha* populations have been declining, leading to increases in *M. leidyi*; in the

Sargasso Sea, overall salp populations have been stable, with only small increases over time in *T. democratica* and *C. polae*. If these changes in populations and community composition continue, they have the potential to significantly impact both prey abundance and vertical carbon flux in both regions, with further implications for commercial fisheries and carbon sequestration.

REFERENCES

Boynton WR, Kemp WM, Barnes JM, Matteson LL, Rohland FM, Jasinski DA, Kimble HL (1993) Ecosystem Processes Component Level 1 Interpretive Report No. 10. Chesapeake Biological Laboratory, University of Maryland System, Solomons, MD 20688-0038. Ref. No. [UMCEES]CBL 93-030a

Breitburg DL, Fulford RS (2006) Oyster-sea nettle interdependence and altered control within the Chesapeake Bay ecosystem. Estuaries Coasts 29(5): 776-784

Cargo DG, King DR (1990) Forecasting the abundance of the sea nettle, *Chrysaora quinquecirrha*, in the Chesapeake Bay. Estuaries 13(4): 486-491

Caron DA, Madin LP, Cole JJ (1989) Composition and degradation of salp fecal pellets: implications for vertical flux in oceanic environments. J Mar Res 47: 829-850

Goldthwait SA, Steinberg DK (2008) Elevated biomass of mesozooplankton and enhanced fecal pellet flux in cyclonic and mode-water eddies in the Sargasso Sea. Deep-Sea Res II 55: 1360-1377

Hagy III JD, Boynton WR, Jasinski DA (2005) Modelling phytoplankton deposition to Chesapeake Bay sediments during winter-spring: interannual variability in relation to river flow. Est Coast Shelf Sci 62: 25-40

Hagy III JD, Boynton WR, Keefe CW, Wood KV (2004) Hypoxia in Chesapeake Bay, 1950–2001: Long-term change in relation to nutrient loading and river flow. Estuaries 27: 634–658

Kimmel DG, Boynton WR, Roman MR (2012) Long-term decline in the calanoid copepod *Acartia tonsa* in central Chesapeake Bay, USA: An indirect effect of eutrophication?. Est Coast Shelf Sci 101: 76-85

Lebrato M, Mendes PJ, Steinberg DK, Cartes JE, Jones BM, Birsa LM, Benavides R, Oschlies A (2013) Jelly biomass sinking speed reveals a fast carbon export mechanism. Limnol Oceanogr 58(3): 1113–1122.

Lebrato M, Pitt KA, Sweetman AK, Jones DOB, Cartes JE, Oschlies A, Condon RH, Molinero JC, Adler L, Gaillard C, Lloris D, Billett DSM (2012) Jelly-falls historic and recent observations: a review to drive future research directions. Hydrobiologia 690: 227–245

Matsueda H, Handa N, Inoue I, Takano H (1986) Ecological significance of salp fecal pellets collected by sediment traps in the eastern North Pacific. Mar Biol 91: 421-431

McGillicuddy DJ, Anderson LA, Bates NR, Bibby T, Buesseler KO, Carlson C, Davis CS, Ewart C, Falkowski PG, Goldthwait SA, Hansell DA, Jenkins WJ, Johnson R, Kosnyrev VK, Ledwell JR, Li QP, Siegel DA, Steinberg DK (2007) Eddy/wind interactions stimulate extraordinary mid-ocean plankton blooms. Science 316: 1021−1026

Najjar RG, Pyke CR, Adams MB, Breitburg D, Hershner C, Kemp M, Howarth R, Mulholland MR, Paolissso M, Secor D, Sellner K, Wardrop D, Wood R (2010) Potential climate-change impacts on the Chesapeake Bay. Est Coast Shelf Sci 86: 1-20

Purcell JE, Cowan Jr. JH (1995) Predation by the scyphomedusan *Chrysaora quinquecirrha* on *Mnemiopsis leidyi* ctenophores. Mar Ecol Prog Ser 128: 63-70

Purcell JE, Cresswell FP, Cargo DG, Kennedy VS (1991) Differential ingestion and

digestion of bivalve larvae by the scyphozoan *Chrysaora quinquecirrha* and the ctenophore *Mnemiopsis leidyi*. Biol Bull 180: 103-111

Purcell JE, Decker MB (2005) Effects of climate on relative predation by scyphomedusae and ctenophores on copepods in Chesapeake Bay during 1987-2000. Limnology and Oceanography 50(1): 376-387

Purcell JE, White JR, Roman MR (1994). Predation by gelatinous zooplankton and resource limitation as potential controls of *Acartia tonsa* copepod populations in Chesapeake Bay. Limnol Oceanogr 39: 263-278

Richardson AJ, Bakun A, Hays GC, and Gibbons MJ (2009) The jellyfish joyride: causes, consequences and management responses to a more gelatinous future. Trends Ecol Evol 24: 312–22

Roden EE, Tuttle JH, Boynton WR, Kemp WM (1995) Carbon cycling in mesohaline Chesapeake Bay sediments 1: POC deposition rates and mineralization pathways. J Mar Res 53: 799-819

Saba VS, Friedrichs MAM, Carr M-E, Antoine D, Armstrong RA, Asanuma I, Aumont O, Bates NR, Behrenfeld MJ, Bennington V, Bopp L, Bruggemann J, Buitenhuis ET, Church MJ, Ciotti AM, Doney SC, Dowell M, Dunne J, Dutkiewicz S, Gregg W, Hoepffner N, Hyde KJW, Ishizaka J, Karneda T, Karl DM, Lima I, Lomas MW, Marra J, McKinley GA, Mélin F, Moore JK, Morel A, O'Reilly J, Salihoglu B, Scardi M, Smyth TJ, Tang S, Tjiputra J, Uitz J, Vichi M, Waters K, Westberry TK, Yool A (2010) Challenges of modeling depth-integrated marine primary productivity over multiple decades: A case study at BATS and HOT. Global Biogeochemical Cycles 24: GB3020

Sexton MA, Hood RR, Sarkodee-adoo J, Liss AM (2010) Response of *Chrysaora quinquecirrha* medusae to low temperature. Hydrobiologia 645: 125-133

Shatova O, Koweek D, Conte MH, Weber JC (2012) Contribution of zooplankton fecal pellets to deep ocean particle flux in the Sargasso Sea assessed using quantitative image analysis. J Plankton Res 34(10): 905–921

Steinberg DK, Carlson CA, Bates NR, Goldthwait SA, Madin LP, Michaels AF (2000) Zooplankton vertical migration and the active transport of dissolved organic and inorganic carbon in the Sargasso Sea. Deep-Sea Res I 47: 137-158

VITA

JOSHUA PAUL STONE

Born in McKeesport, PA on February 10, 1988. Was homeschooled through high school, and graduated in May, 2006. Earned a Bachelor of Science in Biology and a Bachelor of Arts in Spanish in May, 2010 from Messiah College, Grantham, PA. Worked as a Biological Aide for Blackwater National Wildlife Refuge seasonally from 2006 to 2009. Entered the Masters program at the Virginia Institute of Marine Science, College of William & Mary in August, 2010 under graduate advisor Dr. Deborah K. Steinberg and bypassed into the Ph.D. program in 2012.